CR-171826

LMSC-HREC TR D867400-I C.1

HIGH ALTITUDE CHEMICALLY REACTING GAS PARTICLE MIXTURES VOLUME I - A THEORETICAL ANALYSIS AND DEVELOPMENT OF THE NUMERICAL SOLUTION

August 1984

CONTRACT NAS9-16256

Prepared for

National Aeronautics and Space Administration
Aerodynamic Systems Analysis Section
Johnson Space Center, Houston, TX 77058

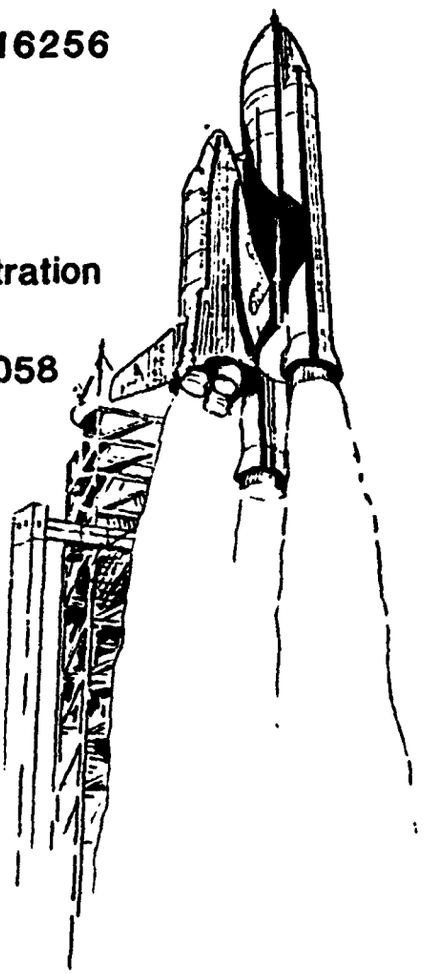

by

S. D. Smith

Lockheed
Missiles & Space Company, Inc
Huntsville Research & Engineering Center
4800 Bradford Drive, Huntsville, AL 35807

FOREWORD

This document is Volume I of a three volume report describing the Reacting and Multi-Phase (RAMP2) computer code developed by the Computational Mechanics Section of Lockheed's Huntsville Research & Engineering Center, Huntsville, Alabama. Volume I describes the overall contractural effort and the theory and numerical solution for the computer code. Volume II provides a detailed description of all the elements used in the RAMP2 code, and Volume III is the program user's and applications manual.

Documentation of the computer code was prepared in partial fulfillment of Contract NAS9-16256 with the NASA-Lyndon B. Johnson Space Center, Houston, Texas. The contracting officer's technical representative for this study was Mr. Barney B. Roberts, ET41.

The author acknowledges the efforts of Dr. Terry F. Greenwood of NASA-Marshall Space Flight Center and Mr. S.J. Robertson of Lockheed-Huntsville, both of whom contributed to the development of the RAMP2 code.

Companion documents to this report include a users and applications manual for RAMP2 computer code; a computer program maintenance manual for RAMP2; a report which describes the modifications made to the NASA-Lewis TRAN72 computer code; the original documentation of the NASA-Lewis TRAN 72 computer code; and the original documentation of the Boundary Layer Integral Matrix (BLIMPJ) computer code. These documents are, respectively:

- "High Altitude Chemically Reacting Gas-Particle Mixtures - Volume II - Program Manual for RAMP2," LMSC-HREC TR D867400-II.

- "High Altitude Chemically Reacting Gas-Particle Mixtures - Volume III - Computer Code User's and Applications Manual," LMSC-HREC TR D867400-III.

- "User's Guide for TRAN72 Computer Code Modified for Use with RAMP and VOFMOC Flowfield Codes," LMSC-HREC TM D390409.

- Svehla, R.A., and B.J. McBride, "FORTRAN IV Computer Program for Calculation of Thermodynamics and Transport Properties of Complex Chemical Systems," NASA TN D-7056, January 1976.

- Evans, R.M., "Boundary Layer Integral Matrix Procedure BLIMP-J User's Manual," Aerotherm UM-75-64, July 1975.

CONTENTS

SYMBOLS AND NOTATION

Symbol	Description
A^j	parameter defined by Eq. (3.46), 1/sec; area, ft^2
a	speed of sound, ft/sec
B^j	parameter defined by Eq. (3.86c)
C	parameter defined by Eq. (3.83), $ft^2/sec^2/^oR$
C_D	drag coefficient, dimensionless
c_p	specific heat at constant pressure, $ft^2/sec^2/^oR$
c_v	specific heat at constant volume, $ft^2/sec^2/^oR$
D_f	drag force, lbf
D/Dt	substantial derivative
dv	an element of volume, ft^3
$\hat{e}$	unit vector, dimensionless
E	energy in the gas-particle system control volume, ft^2/sec^2
F	interpolation factor, dimensionless; or total force acting on the system defined by Eq. (3.30), lbf
f	drag coefficient parameter ($C_D/C_{D_{Stokes}}$), dimensionless
G	Nusselt number parameter defined by Eq. (3.77) dimensionless
H	total enthalpy, ft^2/sec^2
h	local enthalpy, ft^2/sec^2
I_{sp}	specific impulse, lbf-sec/lbm
K	particle heat transfer film coefficient defined by Eq. (3.76), lbm/sec/^{o}R/ft
k	thermal conductivity of gas, lbm/sec/^{o}R

Symbol	Description
M	Mach number, dimensionless; or momentum, lbm-ft/sec
$\dot{m}$	mass flow rate, slug/sec
m^j	density of a particle based on a unit volume of particles, slug/ft^3
NG	index denoting number of discrete gaseous species considered
NP	index denoting number of discrete particles considered
NS	index denoting number of discrete species considered = NG+NP
Nu	Nusselt number, dimensionless
$\vec{n}$	unit normal vector
P	pressure, lbf/ft^2
P_i	partial pressure of species i, lbf/ft^2
Pr	Prandtl number, dimensionless
Q	heat transferred to or from a gas-particle system control volume, Btu
q	velocity, ft/sec
R	gas constant, ft^2/sec^2/^{o}R
Re	Reynolds number, dimensionless
r^j	particle radius, ft
S	surface area of a gas-particle system control volume; ft^2; entropy, ft^2/sec^2/^{o}R
T	temperature, ^{o}R
t	time, sec
u, v	velocity components, ft/sec
V	volume of a gas-particle system control volume, ft^3
W	work performed on or by the gas-particle system control volume, ft^2/sec^2

Symbol	Description
$\dot{w}$	production rate, lbm/sec
x, r	position coordinates, ft
Greek	
α	accommodation coefficient, dimensionless; or Mach angle, radians
β	characteristic slope, radians
γ	specific heat ratio, dimensionless
Φ	any extensive quantity of the element dv
$\bar{\bar{\delta}}$	Kronecker delta
δ	0, 1 for two-dimensional or axisymmetric flow, respectively
$\bar{\bar{\tau}}$	viscous stress tensor, lbf/ft^2
ϵ	emissivity, dimensionless
∇	nabla
θ	inclination of the flow vector with respect to the x-axis, radians
μ	chemical potential, cal/gm
ν	viscosity, $lbf\text{-}sec/ft^2$
λ	equation modifier
ρ	density, $slug/ft^3$
$\bar{\bar{\sigma}}$	surface stress tensor, lbf/ft^2
σ	Stefan-Boltzman constant, ft^2/sec^3
ψ	particle stream function, lbm-sec/ft
Σ	indicates summation, $\sum_{j=1}^{N}$
χ	species mass fraction
∂	indicates partial derivative

Subscripts	Description
I	indicates initial data surface
i	indicates the quantity pertaining to species i
L	denotes local surface conditions
m	indicates the quantity pertaining to the gas-particle mixture
n	indicates n^{th} data surface
w	denotes nozzle wall conditions
x, y	denotes partial differentiation in the x and y (or r) directions

Superscripts	
$\rightarrow$	denotes a vector quantity
$-$	denotes an average value over a step length
j	indicates the quantity pertaining to a particle specie

1. INTRODUCTION AND SUMMARY

The overall objective of this study was to deliver a nozzle-plume flowfield code that has capabilities which do not presently exist in a single computer code. The RAMP code (Refs. 1 and 2), developed by Lockheed under government funding, was chosen as the basic code from which to work. The basic RAMP code is of modular construction and has the following capabilities:

- Two-phase with two-phase transonic solution
- Two-phase, reacting gas (chemical equilibrium reaction kinetics), supersonic inviscid nozzle/plume solution
- Operational for inviscid solutions at both high and low altitudes.

During the course of the study the following capabilities were added to the code to produce the RAMP2 program:

- Direct interface with JANNAF SPF code (Ref. 3)
- Shock capturing finite difference numerical operator
- Two-phase, equilibrium/frozen, boundary layer analysis
- Variable oxidizer-to-fuel ratio transonic solution
- Improved two-phase transonic solution
- Two-phase real gas semi-empirical nozzle boundary layer expansion
- Continuum limit criteria
- Sudden freeze free molecular calculation beyond the continuum limit
- Interface between the Lockheed Plume Impingement Program (PLIMP) Ref. 4.

Most of the above capabilities already existed in other computer codes. These codes were incorporated into the RAMP code to enhance its usefulness. The emphasis of this effort was to improve the capability of the program to treat phenomena which significantly affect high altitude plumes.

The contents of this volume along with the other two volumes (Refs. 4 and 5) are designed to enable the user to easily, efficiently, and accurately apply the RAMP2 codes to calculate rocket exhaust nozzle and plume flow fields to solve practical engineering design problems.

RAMP2 consists of three basic computational modules: the TRAN72 program for generating equilibrium thermodynamic and transport data, the RAMP2F code for solving the flow field, and the BLIMPJ code used to calculate the nozzle boundary layer. Because of computer storage limitations the three programs must be executed separately; however, communication between the programs has been provided via temporary files so that, except for separate executions, they can be considered as one program.

Detailed descriptions of the TRAN72 (Ref. 6) and BLIMPJ (Ref. 7) have not been included, although Volume II contains a brief description of the subroutines of each of the codes. Section 4 of Volume III contains information on how to use and input the TRAN72 code, and Section 5 contains a brief discussion of the BLIMPJ code. Complete descriptions of the two codes are available in Refs. 6 and 7.

Solid propellant motors are frequently utilized to provide launch vehicle boost and stage separation. Most solid rocket motor propellants contain metal additives which increase the energy content of the system and suppress combustion pressure instabilities. The presence of metal additives results in condensed products in the nozzle-exhaust flow fields. This can create a number of adverse effects.

Condensed products (i.e., particulate aluminum oxide, etc.) being inert can do no expansion work. Consequently the particles are accelerated through the flow field via drag exerted on the gas by the viscous shearing action between the gas and particulate phases. Since the particles do no expansion work, the gas phase cools more rapidly than the particles. The particles at any given location are thus at a higher temperature than the gas so that heat is thus transferred from the particles to the gas by conduction and radiation. The net result is that the gas phase expends useful work in accelerating the particles while acquiring heat from the particles. This is an irreversible, non-adiabatic process in the gas phase expansion.

Exhaust plumes create hostile environments to surfaces immersed in the flow. These are in the form of structural loads, contamination, and heating. Heating results from both gas and condensates impinging on the surfaces. Particulates in the flow can also cause surface erosion and other structural damage.

Exhaust plume applications and plume impingement problems typically occur during launch, staging, and rendezvous. The current Space Shuttle design offers several illustrations of areas where exhaust plume flowfield properties and flow structure must be known. This is schematically illustrated in Fig. 1-1 which indicates potential plume related problems from solid rocket motors. During the Space Shuttle launch the solid rocket booster motor exhaust plumes impinge on the launch stand hardware. While the launch vehicle is in the vicinity of the launch pad, reradiation from the launch pad to the Orbiter is a potential problem. The solid rocket motor exhaust plume affects the Shuttle base drag and aerodynamics during the boost phase. The solid rocket separation motors mounted on the booster motor's forward and aft ends that are used to effect stage separation can potentially subject the Orbiter and external hydrogen/oxygen tank to a rather severe environment.

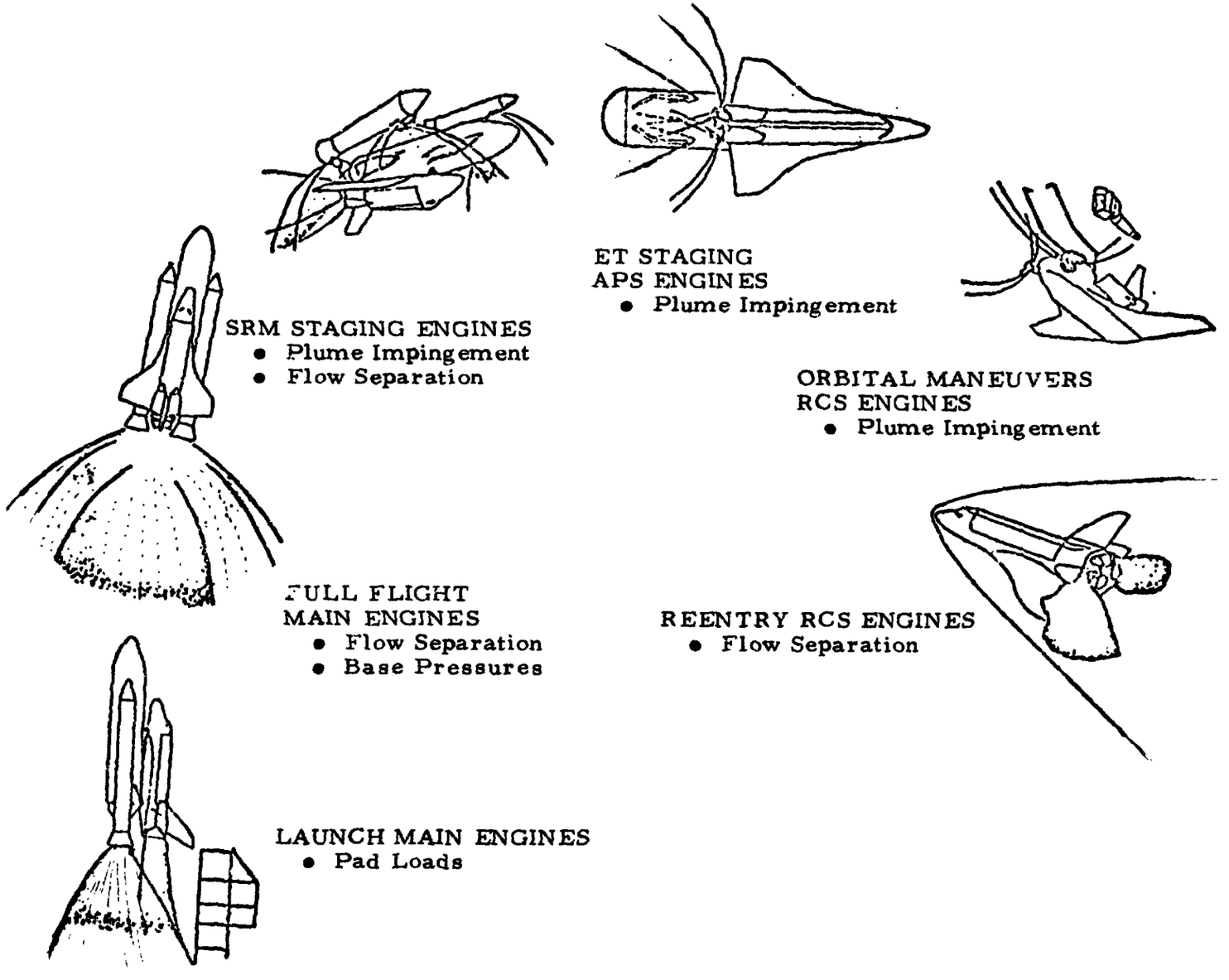

Fig. 1-1 - Mission Profile Illustrating Rocket Plumes Associated with Various Shuttle Operations

Exhaust impingement applications require a detailed definition of the gaseous plume structure as well as particle trajectories and dynamic properties. Plume simulation studies require that plume shapes be known. The exit plane pressure must be known along with the gas thermodynamics. To adequately describe the flowfield properties, the mutual effect of gas on particle and particle on gas must be calculated. Also "real gas" effects can be significant and should be included in the gasdynaic considerations.

Solutions for the supersonic flow of a gas-particle mixture follow one of two approaches: (a) a fully coupled solution in which momentum and energy are exchanged between the gas and particle phases (Refs. 8, 9, and 10), and (b) an uncoupled solution (Ref. 11) in which particle trajectories are traced through nozzle-exhaust plume flows. The uncoupled solution considers "real gas" effects; however, it treats only gas effects on the particle and is more applicable for low aluminum content propellants. The coupled solutions are primarily performance oriented. These solutions readily permit treatment of highly aluminized propellants but are restructured to constant thermodynamic properties. The performance code developed by Kliegel (Ref. 10) was subsequently utilized to trace liquid droplets in predicting contamination to surfaces (Ref. 12).

Applications discussed previously require a knowledge of the flowfield structure. Previous studies (Refs. 13, 14, and 15) indicated the need to include the treatment of "real gas" effects in nozzle-plume calculations. The decision was subsequently made to extend the coupled gas-particle solution (Refs. 8 and 9) to include the treatment of gas thermochemistry (chemical equilibrium and chemical kinetics). The choice of computation scheme and computer code becomes more obvious after examination of anticipated applications.

The metnod-of-characteristics has proven to be a reliable numerical solution for nozzle-plume applications (Ref. 16). Existing gas-particle performance codes utilize the method of characteristics which indicated that an operational nozzle-exhaust plume code could be obtained with a minimum of numerical solution development. The gas-particle capability has been incorporated into a streamline-normal code (Ref. 17) which utilizes the method of characteristics to solve for local flow properties. There are several reasons for choosing this approach:

- Numerical difficulties encountered in highly expanded flow are circumvented.
- The streamline-normal technique has a built-in mechanism for tracing particle streamlines.
- Transition flow between the continuum and free molecular flow regime is more readily treated.

The code, in its present form, will handle the flow problems which exhibit or have any of the following characteristics:

- Supersonic Inviscid Flow
- Highly Underexpanded Nozzles
- Highly Overexpanded Nozzles
- Shock Waves
- Sliplines
- Solid Walls
- Pressure Boundary
- Nonequilibrium Chemistry (Finite Rate)
- Equilibrium Chemistry
- Ideal Chemistry
- Free Molecular Flow
- Two-Phase Flow
- Oxidizer-to-Fuel (O/F) Ratio Gradients
- Nozzle Boundary Layer.

This report summarizes the improvements which were made under this contract to increase the capability of the RAMP program. In addition, this report presents a detailed development of the equations governing the supersonic flow of a chemically reacting gas-particle mixture. Development of the governing relations follows to a large extent the work of Kliegel. Basic assumptions are stated and the set of partial differential equations describing the gas-particle system are developed. These relations are then cast in "characteristic" form and the corresponding difference equations written. Details of the numerical solution are described for the various data point types. The presentation is then concluded with a description of the numerical integration of the conservation equations.

In addition to a description of the above analysis techniques, appendixes are included which discuss: (1) particle drag and heat transfer coefficients; (2) non-isoenergetic gas-phase flow treatment; (3) chemical equilibrium calculations in gas-particle flows; (4) non-continuum flow expansions; and (5) integration of the finite-rate chemical kinetic equations.

2. SUMMARY OF STUDY PERFORMED FOR CONTRACT NAS9-16256

A precise knowledge of local flow properties in nozzles and exhaust plumes is necessary for performance, radiation, attenuation, heat transfer and impingement analyses. The reacting and multiphase (RAMP) computer program is designed to give detailed flowfield information in the supersonic region of a reacting multi-phase, two-dimensional or axisymmetric flow field. The boundaries of the flow field may be solid such as in a nozzle or "free" such as in a plume. The analysis may be utilized therefore to predict performances as well as plume characteristics of a given engine system. A printed record of the program results is given for user inspection while a binary tape is provided for subsequent manipulation by other analyses.

The flow of a gas-particle mixture is described by the equations for conservation of mass, conservation of momentum, and conservation of energy. In the gaseous phase the state variables P, ρ, R and T are related by the equation of state while for the particulate phase the equations are for the particle drag, particle heat balance and the particle equation of state. Development of these equations is based on the following assumptions:

1. The particles are spherical in shape.
2. The particle internal temperature is uniform.
3. The gas and particles exchange thermal energy by convection and radiation (optional).
4. The gas obeys the perfect gas law and is either frozen and/or in chemical equilibrium, or is in chemical non-equilibrium.
5. The pressure of the gas and the drag of the particles contribute to the force acting on the control volume.

6. The gas is inviscid except for the drag it exerts on the particles.

7. There are no particle interactions.

8. The volume occupied by the particles is negligible.

9. There is no mass exchange between the phases.

10. A discrete number of particles, each of different size or chemical species is chosen to represent the actual continuous particle distribution.

11. The particles are inert.

The supersonic two-phase solution accepts the starting line provided by the internally calculated transonic solution as well as other pertinent data supplied through the read function. The equations of motion under the assumptions just listed are hyperbolic and permit the use of a forward marching scheme; a streamline/normal grid structure is employed where the step lengths in the axial and radial directions are under program control. Both BCD (printer) and unformatted binary output tapes are produced. A Prandtl-Meyer expansion of the gas phase and a free boundary calculation are employed to treat the plume flow solution. The run is terminated when pre-specified problem limits are reached.

The two-phase flow analysis will treat an extremely wide range of operating conditions. With few exceptions the limitations are imposed by the theory rather than numerical considerations. In this discussion dimension statement sizes which are arbitrarily set are not considered a limitation. The true limitations are:

- Supersonic regions influenced by embedded subsonic regions.
- Vacuum or limiting expansion limitation - a small region of the expansion fan for a vacuum expansion cannot be treated where the Mach number is so large that treatment by continuous flow assumptions becomes meaningless (this limitation is both numerical and theoretical).
- For two-phase flow the lower boundary can only be horizontal (i.e., nozzle centerline).

During the course of the study the following capabilities have been added to the code.

- Direct interface with JANNAF SPF code
- Shock capturing finite difference numerical operator
- Two-phase, equilibrium/frozen, boundary layer analysis
- Variable oxidizer-to-fuel ratio transonic solution
- Improved two-phase transonic solution
- Two-phase real gas semi-empirical nozzle boundary layer expansion
- Continuum limit criteria
- Sudden freeze free molecular calculation beyond the continuum limit.
- Interface with Plume Impingement models, and
- Documentation.

2.1 MODIFICATIONS TO THE RAMP CODE

This section deals with the modifications which were incorporated into the RAMP code under this contract.

2.1.1 JANNAF Standard Plume Flowfield (SPF) Code Interface

To perform a plume calculation, the SPF code (Ref. 3) requires nozzle exit properties as initial conditions. The RAMP code was modified to punch or put on tape exit plane data in the format that the SPF code uses. The code will punch data for both single and two-phase cases.

At present, the SPF code can accept a single chemical species distribution which must be applied at all points across the exit. The RAMP code can have a distribution of species, so it was necessary to mass flow average the

species distributions across the exit plane to produce a single set of species. This restriction can be easily removed whenever SPF has the capability to handle spatial variations in chemical species.

The code is set up to punch the species information for the various chemical systems that are available in the SPF code. The user must specify which system to punch. If the thermodynamic data are input to the RAMP code using cards then the species mole fractions that are to be punched for the SPF code must be input for the appropriate system in the same order as listed in Table 2-1. For finite rate cases these species are determined inside the code and need not be input. The user may also input another system. Additionally, ideal gas cases can also be handled.

Table 2-1

SPF CHEMICAL SYSTEMS

System 1 – Hydrogen/Oxygen

$H, H_2, H_2O, N_2, O, OH, O_2$

System 2 – Carbon/Hydrogen/Oxygen

$CO, CO_2, H, H_2, H_2O, N_2, O, OH, O_2$

System 3 – Carbon/Hydrogen/Oxygen/Chlorine

$A\ell_2O_3(S), CO, CO_2, C\ell, C\ell_2, H, H_2, H_2O, HC\ell, N_2, O, OH, O_2$

System 4 – Carbon/Hydrogen/Oxygen/Chlorine/Fluorine

$CO, CO_2, C\ell, C\ell_2, F, F_2, H, H_2, H_2O, HC\ell, HF, N_2, O, OH, O_2$

System 5 – Hydrogen/Oxygen/Boron

$BO, BO_2, B_2O_3, H, H_2, H_2O, HBO_2, N_2, O, OH, O_2$

System 6 – Hydrogen/Oxygen/Boron/Chlorine/Fluorine

$BF, BF_2, BF_3, BO, BOC\ell, BOF, BO_2, B_2O_3, CO, CO_2, C\ell, C\ell_2$
$F, F_2, H, H_2, H_2O, HBO_2, HC\ell, HF, N_2, O, OH, O_2$

2.1.2 Shock Capturing Finite Difference Operator

The original RAMP code has the logic for computing any number of right or left-running shocks using shock fitting techniques. This logic was partially checked out under previous efforts. It is desirable to have the capability to treat shocks that can occur in some nozzles. Shock capturing schemes require no special equations or program logic and are reliable. For most nozzle flows, existing shock capturing techniques are sufficiently powerful to treat the shocks. Additionally, in order to directly interface with the SPF code, it would be desirable to use a shock capturing numerical operator.

For the above reasons a shock capturing algorithm was added to the code. The methodology, equations and grid system which was incorporated into the code is identical to the SPF code (Ref. 3). To obtain more information on the scheme the reader is referred to Ref. 3.

For the shock capturing option, the computational grid is composed of vertical lines and a radial coordinate system normalized by the local wall coordinate. This approach as taken to alleviate the problem of inserting a point per line for a Cartesian system. The computational procedure is as follows: the forward marching algorithm is used to compute the flowfield properties at all interior points. Flowfield properties at the wall are obtained via the method-of-characteristics solution. Once the wall has been computed, the coordinate system is transformed and the axis and interior points are solved.

To check out the validity of the shock capturing option, comparisons were made with known method-of-characteristics solutions. Figure 2-1 presents pressure distribution along a nozzle centerline and wall for various calculational techniques. As can be seen from the figure, the shock capturing solution is identical to the characteristics and SPF solutions.

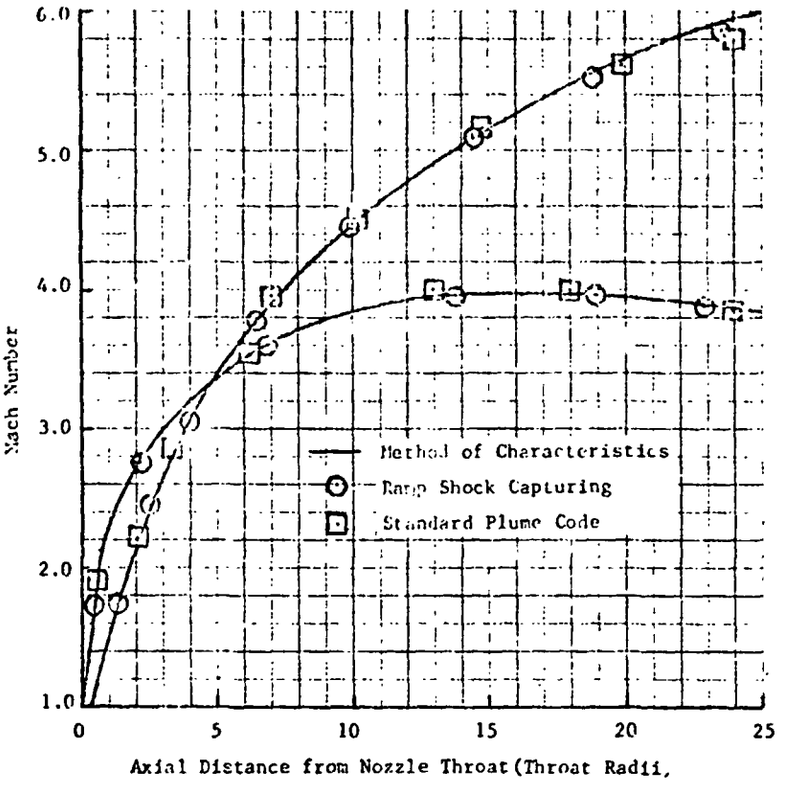

Fig. 2-1 Nozzle Wall and Centerline Mach Number Distributions Using Various Calculation Techniques

2.1.3 Two-Phase, Equilibrium/Frozen, Boundary Layer Analysis

Nozzle boundary layers are known to influence certain regions of nozzle flow and high altitude exhaust plumes (Refs. 18, 19 and 20). For nozzle designers, the nozzle boundary layer is important in determining the thermal loads to the nozzle, performance losses due to heat transfer and effects on the nozzle pressure distribution due to the displacement thickness effect on the inviscid flow structure. For spacecraft designers the nozzle boundary layer is important because of its effect on the exhaust plume. At high altitudes the nozzle boundary layer causes the plume to expand to large angles (approximately 180 deg). In these backflow regions, spacecraft and sensitive surfaces are subjected to unwanted contamination, forces, moments and heating rates. For some applications the radiative properties of the expanded boundary layer flow is importan . Thus, it is easy to see that for many applications the nozzle wall boundary layer is an important factor.

To date there have been numerous techniques used to account for boundary layer effects of the nozzle and exhaust plume flow fields. Lockheed-Huntsville has an option in the MOC and PIP code (Ref. 21, a version of RAMP) which superimposes a power law boundary layer profile based on a flat plate boundary layer thickness on the exit plane start line. The profile can contain a total temperature variation which has been found to be important (Ref. 21) in the back flow region of the plume. This is a very simplified approach and the method of determining the boundary layer thickness is very crude. Lockheed-Huntsville personnel and other investigators have used various boundary layer codes and the inviscid nozzle results to generate a better set of boundary layer properties which were then superimposed on the nozzle exit plane inviscid results. Next, some investigators have gone a step further and iteratively solved the inviscid nozzle and boundary layer to determine the effect of the boundary layer on the nozzle flow field. Finally, it is possible to do a fully viscous nozzle solution with a method such as Lockheed-Huntsville's GIM code (Ref. 22). However, a fully viscous nozzle solution is beyond the scope of this effort. It should

be noted that all techniques except the first require a tremendous amount of effort and hand calculations to finally obtain a plume solution. The purpose of this task was to automate the boundary layer nozzle solution to arrive at an exit plane start line which includes all the effects mentioned above.

The BLIMPJ boundary layer code (Ref. 7) was chosen for the solution of the nozzle wall boundary layer. BLIMPJ is a JANNAF standard boundary layer code for determining boundary layer effects on the performance of a rocket engine. The BLIMPJ code is set up to handle nozzle flows, equilibrium or frozen chemistry, uses the JANNAF standard thermochemistry curve fits and has numerous ways of treating the nozzle wall that allow it to treat liquid engines as well as solid motors with and without ablative walls. At present, the interface between RAMP and BLIMPJ allows only the following wall options: adiabatic wall, steady state energy balance or a specified temperature distribution. The adiabatic wall option is the default option in the code. The remaining wall options in the BLIMPJ code could be used with a few modifications to the RAMP code. In addition to wall boundary condition options, the user may also select laminar, turbulent, frozen, or equilibrium flows or let the code default to turbulent, equilibrium. If the turbulent boundary layer option is used, the flow will transition to a turbulent profile when the Reynolds number based on momentum thickness exceeds 250.

All input data for the boundary layer solution are generated inside the RAMP code except the nozzle wall temperature distribution, if that option is specified. Chemical species must be input if the thermochemistry data for the inviscid solution was input via cards.

The BLIMPJ code was too large for conversion to a module for the RAMP code, so if it is desired to generate a nozzle boundary layer and obtain a viscous exit plane start line it is first necessary to run the RAMP code to calculate the inviscid nozzle solution. The RAMP code generates a file with the BLIMPJ input data on it. The BLIMPJ code is then executed (no data

cards). The BLIMPJ results are printed out and stored on a file for subsequent use by the RAMP code. The RAMP code is then reexecuted with just a single input card and an exit plane vertical or normal start line is generated. The exit plane start line has the results of the inviscid nozzle and boundary layer solutions merged. This capability is a considerable improvement over previous methods which required many hand calculations, cross plotting, etc.

For most rocket motors the boundary layer is fairly thin (approximately 5 to 10% of exit diameter) and the resultant effect on inviscid flow properties is minimal. For these cases one pass through the inviscid nozzle solution and boundary layer calculation is adequate. The boundary layer results will then be superimposed on the inviscid nozzle solution and an exit plane start line with boundary layer effects will be generated which can be used to perform a plume expansion.

Some low pressure or low thrust motors have boundary layers which contain a significant portion of the total mass flow of the system. In these cases the entire solution should be iterated for by making two passes through the inviscid nozzle and boundary layer calculations. After the initial nozzle and boundary layer solution has been completed, the nozzle solutions will be calculated with the actual wall contour adjusted by the local displacement thickness which was determined from the boundary layer calculation. The boundary layer solution will then be rerun using the new edge conditions from the second nozzle calculation. The results will then be superimposed on the original nozzle contour and second flowfield solution and an exit startline will be output or saved. This capability is not presently operational. However, for these cases the boundary layer solution is solved a second time with new edge conditions taken from the inviscid results at the edge of the first BLIMPJ boundary layer. Thus, the inviscid and viscous results match very well at the boundary layer edge. This option is controlled internal to the program and requires no user interface.

2.1.4 Particle Tracing Through Boundary Layer

Any particulate matter (Al_2O_3-solids or unburned propellant droplets in liquid motors) which might enter the nozzle wall boundary layer could be influenced by the boundary layer to be expanded into the backflow region. Thus, there may be certain motor/nozzle configurations in which it is necessary to track particles through the boundary layer in order to obtain the most accurate representation of the nozzle flow properties at the exit plane.

Lockheed-Huntsville added a particle streamline tracing module to the nozzle code. The code which was used as the basic building block or this module was used in predicting the IUS, SSUS particle distributions published in Ref. 23. This code uses initial particle properties (velocity, flow angle, temperature and density) and traces the particles through a known flow field. This option is user-selectable. The basic method used is shown in Fig. 2-2.

After the inviscid nozzle solution and boundary layer solutions have been completed, the RAMP code is re-executed and logic is handed off to the particle trajectory tracing module. The first step is to search the boundary layer edge location in the inviscid nozzle solution to determine if any particles are found to penetrate the boundary layer. Then for each particular size group which has been found to penetrate the boundary layer a distribution of individual particle properties will be determined (interpolated off nozzle solution tape) at several stations along the boundary layer edge. This will be done for each size group. Next a map of the boundary layer properties will be generated using the boundary layer data tape. Finally, each particle streamline will be traced through this mapped flow field and particle properties will be determined at the previously determined exit plane. The effect of the particles on the boundary layer flow properties due to energy and momentum interchange are not considered.

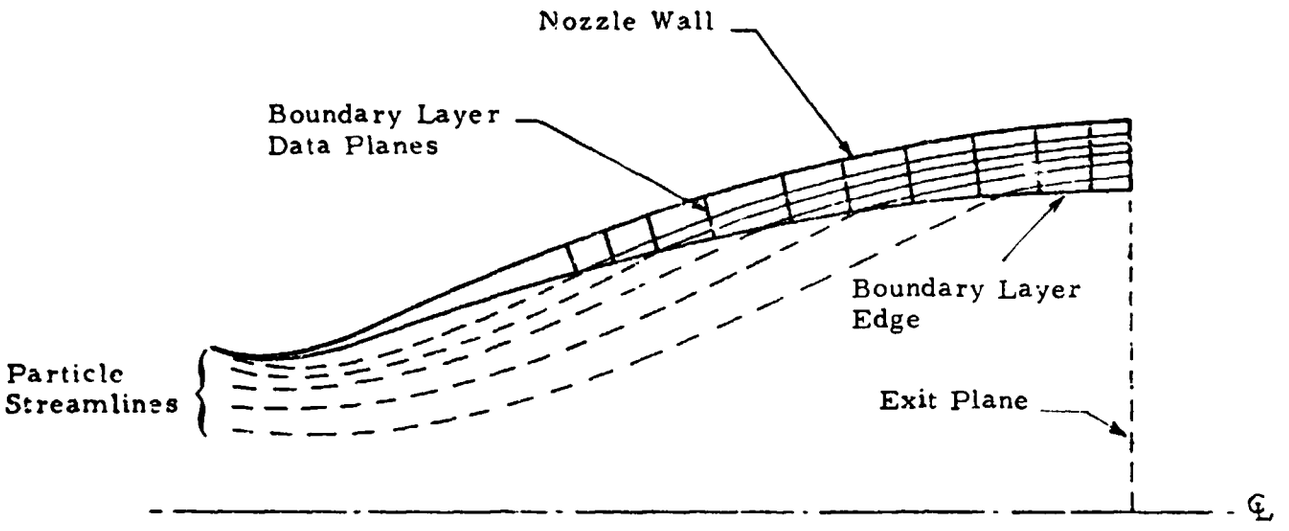

Fig. 2-2 Schematic of Particle Trajectory Tracing Method to be Used in the Inviscid Nozzle Code

Finally, the boundary layer results, the inviscid nozzle solution and the particle properties in the boundary layer are merged and an exit plane start line for a RAMP restart or SPF run will be generated.

Several cases have been executed using the particle trajectory option. Figure 2-3 presents some results of the Large Boeing IUS motor calculations which illustrate the effect the boundary layer can have on the particle properties. The axial distribution of a particle limiting streamline temperature and velocity are shown for both the inviscid and viscous calculations.

2.1.5 Boundary Layer Expansion at Lip

Another required capability of the nozzle code is a fully automated technique to expand the boundary layer at the lip. After an exit plane start line has been generated it is very straightforward to use the Prandtl-Meyer relationship to expand the flow. The key point here is to get a fully supersonic start line. Numerous investigators have made various assumptions to obtain start lines for plume solutions that account for the nozzle wall boundary layer. The various techniques will be discussed briefly.

Perhaps the most simple method of obtaining a supersonic start line is to discard the subsonic portion of the boundary layer (Refs. 18 and 24) and adjust the spatial distribution of boundary layer points up to the lip. This method throws mass away from the system and will affect the results in the backflow region. For nozzles which have thin turbulent boundary layers, these effects are probably minimal. For very viscous nozzles (low pressure) or laminar boundary layers the effects of this assumption could severely compromise the plume results in the backflow region (greater than 90 deg). It should be noted that this technique could consider total temperature variations through the boundary layer.

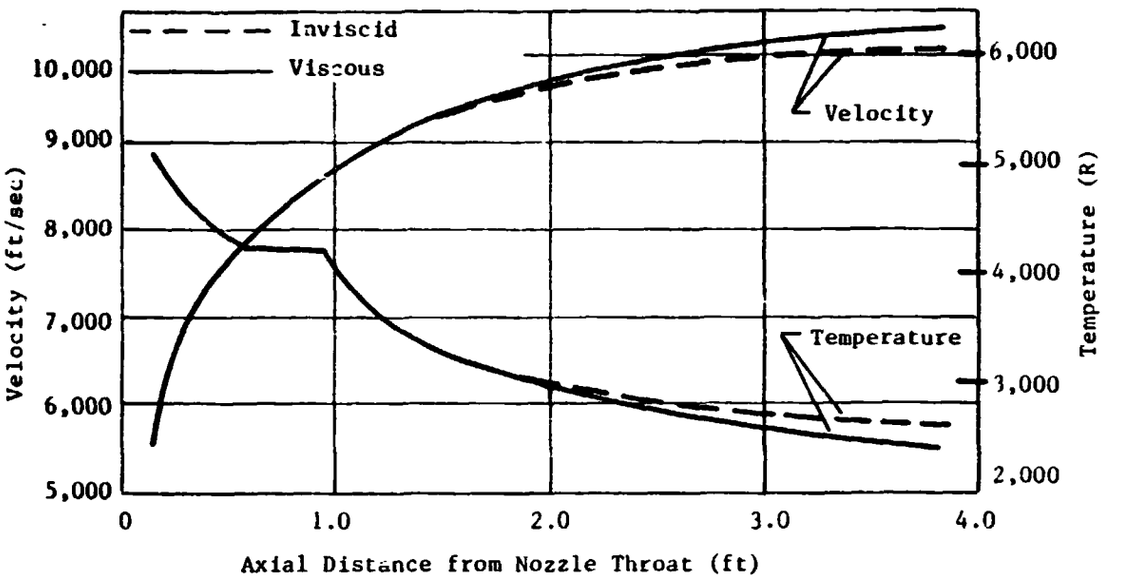

Fig. 2-3 Large Boeing Motor 0.5 micron Radius Particle Limiting Streamline Temperature and Velocity Distributions for Calculations With and Without the Nozzle Boundary Layer

Seubold (Ref. 25) used the technique of replacing the subsonic portion of the boundary layer with mass average properties at a slightly supersonic value. This resulted in a layer of constant properties near the wall. The resultant plume flow had the correct mass flow but did not consider the total temperature variations.

The first two techniques assumed that the static pressure through the boundary layer is constant. Near the lip, however, the subsonic portion of the boundary layer is influenced by the expansion process (Refs. 26, 27, and 28) as shown in Fig. 2-4. For highly underexpanded flows the sonic line has been found to attach to the lip (Ref. 26) so that the flow at the wall must rapidly accelerate when it gets near the lip and the static pressure rapidly decreases. For overexpanded flows the subsonic flow merely stays subsonic as it negotiates the lip so that downstream flow conditions can feed back up into the boundary layer.

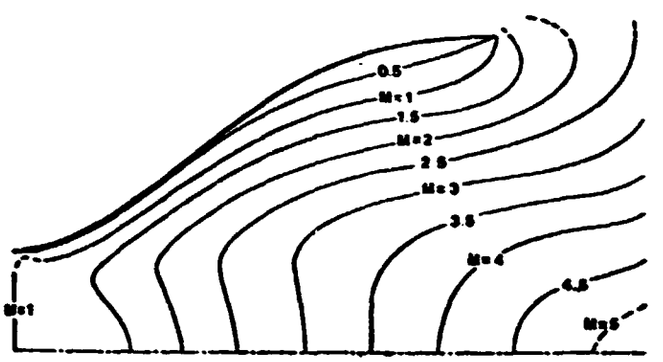

Fig. 2-4 Mach Number Contours for an Underexpanded Axially Symmetric Nozzle (Case 6)

Cooper (Ref. 29) went a little further than the first two approaches as far as treatment of the subsonic flow expanding to the sonic lip conditions. He assumed that the flow (M=0 at wall) just upstream of the lip expanded to M=1 at the lip. Since the static pressure upstream of the lip at the wall was the same as the wall total pressure and the freestream static pressure, the only way for M=1 to be reached at the lip was for the wall static pressure to drop. Therefore, there will be a static pressure distribution across the flow at the lip. It was then assumed that the static pressure at a specified point in the boundary layer is not affected by the expansion and the pressure distribution is faired into the known lip conditions. This method is not totally rigorous but does include boundary layer effects and has been shown to result in good comparisons with some experimental data in the backflow region.

Finally, there are exact solutions to the corner flow problem. Bird (Ref. 26) uses a direct simulation Monte Carlo method. He set his model up so that it would compute the entire nozzle or the region near the throat. He predicts the attachment of the sonic line for underexpanded nozzles. Baum (Ref. 28) uses a finite difference method along with boundary layer equations to describe the subsonic portion of the boundary layer. His application was for base flow about blunt bodies and compares well with data. Finally, the previously mentioned GIM code can be used to exactly solve the corner problem. All three of these methods are very complex and are outside the scope of this effort.

In the present version of the code the method of Seubold was incorporated. Total temperature variations are included and the mass flow in the boundary layer is conserved. Plume calculations using this method were made for a 5 lbf bipropellant motor. The mass flux predictions as shown in Fig. 2-5 compare very well with experimental data.

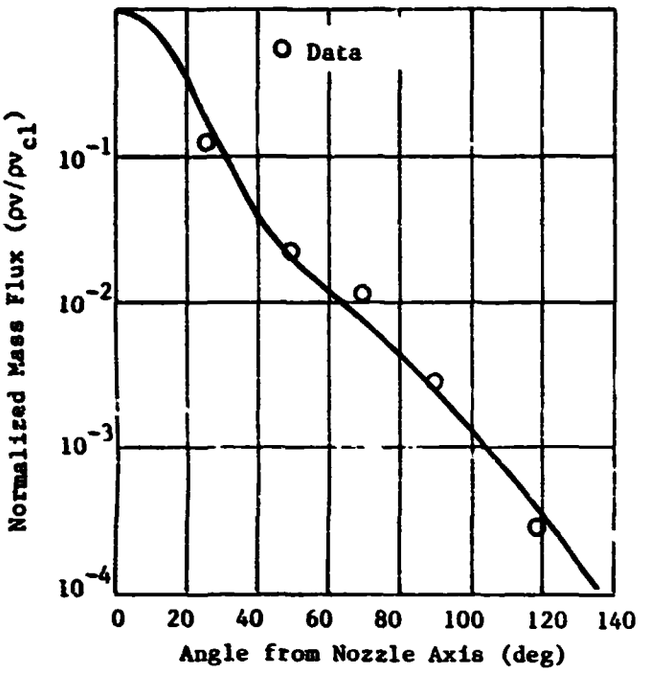

Fig. 2-5 Mass Flux Normalized by Centerline Mass Flux vs Angle from Plume Centerline for 5 lbf Bipropellant Motor

2.1.6 Variable Oxidizer-to-Fuel Ratio Transonic Solution

Solution of the subsonic-transonic region of a liquid rocket engine can vary in complexity from a simple one-dimensional variable O/F streamtube analysis (Ref. 30) to the most detailed model such as that of the Distributed Energy Release (DER, Ref. 31) model. The streamtube analysis performs a multizone one-dimensional calculation to the sonic point given a known O/F distribution just downstream of the injection face. The DER program is a complex model which is initiated upstream of the injector face and continues the solution up through the sonic line. The DER code was used to initiate nozzle solutions in Ref. 32 but is not particularly easy to use and input and requires a good bit of user experience to successfully execute. For

these reasons it is not utilized in the nozzle code. On the other hand, a one-dimensional streamtube analysis does not account for two-dimensional effects. A time-dependent scheme (Ref. 33) is a compromise between these two schemes. The approach includes the radial momentum equation which results in a set of mixed partial differential equations. The solution procedure is an unsteady time-dependent finite difference technique with equilibrium chemistry. This technique has both the equilibrium and variable O/F chemistry option and has been utilized (Refs. 34 and 35) previously with excellent results. This code has been incorporated into the RAMP code as a module and has been executed for all combinations of ideal and equilibrium chemistry, constant and variable O/F distributions. Additional inputs required by this module are: (1) combustion chamber geometry down to the throat; (2) average O/F ratio; (3) location of the initial data surface to start the transonic solution; (4) location of the nozzle throat, and; (5) the O/F distribution at the initial data surface.

Figure 2-6 presents some results of the variable O/F calculations for the Space Shuttle Reaction Control System engine. Exit plane distributions

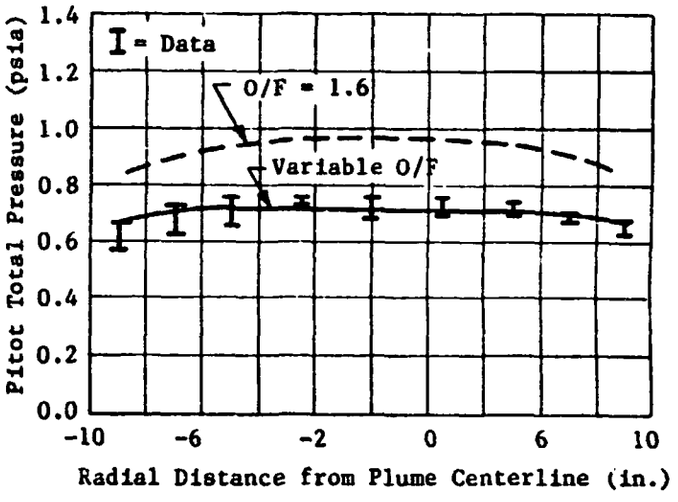

Fig. 2-6 Comparison of RAMP Calculation for Space Shuttle RCS Motor Plume with Pitot Pressure Survey Taken at 45 in. from Nozzle Exit Plane

of pressure and temperature are presented for both constant and variable O/F assumptions. The constant O/F calculation was performed assuming Mach 1.05 at the throat. The variable O/F calculation was initiated upstream of the nozzle throat at the point where the nozzle begins to contract. The O/F distribution at this location was inferred from the injector pattern and incoming mass flow distribution.

2.1.7 Improved Two-Phase Transonic Solution

The original transonic module which was incorporated into the RAMP code could handle throat radii of curvature to throat radius ratios above 1.5. Many solid motors have radii of curvature ratios smaller than 1. To alleviate this limitation the improved approximate transonic module was taken from the new Standard Performance Prediction program (SPP, Ref. 36) and put into the RAMP code.

Many transonic solutions using this module have been run for varying upstream and downstream radii of curvature ratios.

2.1.8 Continuum Limit Criteria

There have been numerous studies over the past several years concerning methods of determining where continuum flow breaks down and free molecular flow begins. Examples of these criteria are the Knudsen number criteria, criteria based on Mach and Reynolds number, and the "breakdown parameter" as proposed by G.A. Bird (Ref. 37).

The present version of the program uses an average Knudsen number to check for transition from continuum to "free molecular" flow regimes where the average Knudsen number between the old streamline base point is calculated via the following equation:

$$Kn = .788539\ (\bar{M}^2/\bar{R}_E) \left| \ln T_1 - \ln T_2 \right| /dS$$

where the properties are averaged between the old (1) and new (2) streamline points. The flow regime is determined by checking the calculated Knudsen number against the input Knudsen number for criteria translational freezing. Once the flow regime has been determined the appropriate specific heat ratio (gamma) and total conditions are calculated. A Knudsen number of 10 is standardly used to check for transition.

The criteria of Bird (Ref. 37) have also been included in the program. The Bird criteria specifies where the continuous flow equations start to break down. This is not necessarily the location in the flow where the flow goes free molecular.

Bird's breakdown criteria

$$P = \frac{q}{v} \frac{d\rho}{ds}$$

is calculated at each point on the normal. If the breakdown parameter of 0.05 is exceeded, the code points out the location on the normal where P = 0.05. The collision frequency v is calculated using the hard sphere relationship:

$$v = \frac{5}{4} \frac{\rho RT}{\mu}$$

The code does keep track of the continuum "breakdown criteria" and locates the surface in the plume where the "breakdown criterion" of 0.05 is located. In the future the appropriate data at this surface will be stored so that this information may be passed along to a full Monte Carlo solution. An example of the application of the Knudsen number and Bird breakdown criteria is shown in Fig. 2-7.

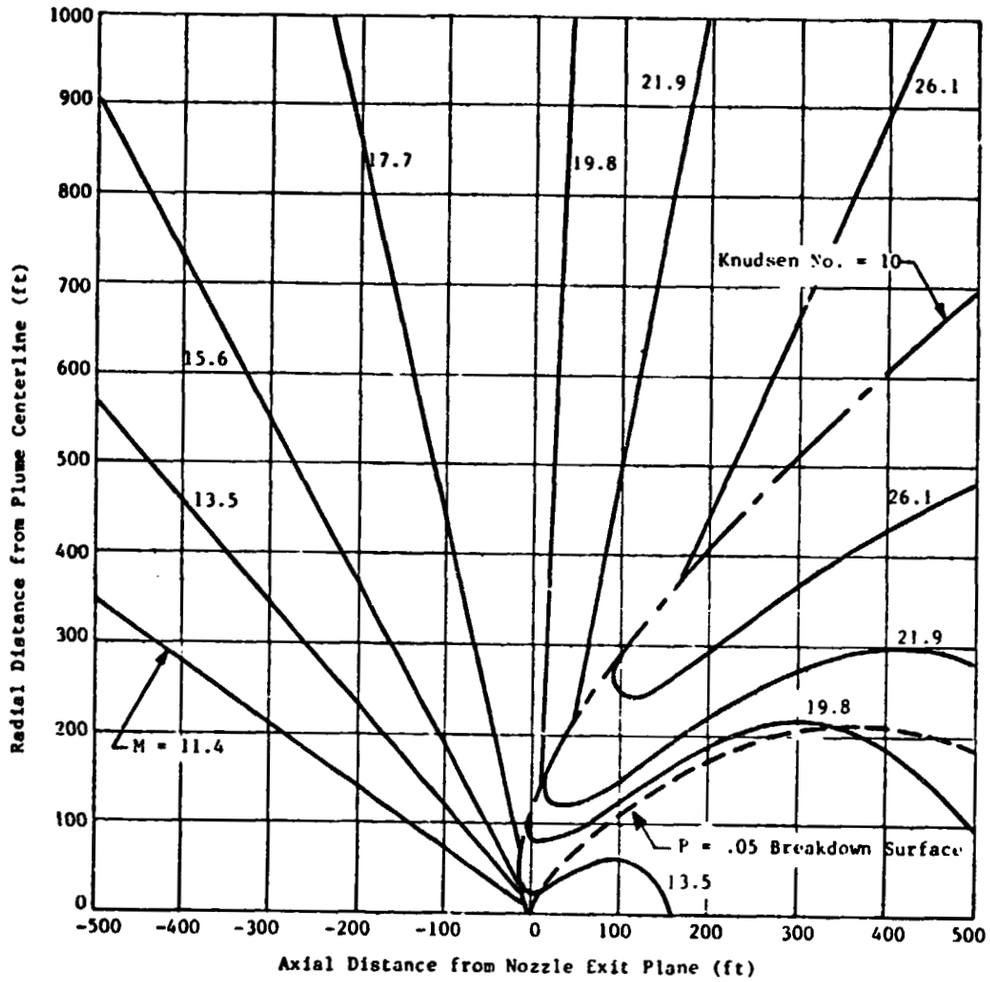

Fig. 2-7 Large Boeing Motor Exhaust Plume Mach Number Contours

The Interim Upper Stage (IUS) is used to boost payloads from near earth orbit to higher orbits. This stage uses solid rocket motors as propulsion. From a payload and stage design standpoint it is necessary to define the exhaust plume. The RAMP code is especially suited to calculating the IUS exhaust plume including all the driving phenomena: equilibrium/frozen thermochemistry with total enthalpy variations, two-phase flow, nozzle wall boundary layer, and free molecular flow. Figure 2-7 presents contour plots for Mach number in the exhaust plume. Shown on this figure is the Knudsen number of 10 and the continuum breakdown surface corresponding to the Bird breakdown criteria of 0.05. Beyond the Knudsen number 10 contour the flow was treated as free molecular.

2.1.9 Free Molecular Flow Option

A "sudden freeze" free molecular flow option has been incorporated into the code. Once the specified Knudsen number criteria have been exceeded the flow is frozen. (Specific heat ratio, molecular weight, velocity and temperature along a gas streamline is held constant.) At this point the streamline is assumed to expand at a constant flow angle and the density varies according to the streamtube area. This option allows the calculations to be performed in the backflow region (>90 deg) of the plume. Numerous cases have been run for several hundred nozzle exit diameters.

2.1.10 Interface with Plume Impingement Model

Specification of the amount and type of plume exhaust products at a surface immersed in a rocket plume is important for determination of spacecraft surface degradation. After an adequate representation of the characteristics of the exhaust plume has been performed it is necessary to relate the spatial characteristics of the plume to a surface that is immersed in the plume.

Under previous studies, Lockheed-Huntsville developed the Lockheed Plume Impingement code (Ref. 38). This program will provide forces, moments and heating rates to bodies immersed in the exhaust plume generated by the Lockheed Method-of-Characteristics Program (Ref. 16).

The Plume Impingement Program (PLIMP) has been modified so that it can use the results of the RAMP2 code to predict forces, moments and heating rates due to plume impingement. Additionally, the PLIMP code has been modified to determine the types and amounts of plume species at any given location of a body immersed in the exhaust plume. This version of the PLIMP program is available with RAMP2.

3. FUNDAMENTAL EQUATIONS FOR STEADY FLOW OF REACTING GAS-PARTICLE MIXTURES

3.1 BASIC ASSUMPTIONS FOR THE GOVERNING EQUATIONS

The flow of a gas-particle mixture is described by the equations for conservation of mass, conservation of momentum and conservation of energy. In the gaseous phase the state variables, P, ρ, R and T are related by the equation of state while for the particulate phase the equations are for the particle drag, particle heat balance and the particle equation of state. Development of these equations is based on the following assumptions:

1. The particles are spherical in shape.
2. The particle internal temperature is uniform.
3. The gas and particles exchange thermal energy by convection and radiation (optional).
4. The gas obeys the perfect gas law and is either frozen and/or in chemical equilibrium, or is in chemical nonequilibrium.
5. The forces acting on the control volume are the pressure of the gas and the drag of the particles.
6. The gas is inviscid except for the drag it exerts on the particles.
7. There are no particle interactions.
8. The volume occupied by the particles is negligible.
9. There is no mass exchange between the phases.
10. A discrete number of particles, each of different size or chemical species, is chosen to represent the actual continuous particle distribution.
11. The particles are inert.

These are basically the same as originally stated by Kliegel except for the provision to: (a) calculate the radiation exchange between the gas and particle phase (assumption 3); (b) the gas phase can be either frozen, in chemical

equilibrium, or chemical non-equilibrium (assumption 4). The total mass and energy of the gas-particle system are not constant since provisions are made for particle streamlines to penetrate the exhaust plume boundary.

3.2 GOVERNING EQUATIONS FOR THE GAS-PARTICLE MIXTURES

3.2.1 Continuity Equation

The various forms of the continuity equation for chemically reacting gas-particle mixtures are derived in this section. The forms of the equation derived, in order are:

1. Species Continuity Equation	(3.6)
2. Global Continuity Equation/(Steady State)	(3.13)/(3.27)
3. Gas Continuity Equation	(3.19)
4. Particle Continuity Equation	(3.20)
5. Species Continuity Equations as a Function of Mass Fraction/(Steady State)	(3.25)/(3.29)
6. Particle Continuity Equation for Each Particle species j/(Steady State)	(3.26)/(3.28)

Consider a chemically reacting gas-particle mixture flowing through some arbitrary stationary control volume, v, (Fig. 3-1)bounded by the control surface, S.

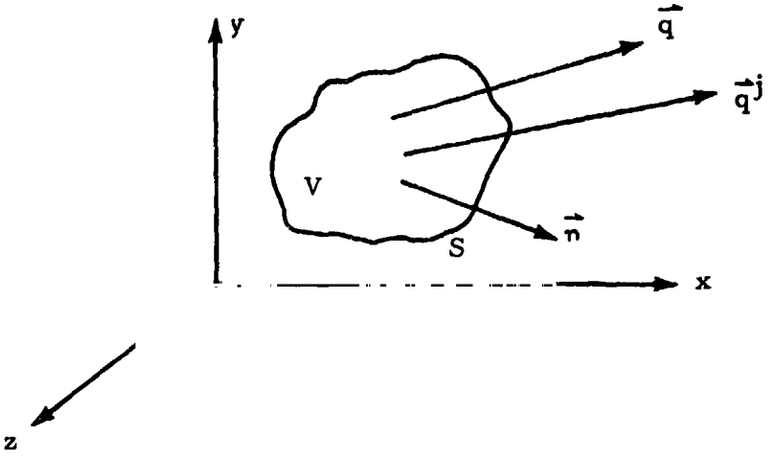

Fig. 3-1 - Control Volume for the System of Equations

For such a flow system, Reynold's Transport theorem states that:

$$\frac{D}{Dt}\int_V A\,dv = \int_V \frac{\partial A}{\partial t}\,dV + \int_S A\,\vec{q}\cdot\vec{n}\,dS; \qquad (3.1)$$

where A = any arbitrary parameter.

Applying the Gauss, or Divergence theorem

$$\int_S \vec{B}\cdot\vec{n}\,dS = \int_V \nabla\cdot\vec{B}\,dV\ ; \qquad (3.2)$$

where B = any arbitrary vector quantity

to Eq. (3.1) yields:

$$\frac{D}{Dt}\int_V A\,dV = \int_V \frac{\partial A}{\partial t}\,dV + \int_V \nabla\cdot A\vec{q}\,dV\ . \qquad (3.3)$$

Furthermore, the substantial or Euler's derivative may be written in the form:

$$\frac{DA}{Dt} = \frac{\partial A}{\partial t} + \vec{q}\cdot\nabla A\ . \qquad (3.4)$$

In a flow system of gas-particle mixtures in which chemical reactions take place, the principle of conservation of mass of each chemical species may be written as:

$$\frac{D}{Dt}\int_V \rho_i\,dV - \int_V \dot{w}_i\,dV = 0 \qquad i = 1, NS; \qquad (3.5)$$

where $\dot{w}_i$ = production rate of species i due to either internal or external sources such as chemical reactions and mass additions.

Applying Eq. (3.3) to the first term of Eq. (3.5)

$$\frac{D}{Dt}\int_V \rho_i\,dV = \int_V \frac{\partial \rho_i}{\partial t}\,dV + \int_V \nabla\cdot\rho_i\,\vec{q}_i\,dV \qquad i = 1, NS\ ,$$

substituting the result back into Eq.(3.5)

$$\int_V \frac{\partial \rho_i}{\partial t}\, dV + \int_V \nabla \cdot \rho_i \vec{q}_i\, dV - \int_V \dot{w}_i\, dV = 0 \qquad i = 1, NS ,$$

and rearranging terms yields

$$\int_V \frac{\partial \rho_i}{\partial t}\, dV = - \int_V \nabla \cdot \rho_i \vec{q}\, dV + \int_V \dot{w}_i\, dV \qquad i = 1, NS .$$

The above equation simply states that, for species i, the mass rate of increase inside the control volume is equal to the net rate of mass flow into the control volume plus the rate of mass produced due to chemical reactions and mass addition. In the following, we shall, however, exclude mass addition from external sources.

Combining the integrands under one integral

$$\int_V \left(\frac{\partial \rho_i}{\partial t} + \nabla \cdot \rho_i \vec{q}_i - \dot{w}_i \right) dV = 0 \qquad i = 1, NS ,$$

and noting that the volume V under consideration is arbitrary; the only way for the above equation to be valid for all V is for the integrand to vanish. We therefore have

$$\frac{\partial \rho_i}{\partial t} + \nabla \cdot \rho_i \vec{q}_i - \dot{w}_i = 0 \qquad i = 1, NS . \tag{3.6}$$

Equation (3.6) is known as the species continuity equation. It is valid for each chemical species at each internal quantum state. We shall, however, assume that the various internal modes of motion are fully excited and are in equilibrium with each other. It is well known that this is approximately the case for the translational and rotational degrees of freedom where the equilibrium value is attained in a few collisions. In general, the vibrational degree of freedom approaches the equilibrium state somewhat more slowly,

except at very high temperatures. As chemical reactions usually occur at high temperatures, this approximation is often justified. The global continuity equation can now be derived by summing Eq.(3.6) for all species present.

$$\sum_{i=1}^{NS}\left(\frac{\partial \rho_i}{\partial t} + \nabla \cdot \rho_i \vec{q}_i - \dot{w}_i\right) = 0$$

or

$$\frac{\partial}{\partial t}\sum_{i=1}^{NS}\rho_i + \nabla \cdot \sum_{i=1}^{NS}\rho_i \vec{q}_i - \sum_{i=1}^{NS}\dot{w}_i = 0 \qquad (3.7)$$

To arrive at the final form of the global continuity equation, it is necessary to take a closer look at the flow system.

In the flow system analyzed, the time variation of the thermodynamic functions is slow compared to the longest relaxation time of the system. Therefore, the assumption that thermodynamic local equilibrium exists can be made. In such a system, the thermodynamic quantities for the nonequilibrium system are the same functions of the local state variables as the corresponding equilibrium thermodynamic quantities. Therefore, the partial specific quantity ϕ_i in an arbitrary volume element dV of a nonequilibrium system may be defined by the equilibrium relation

$$\overline{\phi}_i = \left(\frac{\partial \Phi}{\partial m_i}\right)_{T, P, m_i}$$

The quantities being held constant during the differentiation are the locally defined temperature T, pressure P, and the masses m_j of the other NS-1 species.

The specific quantity ϕ_m (Φ per unit mass) is given in terms of the partial specific quantities $\overline{\phi}_i$ by

$$\rho_m \phi_m = \sum_{i}^{NS}\rho_i \overline{\phi}_i \qquad i = 1, NS;$$

where the relationship between the mass density ρ_m of the mixture and the species density ρ_i is given by

$$\rho_m = \sum_{i=1}^{NS} \rho_i = \text{fluid density} \tag{3.8}$$

The specific velocity, $\vec{q}_m$, specific enthalpy, h_m, and specific internal energy, e_m are given by:

$$\rho_m \vec{q}_m = \sum_{i=1}^{NS} \rho_i \vec{q}_i \tag{3.9}$$

$$\rho_m h_m = \sum_{i=1}^{NS} \rho_i h_i \tag{3.10}$$

and

$$\rho_m e_m = \sum_{i=1}^{NS} \rho_i e_i \tag{3.11}$$

Substituting Eqs. (3.8) and (3.9) into (3.7),

$$\frac{\partial \rho_m}{\partial t} + \nabla \cdot \rho_m \vec{q}_m - \sum_{i=1}^{NS} \dot{w}_i = 0 ,$$

and noting that for a closed system, the total mass for chemical reactions is conserved

$$\sum_{i=1}^{NS} \dot{w}_i = 0 ; \tag{3.12}$$

Equation (3.7) reduces to

$$\frac{\partial \rho_m}{\partial t} + \nabla \cdot \rho_m \vec{q}_m = 0 . \tag{3.13}$$

Equation (3.13) is known as the global continuity equation. It can be written alternatively as

$$\frac{D\rho_m}{Dt} + \rho_m \nabla \cdot \vec{q}_m = 0$$

by means of the substantial derivative.

Equations (3.8),(3.9) and (3.12) can be rewritten in terms of gaseous and particle species as follows:

Equation (3.8)

$$\rho_m = \sum_{i=1}^{NS} \rho_i = \rho + \sum_{j=1}^{NP} \rho^j ; \tag{3.14}$$

Equation (3.9):

$$\rho_m \vec{q}_m = \sum_{i=1}^{NS} \rho_i \vec{q}_i = \rho \vec{q} + \sum_{j=1}^{NP} \rho^j \vec{q}^{\,j} \tag{3.15}$$

Equation (3.12):

$$\sum_{i=1}^{NS} \dot{w}_i = 0 = \dot{w} + \sum_{j=1}^{NP} \dot{w}^j = 0 \tag{3.16}$$

Assuming that reactions of the form A(gas) + B(gas) $\rightleftharpoons$ C(particle) + D(particle) do not contribute significantly to the system (interchange of phases is negligible due to chemical reactions), Eq.(3.16) implies that

$$\dot{w} = 0 \quad \text{and} \quad \sum_{j=1}^{NP} \dot{w}^j = 0 . \tag{3.17}$$

Substituting Eqs.(3.14) through (3.17) into Eq. (3.7)

$$\frac{\partial}{\partial t}\left(\rho + \sum_{j=1}^{NP} \rho^j\right) + \nabla \cdot \left(\rho \vec{q} + \sum_{j=1}^{NP} \rho^j \vec{q}^{\,j}\right) - \cancelto{0}{\dot{w}} - \cancelto{0}{\sum_{j=1}^{NP} \dot{w}^j} = 0 ,$$

and rearranging terms yields

$$\frac{\partial \rho}{\partial t} + \nabla \cdot \rho \vec{q} + \sum_{j=1}^{NP} \left(\frac{\partial \rho^j}{\partial t} + \nabla \cdot \rho^j \vec{q}^{\,j}\right) = 0 \tag{3.18}$$

Since the gaseous species and particle species do not interchange phases, both contributions must vanish. Therefore

$$\frac{\partial \rho}{\partial t} + \nabla \cdot \rho \vec{q} = 0 \tag{3.19}$$

and

$$\sum_{j=1}^{NP} \left(\frac{\partial \rho^j}{\partial t} + \nabla \cdot \rho^j \vec{q}^j \right) = 0 \tag{3.20}$$

Equation (3.19) is known as the gas continuity equation and is valid when applied to the system of gas species. Equation (3.20) is known as the particle continuity equation and is valid when applied to the system of particle species.

The species continuity Eq. (3.6) may be written in a more convenient form by making use of the gas continuity equation and introducing the mass fraction of species i. In general, the mass fraction of species i may be defined as:

$$\chi_i = \frac{\rho_i}{\rho_m} . \tag{3.21}$$

Substituting χ_i into the species continuity Eq. (3.6)

$$\frac{\partial}{\partial t} (\chi_i \rho_m) + \nabla \cdot \chi_i \rho_m \vec{q}_i - \dot{w}_i = 0; \quad i = 1, NS$$

expanding the first term

$$\rho_m \frac{\partial \chi_i}{\partial t} + \chi_i \frac{\partial \rho_m}{\partial t} + \nabla \cdot \chi_i \rho_m \vec{q}_i - \dot{w}_i = 0 \qquad i = 1, NS \tag{3.21a}$$

and applying the vector identity

$$\nabla \cdot \chi_i \rho_m \vec{q}_i = \nabla \cdot (\chi_i (\rho_m \vec{q}_i)) = \nabla \chi_i \cdot \rho_m \vec{q}_i + \chi_i (\nabla \cdot \rho_m \vec{q}_i)$$

results in

$$\rho_m \left(\frac{\partial \chi_i}{\partial t} + \vec{q}_i \cdot \nabla \chi_i \right) + \chi_i \left(\frac{\partial \rho_m}{\partial t} + \nabla \cdot \rho_m \vec{q}_i \right) - \dot{w}_i = 0 \qquad i = 1, NS \qquad (3.22)$$

By limiting the system to only gas phase reactions (no reactions in the particulate phase) the species mass fraction χ_i may be redefined as:

$$\chi_i = \rho_i / \rho \qquad (3.23)$$

Assuming all gaseous species have velocity $\vec{q}_i = \vec{q}$, Eq. (3.22) becomes

$$\rho \left(\frac{\partial \chi_i}{\partial t} + \vec{q}_i \cdot \nabla \chi_i \right) + \chi_i \left(\frac{\partial \rho}{\partial t} + \nabla \cdot \rho \vec{q} \right) - \dot{w}_i = 0 \qquad i = 1, NS \qquad (3.24)$$

Applying the gas continuity equation to the above expression the second term is set equal to zero and Eq. (3.24) becomes:

$$\rho \left(\frac{\partial \chi_i}{\partial t} + \vec{q}_i \cdot \nabla \chi_i \right) - \dot{w}_i = 0 \qquad i = 1, NS$$

The final form of Eq. (3.24) is obtained by applying substantial derivative, Eq. (3.4) to yield

$$\rho \frac{D\chi_i}{Dt} - \dot{w}_i = 0 \qquad i = 1, NS \qquad \text{species continuity equation} \qquad (3.25)$$

Under the above assumption that there are no particle reactions, Eq. (2.20) for each particle species j becomes:

$$\frac{\partial \rho^j}{\partial t} + \nabla \cdot \rho^j \vec{q}^j = 0 \qquad j = 1, NP \qquad \text{particle continuity equation} \qquad (3.26)$$

For steady state flow processes, Eqs. (3.13), (3.26) and (3.25) become:

Equation (3.13)

$$\nabla \cdot \rho_m \vec{q}_m = 0 \qquad \text{global continuity equation} \qquad (3.27)$$

Equation (3.26)

$$\nabla \cdot \rho^j \vec{q}^j = 0 \qquad j = 1, NP \qquad \text{particle continuity equation, and} \qquad (3.28)$$

Equation (3.25)

$$\rho \vec{q}_i \cdot \nabla X_i - \dot{w}_i = 0 \qquad i = 1, NS \qquad \text{species continuity equation} \qquad (3.29)$$

3.2.2 Momentum Equation

The various forms of the global momentum equation for a chemically reacting gas-particle mixture are derived in this section. The forms of the equation derived, in order are:

1. General Global Momentum Equation (3.42)
2. General Global Momentum Equation with particle drag effects (3.49)
3. Global Momentum Equation for steady state, inviscid, no body force flow (3.50)

The linear momentum of an element of mass m is a vector quantity defined as $m\vec{q}_m$. The fundamental statement of Newton's law for an inertial reference is given in terms of momentum as

$$\vec{F} - \frac{D}{Dt}(m_m \vec{q}_m) = 0 \qquad (3.30)$$

To derive the general global momentum equation the two terms of Eq. (3.30) will be analyzed separately.

The total force acting on the system may be represented as the sum of the surface force distributions (force distributions acting on the boundary of the system) and body force distributions (force distributions acting on the material inside the system) as follows:

$$\vec{F} = \int_S \overline{\overline{\sigma}} \cdot \vec{n}\, dS + \int_V \sum_{i=1}^{NS} \rho_i \vec{f}_i\, dV \tag{3.31}$$

The surface force term may be converted into a volume integral by applying Gauss' theorem, Eq. (3.2). Therefore,

$$\vec{F} = \int_V \nabla \cdot \overline{\overline{\sigma}}\, dV + \int_V \sum_{i=1}^{NS} \rho_i \vec{f}_i\, dV \tag{3.32}$$

The surface stress tensor, $\overline{\overline{\sigma}}$ may be written in the form:

$$\overline{\overline{\sigma}} = -P\overline{\overline{\delta}} + \overline{\overline{\tau}} \tag{3.33}$$

and

$$\nabla \cdot \overline{\overline{\sigma}} = -\nabla P + \nabla \cdot \overline{\overline{\tau}} \tag{3.34}$$

Substituting Eq. (3.34) into Eq. (3.32), the total force acting on the system may be written in the form

$$\vec{F} = \int_V (-\nabla P + \nabla \cdot \overline{\overline{\tau}})\, dV + \int_V \sum_{i=1}^{NS} \rho_i \vec{f}_i\, dV ;$$

or, upon combining terms

$$\vec{F} = \int_V \left(-\nabla P + \nabla \cdot \overline{\overline{\tau}} + \sum_{i=1}^{NS} \rho_i \vec{f}_i\right) dV \tag{3.35}$$

The momentum term $m_m \vec{q}_m$ in Eq.(3.30) may be rewritten in the form

$$m_m \vec{q}_m = \int_V \sum_{i=1}^{NS} \rho_i \vec{q}_i \, dV ;$$

from which the substantial derivative can then be written

$$\frac{D}{Dt} (m_m \vec{q}_m) = \frac{D}{Dt} \int_V \sum_{i=1}^{NS} \rho_i \vec{q}_i \, dV . \qquad (3.36)$$

Applying Reynold's transport theorem Eq.(3.3) to Eq.(3.36)

$$\frac{D}{Dt} (m_m \vec{q}_m) = \int_V \frac{\partial}{\partial t} \sum_{i=1}^{NS} \rho_i \vec{q}_i \, dV + \int_V \nabla \cdot \sum_{i=1}^{NS} \rho_i \vec{q}_i \vec{q}_i \, dV ;$$

rearranging terms

$$\frac{D}{Dt} (m_m \vec{q}_m) = \int_V \left\{ \frac{\partial}{\partial t} \sum_{i=1}^{NS} \rho_i \vec{q}_i + \nabla \cdot \sum_{i=1}^{NS} \rho_i \vec{q}_i \vec{q}_i \right\} dV ; \qquad (3.37)$$

and rewriting the results in terms of the gaseous and particle species results in:

$$\frac{D}{Dt} (m_m \vec{q}_m) = \int_V \left\{ \frac{\partial}{\partial t} \left(\rho \vec{q} + \sum_{j=1}^{NP} \rho^j \vec{q}^j \right) + \nabla \cdot \left(\rho \vec{q} \vec{q} + \sum_{j=1}^{NP} \rho^j \vec{q}^j \vec{q}^j \right) \right\} dV$$

or,

$$\frac{D}{Dt} (m_m \vec{q}_m) = \int_V \left\{ \frac{\partial}{\partial t} (\rho \vec{q}) + \nabla \cdot \rho \vec{q} \vec{q} + \sum_{j=1}^{NP} \left[\frac{\partial}{\partial t} (\rho^j \vec{q}^j) + \nabla \cdot \rho^j \vec{q}^j \vec{q}^j \right] \right\} dV \qquad (3.38)$$

Substituting Eqs.(3.35) and (3.38) into Eq.(3.30), dropping the integral notation and rearranging the terms yields

$$\frac{\partial}{\partial t}(\rho \vec{q}) + \nabla \cdot \rho \vec{q}\vec{q} + \sum_{j=1}^{NP}\left[\frac{\partial}{\partial t}(\rho^j \vec{q}^j) + \nabla \cdot \rho^j \vec{q}^j \vec{q}^j\right] = -\nabla P + \nabla \cdot \bar{\bar{\tau}} + \sum_{i=1}^{NS} \rho_i \vec{f}^i \qquad (3.39)$$

Expanding the first two terms of Eq. (3.39)

$$\frac{\partial}{\partial t}(\rho \vec{q}) + \nabla \cdot \rho \vec{q}\vec{q} = \rho \frac{\partial \vec{q}}{\partial t} + \vec{q}\frac{\partial \rho}{\partial t} + \rho \vec{q} \cdot \nabla \vec{q} + \vec{q}\nabla \cdot \rho \vec{q}; \qquad (3.39a)$$

and then applying the gas continuity Eq. (3.19)

$$\frac{\partial \rho}{\partial t} + \nabla \cdot \rho \vec{q} = 0$$

to the results, yields

$$\frac{\partial}{\partial t}(\rho \vec{q}) + \nabla \cdot \rho \vec{q}\vec{q} = \rho\left(\frac{\partial \vec{q}}{\partial t} + \vec{q} \cdot \nabla \vec{q}\right) \qquad (3.40)$$

The third term of Eq.(3.39) may be manipulated in a like manner using the particle continuity Eq.(3.26) to yield:

$$\sum_{j=1}^{NP}\left[\frac{\partial}{\partial t}(\rho^j \vec{q}^j) + \nabla \cdot \rho^j \vec{q}^j \vec{q}^j\right] = \sum_{j=1}^{NP} \rho^j \left(\frac{\partial \vec{q}^j}{\partial t} + \vec{q}^j \cdot \nabla \vec{q}^j\right) \qquad (3.41)$$

Substituting Eqs.(3.40) and (3.41) back into Eq.(3.39) results in:

$$\rho\left(\frac{\partial \vec{q}}{\partial t} + \vec{q} \cdot \nabla \vec{q}\right) + \sum_{j=1}^{NP} \rho^j \left(\frac{\partial \vec{q}^j}{\partial t} + \vec{q}^j \cdot \nabla \vec{q}^j\right) = -\nabla P + \nabla \cdot \bar{\bar{\tau}} + \sum_{i=1}^{NS} \rho_i \vec{f}_i;$$

or in terms of the substantial derivative, Eq. (3.4),

$$\rho \frac{D}{Dt}\vec{q} + \sum_{j=1}^{NP} \rho^j \frac{D}{Dt}\vec{q}^j = -\nabla P + \nabla \cdot \bar{\bar{\tau}} + \sum_{i=1}^{NS} \rho_i \vec{f}_i \qquad (3.42)$$

Equation (3.42) is the general global momentum equation. In this equation, the five terms are, respectively: (1) the non-stationary and convective rate of change of momentum per unit volume of the gaseous species; (2) the non-stationary and convective rate of change of momentum per unit volume of the particle species; (3) the net hydrostatic pressure force; (4) the viscous stress force acting on the surface of the unit volume; and (5) the body forces per unit volume.

Since it is assumed that all forces are negligible, except that of the pressure of the gas and the particle drag, the only force exerted on the particle is a drag force $\vec{D}_f^j$ caused by the relative motion between the gas and the particle. Figure 3-2 illustrates a spherical particle in a gas flow field.

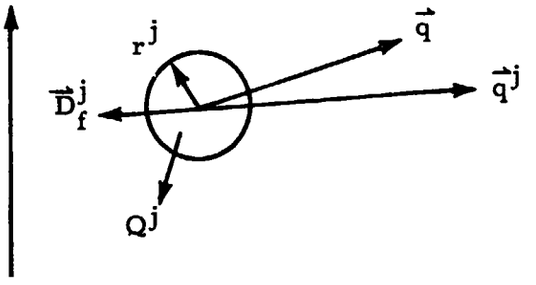

Fig. 3-2 - Particle Momentum and Heat Transfer Model

To determine the effects of particle drag on the global momentum equation, Newton's Second Law is applied to the drag forces $\vec{D}_f^j$ acting on particle species j.

$$\vec{D}_f^j = \frac{D}{Dt}(m\vec{q})^j$$

or rewritten in terms of particle density

$$\vec{D}_f^j = \frac{D}{Dt}\left[m^j \frac{4}{3} \pi (r^j)^3 \vec{q}^j\right] = \frac{4}{3} \pi (r^j)^3 m^j \frac{D}{Dt} \vec{q}^j .$$

In general, the drag force on a spherical particle may be written in the form:

$$\vec{D}_f^j = C_D^j \pi (r^j)^2 \left(\frac{1}{2} \rho \Delta\vec{q}^j |\Delta\vec{q}^j|\right)$$

where

$$\Delta\vec{q}^j = \vec{q} - \vec{q}^j . \tag{3.43}$$

Equating the two expressions for particle drag

$$\frac{4}{3} \pi (r^j)^3 m^j \frac{D}{Dt} \vec{q}^j = C_D^j \pi (r^j)^2 \frac{1}{2} \rho \Delta\vec{q}^j |\Delta\vec{q}^j|;$$

and rearranging terms yields:

$$\frac{D}{Dt} \vec{q}^j = \frac{3}{8}\left(\frac{\rho C_D^j}{m^j r^j}\right) \Delta\vec{q}^j |\Delta\vec{q}^j| \tag{3.44}$$

Equation (3.44) can be simplified by referencing to the Stokes flow regime (Reynolds number is less t. .n 1) in the following manner.

Define

$$f^j = \frac{C_D^j}{C_{D_{Stokes}}}$$

where

$$C_D\Big)_{Stokes} = \frac{24}{Re} , \quad Nu = 2 .$$

Therefore,

$$C_D^j = \frac{24 f^j}{Re} = 24 f^j \left(\frac{\nu}{2 r^j \rho |\Delta\vec{q}^j|}\right). \tag{3.45}$$

Substituting Eq.(3.45) into Eq.(3.44) and defining the parameter

$$A^j = \frac{9}{2}\left[\frac{\nu f^j}{m^j r^{j^2}}\right]; \tag{3.46}$$

the momentum balance becomes

$$\frac{D}{Dt}\vec{q}^j = A^j \Delta\vec{q}^j . \tag{3.47}$$

Expanding the substantial derivative by means of Eq.(3.4), Eq.(3.47) becomes

$$\frac{\partial}{\partial t}\vec{q}^j + \vec{q}^j \cdot \nabla\vec{q}^j = A^j \Delta\vec{q}^j = \frac{D\vec{q}^j}{Dt} . \tag{3.48}$$

Substituting Eq.(3.47) into the general global momentum equation results in:

$$\rho \frac{D\vec{q}}{Dt} + \sum_{j=1}^{NP} \rho^j A^j \Delta\vec{q}^j = -\nabla P + \nabla \cdot \bar{\bar{\tau}} + \sum_{i=1}^{NS} \rho_i \vec{f}_i \tag{3.49}$$

Equation (3.49) is the general global momentum equation with particle drag effects.

For the case in which the flow may be described as steady state, inviscid and no body forces present Eq.(3.49) becomes:

$$\rho \vec{q} \cdot\nabla\vec{q} + \sum_{j=1}^{NP} \rho^j A^j \Delta\vec{q}^j = -\nabla P . \tag{3.50}$$

We note at this point that chemical reactions do not alter the forms of the global continuity equation or equations of motion.

Equation (3.50) will be expanded now for later use in the derivation of the energy equation. For an arbitrary vector $\vec{A}$ the following identity exists

$$\vec{A} \cdot \nabla\vec{A} = \frac{1}{2}\nabla (\vec{A} \cdot \vec{A}) - \vec{A} \times (\nabla \times \vec{A}) . \tag{3.51}$$

Applying this identity to the first term in Eq. (3.50)

$$\rho \vec{q} \cdot \nabla \vec{q} = \frac{1}{2} \rho \nabla(\vec{q} \cdot \vec{q}) - \rho \vec{q} \times (\nabla \times \vec{q}) ;$$

substituting the results back into Eq. (3.50)

$$\frac{1}{2} \rho \nabla(\vec{q} \cdot \vec{q}) - \rho \vec{q} \times (\nabla \times \vec{q}) + \sum_{j=1}^{NP} \rho^j A^j \Delta \vec{q}^j = - \nabla P ;$$

and rearranging terms yields

$$\frac{1}{2} \nabla(\vec{q} \cdot \vec{q}) = \vec{q} \times (\nabla \times \vec{q}) - \frac{1}{\rho} \sum_{j=1}^{NP} \rho^j A^j \Delta \vec{q}^j - \frac{\nabla P}{\rho} \qquad (3.52)$$

3.2.3 Energy Equation

The various forms of the energy equation for a chemically reacting gas-particle mixture are derived in this section. The forms of the equation derived are:

1. General Global Energy Equation Neglecting the Effects of Radiation (3.74)
2. General Particle Energy Balance Equation (3.84)
3. General Global Energy Equation with Radiation Effects (3.85)
4. Global Energy Equation with Radiation Effects for Flow Described as Steady State, Adiabatic, Inviscid, and No Body Forces Present. (3.105)

The most general form of the energy equation, according to the first law of thermodynamics or the law of conservation of energy can be written as

$$\frac{DE}{Dt} - \frac{dQ}{dt} + \frac{dW}{dt} = 0 \qquad (3.53)$$

The energy E in the control volume may be written in terms of the species present as

$$E = \int_V \sum_{i=1}^{NS} \rho_i \, e_i \, dV \; ;$$

where

$$e_i = i_i + \frac{q_i^2}{2} + \frac{q_i}{g_c} Z_i \qquad i = 1, NS \tag{3.54}$$

i_i = internal energy of species i per unit mass

$\frac{q_i^2}{2}$ = kinetic energy of species i per unit mass

$\frac{q_i}{g_c} Z_i$ = potential energy of species i per unit mass.

The substantial derivative can then be written

$$\frac{DE}{Dt} = \frac{D}{Dt} \int_V \sum_{i=1}^{NS} \rho_i \, e_i \, dV \; ;$$

and expanded by applying Eq.(3.3) to yield

$$\frac{DE}{Dt} = \int_V \frac{\partial}{\partial t} \sum_{i=1}^{NS} \rho_i \, e_i \, dV + \int_V \nabla \cdot \sum_{i=1}^{NS} \rho_i \, e_i \, \vec{q}_i \, dV \; . \tag{3.55}$$

Recalling that the total force acting on the control volume according to Eq. (3.31) is

$$\vec{F} = \int_S \bar{\bar{\sigma}} \cdot \vec{n} \, dS + \int_V \sum_{i=1}^{NS} \rho_i \, \vec{f}_i \, dV \; ;$$

and applying the definition for the rate at which work is performed on or by the control volume $dW/dt = -\vec{q} \cdot F$,

one obtains

$$\frac{dW}{dt} = -\int_S \vec{q} \cdot \overline{\overline{\sigma}} \cdot \vec{n}\, dS - \int_V \sum_{i=1}^{NS} \vec{q}_i \cdot \rho_i \vec{f}_i\, dV$$

The surface integral may be converted into a volume integral by applying Gauss' theorem, Eq.(3.2). Therefore,

$$\frac{dW}{dt} = -\int_V \nabla \cdot (\overline{\overline{\sigma}} \cdot \vec{q})\, dV - \int_V \sum_{i=1}^{NS} \vec{q}_i \cdot \rho_i \vec{f}_i\, dV .$$

Recalling the definition of the surface stress tensor $\overline{\overline{\sigma}}$, Eq. (3.33)

$$\overline{\overline{\sigma}} = -P\overline{\overline{\delta}} + \overline{\overline{\tau}} ,$$

and taking the dot product

$$\overline{\overline{\sigma}} \cdot \vec{q} = -P\vec{q} + \overline{\overline{\tau}} \cdot \vec{q} ,$$

the first volume integral in the above equation may be written as

$$\int_V \nabla \cdot (-P\vec{q} + \overline{\overline{\tau}} \cdot \vec{q})\, dV . \qquad (3.56)$$

Substituting Eq.(3.56) back into the expression for dW/dt

$$\frac{dW}{dt} = -\int_V \nabla \cdot (-P\vec{q} + \overline{\overline{\tau}} \cdot \vec{q}) - \int_V \sum_{i=1}^{NS} \vec{q}_i \cdot \rho_i \vec{f}_i\, dV ,$$

combining integrals

$$\frac{dW}{dt} = -\int_V \left[\nabla \cdot (-P\vec{q} + \overline{\overline{\tau}} \cdot \vec{q}) + \sum_{i=1}^{NS} \vec{q}_i \cdot \rho_i \vec{f}_i\right] dV ,$$

and expanding terms yields

$$\frac{dW}{dt} = \int_V \left[\nabla \cdot P\vec{q} - \nabla \cdot (\overline{\overline{\tau}} \cdot \vec{q}) - \sum_{i=1}^{NS} \vec{q}_i \cdot \rho_i \vec{f}_i\right] dV . \qquad (3.57)$$

The rate at which heat is transferred to or from the control volume may be written in the form

$$\frac{dQ}{dt} = \int_S \vec{Q} \cdot \vec{n}\, dS ,$$

or in terms of a volume integral by applying Gauss' theorem, Eq.(2.2)

$$\frac{dQ}{dt} = \int_V \nabla \cdot \vec{Q}\, dV , \tag{3.58}$$

where $\vec{Q}$ is the conduction heat flux vector.

Substituting Eqs.(3.55),(3.57) and(3.58) into Eq.(3.53) and dropping the integral notation results in

$$\frac{\partial}{\partial t} \sum_{i=1}^{NS} \rho_i e_i + \nabla \cdot \sum_{i=1}^{NS} \rho_i e_i \vec{q}_i - \nabla \cdot \vec{Q} + \nabla \cdot P\vec{q} - \nabla \cdot (\bar{\bar{\tau}} \cdot \vec{q}) - \sum_{i=1}^{NS} \vec{q}_i \cdot \rho_i \vec{f}_i = 0 . \tag{3.59}$$

Equation (3.59) is the general global energy equation neglecting the effects of radiation. This equation is based on a unit volume. The six terms are, respectively: (1) and (2) thetotal rate of increase of internal, kinetic and potential energy caused by local and convective changes; (3) the heat conducted to or from the control volume; (4) and (5) the work done on the fluid element due to surface forces; and (6) the work done on the element by the body forces.

In deriving Eq.(3.59), all that has been neglected is the energy transferred due to radiation, which if necessary, can be added to the equation as an extra term. Radiation effects will be determined later in this section.

The microscopic quantum effects (interchange of energy and mass) are not considered in Eq.(3.59) as it has been implied by the classical first law of thermodynamics. The general global energy equation will now be expanded and written in terms of the gaseous and particle species present.

Recall that

$$e_i = i_i + \frac{q_i^2}{2} + \frac{q_i}{g_c} Z_i \qquad i = 1, NS \; . \tag{3.54}$$

If the potential energy term is combined with the body force term, Eq. (3.54) may be rewritten in the form

$$e_i = i_i + \frac{q_i^2}{2} \qquad i = 1, NS \tag{3.60}$$

Defining the specific enthalpy of species i as

$$h_i = i_i + \frac{P_i}{\rho_i} \qquad i = 1, NS \tag{3.61}$$

where P_i = partial pressure of species i
and combining Eqs. (3.60) and (3.61) yields

$$e_i = h_i - \frac{P_i}{\rho_i} + \frac{q_i^2}{2}$$

Next, define the total enthalpy per unit mass of species i as

$$H_i = h_i + \frac{q_i^2}{2} \; . \tag{3.62}$$

Therefore, the expression for e_i becomes

$$e_i = H_i - \frac{P_i}{\rho_i} \; .$$

Substituting the expression for e_i into Eq. (3.59) results in

$$\frac{\partial}{\partial t} \sum_{i=1}^{NS} \rho_i \left(H_i - \frac{P_i}{\rho_i} \right) + \nabla \cdot \sum_{i=1}^{NS} \rho_i \left(H_i - \frac{P_i}{\rho_i} \right) \vec{q}_i - \nabla \cdot \vec{Q} + \nabla \cdot P\vec{q} - \nabla \cdot (\bar{\bar{\tau}} \cdot \vec{q}) - \sum_{i=1}^{NS} \vec{q}_i \cdot \rho_i \vec{f}_i = 0 \tag{3.62a}$$

The pressure P may be expressed as the sum of the partial pressures as follows

$$P = \sum_{i=1}^{NS} P_i \ . \tag{3.63}$$

Substituting Eq. (3.63) into Eq. (3.62a)

$$\frac{\partial}{\partial t} \sum_{i=1}^{NS} \rho_i H_i - \frac{\partial P}{\partial t} + \nabla \cdot \sum_{i=1}^{NS} \rho_i \vec{q}_i H_i - \nabla \cdot \sum_{i=1}^{NS} P_i \vec{q}_i - \nabla \cdot \vec{Q}$$

$$+ \nabla \cdot P\vec{q} - \nabla \cdot (\bar{\bar{\tau}} \cdot \vec{q}) - \sum_{i=1}^{NS} \vec{q}_i \cdot \rho_i \vec{f}_i = 0$$

and noting that

$$\nabla \cdot \sum_{i=1}^{NS} \vec{q}_i P_i = \nabla \cdot P\vec{q} \ ,$$

the above equation becomes

$$\frac{\partial}{\partial t} \sum_{i=1}^{NS} \rho_i H_i - \frac{\partial P}{\partial t} + \nabla \cdot \sum_{i=1}^{NS} \rho_i \vec{q}_i H_i - \nabla \cdot \vec{Q} - \nabla \cdot (\bar{\bar{\tau}} \cdot \vec{q}) - \sum_{i=1}^{NS} \vec{q}_i \cdot \rho_i \vec{f}_i = 0 \tag{3.64}$$

From the assumption that thermodynamic local equilibrium exists, the following expressions may be written in terms of the gaseous and particle species:

$$\sum_{i=1}^{NS} \rho_i H_i = \rho H + \sum_{j=1}^{NP} \rho^j H^j \tag{3.65}$$

and,

$$\sum_{i=1}^{NS} \rho_i \vec{q}_i H_i = \rho \vec{q} H + \sum_{j=1}^{NP} \rho^j \vec{q}^j H^j \tag{3.66}$$

Substituting Eqs. (3.65) and (3.66) into Eq. (3.64)

$$\frac{\partial}{\partial t} \left(\rho H + \sum_{j=1}^{NP} \rho^j H^j \right) - \frac{\partial P}{\partial t} + \nabla \cdot \left(\rho \vec{q} H + \sum_{j=1}^{NP} \rho^j \vec{q}^j H^j \right) - \nabla \cdot \vec{Q} - \nabla \cdot (\bar{\bar{\tau}} \cdot \vec{q})$$

$$- \sum_{i=1}^{NS} \vec{q}_i \cdot \rho_i \vec{f}_i = 0,$$

and rearranging terms yields

$$\frac{\partial}{\partial t}(\rho H) + \nabla \cdot \rho \vec{q} H + \sum_{j=1}^{NP}\left[\frac{\partial}{\partial t}(\rho^j H^j) + \nabla \cdot \rho^j \vec{q}^j H^j\right] = \frac{\partial P}{\partial t} + \nabla \cdot (\bar{\bar{\tau}} \cdot \vec{q}) + \sum_{i=1}^{NS} \vec{q}_i \cdot \rho_i \vec{f}_i + \nabla \cdot \vec{Q}; \quad (3.67)$$

where

$$H = h + q^2/2 \quad (3.68)$$

$$H^j = h^j + (q^j)^2/2 . \quad (3.69)$$

Expanding the first two terms of Eq. (3.67)

$$\rho \frac{\partial H}{\partial t} + H \frac{\partial \rho}{\partial t} + \rho \vec{q} \cdot \nabla H + H \nabla \cdot \rho \vec{q} ,$$

and rearranging terms yields

$$\rho \left(\frac{\partial H}{\partial t} + \vec{q} \cdot \nabla H\right) + H \left(\frac{\partial \rho}{\partial t} + \nabla \cdot \rho \vec{q}\right) .$$

Recalling the gas continuity Eq. (3.19)

$$\frac{\partial \rho}{\partial t} + \nabla \cdot \rho \vec{q} = 0 ,$$

and applying the definition of the substantial derivative to the first term in the above expression

$$\frac{\partial H}{\partial t} + \vec{q} \cdot \nabla H = \frac{DH}{Dt} ,$$

the first two terms of Eq. (3.67) reduce to

$$\frac{\partial}{\partial t}(\rho H) + \nabla \cdot \rho \vec{q} H = \rho \frac{DH}{Dt} . \quad (3.70)$$

The third term of Eq.(3.67) may be manipulated in a like manner. Expanding

$$\sum_{j=1}^{NP}\left(\rho^j \frac{\partial H^j}{\partial t} + H^j \frac{\partial \rho^j}{\partial t} + \rho^j \vec{q}^j \cdot \nabla H^j + H^j \nabla \cdot \rho^j \vec{q}^j\right),$$

and rearranging terms yields

$$\sum_{j=1}^{NP}\left[\rho^j\left(\frac{\partial H^j}{\partial t} + \vec{q}^j \cdot \nabla H^j\right)\right] + \sum_{j=1}^{NP}\left[H^j\left(\frac{\partial \rho^j}{\partial t} + \nabla \cdot \rho^j \vec{q}^j\right)\right].$$

Recalling the particle continuity Eq. (3.26)

$$\frac{\partial \rho^j}{\partial t} + \nabla \cdot \rho^j \vec{q}^j = 0 \qquad j = 1, NP,$$

and applying the definition of the substantial derivative to the first term in the above expression

$$\frac{\partial H^j}{\partial t} + \vec{q}^j \cdot \nabla H^j = \frac{DH^j}{Dt},$$

the third term of Eq.(3.67) reduces to

$$\sum_{j=1}^{NP}\left[\frac{\partial}{\partial t}(\rho^j H^j) + \nabla \cdot \rho^j \vec{q}^j H^j\right] = \sum_{j=1}^{NP} \rho^j \frac{DH^j}{Dt}. \tag{3.71}$$

Substituting Eqs.(3.70) and (3.71) into Eq.(3.67) results in

$$\rho \frac{DH}{Dt} + \sum_{j=1}^{NP} \rho^j \frac{DH^j}{Dt} = \frac{\partial P}{\partial t} + \nabla \cdot (\bar{\bar{\tau}} \cdot \vec{q}) + \sum_{i=1}^{NS} \vec{q}_i \cdot \rho_i \vec{f}_i + \nabla \cdot \vec{Q}. \tag{3.72}$$

Recall that

$$H^j = h^j + \frac{(q^j)^2}{2}. \tag{3.69}$$

Therefore,

$$\frac{DH^j}{Dt} = \frac{Dh^j}{Dt} + \frac{1}{2}\frac{D(q^j)^2}{Dt} = \frac{Dh^j}{Dt} + \frac{1}{2}\frac{D}{Dt}(\vec{q}^j \cdot \vec{q}^j)$$

or,

$$\frac{DH^j}{Dt} = \frac{Dh^j}{Dt} + \frac{1}{2}\left(\vec{q}^j \cdot \frac{D\vec{q}^j}{Dt} + \vec{q}^j \cdot \frac{D\vec{q}^j}{Dt}\right) = \frac{Dh^j}{Dt} + \frac{1}{2}\left(2\vec{q}^j \cdot \frac{D\vec{q}^j}{Dt}\right)$$

finally,

$$\frac{DH^j}{Dt} = \frac{Dh^j}{Dt} + \vec{q}^j \cdot \frac{D\vec{q}^j}{Dt} . \tag{3.73}$$

Substituting Eq.(3.73) into Eq.(3.72) results in

$$\rho \frac{DH}{Dt} + \sum_{j=1}^{NP} \rho^j \left(\frac{Dh^j}{Dt} + \vec{q}^j \cdot \frac{D\vec{q}^j}{Dt}\right) = \frac{\partial P}{\partial t} + \nabla \cdot (\bar{\bar{\tau}} \cdot \vec{q}) + \sum_{i=1}^{NS} \vec{q}_i \cdot \rho_i \vec{f}_i + \nabla \cdot \vec{Q} \tag{3.74}$$

Equation (3.74) is the general global energy equation written in terms of the gaseous and particle species.

To determine the effect of particle/gas conduction and radiation, the particle energy balance for the j^{th} particle is written as follows:

$$\frac{DQ^j}{Dt} = -K^j\left[4\pi (r^j)^2\right](T^j - T) - \sigma 4\pi (r^j)^2 \left[\epsilon^j (T^j)^4 - \alpha^j T^4\right]; \tag{3.75}$$

where

$$K^j = \frac{k N_u^j}{2r^j} = \text{particle heat transfer film coefficient.} \tag{3.76}$$

Defining the Nusselt number parameter

$$G^j = \frac{N_u^j}{(Nu)_{Stokes}} \tag{3.77}$$

where

$$(Nu)_{Stokes} = 2 ; \tag{3.78}$$

the particle heat transfer film coefficient may be rewritten as

$$K^j = \frac{k G^j}{r^j} . \tag{3.79}$$

Furthermore the heat quantity of the particle is defined as

$$Q^j = m^j \frac{4\pi}{3} (r^j)^3 h^j . \tag{3.80}$$

Differentiating Eq. (3.80)

$$\frac{DQ^j}{Dt} = m^j \frac{4}{3} \pi (r^j)^3 \frac{Dh^j}{Dt} ,$$

rearranging terms

$$\frac{Dh^j}{Dt} = \frac{3}{4\pi m^j (r^j)^3} \frac{DQ^j}{Dt} ,$$

and substituting the above results, with the expression for K^j back into Eq.(3.75), the particle energy balance equation becomes

$$m^j \frac{4\pi}{3} (r^j)^3 \frac{Dh^j}{Dt} = - \frac{k G^j}{r^j} \left[4\pi (r^j)^2\right] (T^j - T) - \sigma 4\pi (r^j)^2 \left[\varepsilon^j (T^j)^4 - \alpha^j T^4\right] .$$

Solving for Dh^j/Dt in the above equation

$$\frac{Dh^j}{Dt} = - \frac{k G^j}{(r^j)^2} \frac{3}{m^j} (T^j - T) - \frac{3\sigma}{m^j r^j} \left[\varepsilon^j (T^j)^4 - \alpha^j T^4\right] , \tag{3.81}$$

and recalling Eq. (3.46)

$$A^j = \frac{9}{2} \frac{\nu f^j}{m^j r^j{}^2} \tag{3.46}$$

the equation for Dh^j/Dt may be written as

$$\frac{Dh^j}{Dt} = - \frac{2k}{3} \frac{G^j A^j}{\nu f^j} (T^j - T) - \frac{3\sigma}{m^j r^j} \left[\varepsilon^j (T^j)^4 - \alpha^j T^4\right] . \tag{3.82}$$

Equation (3.82) may be simplified by letting

$$C^j = \frac{G^j c_p}{f^j Pr} = \frac{k G^j}{\nu f^j} \tag{3.83}$$

Therefore,

$$\frac{Dh^j}{Dt} = -\frac{2}{3} A^j C^j (T^j - T) - \frac{3\sigma}{m^j r^j} \left[\mathcal{E}^j (T^j)^4 - \alpha^j T^4 \right]. \tag{3.84}$$

This is the general particle energy balance equation. The temperature of the particle depends upon its state, where the state may be a liquid, a liquid in the process of solidifying, or a solid. The temperature is uniquely related to the particle enthalpy by the equation of state $T^j = f(h^j)$, tabulated.

Substituting Eqs. (3.47) and (3.84) into the general global energy Eq. (3.74) yields

$$\rho \frac{DH}{Dt} + \sum_{j=1}^{NP} \left\{ -\frac{2}{3} \rho^j A^j C^j (T^j - T) - \frac{3\sigma}{m^j r^j} \rho^j \left[\mathcal{E}^j (T^j)^4 - \alpha^j T^4 \right] + \vec{q}^j \cdot \rho^j A^j \Delta\vec{q}^j \right\}$$

$$= \frac{\partial P}{\partial T} + \nabla \cdot (\bar{\bar{\tau}} \cdot \vec{q}) + \sum_{i=1}^{NS} \vec{q}_i \cdot \rho_i \vec{f}_i + \nabla \cdot \vec{Q} \ . \tag{3.85}$$

This is the general global energy equation with radiation effects.

Expanding the first term of the above equation

$$\rho \frac{DH}{Dt} = \rho \left(\frac{\partial H}{\partial t} + \vec{q} \cdot \nabla H \right),$$

and applying the definition for total specific enthalpy

$$H = h + \frac{q^2}{2} \ ; \tag{3.68}$$

the first term becomes

$$\rho \frac{DH}{Dt} = \rho \frac{\partial H}{\partial t} + \rho \vec{q} \cdot \nabla h + \rho \vec{q} \cdot \frac{1}{2} \nabla (\vec{q} \cdot \vec{q}) \ .$$

Recalling the momentum balance relationship

$$\frac{1}{2}\nabla(\vec{q}\cdot\vec{q}) = \vec{q}\times(\nabla\times\vec{q}) - \frac{1}{\rho}\sum_{j=1}^{NP}\rho^j A^j \Delta\vec{q}^j - \frac{\nabla P}{\rho}, \tag{3.52}$$

and substituting it into the above equation yields

$$\rho\frac{DH}{Dt} = \rho\frac{\partial H}{\partial t} + \rho\vec{q}\cdot\left(\nabla h - \frac{\nabla P}{\rho}\right) + \rho\vec{q}\cdot\left[\vec{q}\times(\nabla\times\vec{q})\right] - \vec{q}\cdot\sum_{j=1}^{NP}\rho^j A^j\Delta\vec{q}^j. \tag{3.86}$$

This expression may be further simplified by noting that for an arbitrary vector $\vec{A}$ the following identity exists:

$$\vec{A}\cdot[\vec{A}\times(\nabla\times\vec{A})] = 0.$$

Applying the above identity to Eq. (3.86)

$$\rho\frac{DH}{Dt} = \rho\frac{\partial H}{\partial t} + \rho\vec{q}\cdot(\nabla h - \frac{\nabla P}{\rho}) - \vec{q}\cdot\sum_{j=1}^{NP}\rho^j A^j\Delta\vec{q}^j, \tag{3.86a}$$

and substituting the result back into Eq.(3.85) yields

$$\rho\frac{\partial H}{\partial t} + \rho\vec{q}\cdot(\nabla h - \frac{\nabla P}{\rho}) - \vec{q}\cdot\sum_{j=1}^{NP}\rho^j A^j\Delta\vec{q}^j + \sum_{j=1}^{NP}\left\{-\frac{2}{3}\rho^j A^j C^j (T^j - T)\right.$$

$$\left. - \frac{3\sigma}{m^j r^j}\rho^j\left[\epsilon^j (T^j)^4 - \alpha^j T^4\right] + \vec{q}^j\cdot\rho^j A^j\Delta\vec{q}^j\right\} = \frac{\partial P}{\partial t} + \nabla\cdot(\bar{\bar{\tau}}\cdot\vec{q})$$

$$+\sum_{i=1}^{NS}\vec{q}_i\cdot\rho_i\vec{f}_i + \nabla\cdot\vec{Q}.$$

For the case in which the flow may be described as steady state, adiabatic, inviscid and no body forces present the above equation becomes:

$$\rho\vec{q}\cdot(\nabla h - \frac{\nabla P}{q}) - \vec{q}\cdot\sum_{j=1}^{NP}\rho^j A^j\Delta\vec{q}^j + \sum_{j=1}^{NP}\left\{-\frac{2}{3}\rho^j A^j C^j (T^j - T)\right.$$

$$\left. - \frac{3\sigma}{m^j r^j}\rho^j\left[\epsilon^j (T^j)^4 - \alpha^j T^4\right] + \vec{q}^j\cdot\rho^j A^j\Delta\vec{q}^j\right\} = 0 \tag{3.86b}$$

This equation can be reduced to a simpler form by letting

$$B^j = \vec{q} \cdot \Delta\vec{q}^j - \vec{q}^j \cdot \Delta\vec{q}^j + \frac{2}{3} C^j (T^j - T) + \frac{3\sigma}{A^j m^j r^j} \left[\epsilon^j (T^j)^4 - \alpha^j T^4 \right] \quad (3.86c)$$

Therefore, the global energy equation becomes

$$\rho\vec{q} \cdot (\nabla h - \frac{\nabla P}{\rho}) - \sum_{j=1}^{NP} \rho^j A^j B^j = 0 \quad (3.87)$$

To expand the term in parenthesis in the above equation, it is necessary to examine the fundamental thermodynamic relationship for a system in which chemical reactions are occurring.

3.3 GASEOUS THERMODYNAMIC RELATIONS

Assumption 4 given in Section 3.1 states that the gas obeys the perfect gas law and is in chemical equilibrium, nonequilibrium or is chemically frozen. A chemically frozen gas is one in which the gas stops reacting at a given species concentration so that the molecular weight along a streamline remains at a fixed value and the ratio of specific heats is a function of temperature only. However, for the chemically reacting case the local chemical species concentrations will change in accordance with type of chemistry assumption considered for a respective analysis.

In the high-temperature low-velocity regions of the flow field, an equilibrium chemistry calculation for the gas phase is a good assumption. Local residence times of the flow are sufficiently long for all chemical reactions to proceed to completion. However, as the flow accelerates through the nozzle and exhaust plume the local flow residence time becomes less than that required for the chemical reactions to reach completion. Significant deviations from the chemical equilibrium conditions occur and ultimately the flowfield chemistry usually approaches a frozen condition. This calculation is treated best by including the kinetics in the gasdynamic calculation, thereby avoiding the problem of choosing either an equilibrium or frozen chemical analysis.

The development of the gas thermodynamic relations and the corresponding contribution to the gasdynamic relations will consider the chemical kinetics. Appendix C addresses the equilibrium chemistry analysis for gas-particle flows. Appendix E discusses the nonequilibrium chemistry analysis. Finally, a summary of the applicable equations for chemical nonequilibrium and chemical equilibrium flow is presented in Section 4.2.3.

Consider only the gas phase portion of the flow system in which there are NS-NP different species present. If the mass fraction of each species i is constant, the specific enthalpy, h, of the gas depends only on specific entropy, S, and pressure, P. However, for a variable composition

$$h = h\,(S, P, \chi_1, \chi_2, \ldots, \chi_{NS-NP})$$

and thus the total differential of h is

$$dh = \left.\frac{\partial h}{\partial S}\right|_{P,\chi_i} dS + \left.\frac{\partial h}{\partial P}\right|_{S,\chi_i} dP + \sum_{i=1}^{NS-NP} \left.\frac{\partial h}{\partial \chi_i}\right|_{S,P,\chi_j} d\chi_i \,.$$

In this expression the subscript χ_i implies that the mass fractions of all species are constant during the variation in question. On the other hand, the last term in the equation is a sum of partials in each of which the S and P are constant, together with all but one of the mass fractions.

For constant mass fractions the total differential of h may be written as

$$dh = T\,dS + \frac{1}{\rho}\,dP \,.$$

Therefore,

$$\left.\frac{\partial h}{\partial S}\right|_{P,\chi_i} = T \quad \text{and} \quad \left.\frac{\partial h}{\partial P}\right|_{S,\chi_i} = \frac{1}{\rho}$$

By defining the chemical potential μ_i as

$$\mu_i = \left.\frac{\partial h}{\partial \chi_i}\right|_{S,P,\chi_j} = h_i = \text{specific enthalpy of species i}$$

the fundamental thermodynamic relationship for a system in which chemical reactions are occurring may be written in the form

$$dh = T\,dS + \frac{dP}{\rho} + \sum_{i=1}^{NS-NP} \mu_i\, d\chi_i \tag{3.88}$$

The above equation may be rewritten as

$$\nabla h - \frac{\nabla P}{\rho} = T\nabla S + \sum_{i=1}^{NS-NP} \mu_i\, \nabla\chi_i \tag{3.89}$$

Since the pressure is a function of the gas state variables (ρ, S)

$$P = P(\rho, S)\ , \tag{3.90}$$

the expression for ∇P may be written

$$\nabla P = \left(\frac{\partial P}{\partial \rho}\right)_S \nabla\rho + \left(\frac{\partial P}{\partial S}\right)_\rho \nabla S\ .$$

Noting that

$$a^2 \equiv \left(\frac{\partial P}{\partial \rho}\right)_S \tag{3.91}$$

and,

$$\left(\frac{\partial P}{\partial S}\right)_\rho = \frac{P}{c_p - R} \qquad \text{Bridgeman's Equation} \tag{3.92}$$

where a, c_p and R are local thermodynamic equilibrium properties, ∇P becomes

$$\nabla P = a^2\,\nabla\rho + \frac{P}{c_p - R}\,\nabla S\ .$$

Rearranging terms in the above expression

$$\nabla S = \left(\frac{c_p - R}{P}\right)(\nabla P - a^2\,\nabla\rho)\ , \tag{3.93}$$

and utilizing the equation of state for an ideal gas

$$P = \rho R T , \tag{3.94}$$

Eq. (3.93) becomes:

$$\nabla S = \left(\frac{c_p - R}{\rho R T}\right)(\nabla P - a^2 \nabla \rho) . \tag{3.95}$$

Multiplying through by T

$$T \nabla S = \left(\frac{c_p - R}{\rho R}\right)(\nabla P - a^2 \nabla \rho) , \tag{3.96}$$

and rearranging terms yields

$$T \nabla S = \left(\frac{c_p}{R} - 1\right)\left(\frac{\nabla P}{\rho} - \frac{a^2 \nabla \rho}{\rho}\right) . \tag{3.97}$$

Substituting Eq.(3.97) into Eq.(3.89) results in

$$\nabla h - \frac{\nabla P}{\rho} = \left(\frac{c_p}{R} - 1\right)\left(\frac{\nabla P}{\rho} - \frac{a^2 \nabla \rho}{\rho}\right) + \sum_{i=1}^{NS-NP} \mu_i \chi_i . \tag{3.98}$$

Since particle species are not considered in the chemical reactions, the summation term upper limit may be defined as

$$NG = NS - NP \tag{3.99}$$

where NG = number of gas species present.

Equation (3.98) then becomes

$$\nabla h - \frac{\nabla P}{\rho} = \left(\frac{c_p}{R} - 1\right)\left(\frac{\nabla P}{\rho} - \frac{a^2 \nabla \rho}{\rho}\right) + \sum_{i=1}^{NG} \mu_i \nabla \chi_i . \tag{3.100}$$

Substituting Eq.(3.100) into the global energy Eq.(3.87)

$$\rho \vec{q} \cdot \left[\left(\frac{c_p}{R} - 1 \right) \left(\frac{\nabla P}{\rho} - \frac{a^2 \nabla \rho}{\rho} \right) + \sum_{i=1}^{NG} \mu_i \nabla X_i \right] - \sum_{j=1}^{NP} \rho^j A^j B^j = 0 ,$$

and expanding the dot product results in

$$\left(\frac{c_p}{R} - 1 \right) (\vec{q} \cdot \nabla P - \vec{q} \cdot a^2 \nabla \rho) + \rho \sum_{i=1}^{NG} \mu_i \vec{q} \cdot \nabla X_i - \sum_{j=1}^{NP} \rho^j A^j B^j = 0 \qquad (3.101)$$

Equation (3.101) is the expanded form of the global energy equation for flow described as steady state, adiabatic, inviscid and no body forces present.

Dividing through by $(c_p/R - 1)$ yields

$$\vec{q} \cdot \nabla P - a^2 \vec{q} \cdot \nabla \rho + \frac{\rho}{c_p/R - 1} \sum_{i=1}^{NG} \mu_i \frac{DX_i}{Dt} - \frac{1}{c_p/R - 1} \sum_{j=1}^{NP} \rho^j A^j B^j = 0. \qquad (3.102)$$

Recalling the species continuity equation

$$\rho \frac{DX_i}{Dt} = \dot{w}_i \qquad i = 1, NS , \qquad (3.25)$$

and letting,

$$B_1^j = \frac{B^j}{c_p/R - 1} \qquad (3.103)$$

and

$$\psi_1 = \frac{1}{c_p/R - 1} \sum_{i=1}^{NG} \mu_i \dot{w}_i , \qquad (3.104)$$

the final form of Eq.(3.102) becomes

$$\vec{q} \cdot \nabla P - a^2 \vec{q} \cdot \nabla \rho + \psi_1 - \sum_{j=1}^{NP} \rho^j A^j B_1^j = 0 . \qquad (3.105)$$

3.4 SUMMARY OF THE GOVERNING EQUATIONS FOR STEADY, ADIABATIC, NONEQUILIBRIUM FLOWS OF REACTING GAS-PARTICLE MIXTURES WITHOUT TRANSPORT OR BODY FORCE EFFECTS

The system of basic governing equations for any reacting flow field have now been derived. When the reactions between components of the gas mixture are known and the boundary conditions adequately specified, one should be able to solve the nonequilibrium flow system.

The pertinent equations derived in this section are summarized as follows:

Continuity equation for steady state flow

$$\nabla \cdot \rho \vec{q} = 0 \qquad \text{gas continuity equation} \qquad (3.19)$$

$$\nabla \cdot \rho^j \vec{q}^j = 0 \quad j = 1,NP \qquad \text{particle continuity equation} \qquad (3.26)$$

$$\rho \vec{q} \cdot \nabla X_i - \dot{w}_i = 0 \quad i = 1,NS \qquad \text{species continuity equation} \qquad (3.25)$$

Momentum equation for steady state, inviscid flow with no body forces

$$\rho \vec{q} \cdot \nabla \vec{q} + \sum_{j=1}^{NP} \rho^j A^j \Delta \vec{q}^j + \nabla P = 0 \qquad \text{global (gas + particle) momentum equation} \qquad (3.50)$$

where

$$A^j = \frac{9}{2}\left[\frac{\nu f^j}{m^j r^{j^2}}\right] \qquad (3.46)$$

$$\rho^j \vec{q}^j \cdot \nabla \vec{q}^j - \rho^j A^j \nabla \vec{q}^j = 0 \quad j = 1,NP \qquad \text{particle momentum equation} \qquad (3.47)$$

Energy equation for steady state, inviscid flow, with no body forces and no heat loss from the gas-particle system

$$\vec{q} \cdot \nabla P - a^2 \vec{q} \cdot \nabla \rho - \sum_{j=1}^{NP} \rho^j A^j B_1^j + \psi_1 = 0 \qquad \text{global energy equation} \qquad (3.105)$$

where

$$B_1^j = \frac{1}{c_p/R - 1}\left\{\vec{q}\cdot\Delta\vec{q}^j - \vec{q}^j\cdot\Delta\vec{q}^j + \frac{2}{3}C^j(T^j - T) + \frac{3\sigma}{A^j m^j r^j}\left[\mathcal{E}^j(T^j)^4 - \alpha^j T^4\right]\right\} \quad (3.103)$$

$$\Delta\vec{q}^j = \vec{q} - \vec{q}^j \quad (3.43)$$

and

$$C^j = \frac{k G^j}{\nu f^j} \quad (3.83)$$

$$\vec{q}^j\cdot\nabla h^j + \frac{2}{3}A^j C^j(T^j - T) + \frac{3\sigma}{m^j r^j}\left[\mathcal{E}^j(T^j)^4 - \alpha^j T^4\right] = 0 \quad j = 1, NP \quad (3.84)$$

particle energy balance equation

4. THE METHOD OF CHARACTERISTICS SOLUTION

The set of equations summarized in Section 3.4 are applicable for flow calculations in both the subsonic and supersonic regimes. Examination of the equations reveals that a closed form solution is not possible, thus necessitating a numerical solution to obtain the flowfield properties. The choice of the numerical solution is governed by the application and the flow regime of interest.

The current study addresses the nozzle-plume flowfield where the flow is everywhere supersonic except for those regions in the immediate vicinity downstream of a normal shock. Treatment of these regions are considered beyond the scope of this study, thus reducing the problem to one of analyzing a supersonic flowfield. For supersonic flow applications the method-of-characteristics provides a reliable method for numerically solving the set of governing equations. The method is characterized by rapid convergence of the numerical solution and has been shown to be unconditionally stable. This method is the one chosen for the current study.

A number of investigators (Refs. 8,9 and 10) have developed solutions employing the method-of-characteristics. In "characteristic form" the relations are transformed to a set of differential equations which apply along the characteristic directions. Prozan (Ref. 16) developed a nozzle-plume solution which includes gas thermochemistry considerations. Kliegel (Ref. 9) and Hoffman (Ref. 8) extended the method-of-characteristics to include the treatment of gas-particle flows. The present study followed the work of Prozan in the treatment of the gas equilibrium thermochemistry considerations and that of Thoenes, etc., (Ref. 39) for chemical kinetics. These considerations have been combined with the coupled gas-particle solution as formulated by Kliegel.

The original formulation by Prozan utilized the enthalpy-entropy-velocity form of the compatibility equations, i.e., independent variables are the velocity, total enthalpy and entropy. Prozan showed that the thermochemistry calculations could be uncoupled from the gasdynamic solution. Consequently the thermodynamics were calculated in terms of the independent variables, V, H, S and retrieved via interpolation from tables as needed by the characteristic solution. The routines became an integral part of the streamline normal code developed by Ruo (Ref. 17) from which the RAMP code evolved. Consequently the V, H, S form is used in the present analysis for chemical equilibrium calculations. However, when kinetics or transition between the continuum or non-continuum flow is to be treated, use of the pressure-density-velocity form of compatibility equations is more appropriate. Therefore development of both forms is given in the following sections.

4.1 DEVELOPMENT OF THE CHARACTERISTIC CURVES

The governing flow equations summarized in Section 3.4 may be written in the following expanded two-dimensional (or axisymmetric) form:

Continuity equation for steady state, particle species not considered in the chemical reactions

(3.19) $$\rho u_x + \rho v_y + u\rho_x + v\rho_y + \frac{\delta \rho v}{y} = 0 \qquad (4.1)$$

(3.26) $$\rho^j u_x^j + \rho^j v_y^j + u^j \rho_x^j + v^j \rho_y^j + \frac{\delta \rho^j v^j}{y} = 0 \qquad j = 1, NP \qquad (4.2)$$

(3.25) $$\rho u \, (\chi_i)_x + \rho v \, (\chi_i)_y - \dot{w}_i = 0 \qquad i = 1, NG \qquad (4.3)$$

Momentum equation for steady state, inviscid flow, with no body forces

(3.50) $$\rho u u_x + \rho v u_y + P_x + \sum_{j=1}^{NP} \rho^j A^j (u - u^j) = 0 \qquad (4.4)$$

$$\rho u v_x + \rho v v_y + P_y + \sum_{j=1}^{NP} \rho^j A^j (v - v^j) = 0 \qquad (4.5)$$

(3.47)
$$\rho^j u^j u_x^j + \rho^j v^j u_y^j - \rho^j A^j (u - u^j) = 0 \quad j = 1, NP \qquad (4.6)$$

$$\rho^j u^j v_x^j + \rho^j v^j v_y^j - \rho^j A^j (v - v^j) = 0 \quad j = 1, NP \qquad (4.7)$$

Energy equation for steady state, inviscid flow, with no body forces and no heat loss from the gas-particle system

(2 105)
$$u P_x + v P_y - a^2 u \rho_x - a^2 v \rho_y - \sum_{j-1}^{NP} \rho^j A^j B_1^j + \psi_1 = 0 \qquad (4.8)$$

(3.84)
$$\rho^j u^j h_x^j + \rho^j v^j h_y^j + \frac{2}{3} \rho^j A^j C^j (T^j - T) + \frac{3 \rho^j \sigma}{m^j r^j} \left[\epsilon^j (T^j)^4 - \alpha^j T^4 \right] = 0 \quad j = 1, NP \qquad (4.9)$$

The corresponding coordinate system used in this analysis is presented in Fig. 4-1.

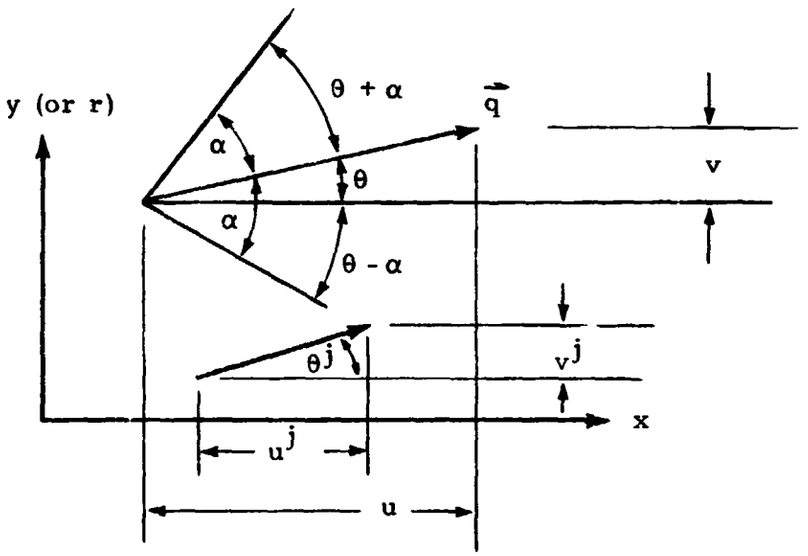

Fig. 4-1 - Coordinate System Used in the Development of the Characteristic and Compatibility Equations

To minimize the amount of "bookkeeping" that would be required in the development of the characteristic equations the governing flow Eqs. (4.1) through (4.9) will be written in the following general form

$$L_m = a_{mn} \frac{\partial \phi_n}{\partial x} + b_{mn} \frac{\partial \phi_n}{\partial y} + c_m \quad \text{for } n = 1,N \text{ and } m = 1,N \tag{4.10}$$

where:

$N = 4 + 4NP + NG$

ϕ_n represents the dependent variables $u, v, P, \rho, u^j, v^j, \rho^j, h^j$ and χ_i

a_{mn} and b_{mn} are coefficients.

If we let

$$\left.\begin{aligned}
\phi_1 &= u \\
\phi_2 &= v \\
\phi_3 &= P \\
\phi_4 &= \rho \\
\phi_{4j+1} &= u^j \quad j = 1,NP \\
\phi_{4j+2} &= v^j \quad j = 1,NP \\
\phi_{4j+3} &= \rho^j \quad j = 1,NP \\
\phi_{4j+4} &= h^j \quad j = 1,NP \\
\phi_{4+4NP+i} &= \chi_i \quad i = 1,NG;
\end{aligned}\right\} \tag{4.11}$$

equation (4.10) can be rewritten as

$$\begin{aligned}
L_m = {} & a_{m1} u_x + b_{m1} u_y + a_{m2} v_x + b_{m2} v_y + a_{m3} P_x + b_{m3} P_y \\
& + a_{m4} \rho_x + b_{m4} \rho_y + a_{m5} u^1_x + b_{m5} u^1_y + a_{m6} v^1_x + b_{m6} v^1_y \\
& + a_{m7} \rho^1_x + b_{m7} \rho^1_y + a_{m8} h^1_x + b_{m8} h^1_y + \ldots \\
& + a_{m,4j+1} u^j_x + b_{m,4j+1} u^j_y + \ldots + a_{m,4j+4} h^j_x + b_{m,4j+4} h^j_y + \ldots \\
& + a_{m,4+4NP+i} (\chi_i)_x \; b_{m,4+4NP+i} (\chi_i)_y + \sum_{m=1}^{N} c_m \quad \text{for } m = 1,N
\end{aligned} \tag{4.12}$$

We then have N independent, linear nonhomogeneous equations written in N unknown derivatives. The N linear equations for L_m may be combined to form a single differential operator by employing arbitrary multipliers and summing. Thus,

$$L = \sum_{m=1}^{N} \sigma_m L_m = 0 \tag{4.13}$$

where σ_m = arbitrary multipliers.

Assuming that the following relation holds,

$$a_{mn} \sigma_m \frac{dy}{dx} = b_{mn} \sigma_m \quad \text{for } n = 1,N \text{ and } m = 1,N; \tag{4.14}$$

Eq. (4.13) can be rewritten in the form of an ordinary differential equation. Substitution of Eqs. (4.10) and (4.14) into Eq. (4.13) yields

$$L = \sum_{m=1}^{N} (\sigma_m a_{mn} \frac{\partial \phi_n}{\partial x} + \sigma_m a_{mn} \frac{dy}{dx} \frac{\partial \phi_n}{\partial y} + c_m \sigma_m) = 0$$

or

$$L = \sum_{m=1}^{N} (\sigma_m a_{mn} \frac{\partial \phi_n}{\partial x} dx + \sigma_m a_{mn} \frac{\partial \phi_n}{\partial y} dy + c_m \sigma_m dx) = 0$$

and finally,

$$L = \sum_{m=1}^{N} (\sigma_m a_{mn} d\phi_n + c_m \sigma_m dx) = 0 \quad n = 1,N . \tag{4.15}$$

Equation (4.15) is the generalized compatibility equation and is valid if and only if Eq. (4.14) is true.

Equation (4.14) may be rewritten in the form

$$\sigma_m (a_{mn} \frac{dy}{dx} - b_{mn}) = 0 \quad n = 1,N \text{ and } m = 1,N . \tag{4.16}$$

If Eq. (4.16) has a solution other than trivial, i.e., all $\sigma_m = 0$, then the determinant of the coefficients of σ_m must be zero. Therefore:

$$D = \left| a_{mn} \frac{dy}{dx} - b_{mn} \right| = 0 \qquad n = 1,N \text{ and } m = 1,N \tag{4.17}$$

The equation D = 0 is called the characteristic equation for the system of equations (4.16). On expanding the determinant, it is seen that Eq. (4.17) is an algebraic equation of degree N and thus has N real roots. These roots are called the characteristic roots.

To analyze the determinant D, begin by substituting Eqs. (4.1), (4.4), (4.5) and (4.8) into Eq. (4.12), and putting the results into a matrix of the form:

$$\lambda = \begin{vmatrix} a_{11}, b_{11} & a_{12}, b_{12} & a_{13}, b_{13} & a_{14}, b_{14} \\ a_{21}, b_{21} & a_{22}, b_{22} & a_{23}, b_{23} & a_{24}, b_{24} \\ a_{31}, b_{31} & a_{32}, b_{32} & a_{33}, b_{33} & a_{34}, b_{34} \\ a_{41}, b_{41} & a_{42}, b_{42} & a_{43}, b_{43} & a_{44}, b_{44} \end{vmatrix} \tag{4.18}$$

This yields

$$\lambda_1 = \begin{vmatrix} \rho, 0 & 0, \rho & 0, 0 & u, v \\ \rho u, \rho v & 0, 0 & 1, 0 & 0, 0 \\ 0, 0 & \rho u, \rho v & 0, 1 & 0, 0 \\ 0, 0 & 0, 0 & u, v & -a^2 u, -a^2 v \end{vmatrix} \tag{4.19}$$

and

$$\begin{aligned} C_1 &= \frac{\delta \rho v}{y} \\ C_2 &= \sum_{j=1}^{NP} \rho^j A^j (u - u^j) \end{aligned} \tag{4.20}$$

$$C_3 = \sum_{j=1}^{NP} \rho^j A^j (v - v^j)$$

$$C_4 = \psi_i - \sum_{j=1}^{NP} \rho^j A^j B_1^j \qquad (4.20)\ \text{Cont'd}$$

Next, substituting Eqs. (4.2), (4.6), (4.7) and (4.9) into Eq. (4.12) with j = 1 (for the first particle) and putting the results into a matrix of the form of (3.18) yields

$$\lambda_2^1 = \begin{vmatrix} \rho^1, 0 & 0, \rho^1 & u^1, v^1 & 0, 0 \\ \rho^1 u^1, \rho^1 v^1 & 0, 0 & 0, 0 & 0, 0 \\ 0, 0 & \rho^1 u^1, \rho^1 v^1 & 0, 0 & 0, 0 \\ 0, 0 & 0, 0 & 0, 0 & \rho^1 u^1, \rho^1 v^1 \end{vmatrix} \qquad (4.21)$$

and

$$\left.\begin{aligned} C_5 &= \frac{\delta \rho^1 v^1}{y} \\ C_6 &= -\rho^1 A^1 (u - u^1) \\ C_7 &= -\rho^1 A^1 (v - v^1) \\ C_8 &= \rho^1 \psi_2^1 \end{aligned}\right\} \qquad (4.22)$$

where

$$\psi_2^j = \frac{2}{3} A^j C^j (T^j - T) + \frac{3\sigma}{m^j r^j} \left[\epsilon^j (T^j)^4 - \alpha^j T^4 \right]. \qquad (4.23)$$

Repeating for each particle, j, and generalizing yields

$$\lambda_2^j = \begin{vmatrix} \rho^j, 0 & 0, \rho^j & u^j, v^j & 0, 0 \\ \rho^j u^j, \rho^j v^j & 0, 0 & 0, 0 & 0, 0 \\ 0, 0 & \rho^j u^j, \rho^j v^j & 0, 0 & 0, 0 \\ 0, 0 & 0, 0 & 0, 0 & \rho^j u^j, \rho^j v^j \end{vmatrix} \quad j = 1, NP \qquad (4.24)$$

and

$$\left.\begin{aligned} C_{4j+1} &= \frac{\delta \rho^j v^j}{y} \\ C_{4j+2} &= -\rho^j A^j (u - u^j) \\ C_{4j+3} &= -\rho^j A^j (v - v^j) \\ C_{4j+4} &= \rho^j \psi_2^j \end{aligned}\right\} \quad j = 1, NP \tag{4.25}$$

Substituting Eq.(4.3) into Eq. (4.12)

$$\left.\begin{aligned} a_{m,\,4+4NP+i} &= 0 \quad \text{if} \quad m \neq n \qquad n = 4+4NP+i \\ &= \rho u \quad \text{if} \quad m = n \\ b_{m,\,4+4NP+i} &= 0 \quad \text{if} \quad m \neq n \\ &= \rho v \quad \text{if} \quad m = n \end{aligned}\right\} \tag{4.26}$$

$$c_{4+4NP+i} = -\dot{w}_i \qquad i = 1, NG; \tag{4.27}$$

and rewriting in the matrix form of (4.18) yields

$$\lambda_3 = \begin{vmatrix} \rho u, \rho v & 0, 0 & \cdots & 0, 0 \\ 0, 0 & & & \vdots \\ \vdots & & & \vdots \\ \vdots & \rho u, \rho v & & \vdots \\ \vdots & & \ddots & 0, 0 \\ 0, 0 & 0, 0 & \cdots & \rho u, \rho v \end{vmatrix} \tag{4.28}$$

If all of the coefficients of Eq.(4.12) were put into a single matrix of the form:

$$\lambda = \begin{vmatrix} a_{11}, b_{11} & a_{12}, b_{1} & \cdots & a_{1N}, b_{1N} \\ a_{21}, b_{21} & & & \vdots \\ \vdots & & & \vdots \\ \vdots & & & \vdots \\ a_{N1}, b_{N1} & \cdots & & a_{NN}, b_{NN} \end{vmatrix} \tag{4.29}$$

where

$$N = 4 + 4NP + NG ;$$

the result would be the diagonal matrix

$$\lambda = \begin{vmatrix} \lambda_1 & 0 & 0 \ldots 0 \ldots & 0 & 0 \\ 0 & \lambda_2^1 & 0 \ldots 0 \ldots & 0 & 0 \\ 0 & 0 & \lambda_2^2 \ldots 0 \ldots & 0 & 0 \\ 0 & 0 & 0 \ldots 0 \ldots & 0 & 0 \\ 0 & 0 & 0 \ldots \lambda_2^j \ldots & 0 & 0 \\ 0 & 0 & 0 \ldots 0 \ldots & 0 & 0 \\ 0 & 0 & 0 \ldots 0 \ldots & \lambda_2^{NP} & 0 \\ 0 & 0 & 0 \ldots 0 \ldots & 0 & \lambda_3 \end{vmatrix} \qquad (4.30)$$

Examining matrix (4.30), from which the coefficients a_{mn} and b_{mn} for determinant D will come, it can be seen that D will have the same form as matrix (4.30). That is:

$$D = \begin{vmatrix} D_1 & 0 & 0 \ldots 0 \ldots & 0 & 0 \\ 0 & D_2^1 & 0 \ldots 0 \ldots & 0 & 0 \\ 0 & 0 & D_2^2 \ldots 0 \ldots & 0 & 0 \\ 0 & 0 & 0 \ldots 0 \ldots & 0 & 0 \\ 0 & 0 & 0 \ldots D_2^j \ldots & 0 & 0 \\ 0 & 0 & 0 \ldots 0 \ldots & 0 & 0 \\ 0 & 0 & 0 \ldots 0 \ldots & D_2^{NP} & 0 \\ 0 & 0 & 0 \quad 0 \ldots & 0 & D_3 \end{vmatrix} \qquad (4.31)$$

where

$|D_1|$ obtains its elements from λ_1

$|D_2^1|$ from λ_2^1, etc.

For purposes of simplification, let:

$$\left.\begin{aligned} S &= u\frac{dy}{dx} - v \\ S^j &= u^j\frac{dy}{dx} - v^j \\ y' &= \frac{dy}{dx} \end{aligned}\right\} \qquad (4.32)$$

Substituting the coefficients from matrix (4.19) into matrix (4.17) and using Eq. (4.32) results in

$$\left|D_1\right| = \begin{vmatrix} \rho y' & -\rho & 0 & S \\ \rho S & 0 & y' & 0 \\ 0 & \rho S & -1 & 0 \\ 0 & 0 & S & -a^2 S \end{vmatrix} . \qquad (4.33)$$

Matrix (4.33) may be rewritten in the form

$$\left|D_1\right| = \sum_{j=1}^{4} d_{ij}\,(-1)^{i+j} N_{ij} , \qquad (4.34)$$

where

d_{ij} = elements of D_1

and

N_{ij} = the minor of d_{ij} .

Utilizing Eq. (4.34) and letting i = 3, Eq. (4.33) becomes

$$\left|D_1\right| = \cancel{d_{31}}^{\,0}\,(-1)^4 N_{31} + d_{32}\,(-1)^5 N_{32} + d_{33}\,(-1)^6 N_{33} + \cancel{d_{34}}^{\,0}\,(-1)^7 N_{34} .$$

Expanding terms

$$\left|D_1\right| = -\rho S \begin{vmatrix} \rho y' & 0 & S \\ \rho S & y' & 0 \\ 0 & S & -a^2 S \end{vmatrix} + (-1) \begin{vmatrix} \rho y' & -\rho & S \\ \rho S & 0 & 0 \\ 0 & 0 & -a^2 S \end{vmatrix} ;$$

performing the necessary matrix algebra

$$\left|D_1\right| = -\rho S\left[-\rho a^2 S(y')^2 + \rho S^3\right] - 1\ (-\rho^2 a^2 S^2) \quad ;$$

and combining terms yields

$$\left|D_1\right| = \rho^2 S^2\left[a^2(y')^2 - S^2 + a^2\right] .$$

Substituting the expressions for S and y' from Eqs. (4.32)

$$\left|D_1\right| = \rho^2\left(u\frac{dy}{dx} - v\right)^2\left[a^2\left(\frac{dy}{dx}\right)^2 - \left(u\frac{dy}{dx} - v\right)^2 + a^2\right] ;$$

expanding

$$\left|D_1\right| = \rho^2\left(u\frac{dy}{dx} - v\right)^2\left[a^2\left(\frac{dy}{dx}\right)^2 - u^2\left(\frac{dy}{dx}\right)^2 + 2uv\frac{dy}{dx} - v^2 + a^2\right];$$

and recombining terms yields the final form of $\left|D_1\right|$.

$$\left|D_1\right| = \rho^2\left(u\frac{dy}{dx} - v\right)^2\left[(a^2 - u^2)\left(\frac{dy}{dx}\right)^2 + 2uv\frac{dy}{dx} + (a^2 - v^2)\right]. \qquad (4.35)$$

The same procedure is applied to matrix (4.24). Substituting the coefficie from matrix (4.24) into matrix (4.17) and using Eqs. (4.32) results in

$$\left|D_2^j\right| = \begin{vmatrix} \rho^j y' & -\rho^j & S^j & 0 \\ \rho^j S^j & 0 & 0 & 0 \\ 0 & \rho^j S^j & 0 & 0 \\ 0 & 0 & 0 & \rho^j S^j \end{vmatrix} \quad j = 1, NP . \qquad (4.36)$$

Utilizing Eq. (4.34) and letting i = 2, Eq. (4.36) becomes

$$\left|D_2^j\right| = d_{21}(-1)^3 N_{21} + \cancel{d_{22}}^{0}(-1)^4 N_{22} + \cancel{d_{23}}^{0}(-1)^5 N_{23} + \cancel{d_{24}}^{0}(-1)^6 N_{24}$$

Expanding terms, performing the necessary matrix algebra

$$\left|D_2^j\right| = \rho^j S^j (-1) \begin{vmatrix} -\rho^j & S^j & 0 \\ \rho^j S^j & 0 & 0 \\ 0 & 0 & \rho^j S^j \end{vmatrix} = -\rho^j S^j \left[-(\rho^j)^2 (S^j)^3\right],$$

and combining terms yield

$$\left|D_2^j\right| = (\rho^j)^3 (S^j)^4 .$$

Substituting the expression for S^j from Eq.(4.32) yields the final form of $\left|D_2^j\right|$

$$\left|D_2^j\right| = (\rho^j)^3 \left(u^j \frac{dy}{dx} - v^j\right)^4 . \qquad (4.37)$$

Finally, the same procedure is applied to matrix (4.28). Substituting the coefficients from matrix (4.28) into matrix (4.17) and using Eq. (4.32) results in

$$\left|D_3\right| = \begin{vmatrix} \rho S & 0 & \cdots & 0 \\ 0 & \rho S & & \vdots \\ \vdots & & \ddots & \vdots \\ 0 & \cdots & \cdots & \rho S \end{vmatrix} = (\rho S)^{NG} .$$

Substituting the expression for S from Eq. (4.32) yields

$$\left|D^3\right| = \rho^{NG} \left(u \frac{dy}{dx} - v\right)^{NG} . \qquad (4.38)$$

Since the matrices $|D_1|$ through $|D_3|$ are the diagonal elements of matrix $|D|$, the characteristic equation for the system of Eq.(4.16) can be written as

$$\left|D\right| = \left|D_1\right| * \left|D_2^1\right| * \cdots * \left|D_2^j\right| * \cdots * \left|D_2^{NP}\right| * \left|D_3\right| = 0 \qquad (4.39)$$

Substituting Eqs.(4.35), (4.37) and (4.38) into Eq. (4.39)

$$|D| = \rho^2 \left(u \frac{dy}{dx} - v\right)^2 \left[(a^2 - u^2)\left(\frac{dy}{dx}\right)^2 + 2uv \frac{dy}{dx} + (a^2 - v^2)\right] \rho^{NG} \left(u \frac{dy}{dx} - v\right)^{NG}$$

$$(\rho^j)^3 \left(u^j \frac{dy}{dx} - v^j\right)^4 = 0 ,$$

and combining terms the final form of the characteristic equation becomes:

$$|D| = \left(u \frac{dy}{dx} - v\right)^{2+NG} \left[(a^2 - u^2)\left(\frac{dy}{dx}\right)^2 + 2uv \frac{dy}{dx} + (a^2 - v^2)\right] (\rho^j)^3 \left(u^j \frac{dy}{dx} - v^j\right)^4 = 0 \qquad (4.40)$$

Realizing that $\rho^j \neq 0$, the characteristic roots of Eq.(4.40) are determined by setting each of the three remaining terms to zero and solving for dy/dx.

Setting the first term to zero

$$\left(u \frac{dy}{dx} - v\right)^{2+NG} = 0 ,$$

and solving for dy/dx results in

$$\frac{dy}{dx} = \frac{v}{u} = \tan\theta . \qquad (4.41)$$

Setting the fourth term to zero

$$\left(u^j \frac{dy}{dx} - v^j\right)^4 = 0, \qquad j = 1, NP$$

and solving for dy/dx results in

$$\frac{dy}{dx} = \frac{v^j}{u^j} = \tan\theta^j \qquad j = 1, NP . \qquad (4.42)$$

Referring to Fig. 4-1, Eqs.(4.41) and (4.42) shows that each of the characteristics is inclined at an angle tangent to the gas velocity vector and particle velocity vectors respectively. Thus we see that the characteristics are identical with the gas streamlines and particle streamlines of the flow.

The final characteristic root is obtained by setting the second term in Eq. (4.40) to zero

$$(a^2 - u^2)\left(\frac{dy}{dx}\right)^2 + 2uv\,\frac{dy}{dx} + (a^2 - v^2) = 0\ ,$$

and solving for dy/dx in the following manner:

Applying the quadratic formula

$$\frac{dy}{dx} = \frac{-2uv \pm \sqrt{4u^2v^2 - 4(a^2 - u^2)(a^2 - v^2)}}{2(a^2 - u^2)}\ ;$$

expanding the terms under the square root

$$\frac{dy}{dx} = \frac{-2uv \pm 2\sqrt{u^2v^2 - a^4 + a^2v^2 + a^2u^2 - u^2v^2}}{2(a^2 - u^2)}\ ;$$

dividing through by 2 and combining terms under the square root

$$\frac{dy}{dx} = \frac{-uv \pm \sqrt{a^2(u^2 + v^2) - a^4}}{a^2 - u^2}$$

and finally moving a^4 outside the square root yields

$$\frac{dy}{dx} = \frac{-uv \pm a^2\sqrt{(u^2 + v^2)/a^2 - 1}}{a^2 - u^2} \qquad (4.43)$$

The first term in the square root may be simplified by utilizing the definition of the gas Mach number

$$M = q/a$$

or

$$M^2 = \frac{q^2}{a^2} = \frac{u^2 + v^2}{a^2}\ . \qquad (4.44)$$

Substituting Eq. (4.44) into Eq. (4.43) yields

$$\frac{dy}{dx} = \frac{-uv \pm a^2\sqrt{M^2 - 1}}{a^2 - u^2} \qquad (4.45)$$

Referring to Fig. 4-1, the following relations may be written:

$$u = q\cos\theta \tag{4.46}$$

$$v = q\sin\theta \tag{4.47}$$

$$\alpha = \sin^{-1}(1/M) = \sin^{-1}(a/q) \tag{4.48}$$

and

$$a = q\sin\alpha \tag{4.49}$$

$$\cot\alpha = \sqrt{M^2 - 1} \tag{4.50}$$

Substituting Eqs. (4.46) through (4.50) into Eq. (4.45)

$$\frac{dy}{dx} = \frac{-q^2\cos\theta\sin\theta \pm q^2\sin^2\alpha\cot\alpha}{q^2(\sin^2\alpha - \cos^2\theta)} ;$$

dividing through by q^2

$$\frac{dy}{dx} = \frac{-\cos\theta\sin\theta \pm \sin\alpha\cos\alpha}{\sin^2\alpha - \cos^2\theta} ;$$

and multiplying the numerator and denominator by -1 yields

$$\frac{dy}{dx} = \frac{\cos\theta\sin\theta \mp \sin\alpha\cos\alpha}{\cos^2\theta - \sin^2\alpha} \tag{4.51}$$

To simplify Eq. (4.51) consider the following trigonometric identities:

$$\sin(\theta \mp \alpha) = \sin\theta\cos\alpha \mp \cos\theta\sin\alpha , \tag{4.52}$$

$$\cos(\theta \pm \alpha) = \cos\theta\cos\alpha \mp \sin\theta\sin\alpha , \tag{4.53}$$

and

$$\cos^2\theta - \sin^2\alpha = \cos(\theta + \alpha)\cos(\theta - \alpha) . \tag{4.54}$$

Multiplying Eq. (4.52) by (4.53)

$$\sin(\theta \mp \alpha)\cos(\theta \pm \alpha) = \cos^2\alpha\sin\theta\cos\theta \mp \sin^2\theta\sin\alpha\cos\alpha \mp \cos^2\theta\sin\alpha\cos\alpha + \sin^2\alpha\sin\theta\cos\theta$$

and combining terms yield

$$\sin(\theta \mp \alpha)\cos(\theta \pm \alpha) = (\sin^2\alpha + \cos^2\alpha)\sin\theta\cos\theta \mp (\sin^2\theta + \cos^2\theta)\sin\alpha\cos\alpha ;$$

or

$$\sin(\theta \mp \alpha) \cos(\theta \pm \alpha) = \cos\theta \sin\theta \mp \sin\alpha \cos\alpha \ . \qquad (4.55)$$

By substituting Eqs.(4.54) and (4.55) into Eq. (4.51) the final form of dy/dx is obtained

$$\frac{dy}{dx} = \frac{\sin(\theta \mp \alpha) \cos(\theta \pm \alpha)}{\cos(\theta + \alpha) \cos(\theta - \alpha)} = \frac{\sin(\theta \mp \alpha)}{\cos(\theta \mp \alpha)} \ ;$$

or

$$\frac{dy}{dx} = \tan(\theta \mp \alpha) \ . \qquad (4.56)$$

Referring again to Fig. 4-1, Eq. (4.56) shows that each of the two characteristics is inclined at the Mach angle to the gas velocity vector. Thus we see that the characteristics are identical with the gas Mach lines of the flow.

In summary, the characteristics of the flow have been found to be the gas streamlines, the particle streamlines (one for each particle species) and the gas Mach lines.

4.2 DEVELOPMENT OF THE COMPATIBILITY EQUATIONS FOR GAS-PARTICLE FLOWS

The relationship assumed in Eq. (4.14)

$$a_{mn} \sigma_m \frac{dy}{dx} = b_{mn} \sigma_m \quad \text{for} \quad n = 1,N \quad \text{and} \quad m = 1,N$$

is valid along each of the characteristics. Therefore, we can now substitute the governing flow equations into Eq.(4.14) and knowing the conditions that exist along each characteristic, solve for the multipliers, σ_m. The corresponding compatibility equations that are valid along each characteristic are then derived by substituting the proper multipliers into the general compatibility equation. The compatibility equations will be first derived in the pressure-density-velocity form. This form of the equations is used by the RAMP computer program when the finite rate chemistry option is utilized. In this form, the local temperature may be solved for directly eliminating

the need for a time consuming iterative solution. The compatibility equations will then be rederived in the enthalpy-entropy-velocity form. This form of the equations is used by the RAMP computer program when the equilibrium and/or frozen chemistry option is utilized. In this form, the thermochemical data generated by the TRAN72 computer program may be used.

4.2.1 Pressure-Density-Velocity Form of the Compatibility Equations

Substituting the governing flow, Eqs. (4.1) through (4.9) into Eq. (4.14) results in

for n = 1:

$$\sigma_1 \rho \frac{dy}{dx} + \sigma_2 \left(\rho u \frac{dy}{dx} - \rho v\right) = 0$$

or

$$\sigma_1 \frac{dy}{dx} + \sigma_2 \left(u \frac{dy}{dx} - v\right) = 0 ; \tag{4.57}$$

for n = 2:

$$-\sigma_1 \rho + \rho \left(u \frac{dy}{dx} - v\right) \sigma_3 = 0$$

or

$$\sigma_1 = \left(u \frac{dy}{dx} - v\right) \sigma_3 ; \tag{4.58}$$

for n = 3:

$$\sigma_2 \frac{dy}{dx} - \sigma_3 + \left(u \frac{dy}{dx} - v\right) \sigma_4 = 0 ; \tag{4.59}$$

for n = 4:

$$\left(u \frac{dy}{dx} - v\right) \sigma_1 - a^2 \left(u \frac{dy}{dx} - v\right) \sigma_4 = 0 ; \tag{4.60}$$

for n = 4j+1:

$$\rho^j \frac{dy}{dx} \sigma_{4j+1} + \rho^j \left(u^j \frac{dy}{dx} - v^j\right) \sigma_{4j+2} = 0 \qquad j = 1, NP;$$

or

$$\frac{dy}{dx} \sigma_{4j+1} + \left(u^j \frac{dy}{dx} - v^j\right) \sigma_{4j+2} = 0 \qquad j = 1, NP ; \tag{4.61}$$

for n = 4j+2:

$$- \rho^j \sigma_{4j+1} + \rho^j \left(u^j \frac{dy}{dx} - v^j\right) \sigma_{4j+3} = 0 \qquad j = 1, NP$$

or

$$\sigma_{4j+1} = \left(u^j \frac{dy}{dx} - v^j\right) \sigma_{4j+3} \qquad j = 1, NP \; ; \tag{4.62}$$

for n = 4j+3:

$$\left(u^j \frac{dy}{dx} - v^j\right) \sigma_{4j+1} = 0 \qquad j = 1, NP \; ; \tag{4.63}$$

for n = 4j+4:

$$\rho^j \left(u^j \frac{dy}{dx} - v^j\right) \sigma_{4j+4} = 0 \qquad j = 1, NP$$

or

$$\left(u^j \frac{dy}{dx} - v^j\right) \sigma_{4j+4} = 0 \qquad j = 1, NP \; ; \tag{4.64}$$

and finally, for n = 4 + 4NP + i:

$$\rho \left(u \frac{dy}{dx} - v\right) \sigma_{4+4NP+i} = 0 \qquad i = 1, NG$$

or,

$$\left(u \frac{dy}{dx} - v\right) \sigma_{4+4NP+i} = 0 \qquad i = 1, NG \; . \tag{4.65}$$

Now, substituting the values of a_{mn} and c_m from Eqs. (4.19), (4.20), (4.24), (4.25) and (4.28) into the generalized compatibility equation (4.15) yields:

$$\begin{aligned} L = {} & (\rho \sigma_1 + \rho u \sigma_2)\, du + (\rho u \sigma_3)\, dv + (\sigma_2 + u\sigma_4)\, dP + (u\sigma_1 - a^2 u\sigma_4)\, d\rho \\ & + \sum_{j=1}^{NP} \Big[(\rho^j \sigma_{4j+1} + \rho^j u^j \sigma_{4j+2})\, du^j + (\rho^j u^j \sigma_{4j+3})\, dv^j + (u^j \sigma_{4j+1})\, d\rho^j \\ & + (\rho^j u^j \sigma_{4j+4})\, dh^j \Big] + \sum_{i=1}^{NG} \rho u \sigma_{4+4NP+i}\, d\chi_i + \left\{ \frac{\delta \rho v}{y} \sigma_1 + \sigma_2 \sum_{j=1}^{NP} \rho^j A^j (u - u^j) \right. \\ & \left. + \sigma_3 \sum_{j=1}^{NP} \rho^j A^j (v - v^j) + \sigma_4 \left(\psi_1 - \sum_{j=1}^{NP} \rho^j A^j B_1^j\right) + \sum_{j=1}^{NP} \left[\frac{\delta \rho^j v^j}{y} \sigma_{4j+1} \right. \right. \end{aligned} \tag{4.66}$$

$$- \rho^j A^j (u - u^j)\, \sigma_{4j+2} - \rho^j A^j (v - v^j)\, \sigma_{4j+3} + \rho^j \psi_2^j\, \sigma_{4j+4} \Big]$$

$$- \sum_{i=1}^{NG} \dot{w}_i\, \sigma_{4+4NP+i} \Bigg\} dx = 0 \quad . \qquad (4.66)$$

(Continued)

Equation (4.66) is the expanded form of the generalized compatibility equation and is used to determine the compatibility equations that are valid along each characteristic.

To determine the compatibility equations that are applied along gas streamlines recall that along gas streamlines

$$\frac{dy}{dx} = \frac{v}{u} \quad . \qquad (4.41)$$

Therefore, Eq. (4.57) becomes:

$$\sigma_1 \frac{dy}{dx} + \sigma_2 \underbrace{(u \frac{dy}{dx} - v)}_{\to 0} = 0 \qquad (4.57)$$

or

$$\sigma_1 = 0 \quad . \qquad (4.67)$$

Equation (4.59) becomes

$$\sigma_2 \frac{dy}{dx} - \sigma_3 + \underbrace{(u \frac{dy}{dx} - v)}_{\to 0} \sigma_4 = 0 \qquad (4.59)$$

or

$$\sigma_2 = \frac{dx}{dy} \sigma_3 = \frac{u}{v} \sigma_3 \quad . \qquad (4.68)$$

Along a gas streamline:

$$u^j \frac{dy}{dx} - v^j \neq 0 \qquad j = 1, NP \quad .$$

Therefore, Eq. (4.63) becomes:

$$(u^j \frac{dy}{dx} - v^j)\, \sigma_{4j+1} = 0 \qquad j = 1, NP \tag{4.63}$$

or

$$\sigma_{4j+1} = 0 \qquad j = 1, NP\,. \tag{4.69}$$

Similarly, Eq. (4.64) becomes

$$(u^j \frac{dy}{dx} - v^j)\, \sigma_{4j+4} = 0 \qquad j = 1, NP \tag{4.64}$$

or

$$\sigma_{4j+4} = 0 \qquad j = 1, NP\,. \tag{4.70}$$

Recalling Eq. (4.69), Eq. (4.62) yields

$$\cancelto{0}{\sigma_{4j+1}} = (u^j \frac{dy}{dx} - v^j)\, \sigma_{4j+3} = 0 \qquad j = 1, NP \tag{4.72}$$

or

$$\sigma_{4j+3} = 0 \qquad j = 1, NP\,. \tag{4.71}$$

Similarly, Eq. (4.61) yields

$$\frac{dy}{dx}\cancelto{0}{\sigma_{4j+1}} + (u^j \frac{dy}{dx} - v^j)\, \sigma_{4j+2} = 0 \qquad j = 1, NP \tag{4.61}$$

or

$$\sigma_{4j+2} = 0 \qquad j = 1, NP\,. \tag{4.72}$$

Substituting Eqs. (4.67) through (4.72) into Eq. (4.66)

$$L = \frac{\rho u^2}{v}\, \sigma_3\, du + \rho u\, \sigma_3\, dv + (\frac{u}{v}\, \sigma_3 + u\, \sigma_4)\, dP + (-a^2 u\, \sigma_4)\, d\rho$$

$$+ \sum_{i=1}^{NG} \rho u\, \sigma_{4+4NP+i}\, d\chi_i \frac{u}{v} \sum_{j=1}^{NP} \rho^j A^j (u - u^j)\, \sigma_3\, dx +$$

$$+ \sum_{j=1}^{NP} \rho^j A^j (v - v^j) \sigma_3 \, dx + \sigma_4 \left(\psi_1 - \sum_{j=1}^{NP} \rho^j A^j B_1^j\right) dx - \sum_{i=1}^{NG} \dot{w}_i \sigma_{4+4NP+i} \, dx = 0 ;$$

and rearranging terms yields

$$L = \left\{ \frac{\rho u^2}{v} du + \rho u \, dv + \frac{u}{v} dP + \sum_{j=1}^{NP} \rho^j A^j \left[\frac{u}{v} (u - u^j) + (v - v^j) \right] dx \right\} \sigma_3$$

$$+ \left\{ u \, dP - a^2 u \, d\rho + \left(\psi_1 - \sum_{j=1}^{NP} \rho^j A^j B_1^j\right) dx \right\} \sigma_4$$

$$+ \sum_{i=1}^{NG} \left[\sigma_{4+4NP+i} \left(\rho u \, d\chi_i - \dot{w}_i \, dx\right) \right] = 0 . \qquad (4.73)$$

Since the remaining multipliers, σ, are arbitrary, their coefficients must be zero. Therefore, the coefficient of σ_3 yields

$$\frac{\rho u^2}{v} du + \rho u \, dv + \frac{u}{v} dP + \sum_{j=1}^{NP} \rho^j A^j \left[\frac{u}{v} (u - u^j) + (v - v^j) \right] dx = 0$$

or

$$\rho u \, du + \rho v \, dv + dP + \sum_{j=1}^{NP} \rho^j A^j \left[(u - u^j) + \frac{v}{u} (v - v^j) \right] dx = 0 \qquad (4.74)$$

Since

$$q^2 = u^2 + v^2 ;$$

$$2q \, dq = 2u \, du + 2v \, dv$$

or

$$q \, dq = u \, du + v \, dv . \qquad (4.75)$$

Substituting Eq. (4.75) into Eq. (4.74), and dividing through by ρ yields:

$$q \, dq + \frac{dP}{\rho} + \frac{1}{\rho} \sum_{j=1}^{NP} \rho^j A^j \left[(u - u^j) + \frac{v}{u} (v - v^j) \right] dx = 0 . \qquad (4.76)$$

$$u\,dP - a^2\,u\,d\rho + \psi_1\,dx - \sum_{j=1}^{NP} \rho^j\,A^j\,B_1^j\,dx = 0$$

or

$$dP - a^2\,d\rho + \frac{\psi_1}{u}\,dx - \frac{1}{u}\sum_{j=1}^{NP} \rho^j\,A^j\,B_1^j\,dx = 0 \qquad (4.77)$$

and finally for the coefficient of $\sigma_{4+4NP+i}$

$$\sum_{i=1}^{NG} (\rho u\,d\chi_i - \dot{w}_i\,dx) = 0$$

or

$$\rho u\,d\chi_i - \dot{w}_i\,dx = 0 \qquad i = 1, NG \qquad (4.78)$$

Equations (4.76), (4.77) and (4.78) are the compatibility equations that apply along the gas streamlines.

To determine the compatibility equations that apply along Mach lines, recall that along each Mach line

$$\frac{dy}{dx} = \tan(\theta \mp \alpha) \qquad (4.56)$$

and,

$$\frac{dy}{dx} \neq \frac{v}{u}\ .$$

Equation (4.60) may be rewritten in the form:

$$(u\,\frac{dy}{dx} - v)\,(\sigma_1 - a^2\,\sigma_4) = 0 \qquad (4.60)$$

Therefore,

$$\sigma_1 - a^2\,\sigma_4 = 0$$

or

$$\sigma_1 = a^2\,\sigma_4\ . \qquad (4.79)$$

Equation (4.57) becomes

$$\sigma_1\,\frac{dy}{dx} + \sigma_2\,(u\,\frac{dy}{dx} - v) = 0$$

$$\sigma_2 = \frac{-a^2 \sigma_4 \, dy/dx}{(u \, dy/dx - v)} \quad . \tag{4.57}$$

Using Eq. (4.32)

$$S = u \frac{dy}{dx} - v \; ; \tag{4.32}$$

the expression for σ_2 becomes

$$\sigma_2 = \frac{-a^2 \sigma_4 \, dy/dx}{S} \tag{4.80}$$

Equation (4.58) becomes

$$\sigma_1 = (u \frac{dy}{dx} - v) \, \sigma_3 \tag{4.58}$$

or

$$\sigma_3 = \frac{\sigma_1}{S} = \frac{a^2 \sigma_4}{S} \tag{4.81}$$

Recall that along a Mach line

$$u^j \frac{dy}{dx} - v^j \neq 0 \qquad j = 1, NP \; .$$

Therefore, Eq. (4.63) yields

$$(u^j \frac{dy}{dx} - v^j) \, \sigma_{4j+1} = 0 \qquad j = 1, NP \tag{4.63}$$

or

$$\sigma_{4j+1} = 0 \qquad j = 1, NP \; . \tag{4.82}$$

Applying Eq. (4.82) to Eq. (4.61)

$$\frac{dv}{dx} \cancelto{0}{\sigma_{4j+1}} + (u^j \frac{dy}{dx} - v^j) \, \sigma_{4j+2} = 0 \qquad j = 1, NP \tag{4.61}$$

or,

$$\sigma_{4j+2} = 0 \qquad j = 1, NP \; . \tag{4.83}$$

Similarly, Eq. (4.62) yields

$$\cancelto{0}{\sigma_{4j+1}} = (u^j \frac{dy}{dx} - v^j) \, \sigma_{4j+3} = 0 \qquad j = 1, NP \tag{4.62}$$

or,

$$\sigma_{4j+3} = 0 \qquad j = 1, NP \; . \tag{4.84}$$

Equation (4.64) yields

$$(u^j \frac{dy}{dx} - v^j)\, \sigma_{4j+4} = 0 \qquad j = 1, NP \tag{4.64}$$

or

$$\sigma_{4j+4} = 0 \qquad j = 1, NP \; . \tag{4.85}$$

Finally, Eq. (4.65)yields

$$(u \frac{dy}{dx} - v)\, \sigma_{4+4NP+i} = 0 \qquad i = 1, NG \tag{4.65}$$

or

$$\sigma_{4+4NP+i} = 0 \qquad i = 1, NG \; . \tag{4.86}$$

Substituting Eqs. (4.79) through (4.86) into Eq. (4.66)

$$L = (\rho a^2 \sigma_4 - \frac{\rho u a^2 \sigma_4}{S} \frac{dy}{dx})\, du + \frac{\rho u a^2 \sigma_4}{S}\, dv + \left(- \frac{a^2 \sigma_4\, dy/dx}{S} + u \sigma_4\right) dP$$

$$+ \cancelto{0}{(u a^2 \sigma_4 - a^2 u \sigma_4)}\, d\rho + \left\{ \frac{\delta \rho v}{y} a^2 \sigma_4 - \frac{a^2 \sigma_4\, dy/dx}{S} \sum_{j=1}^{NP} \rho^j A^j (u - u^j) \right.$$

$$\left. + \frac{a^2 \sigma_4}{S} \sum_{j=1}^{NP} \rho^j A^j (v - v^j) + \sigma_4 \left(\psi_1 - \sum_{j=1}^{NP} \rho^j A^j B_1^j\right) \right\} dx = 0 \; ;$$

and rearranging terms yields

$$L = \left\{ \left(\rho a^2 - \frac{\rho u a^2}{S} \frac{dy}{dx}\right) du + \frac{\rho u a^2}{S}\, dv + \left(u - \frac{a^2}{S} \frac{dy}{dx}\right) dP \right.$$

$$\left. + \left[\frac{\delta \rho v}{y} a^2 + \frac{a^2}{S} \sum_{j=1}^{NP} \rho^j A^j \left[(v - v^j) - (u - u^j) \frac{dy}{dx} \right] + \psi_1 - \sum_{j=1}^{NP} \rho^j A^j B_1^j \right] dx \right\} \sigma_4 = 0$$

Since the multiplier, c_4, is arbitrary, the coefficient must be zero. Therefore,

$$\left(\rho a^2 - \frac{\rho u\, a^2}{S}\frac{dy}{dx}\right)du + \frac{\rho u\, a^2}{S}dv + \left(u - \frac{a^2}{S}\frac{dy}{dx}\right)dP + \frac{\delta\rho v\, a^2}{y}dx$$

$$+\frac{a^2}{S}\sum_{j=1}^{NP}\rho^j A^j\left[(v - v^j) - (u - u^j)\frac{dy}{dx}\right]dx + \psi_1\, dx - \sum_{j=1}^{NP}\rho^j A^j B_1^j\, dx = 0 \quad (4.87)$$

The coefficient of du may be rewritten in the form

$$\rho a^2 - \frac{\rho u\, a^2}{S}\frac{dy}{dx} = \rho a^2\left(\frac{S - u\, dy/dx}{S}\right) = \rho a^2\left(-\frac{v}{S}\right) . \quad (4.88)$$

The coefficient of dP may be rewritten in the form

$$u - \frac{a^2}{S}\frac{dy}{dx} = \frac{uS - a^2\, dy/dx}{S} = \frac{u^2\, dy/dx - uv - a^2\, dy/dx}{S}$$

or

$$u - \frac{a^2}{S}\frac{dy}{dx} = \frac{(u^2 - a^2)\, dy/dx - uv}{S} \quad (4.89)$$

Recalling that

$$\frac{dy}{dx} = \frac{-uv \pm a^2\sqrt{M^2 - 1}}{a^2 - u^2}$$

and rearranging terms

$$(a^2 - u^2)\frac{dy}{dx} = -uv \pm a^2\sqrt{M^2 - 1} ,$$

$$(u^2 - a^2)\frac{dy}{dx} = uv \mp a^2\sqrt{M^2 - 1}$$

finally,

$$(u^2 - a^2)\frac{dy}{dx} - uv = \mp a^2\sqrt{M^2 - 1} . \quad (4.90)$$

C-2

Substituting Eq.(4.90) into Eq.(4.89) yields

$$u - \frac{a^2}{S}\frac{dy}{dx} = \frac{\mp a^2\sqrt{M^2-1}}{S} \tag{4.91}$$

Substituting Eqs.(4.88) and (4.91) into Eq. (4.87)

$$-\frac{a^2}{S}\rho v\,du + \frac{a^2}{S}\rho u\,dv \mp \frac{a^2}{S}\sqrt{M^2-1}\,dP + \frac{\delta\rho v a^2}{y}\,dx$$

$$+\frac{a^2}{S}\sum_{j=1}^{NP}\rho^j A^j\left[(v-v^j)\,dx - (u-u^j)\,dy\right] + \psi_1\,dx - \sum_{j=1}^{NP}\rho^j A^j B_1^j\,dx = 0\,; \tag{4.92}$$

dividing through by $a^2\rho/S$ and rearranging terms yields

$$\left.\begin{aligned} &udv - vdu \mp \sqrt{M^2-1}\frac{dP}{\rho} + \left(\frac{\delta v}{y} + \frac{\psi_1}{\rho a^2}\right)S\,dx \\ &+\frac{1}{\rho}\sum_{j=1}^{NP}\rho^j A^j\left[(v-v^j)\,dx - (u-u^j)\,dy - \frac{S}{a^2}B_1^j\,dx\right] = 0 \end{aligned}\right\} \tag{4.93}$$

Recall that

$$u = q\cos\theta\,, \tag{4.46}$$

$$v = q\sin\theta\,, \tag{4.47}$$

and $dy/dx = \tan(\theta \mp \alpha)$ along each Mach line. (4.56)

Therefore, S dx may be rewritten in the form

$$S\,dx = \left(u\frac{dy}{dx} - v\right)dx = \left(q\cos\theta\tan(\theta \mp \alpha) - q\sin\theta\right)dx$$

and upon rearranging terms

$$S\,dx = q\,dx\left[\cos\theta\frac{\sin(\theta \mp \alpha)}{\cos(\theta \mp \alpha)} - \sin\theta\frac{\cos(\theta \mp \alpha)}{\cos(\theta \mp \alpha)}\right]$$

$$S\,dx = \frac{q\,dx}{\cos(\theta \mp \alpha)} \left[\cos\theta \sin(\theta \mp \alpha) - \sin\theta \cos(\theta \mp \alpha)\right] . \tag{4.94}$$

To simplify the above equation consider the trigonometric identity:

$$\sin\left[(\theta \mp \alpha) \pm \theta\right] = \cos\theta \sin(\theta \mp \alpha) \pm \sin\theta \cos(\theta \mp \alpha) . \tag{4.95}$$

Therefore,

$$S\,dx = \frac{q\,dx}{\cos(\theta \mp \alpha)} \sin\left[(\theta \mp \alpha) - \theta\right] = q\,dx \frac{\sin(\mp \alpha)}{\cos(\theta \mp \alpha)} ,$$

or

$$S\,dx = \mp \frac{q \sin\alpha}{\cos(\theta \mp \alpha)}\,dx . \tag{4.96}$$

From Eqs. (4.46) and (4.47) above the following expressions can be written:

$$du = - q \sin\theta\,d\theta + \cos\theta\,dq \tag{4.97}$$

and

$$dv = q \cos\theta\,d\theta + \sin\theta\,dq . \tag{4.98}$$

Therefore, the first term in Eq. (4.93) may be written as

$$u\,dv - v\,du = q^2 \cos^2\theta\,d\theta + q\,dq \sin\theta \cos\theta + q^2 \sin^2\theta\,d\theta - q\,dq \sin\theta \cos\theta$$

or

$$u\,dv - v\,du = q^2\,d\theta\,(\cos^2\theta + \sin^2\theta)$$

and finally,

$$u\,dv - v\,du = q^2\,d\theta . \tag{4.99}$$

Substituting Eqs. (4.96), (4.99) and (4.50) into Eq. (4.93) yields the final form of the compatibility equations that apply along Mach lines

$$q^2\,d\theta \mp \cot\alpha \frac{dP}{\rho} + \left(\frac{\delta q \sin\theta}{y} + \frac{\psi_1}{\rho a^2}\right)\left(\mp \frac{q \sin\alpha}{\cos(\theta \mp \alpha)}\right) dx + \frac{1}{\rho} \sum_{j=1}^{NP} \rho^j A^j \left[(v - v^j)\,dx - (u - u^j)\right]dy - \frac{S}{a^2} B_1^j\,dx \Big] = 0 \tag{4.100}$$

Finally, to determine the compatibility equations that apply along the particle streamlines recall that along each particle streamline

$$\left(u^j \frac{dy}{dx} - v^j\right)^4 = 0 ,$$

or

$$\frac{dy}{dx} = \frac{v^j}{u^j} = \tan\theta^j \tag{4.42}$$

and that,

$$\frac{dy}{dx} \neq \frac{v}{u} .$$

We may immediately rewrite Eqs. (4.79), (4.80) and (4.81) which were derived for Mach lines.

Equation (4.79)

$$\sigma_1 = a^2 \sigma_4 , \tag{4.101}$$

Equation (4.80)

$$\sigma_2 = -\frac{a^2 \sigma_4}{S} \frac{dy}{dx} , \tag{4.102}$$

Equation (4.81)

$$\sigma_3 = \frac{a^2 \sigma_4}{S} . \tag{4.103}$$

Then applying Eq. (4.42) to Eq. (4.61) yields

$$\frac{dy}{dx} \sigma_{4j+1} + \cancelto{0}{\left(u^j \frac{dy}{dx} - v^j\right)} \sigma_{4j+2} = 0 \qquad j = 1, NP , \tag{4.61}$$

$$\frac{dy}{dx} \sigma_{4j+1} = 0 \qquad j = 1, NP$$

or

$$\sigma_{4j+1} = 0 \qquad j = 1, NP . \tag{4.104}$$

Similarly, Eq. (4.65) yields

$$\left(u \frac{dy}{dx} - v\right) \sigma_{4+4NP+i} = 0 \qquad i = 1, NG \tag{4.65}$$

or,

$$\sigma_{4+4NP+i} = 0 \qquad i = 1, NG \; . \tag{4.105}$$

Substituting Eqs. (4.101) through (4.105) into Eq. (4.66)

$$L = \left(\rho a^2 \sigma_4 - \frac{\rho u a^2}{S} \sigma_4 \frac{dy}{dx}\right) du + \frac{\rho u a^2}{S} \sigma_4 \, dv + \left(u\sigma_4 - \frac{a^2 \sigma_4}{S} \frac{dy}{dx}\right) dP$$

$$+ (u a^2 \sigma_4 - u a^2 \sigma_4) \, d\rho + \sum_{j=1}^{NP} \left[\rho^j u^j \sigma_{4j+2} \, du^j + \rho^j u^j \sigma_{4j+3} \, dv^j\right.$$

$$\left. + \rho^j u^j \sigma_{4j+4} \, dh^j\right] + \frac{\delta \rho v a^2 \sigma_4}{y} \, dx - \frac{a^2 \sigma_4}{S} \frac{dy}{dx} \sum_{j=1}^{NP} \rho^j A^j (u - u^j) \, dx$$

$$+ \frac{a^2 \sigma_4}{S} \sum_{j=1}^{NP} \rho^j A^j (v - v^j) \, dx + \sigma_4 \psi_1 \, dx - \sigma_4 \sum_{j=1}^{NP} \rho^j A^j B_1^j \, dx$$

$$+ \sum_{j=1}^{NP} \left[-\rho^j A^j (u - u^j) \sigma_{4j+2} - \rho^j A^j (v - v^j) \sigma_{4j+3} + \rho^j \psi_2^j \sigma_{4j+4}\right] dx = 0 \; ;$$

and rearranging terms yields:

$$L = \left\{\rho a^2 \left(1 - \frac{u}{S} \frac{dy}{dx}\right) du + \rho a^2 \frac{u}{S} dv + \left(u - \frac{a^2}{S} \frac{dy}{dx}\right) dP + \frac{\delta \rho v a^2}{y} \, dx \right.$$

$$\left. + \frac{a^2}{S} \sum_{j=1}^{NP} \rho^j A^j \left[(v - v^j) \, dx - (u - u^j) \, dy - \frac{S}{a^2} B_1^j \, dx\right] + \psi_1 \, dx \right\} \sigma_4$$

$$+ \sum_{j=1}^{NP} \left[\rho^j u^j \, du^j - \rho^j A^j (u - u^j) \, dx\right] \sigma_{4j+2}$$

$$+ \sum_{j=1}^{NP} \left[\rho^j u^j \, dv^j - \rho^j A^j (v - v^j) \, dx\right] \sigma_{4j+3}$$

$$+ \sum_{j=1}^{NP} \left[\rho^j u^j \, dh^j + \rho^j \psi_2^j \, dx\right] \sigma_{4j+4} = 0 \; . \tag{4.106}$$

Since the remaining multipliers, σ, are arbitrary their coefficients must be zero. Therefore, the coefficient of σ_4 yields

$$\rho a^2 \left(1 - \frac{u}{S}\frac{dy}{dx}\right) du + \rho a^2 \frac{u}{S}\, dv + \left(u - \frac{a^2}{S}\frac{dy}{dx}\right) dP + \frac{\delta \rho v a^2}{y}\, dx$$

$$+ \frac{a^2}{S} \sum_{j=1}^{NP} \rho^j A^j \left[(v - v^j)\, dx - (u - u^j)\, dy - \frac{S}{a^2} B_1^j\, dx\right] + \psi_1\, dx = 0; \qquad (4.107)$$

the coefficient of σ_{4j+2} yields

$$\sum_{j=1}^{NP} \left[\rho^j u^j\, du^j - \rho^j A^j (u - u^j)\, dx\right] = 0 ;$$

or

$$u^j\, du^j = A^j (u - u^j)\, dx \qquad j = 1, NP . \qquad (4.108)$$

Similarly, for the coefficient of σ_{4j+3}

$$\sum_{j=1}^{NP} \left[\rho^j u^j\, dv^j - \rho^j A^j (v - v^j)\, dx\right] = 0$$

or

$$u^j\, dv^j = A^j (v - v^j)\, dx \qquad j = 1, NP ; \qquad (4.109)$$

and finally for the coefficient of σ_{4j+4}

$$\sum_{j=1}^{NP} \left[\rho^j u^j\, dh^j + \rho^j \psi_2^j\, dx\right] = 0$$

or

$$u^j\, dh^j = -\psi_2^j\, dx \qquad j = 1, NP . \qquad (4.110)$$

Recalling that

$$\psi_2^j = \frac{2}{3} A^j C^j (T^j - T) + \frac{3\sigma}{m^j r^j} \left[\epsilon^j (T^j)^4 - \alpha^j T^4\right]; \qquad (4.23)$$

Eq. (4.110) becomes

$$u^j \, dh^j = -\left[\frac{2}{3} A^j C^j (T^j - T) + \frac{3\sigma}{m^j r^j} \left[\epsilon^j (T^j)^4 - \alpha^j T^4\right]\right] dx \qquad j = 1, NP \qquad (4.111)$$

Before evaluating Eq. (4.107) it is necessary to examine Eqs. (4.57) through (4.60) with $S = u\, dy/dx - v$ non-vanishing ($S \neq 0$) as in the case along a particle streamline.

Equation (4.60):

$$S\sigma_1 - a^2 S\sigma_4 = 0$$

or

$$\sigma_1 = a^2 \sigma_4 \; ; \qquad (4.112)$$

Equation (4.58):

$$\sigma_1 = S\sigma_3$$

or

$$\sigma_3 = \sigma_1/S$$

finally,

$$\sigma_3 = \frac{a^2 \sigma_4}{S} \; ; \qquad (4.113)$$

Equation (4.57):

$$\sigma_1 \frac{dy}{dx} + \sigma_2 S = 0$$

or

$$\sigma_2 = -\frac{\sigma_1}{S}\frac{dy}{dx} = -\frac{a^2 \sigma_4}{S}\frac{dy}{dx} \; ; \qquad (4.114)$$

and finally

Equation (4.59):

$$\sigma_2 \frac{dy}{dx} - \sigma_3 + S\sigma_4 = 0 \; . \qquad (4.59)$$

Substituting Eqs. (4.112) through (4.114) into Eq. (4.59) yields

$$-\frac{a^2 \sigma_4}{S}\left(\frac{dy}{dx}\right)^2 - \frac{a^2 \sigma_4}{S} + S\,\sigma_4 = 0$$

or

$$\left[-a^2\left(\frac{dy}{dx}\right)^2 - a^2 + S^2\right]\sigma_4 = 0 \qquad (4.115)$$

In the above equation, either σ_4 is zero or its coefficient is zero.
Along particle streamlines:

$$\frac{dy}{dx} = \frac{v^j}{u^j} \qquad (4.42)$$

Assuming $\sigma_4 = 0$, Eq. (4.115) becomes

$$\left[-a^2\left(\frac{v^j}{u^j}\right)^2 - a^2 + S^2\right] = 0 .$$

Recalling that

$$S = u\frac{dy}{dx} - v$$

or

$$S = u\frac{v^j}{u^j} - v \neq 0 ;$$

Eq. (4.115) may again be rewritten in the form:

$$-a^2\left(\frac{v^j}{u^j}\right)^2 - a^2 + u^2\left(\frac{v^j}{u^j}\right)^2 - 2uv\frac{v^j}{u^j} + v^2 = 0$$

or

$$(u^2 - a^2)\left(\frac{v^j}{u^j}\right)^2 - 2uv\frac{v^j}{u^j} + (v^2 - a^2) = 0$$

Solving for $\frac{v^j}{u^j}$,

$$\frac{v^j}{u^j} = \frac{2uv \pm \sqrt{4u^2v^2 - 4(u^2 - a^2)(v^2 - a^2)}}{2(u^2 - a^2)}$$

upon rearranging terms,

$$\frac{v^j}{u^j} = \frac{uv \pm \sqrt{u^2 v^2 - u^2 v^2 + a^2 v^2 + a^2 u^2 - a^4}}{u^2 - a^2}$$

$$\frac{v^j}{u^j} = \frac{uv \pm \sqrt{a^2 (u^2 + v^2) - a^4}}{u^2 - a^2}$$

$$\frac{v^j}{u^j} = \frac{uv \pm a^2 \sqrt{(u^2 + v^2)/a^2 - 1}}{u^2 - a^2}$$

$$\frac{v^j}{u^j} = \frac{-uv \pm a^2 \sqrt{(u^2 + v^2)/a^2 - 1}}{a^2 - u^2} \quad .$$

This equation has the same solution as Eq. (4.43), that is:

$$\frac{v^j}{u^j} = \tan(\theta \mp \alpha) \quad .$$

However, for a particle streamline,

$$\frac{v^j}{u^j} = \tan\theta^j \quad ;$$

therefore the assumption that the coefficient of σ_4 in Eq. (4.115) vanishes does not apply along particle streamlines, hence the multiplier σ_4 must be equal to zero and Eq. (4.107) is not valid along particle streamlines. In summary, the compatibility equations that apply along particle streamlines are:

$$\frac{dy}{dx} = \frac{v^j}{u^j} = \tan\theta^j \qquad j = 1, NP$$

$$u^j \, du^j = A^j (u - u^j) \, dx \qquad j = 1, NP \tag{4.108}$$

$$u^j \, dv^j = A^j (v - v^j) \, dx \qquad j = 1, NP \tag{4.109}$$

and

$$u^j\, dh^j = -\left[\frac{2}{3} A^j C^j (T^j - T) + \frac{3\sigma}{m^j r^j}\left[\epsilon^j (T^j)^4 - \alpha^j T^4\right]\right] dx \qquad j = 1, NP \quad (4.111)$$

4.2.2 Enthalpy-Entropy-Velocity Form of the Compatibility Equations

Recall the pressure-density-velocity form of the compatibility equations that apply along gas streamlines

$$q\, dq + \frac{dP}{\rho} + \frac{1}{\rho}\sum_{j=1}^{NP} \rho^j A^j \left[(u - u^j) + \frac{v}{u}(v - v^j)\right] dx = 0 \qquad (4.76)$$

$$dP - a^2\, d\rho + \frac{\psi_1}{u}\, dx - \frac{1}{u}\sum_{j=1}^{NP} \rho^j A^j B_1^j\, dx = 0 \qquad (4.77)$$

$$\rho u\, dX_i - \dot{w}_i\, dx = 0 \qquad i = 1, NG \qquad (4.78)$$

Equation (4.76) may be written in the enthalpy-entropy form using the thermodynamic relations

$$T\, dS = dh - \frac{dP}{\rho} - \sum_{i=1}^{NG} \mu_i\, dX_i \qquad (3.88)$$

$$H = h + \frac{q^2}{2} \qquad (3.68)$$

and the definition of the local speed of sound.

From Ref. 9 it is shown that since the particle velocity and temperature do not change through a discontinuity and since there is a finite relaxation time associated with changes in the particle properties, then an infinitesimal weak disturbance must travel at the gas-sonic speed. That is to say, the local speed of sound of the gas-particle mixture is unaffected by the particle and is identical with the speed of sound of the gas; hence, it can be expressed by the following

$$a^2 = \gamma R T .$$

From Eq. (3.68) we may write

$$dH = dh + q\,dq$$

or

$$dh = dH - q\,dq \qquad (4.116)$$

Rearranging Eq. (3.88)

$$\frac{dP}{\rho} = dh - Tds - \sum_{i=1}^{NG} \mu_i\, dX_i ,$$

substituting for dh from Eq. (4.116)

$$\frac{dP}{\rho} = dH - q\,dq - TdS - \sum_{i=1}^{NG} \mu_i\, dX_i$$

and rearranging terms yields

$$\frac{dP}{\rho} + q\,dq = dH - TdS - \sum_{i=1}^{NG} \mu_i\, dX_i . \qquad (4.117)$$

Substituting this result back into Eq. (4.76) yields the final form of the compatibility equation

$$dH - TdS - \sum_{i=1}^{NG} \mu_i\, dX_i + \frac{1}{\rho} \sum_{j=1}^{NP} \rho^j A^j \left[(u - u^j) + \frac{v}{u} (v - v^j) \right] dx = 0 \qquad (4.118)$$

Equation (4.118) may be rewritten using the definition of the local speed of sound.

Solving for temperature

$$T = \frac{q^2 \sin^2 \alpha}{\gamma R} \qquad (4.119)$$

and substituting the result back into Eq. (4.118) yields

$$dH - q^2 \frac{\sin^2\alpha}{\gamma R}\, dS - \sum_{i=1}^{NG} \mu_i\, d\chi_i + \frac{1}{\rho} \sum_{j=1}^{NP} \rho^j A^j \left[(u - u^j) + \frac{v}{u}(v - v^j)\right] dx = 0 \quad (4.120)$$

Next, we examine Eq. (4.78).

Equation (4.78) may be rewritten in the form

$$\rho\, q \cos\theta\, d\chi_i = \dot{w}_i\, dx \qquad i = 1, NG \quad (4.121)$$

or

$$d\chi_i = \frac{\dot{w}_i\, dx}{\rho\, q \cos\theta} \qquad i = 1, NG \quad (4.122)$$

By letting

$$\dot{\chi}_i = \frac{\dot{w}_i}{\rho} ,$$

Eq. (4.122) becomes

$$d\chi_i = \frac{\dot{\chi}_i\, dx}{q \cos\theta} \qquad i = 1, NG$$

or finally,

$$q \cos\theta\, d\chi_i = \dot{\chi}_i\, dx \qquad i = 1, NG . \quad (4.123)$$

Equation (4.77) may be written in the enthalpy-entropy form using the thermodynamic relations

$$T\, dS = \left(\frac{C_p}{R} - 1\right)\left(\frac{dP}{\rho} - \frac{a^2\, d\rho}{\rho}\right) \quad (3.97)$$

and

$$\psi_1 = \frac{1}{C_p/R - 1} \sum_{i=1}^{NG} \mu_i\, \dot{w}_i . \quad (3.104)$$

Rearranging Eq. (3.97)

$$dP - a^2\, d\rho = \frac{\rho\, T\, dS}{(C_p/R - 1)} , \quad (4.124)$$

and substituting for T from Eq. (4.119) yields

$$dP - a^2\, d\rho = \frac{\rho\, q^2 \sin^2\alpha\, dS}{\gamma\,(C_p - R)} \quad . \tag{4.125}$$

Replacing the first two terms of Eq. (4.77) with Eq. (4.125)

$$\frac{\rho\, q^2 \sin^2\alpha\, dS}{\gamma\,(C_p - R)} + \frac{\psi_1}{u}\, dx - \frac{1}{u}\sum_{j=1}^{NP} \rho^j A^j B_1^j\, dx = 0 :$$

substituting for ψ_1 from Eq. (3.104)

$$\frac{\rho\, q^2 \sin^2\alpha\, dS}{\gamma\,(C_p - R)} + \frac{R}{(C_p - R)\,u}\sum_{i=1}^{NG} \mu_i \dot{w}_i\, dx - \frac{1}{u}\sum_{j=1}^{NP} \rho^j A^j B_1^j\, dx = 0 \tag{4.126}$$

and using the relation $\dot{\chi}_i = \dot{w}_i/\rho$ results in

$$\frac{\rho\, q^2 \sin^2\alpha\, dS}{\gamma\,(C_p - R)} + \frac{R\rho}{(C_p - R)\, q\cos\theta}\sum_{i=1}^{NG} \mu_i \dot{\chi}_i\, dx - \frac{1}{u}\sum_{j=1}^{NP} \rho^j A^j B_1^j\, dx = 0 .$$

Dividing through by $\rho R/(C_p - R)$, and recalling Eq. (4.119) yields

$$T\, dS + \frac{1}{q\cos\theta}\sum_{i=1}^{NG} \mu_i \dot{\chi}_i\, dx \frac{(C_p - R)}{u\rho R}\sum_{j=1}^{NP} \rho^j A^j B_1^j\, dx = 0 \tag{4.127}$$

where

$$B_1 = \frac{R}{C_p - R}\left\{\vec{q}\cdot\Delta\vec{q}^j - \vec{q}^j\cdot\Delta\vec{q}^j + \frac{2}{3}C^j\,(T^j - T) + \frac{3\sigma}{A^j m^j r^j}\left[\epsilon^j (T^j)^4 - \alpha^j T^4\right]\right\} \tag{4.103}$$

The final form of the compatibility equations that apply along gas streamlines are summarized as follows:

Equation (4.127)

$$T\, dS + \frac{1}{q\cos\theta}\sum_{i=1}^{NG} \mu_i \dot{\chi}_i\, dx - \frac{(C_p - R)}{u\rho R}\sum_{j=1}^{NP} \rho^j A^j B_1^j\, dx = 0, \tag{4.128}$$

Equation (4.118)

$$dH - T\,dS - \sum_{i=1}^{NG} \mu_i\, d\chi_i + \frac{1}{\rho}\sum_{j=1}^{NP} \rho^j A^j \left[(u - u^j) + \frac{v}{u}(v - v^j)\right] dx = 0 \qquad (4.129)$$

and

Equation (4.123)

$$q \cos\theta\, d\chi_i = \dot{\chi}_i\, dx \qquad i = 1, NG \qquad (4.130)$$

The pressure-density-velocity form of the compatibility equations that apply along Mach lines are

$$q^2\, d\theta \mp \cot\alpha \frac{dP}{\rho} + \left(\frac{\delta q \sin\theta}{y} + \frac{\psi_1}{\rho a^2}\right)\left(\mp \frac{q \sin\alpha}{\cos(\theta \mp \alpha)}\right) dx$$

$$+ \frac{1}{\rho}\sum_{j=1}^{NP} \rho^j A^j \left[(v - v^j)\, dx - (u - u^j)\, dy - \frac{S}{a^2} B_1^j\, dx\right] = 0 . \qquad (4.100)$$

Substituting Eq. (4.117)

$$\frac{dP}{\rho} = dH - T\,dS - q\,dq - \sum_{i=1}^{NG} \mu_i\, d\chi_i \qquad (4.117)$$

into Eq. (4.100)

$$q^2\, d\theta \mp \cot\alpha \left(dH - T\,dS - q\,dq - \sum_{i=1}^{NG} \mu_i\, d\chi_i\right) \mp \frac{q \sin\alpha}{\cos(\theta \mp \alpha)}\left(\frac{\delta q \sin\theta}{y}\right.$$

$$\left. + \frac{\psi_1}{\rho a^2}\right) dx + \frac{1}{\rho}\sum_{j=1}^{NP} \rho^j A^j \left[(v - v^j)\, dx - (u - u^j)\, dy \pm \frac{q \sin\alpha}{\cos(\theta \mp \alpha)\, q^2 \sin^2\alpha} B_1^j\, dx\right] = 0 ;$$

dividing through by q^2, and expanding wherever possible yields:

$$d\theta \mp \frac{\cot\alpha}{q^2}\, dH \pm \frac{\cot\alpha}{q^2}\, T\, dS \pm \frac{\cot\alpha}{q}\, dq \pm \frac{\cot\alpha}{q^2} \sum_{i=1}^{NG} \mu_i\, dX_i$$

$$\mp \frac{\delta \sin\alpha \sin\theta}{\cos(\theta \mp \alpha)\, y}\, dx \mp \frac{\sin\alpha\, \psi_1}{q \rho a^2 \cos(\theta \mp \alpha)}\, dx + \frac{1}{\rho q^2} \sum_{j=1}^{NP} \rho^j A^j \left[(v - v^j)\, dx - (u - u^j)\, dy \right.$$

$$\left. \pm \frac{B_1^j\, dx}{q \sin\alpha \cos(\theta \mp \alpha)} \right] = 0 \qquad (4.131)$$

Equation (4.131) may be rewritten in the following manner:

Recall that

$$T = \frac{q^2 \sin^2\alpha}{\gamma R} \,, \qquad (4.119)$$

$$\psi_1 = \frac{1}{C_p/R - 1} \sum_{i=1}^{NG} \mu_i \dot{w}_i \qquad (4.104)$$

and

$$\dot{X}_i = \frac{\dot{w}_i}{\rho} \,.$$

Therefore, the third term of Eq. (4.131) may be rewritten as

$$\frac{\cot\alpha}{q^2}\, T\, dS = \frac{\cot\alpha\, q^2 \sin^2\alpha}{q^2 \gamma R}\, dS$$

or

$$\frac{\cot\alpha}{q^2}\, T\, dS = \frac{\sin\alpha \cos\alpha}{\gamma R}\, dS \,. \qquad (4.132)$$

The seventh term may be rewritten as

$$\frac{\sin\alpha\, \psi_1\, dx}{q \rho a^2 \cos(\theta \mp \alpha)} = \frac{\sin\alpha \left[\frac{1}{(C_p/R - 1)} \sum_{i=1}^{NG} \mu_i \dot{w}_i \right] dx}{\rho q^3 \sin^2\alpha \cos(\theta \mp \alpha)} \qquad (4.133)$$

or

$$\frac{\sin\alpha\ \psi_1\ dx}{q\rho a^2\cos(\theta \mp \alpha)} = \frac{\dfrac{dx}{C_p\sqrt{R-1}}\displaystyle\sum_{i=1}^{NG}\mu_i\dot{\chi}_i}{q^3\sin\alpha\cos(\theta \mp \alpha)} \quad . \tag{4.133}$$

A portion of the eighth term may be rewritten as

$$\begin{aligned}(v - v^j)\,dx - (u - u^j)\,dy &= dx\left[(v - v^j) - (u - u^j)\frac{dy}{dx}\right] \\ &= dx\left[(v - v^j) - (u - u^j)\tan(\theta \mp \alpha)\right] \\ &= dx\left[(v - v^j)\frac{\cos(\theta \mp \alpha)}{\cos(\theta \mp \alpha)} - (u - u^j)\frac{\sin(\theta \mp \alpha)}{\cos(\theta \mp \alpha)}\right]\end{aligned}$$

finally,

$$(v - v^j)\,dx - (u - u^j)\,dy = \frac{dx}{\cos(\theta \mp \alpha)}\left[(v - v^j)\cos(\theta \mp \alpha) - (u - u^j)\sin(\theta \mp \alpha)\right] . \tag{4.134}$$

Substituting Eqs. (4.132), (4.133) and (4.134) back into Eq. (4.131 yields the final form of the compatibility equations that apply along Mach lines

$$\begin{aligned}&d\theta \pm \frac{\cot\alpha}{q}\,dq \pm \frac{\sin\alpha\cos\alpha\,dS}{\gamma R} \mp \frac{\cot\alpha\,dH}{q^2} \mp \frac{\delta\sin\theta\sin\alpha\,dx}{y\cos(\theta \mp \alpha)} \\ &\pm \frac{dx}{\rho q^2\cos(\theta \mp \alpha)}\sum_{j=1}^{NP}\rho^j A^j\left[\pm (v - v^j)\cos(\theta \mp \alpha) \mp (u - u^j)\sin(\theta \mp \alpha) + \frac{B_1^j}{q\sin\alpha}\right] \\ &\pm \frac{\cot\alpha}{q^2}\sum_{i=1}^{NG}\mu_i\,d\chi_i \mp \frac{\dfrac{dx}{C_p\sqrt{R-1}}\displaystyle\sum_{i=1}^{NG}\mu_i\dot{\chi}_i}{q^3\sin\alpha\cos(\theta \mp \alpha)} = 0\end{aligned} \tag{4.135}$$

4.2.3 Compatibility Equations for Equilibrium and/or Frozen Chemistry

Recall the enthalpy-entropy-velocity form of the compatibility equations.

Along gas streamlines:

$$T\,dS + \frac{1}{q\cos\theta}\sum_{i=1}^{NG}\mu_i\,\dot{\chi}_i\,dx - \frac{(C_p - R)}{u\rho R}\sum_{j=1}^{NP}\rho^j A^j B_1^j\,dx = 0 \qquad (4.128)$$

and

$$dH - T\,dS - \sum_{i=1}^{NG}\mu_i\,d\chi_i + \frac{1}{\rho}\sum_{j=1}^{NP}\rho^j A^j\left[(u-u^j) + \frac{v}{u}(v-v^j)\right]dx = 0\,. \qquad (4.129)$$

Along Mach lines:

$$d\theta \pm \frac{\cot\alpha}{q}\,dq \pm \frac{\sin\alpha\cos\alpha\,dS}{\gamma R} \mp \frac{\cot\alpha\,dH}{q^2} \mp \frac{\delta\sin\theta\sin\alpha\,dx}{y\cos(\theta\mp\alpha)}$$

$$\pm \frac{dx}{\rho q^2\cos(\theta\mp\alpha)}\sum_{j=1}^{NP}\rho^j A^j\left[\pm(v-v^j)\cos(\theta\mp\alpha) \mp (u-u^j)\sin(\theta\mp\alpha) + \frac{B_1^j}{q\sin\alpha}\right]$$

$$\pm \frac{\cot\alpha}{q^2}\sum_{i=1}^{NG}\mu_i\,d\chi_i \mp \frac{\dfrac{dx}{C_p/R-1}\displaystyle\sum_{i=1}^{NG}\mu_i\dot{\chi}_i = 0}{q^3\sin\alpha\cos(\theta\mp\alpha)}\,. \qquad (4.135)$$

For any closed system which is in the state of complete equilibrium the terms

$$\sum_{i=1}^{NG}\mu_i\,d\chi_i$$

and

$$\sum_{i=1}^{NG}\mu_i\,\dot{\chi}_i$$

must be zero (Ref. 40). Furthermore, for chemically frozen flow $\dot{\chi}_i$ and $d\chi_i$ are obviously zero since there are no changes in the chemical species concentration. Therefore, for the case of equilibrium and/or frozen chemistry the above equations reduce to the form:

Along gas streamlines:

$$T\,dS - \frac{(C_p - R)}{u\rho R}\sum_{j=1}^{NP}\rho^j A^j B_1^j\,dx = 0\,, \tag{4.128a}$$

and

$$dH - T\,dS + \frac{1}{\rho}\sum_{j=1}^{NP}\rho^j A^j\left[(u-u^j) + \frac{v}{u}(v-v^j)\right]dx = 0. \tag{4.129a}$$

Along Mach lines:

$$d\theta \pm \frac{\cot\alpha}{q}\,dq \pm \frac{\sin\alpha\cos\alpha\,dS}{\gamma R} \mp \frac{\cot\alpha\,dH}{q^2} \mp \frac{\delta\,\sin\theta\,\sin\alpha\,dx}{y\cos(\theta\mp\alpha)}$$

$$\pm \frac{dx}{\rho q^2\cos(\theta\mp\alpha)}\sum_{j=1}^{NP}\rho^j A^j\left[\pm(v-v^j)\cos(\theta\mp\alpha) \mp (u-u^j)\sin(\theta\mp\alpha) + \frac{B_1^j}{q\sin\alpha}\right] \tag{4.135a}$$

4.2.4 Summary of the Compatibility Equations for Gas-Particle Flows

The characteristics of the flow have been found to be the gas streamlines, gas Mach lines and particle streamlines (one for each particle species).

Pressure-Density-Velocity Form (for Chemical Non-Equilibrium and Transition Flow Applications)

The slope of the gas streamline, θ, is given by

$$\frac{dy}{dx} = \tan\theta \tag{4.41}$$

and the compatibility equations which apply along gas streamlines are:

$$q\,dq + \frac{dP}{\rho} + \frac{1}{\rho}\sum_{j=1}^{NP}\rho^j A^j\left[(u-u^j) + \frac{v}{u}(v-v^j)\right]dx = 0\,, \tag{4.76}$$

$$dP - a^2\,d\rho + \frac{\psi_1}{u}\,dx - \frac{1}{u}\sum_{j=1}^{NP}\rho^j A^j B_j^j\,dx = 0 \tag{4.77}$$

and

$$\rho u \, dX_i - \dot{w}_i \, dx = 0 \qquad i = 1, NG \tag{4.78}$$

The slope of the Mach lines (left running characteristics and right running characteristics) is given by

$$\frac{dy}{dx} = \tan(\theta \mp \alpha) \tag{4.56}$$

and the compatibility equations which apply along each Mach line are:

$$q^2 \, d\theta \mp \cot\alpha \frac{dP}{\rho} + \left(\frac{\delta \, q \sin\theta}{y} + \frac{\psi_1}{\rho a^2} \right) \left(\mp \frac{q \sin\alpha}{\cos(\theta \mp \alpha)} \right) dx$$

$$+ \frac{1}{\rho} \sum_{j=1}^{NP} \rho^j A^j \left[(v - v^j) \, dx - (u - u^j) \, dy - \frac{S}{a^2} B_1^j \, dx \right] = 0 \tag{4.100}$$

Equation (4.100) may be written in the more convenient form

$$d\theta \mp \cot\alpha \frac{dP}{\rho q^2} \mp \frac{\delta \sin\theta \sin\alpha \, dx}{y \cos(\theta \mp \alpha)} \pm \frac{dx}{\rho q^2 \cos(\theta \mp \alpha)} \sum_{j=1}^{NP} \rho^j A^j \left[\pm (v - v^j) \cos(\theta \mp \alpha) \right.$$

$$\left. \mp (u - u^j) \sin(\theta \mp \alpha) + \frac{B_1^j}{q \sin\alpha} \right] \mp \frac{\frac{dx}{C_p/R - 1} \sum_{i=1}^{NG} \mu_i \dot{X}_1}{q^3 \sin\alpha \cos(\theta \mp \alpha)} = 0 \; . \tag{4.136}$$

The particle streamline direction, θ^j, is given by

$$\frac{dy}{dx} = \frac{v^j}{u^j} = \tan\theta^j \qquad j = 1, NP \tag{4.42}$$

and the compatibility equations which apply along particle streamlines are:

$$u^j \, du^j = A^j (u - u^j) \, dx \qquad j = 1, NP \tag{4.108}$$

$$u^j \, dv^j = A^j (v - v^j) \, dx \qquad j = 1, NP \tag{4.109}$$

and

$$u^j\, dh^j = -\left[\frac{2}{3} A^j C^j (T^j - T) + \frac{3\sigma}{m^j r^j}\left[\varepsilon^j (T^j)^4 - \alpha^j T^4\right]\right] dx \qquad j = 1, NP \qquad (4.111)$$

Enthalpy-Entropy-Velocity Form (For Chemical Equilibrium and/or Frozen Flow Applications)

The slope of the gas streamline, θ, is given by

$$\frac{dy}{dx} = \tan\theta \qquad (4.41)$$

and the compatibility equations which apply along gas streamlines are:

$$dH - T\, dS + \frac{1}{\rho}\sum_{j=1}^{NP} \rho^j A^j \left[(u - u^j) + \frac{v}{u}(v - v^j)\right] dx = 0 \qquad (4.129a)$$

$$T\, dS - \frac{(C_p - R)}{u\rho R}\sum_{j=1}^{NP} \rho^j A^j B_1^j\, dx = 0 \qquad (4.128a)$$

where

$$B_1^j = \frac{1}{C_p/R - 1}\left\{\vec{q} \cdot \Delta\vec{q}^j - \vec{q}^j \cdot \Delta\vec{q}^j + \frac{2}{3} C^j (T^j - T) + \frac{3\sigma}{A^j m^j r^j}\left[\varepsilon^j (T^j)^4 - \alpha^j T^4\right]\right\} \qquad (3.103)$$

$$A^j = \frac{9}{2}\left[\frac{\nu f^j}{m^j (r^j)^2}\right] \qquad (3.46)$$

and

$$C^j = \frac{k G^j}{\nu f^j} \qquad (3.83)$$

The slope of the Mach lines is given by

$$\frac{dy}{dx} = \tan(\theta \mp \alpha) \qquad (4.56)$$

and the compatibility equations which apply along each Mach line are:

$$d\theta \pm \frac{\cot\alpha}{q}\, dq \pm \frac{\sin\alpha \cos\alpha\, dS}{\gamma R} \mp \frac{\cot\alpha\, dH}{q^2} \mp \frac{\delta \sin\theta \sin\alpha\, dx}{y \cos(\theta \mp \alpha)}$$

$$\pm \frac{dx}{\rho q^2 \cos(\theta \mp \alpha)} \sum_{j=1}^{NP} \rho^j A^j \left[\pm (v - v^j) \cos(\theta \mp \alpha) \mp (u - u^j) \sin(\theta \mp \alpha) + \frac{B_1^j}{q \sin\alpha} \right] \quad (4.135a)$$

The independent variables are $x, y, q, \theta, P, \rho, u^j, v^j, h^j$ and ρ^j in the Pressure-Density-Velocity form, and $x, y, q, \theta, H, S, u^j, v^j, h^j$ and ρ^j in the Enthalpy-Entropy-Velocity form. 6+4NP unknowns are required to completely define the gas-particle flow at a given location in the flow field. The above equations provide only 6+3NP compatibility relations. This is because a compatibility relation does not exist for the particle density and results from the assumption that the particles do not contribute to the pressure acting on a control volume in the gas-particle system. As originally shown by Kliegel, (Ref.10) this can be resolved by utilizing the following incompressible flow relation to obtain the particle density.

$$d\dot{m}^j = (2\pi)^\delta \rho^j \left\{ u^j (y^j)^\delta\, dy^j - v^j (y^j)^\delta\, dx^j \right\} \quad (4.137)$$

and

δ takes on the values

$\delta = 0$ for two-dimensional flow
$\delta = 1$ for axisymmetric flow

4.3 FINITE DIFFERENCE SOLUTION OF THE COMPATIBILITY EQUATIONS

To solve the system of compatibility equations it is first necessary to write these equations in finite difference form. Notice that the equations describing the particle properties were derived for a discrete particle. To account for more than one particle size or species, n discrete particles are allowed in the numerical solution. The streamline of each additional particle

is an additional characteristic curve; and the solution is obtained by applying the particle compatibility equations independently for each particle along its streamline.

The equations are cast in a form suitable for the calculation of an interior point in the flow field. For special points, such as along the nozzle axis, the nozzle wall, the limiting particle streamline and a free boundary, certain boundary conditions in the flow field are known which allow some of the equations to be discarded. The characteristic net for an interior point is illustrated by Fig. 4-2.

The difference equations for the gas-particle system of compatibility equations in coefficient form is given below.

The slope of the gas streamline, θ, is given by

$$\frac{\Delta y}{\Delta x}_{5-3} = \tan\theta_{5,3} \tag{4.138}$$

and the compatibility equations which apply along gas streamlines are

Pressure-Density-Velocity Form for Finite Rate Chemistry

$$\bar{q}_{5,3}\,\Delta q_{5-3} + \frac{\Delta P_{5-3}}{\bar{\rho}_{5,3}} + C_{3_P} = 0 \tag{4.139}$$

$$\Delta P_{5-3} - \bar{a}^2_{5,3}\,\Delta\rho_{5-3} + C_{2_P} = 0 \tag{4.140}$$

and,

$$\bar{\rho}_{5,3}\,\bar{u}_{5,3}\,\Delta X_{i_{5-3}} - \bar{\dot{w}}_{i_{5,3}}\,\Delta x_{5-3} = 0 \qquad i = 1, NG\ ; \tag{4.141}$$

where the barred values are averages over the step length, and the coefficients are defined as follows:

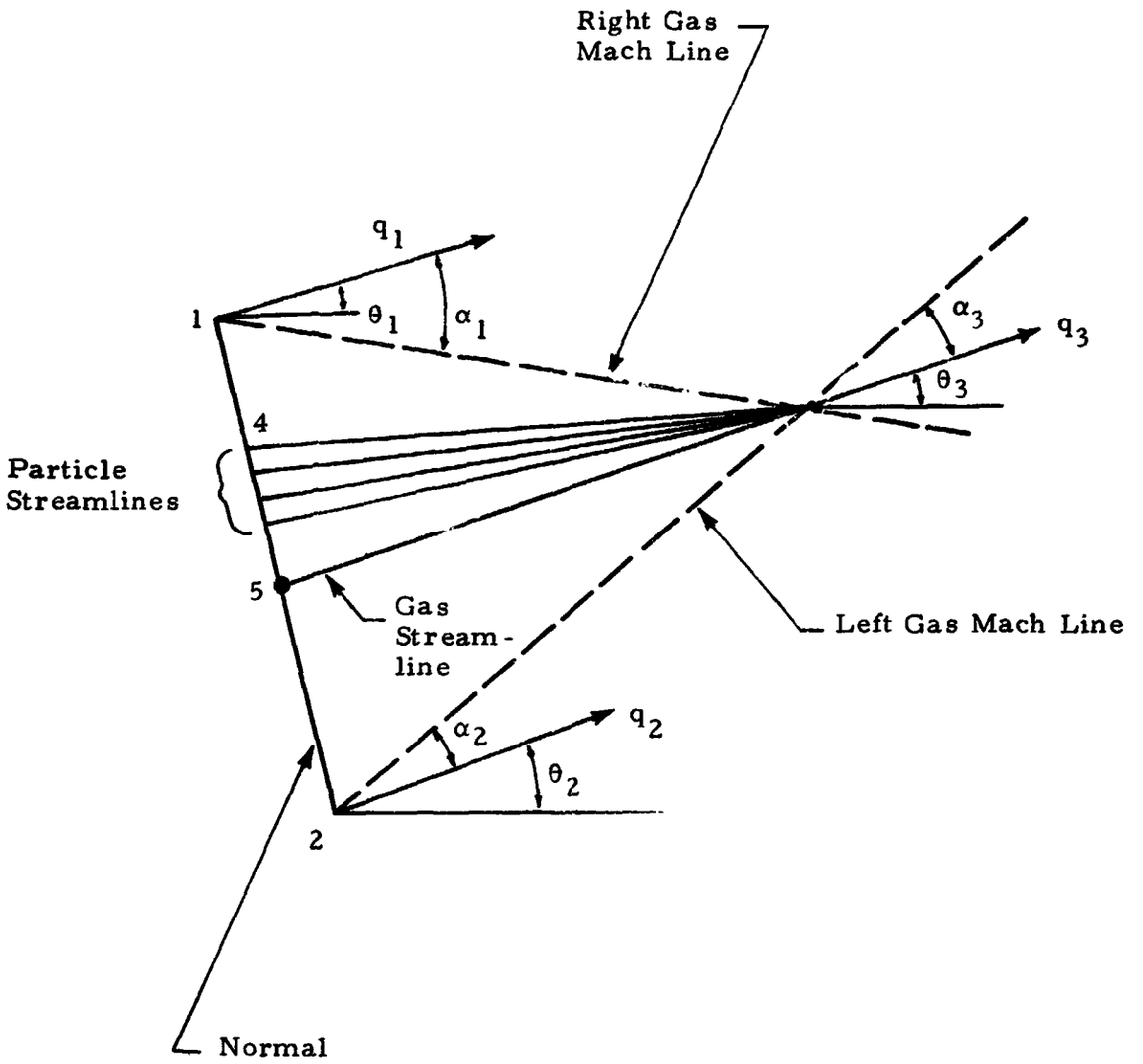

Fig. 4-2 - Characteristic Net for an Interior Point

$$C_{3_p} = \frac{1}{\bar{\rho}_{5,3}} \sum_{j=1}^{NP} \bar{\rho}^j_{5,3} \bar{A}^j_{5,3} \left[(\bar{u}_{5,3} - \bar{u}^j_{5,3}) \cos\bar{\theta}_{5,3} + (\bar{v}_{5,3} - \bar{v}^j_{5,3}) \sin\bar{\theta}_{5,3} \right] \Delta L_{5-3}$$

and

$$C_{2_p} = \left\{ \left[\frac{1}{\frac{\bar{C}_{p_{5,3}}}{\bar{R}_{5,3}} - 1} \right] \sum_{i=1}^{NG} \bar{\mu}_{i_{5,3}} \dot{\bar{w}}_{i_{5,3}} - \sum_{j=1}^{NP} \bar{\rho}^j_{5,3} \bar{A}^j_{5,3} \bar{B}^j_{1_{5,3}} \right\} \frac{\Delta L_{5-3}}{\bar{q}_{5,3}} \quad .$$

ΔL is the step size along the streamline.

Enthalpy-Entropy-Velocity Form for Equilibrium and/or Frozen Chemistry

$$\Delta H_{5-3} = \bar{T}_{5,3} \Delta S_{5-3} - C_{3_p} \tag{4.142}$$

and

$$\Delta S_{5-3} = C_2 \tag{4.143}$$

where

$$C_2 = \left(\frac{\bar{C}_{p_{5,3}}}{\bar{R}_{5,3}} - 1 \right) \left[\sum_{j=1}^{NP} \bar{\rho}^j_{5,3} \bar{A}^j_{5,3} \bar{B}^j_{1_{5,3}} \right] \frac{\Delta L_{5-3}}{\bar{\rho}_{5,3} \bar{T}_{5,3} \bar{q}_{5,3}} \quad .$$

The slope of the Mach lines (left running denoted by subscript 2 and right running denoted by subscript 1) is given by

$$\frac{\Delta y}{\Delta x}_{1,2} = \tan\bar{\beta}_{1,2} \tag{4.144}$$

where

$$\bar{\beta}_{1,2} = \bar{\theta}_{1,2} \mp \lambda_{1,2} \bar{\alpha}_{1,2}$$

and λ takes on the values

$$\lambda_1 = \begin{cases} 1 & \text{for interior solution} \\ 1 & \text{for lower boundary solution} \\ 0 & \text{for upper boundary solution} \end{cases}$$

$$\lambda_2 = \begin{cases} 1 & \text{for interior solution} \\ 0 & \text{for lower boundary solution} \\ 1 & \text{for upper boundary solution.} \end{cases}$$

The compatibility equations which apply along each Mach line are:

Pressure-Density-Velocity Form

$$\Delta\theta_{1,2} \mp Q_{1,2}\,\Delta P_{1,2} - G_{1,2} \pm Cl_{1,2} = 0 \qquad (4.145)$$

where the coefficients are defined as follows

$$Q_{1,2} = \frac{\cos\bar{\alpha}_{1,2}}{\sin\bar{\alpha}_{1,2}\,\bar{q}^2_{1,2}\,\bar{\rho}_{1,2}}$$

$$G_{1,2} = \frac{\delta \sin\bar{\sigma}_{1,2} \sin\bar{\alpha}_{1,2}\,\Delta x_{1,2}}{\bar{y}_{1,2}\cos\bar{\beta}_{1,2}}$$

and

$$Cl_{1,2} = \left\{ \sum_{j=1}^{NP} \bar{\rho}^j_{1,2}\,\bar{A}^j_{1,2} \left[\pm (\bar{v}_{1,2} - \bar{v}^j_{1,2}) \cos\bar{\beta}_{1,2} \mp (\bar{u}_{1,2} - \bar{u}^j_{1,2}) \sin\bar{\beta}_{1,2} \right.\right.$$

$$\left.\left. + \frac{\bar{B}^j_{1,2}}{\bar{q}_{1,2}\sin\bar{\alpha}_{1,2}} \right] \right\} \frac{\Delta x_{1,2}}{\bar{\rho}_{1,2}\,\bar{q}^2_{1,2}\cos\bar{\beta}_{1,2}} \mp \frac{\sum_{i=1}^{NG} \bar{\mu}_{i_{1,2}}\,\bar{\dot{v}}_{i_{1,2}}}{\bar{q}^3_{1,2}\sin\bar{\alpha}_{1,2}\cos\bar{\beta}_{1,2}} \frac{\Delta x_{1,2}}{\dfrac{\bar{C}_{p_{1,2}}}{\bar{R}_{1,2}} - 1} .$$

Enthalpy-Entropy-Velocity Form

$$\Delta\theta_{1,2} \pm Q_{1,2}\,\Delta q_{1,2} \pm B_{1,2} \mp CI_{1,2}\,\Delta H_{1,2} \mp G_{1,2} \pm Cl_{1,2} = 0 \qquad (4.146)$$

where the coefficients are defined as follows

$$Q_{1,2} = \frac{\cos\bar{\alpha}_{1,2}}{\sin\bar{\alpha}_{1,2}\,\bar{q}_{1,2}}$$

$$B_{1,2} = \frac{\sin\bar{\alpha}_{1,2}\cos\bar{\alpha}_{1,2}\,\Delta S_{1,2}}{\bar{\alpha}_{1,2}\,\bar{R}_{1,2}}$$

$$CI_{1,2} = \frac{\cos\bar{\alpha}_{1,2}}{\sin\bar{\alpha}_{1,2}\,\bar{q}^2_{1,2}}$$

$$G_{1,2} = \frac{\delta\sin\bar{\theta}_{1,2}\sin\bar{\alpha}_{1,2}\,\Delta x_{1,2}}{\bar{y}_{1,2}\cos\bar{\beta}_{1,2}}$$

and

$$Cl_{1,2} = \left\{\sum_{j=1}^{NP}\bar{\rho}^j_{1,2}\,\bar{A}^j_{1,2}\left[\pm(\bar{v}_{1,2}-\bar{v}^j_{1,2})\cos\bar{\beta}_{1,2} \mp (\bar{u}_{1,2}-\bar{u}^j_{1,2})\sin\bar{\beta}_{1,2} + \frac{\bar{B}^j_{1,2}}{\bar{q}_{1,2}\sin\bar{\alpha}_{1,2}}\right]\right\}\frac{\Delta x_{1,2}}{\bar{\rho}_{1,2}\,\bar{q}^2_{1,2}\cos\bar{\beta}_{1,2}}$$

Finally, the particle streamline direction, θ^j, is given by

$$\frac{\Delta y^j}{\Delta x^j}\,4\text{-}3 = \tan\bar{\theta}^j_{4,3} \qquad j = 1, NP \qquad (4.147)$$

and the compatibility equations which apply along particle streamlines are:

$$\Delta u^j_{4-3} = \overline{C2}^j_{4,3}\,\Delta x^j_{4-3} \qquad j = 1, NP \tag{4.148}$$

$$\Delta v^j_{4-3} = \overline{C3}^j_{4,3}\,\Delta x^j_{4-3} \qquad j = 1, NP \tag{4.149}$$

and

$$\Delta h^j_{4-3} = \overline{C4}^j_{4,3}\,\Delta x^j_{4-3} \qquad j = 1, NP \tag{4.150}$$

where the coefficients are defined as follows

$$C2^j_{4,3} = A^j_{4,3}\,\frac{(u_{4,3} - u^j_{4,3})}{u^j_{4,3}}$$

$$C3^j_{4,3} = A^j_{4,3}\,\frac{(v_{4,3} - v^j_{4,3})}{u^j_{4,3}} \tag{4.150a}$$

and

$$C4^j_{4,3} = \frac{-\left\{\frac{2}{3}A^j_{4,3}\,C^j_{4,3}\,(T^j_{4,3} - T_{4,3}) + \frac{3\sigma_{4,3}}{m^j_{4,3}\,r^j_{4,3}}\left[\mathcal{E}^j_{4,3}\,(T^j_{4,3})^4 - \alpha^j_{4,3}\,T^4_{4,3}\right]\right\}}{u^j_{4,3}}.$$

The difference form of Kliegel's incompressible flow relation is

$$\Delta\dot{m}^j_{1,2} = (\quad)^{\delta}\,\overline{\rho}^j_{1,2}\left[\overline{u}^j_{1,2}\,(\overline{y}^j_{1,2})^{\delta}\,\Delta y^j_{1,2} - \overline{v}^j_{1,2}\,(\overline{y}^j_{1,2})^{\delta}\,\Delta x^j_{1,2}\right]. \tag{4.151}$$

An iterative solution is employed to determine the properties of the flow at the new point. For the first pass of the solution the barred values are approximated by the conditions at the known points, e.g.,

$$\overline{\theta}_1 = \theta_1$$

After the appropriate set of equations has been solved a new estimate of the barred values is made, e.g.,

$$\overline{\theta}_1 = \frac{\theta_1 + \theta_3}{2}.$$

The iterative process is continued until the desired convergence is reached.

The mechanics of the numerical solution for a typical point are quite involved. Section 7 presents the mechanics of the numerical solution for the different types of points encountered in a typical gas-particle flow problem.

4.4 DEVELOPMENT OF THE PARTICLE DENSITY RELATIONSHIPS

Kliegel's incompressible flow relation

$$d\dot{m}^j = (2\pi)^\delta \rho^j \left| u^j (y^j)^\delta \, dy^j - v^j (y^j)^\delta \, dx^j \right| \qquad (4.137)$$

will now be used to develop the particle density relationships required to solve for the particle density at each of the different types of points encountered in a typical gas-particle flow problem. The particle density relationships will be derived for an interior point, a lower boundary point, a particle limiting streamline point and an upper boundary point. The particle density relationships for the remaining type points (such as a shock point) will not be developed because each is subject to the same boundary conditions as one of the above four cases and therefore yield the same results.

4.4.1 Interior Point Solution

Consider the characteristic net for an interior point

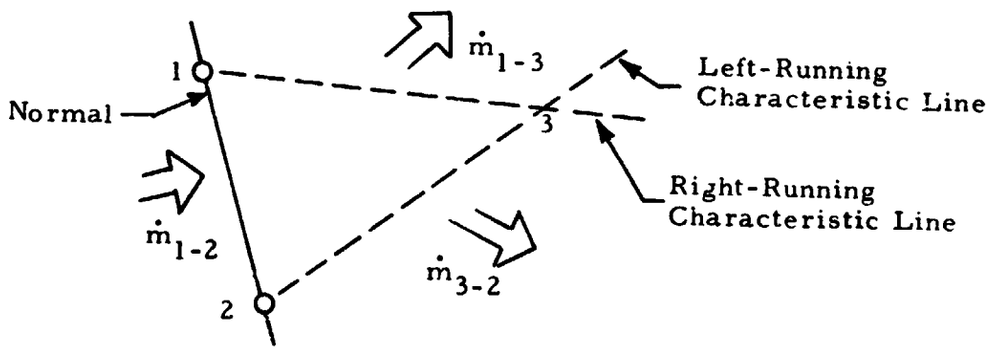

Applying the principle of conservation of mass to the above system, we may write

$$\dot{m}_{1-2} = \dot{m}_{1-3} + \dot{m}_{3-2} \tag{4.152}$$

Each term in the above equation may be solved for by applying Eq. (4.137) between the proper points.

Points 1-3:

$$\dot{m}_{1-3} = (2\pi)^{\delta}\left[\frac{(\rho_1 u_1 + \rho_3 u_3)}{2}\,\frac{(y_1 y_1^{\delta} - y_3 y_3^{\delta})}{2^{\delta}} - \frac{(\rho_1 v_1 + \rho_3 v_3)}{2}\,\frac{(y_1^{\delta} + y_3^{\delta})}{2^{\delta}}\,(x_1 - x_3)\right] \tag{4.153}$$

Points 3-2:

$$\dot{m}_{3-2} = (2\pi)^{\delta}\left[\frac{(\rho_2 u_2 + \rho_3 u_3)}{2}\,\frac{(y_3 y_3^{\delta} - y_2 y_2^{\delta})}{2^{\delta}} - \frac{(\rho_2 v_2 + \rho_3 v_3)}{2}\,\frac{(y_2^{\delta} + y_3^{\delta})}{2^{\delta}}\,(x_3 - x_2)\right] \tag{4.154}$$

and points 1-2:

$$\dot{m}_{1-2} = (2\pi)^{\delta}\left[\frac{(\rho_1 u_1 + \rho_2 u_2)}{2}\,\frac{(y_1 y_1^{\delta} - y_2 y_2^{\delta})}{2^{\delta}} - \frac{(\rho_1 v_1 + \rho_2 v_2)}{2}\,\frac{(y_1^{\delta} + y_2^{\delta})}{2^{\delta}}\,(x_1 - x_2)\right] \tag{4.155}$$

The particle density relationship at point 3 may now be determined by substituting Eqs. (4.153), (4.154) and (4.155) into Eq. (4.152) and solving for ρ_3. Equation (4.152) becomes:

$$\begin{aligned}(\rho_1 u_1 + \rho_2 u_2)\,(y_1 y_1^{\delta} - y_2 y_2^{\delta}) - (\rho_1 v_1 + \rho_2 v_2)\,(y_1^{\delta} + y_2^{\delta})\,(x_1 - x_2) \\ = (\rho_1 u_1 + \rho_3 u_3)\,(y_1 y_1^{\delta} - y_3 y_3^{\delta}) - (\rho_1 v_1 + \rho_3 v_3)\,(y_1^{\delta} + y_3^{\delta})\,(x_1 - x_3) \\ + (\rho_2 u_2 + \rho_3 u_3)\,(y_3 y_3^{\delta} - y_2 y_2^{\delta}) - (\rho_2 v_2 + \rho_3 v_3)\,(y_2^{\delta} + y_3^{\delta})\,(x_3 - x_2)\,.\end{aligned} \tag{4.156}$$

To solve for ρ_3:

expand Eq. (4.156)

$$\rho_1 u_1 (y_1 y_1^{\delta} - y_2 y_2^{\delta}) - \rho_1 v_1 (y_1^{\delta} + y_2^{\delta}) (x_1 - x_2) + \rho_2 u_2 (y_1 y_1^{\delta} - y_2 y_2^{\delta})$$

$$- \rho_2 v_2 (y_1^{\delta} + y_2^{\delta}) (x_1 - x_2) = \rho_3 u_3 (y_1 y_1^{\delta} - y_3 y_3^{\delta})$$

$$- \rho_1 v_1 (y_1^{\delta} + y_3^{\delta}) (x_1 - x_3) + \rho_3 u_3 (y_3 y_3^{\delta} - y_2 y_2^{\delta}) + \rho_1 u_1 (y_1 y_1^{\delta} - y_3 y_3^{\delta})$$

$$+ \rho_2 u_2 (y_3 y_3^{\delta} - y_2 y_2^{\delta}) - \rho_2 v_2 (y_2^{\delta} + y_3^{\delta}) (x_3 - x_2) - \rho_3 v_3 (y_1^{\delta} + y_3^{\delta}) (x_1 - x_3)$$

$$- \rho_3 v_3 (y_2^{\delta} + y_3^{\delta}) (x_3 - x_2) ;$$

combine terms to form coefficients of ρ_1, ρ_2 and ρ_3

$$\rho_1 \left[u_1 (y_1 y_1^{\delta} - y_2 y_2^{\delta}) - v_1 (y_1^{\delta} + y_2^{\delta}) (x_1 - x_2)\right] + \rho_2 \left[u_2 (y_1 y_1^{\delta} - y_2 y_2^{\delta})\right.$$

$$\left. - v_2 (y_1^{\delta} + y_2^{\delta}) (x_1 - x_2)\right] = \rho_3 \left[u_3 (y_1 y_1^{\delta} - y_3 y_3^{\delta} + y_3 y_3^{\delta} - y_2 y_2^{\delta})\right.$$

$$\left. - v_3 (y_1^{\delta} + y_3^{\delta}) (x_1 - x_3) - v_3 (y_2^{\delta} + y_3^{\delta}) (x_3 - x_2)\right]$$

$$+ \rho_1 \left[u_1 (y_1 y_1^{\delta} - y_3 y_3^{\delta}) - v_1 (y_1^{\delta} + y_3^{\delta}) (x_1 - x_3)\right] + \rho_2 \left[u_2 (y_3 y_3^{\delta} - y_2 y_2^{\delta})\right.$$

$$\left. - v_2 (y_2^{\delta} + y_3^{\delta}) (x_3 - x_2)\right] ;$$

isolate ρ_3 and its coefficient

$$\rho_3 \left\{u_3 (y_1 y_1^{\delta} - y_2 y_2^{\delta}) - v_3 \left[(y_1^{\delta} + y_3^{\delta}) (x_1 - x_3) + (y_2^{\delta} + y_3^{\delta}) (x_3 - x_2)\right]\right\}$$

$$= \rho_1 \left[u_1 (y_1 y_1^{\delta} - y_2 y_2^{\delta}) - v_1 (y_1^{\delta} + y_2^{\delta}) (x_1 - x_2) - u_1 (y_1 y_1^{\delta} - y_3 y_3^{\delta})\right.$$

$$+ v_1(y_1^\delta + y_3^\delta)(x_1 - x_3)\Big] + \rho_2\Big[u_2(y_1 y_1^\delta - v_2 y_2^\delta) - v(y_1^\delta + y_2^\delta)(x_1 - x_2)$$

$$- u_2(y_3 y_3^\delta - y_2 y_2^\delta) + v_2(y_2^\delta + y_3^\delta)(x_3 - x_2)\Big] ;$$

combining terms on the right hand side of the equal sign

$$= \rho_1\Big\{u_1(y_3 y_3^\delta - y_2 y_2^\delta) - v_1\Big[(y_1^\delta + y_2^\delta)(x_1 - x_2) - (y_1^\delta + y_3^\delta)(x_1 - x_3)\Big]\Big\}$$

$$+ \rho_2\Big\{u_2(y_1 y_1^\delta - y_3 y_3^\delta) - v_2\Big[(y_1^\delta + y_2^\delta)(x_1 - x_2) - (y_2^\delta + y_3^\delta)(x_3 - x_2)\Big]\Big\} ;$$

and finally solving for ρ_3

$$\rho_3 = \frac{1}{u_3(y_1 y_1^\delta - y_2 y_2^\delta) - v_3\Big[(y_1^\delta + y_3^\delta)(x_1 - x_3) + (y_2^\delta + y_3^\delta)(x_3 - x_2)\Big]}\Big[\rho_1\Big\{u_1(y_3 y_3^\delta - y_2 y_2^\delta)$$

$$- v_1\Big[(y_1^\delta + y_2^\delta)(x_1 - x_2) - (y_1^\delta + y_3^\delta)(x_1 - x_3)\Big]\Big\} + \rho_2\Big\{u_2(y_1 y_1^\delta - y_3 y_3^\delta)$$

$$- v_2\Big[(y_1^\delta + y_2^\delta)(x_1 - x_2) - (y_2^\delta + y_3^\delta)(x_3 - x_2)\Big]\Big\}\Big]. \qquad (4.157)$$

4.4.2 Lower Boundary Point Solution

The lower wall point and free boundary point are the two types of lower boundary points encountered in a typical gas-particle flow problem. To derive a relationship for the particle density at a lower boundary point it will be assumed that: (1) the lower boundary runs parallel to the x-axis (for two-phase only), and (2) the particle streamlines run parallel to the lower boundary when in the vicinity of the lower boundary. These assumptions are valid in nearly all of the flow problems encountered.

Consider the characteristic ne. for a point on a lower boundary

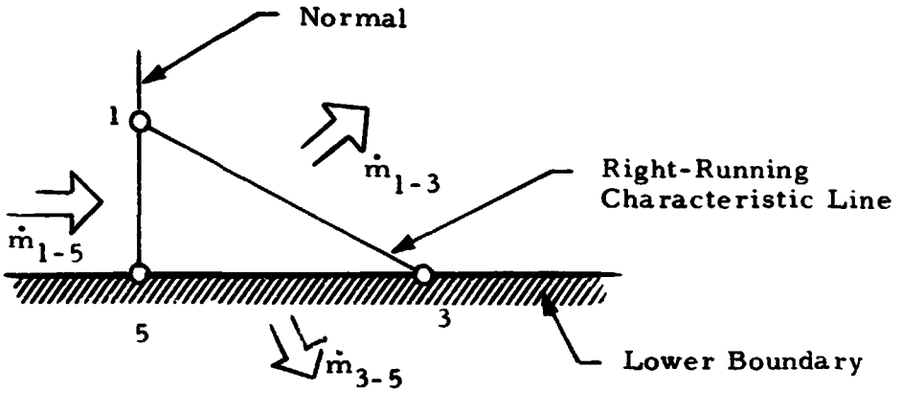

Applying the principle of conservation of mass to the above system, we may write

$$\dot{m}_{1-5} = \dot{m}_{1-3} + \dot{m}_{3-5} . \tag{4.158}$$

Furthermore, from the above assumptions $\dot{m}_{3-5}$, v_5^j and v_3^j may be set equal to zero.

Equation (4.158) then becomes

$$\dot{m}_{1-5} = \dot{m}_{1-3} . \tag{4.159}$$

Each term in the above equation may be solved for by applying Eq. (4.137) between the proper points.

Points 1-5:

$$\dot{m}_{1-5} = (2\pi)^{\delta} \left[\frac{(\rho_1 u_1 + \rho_5 u_5)\, y_1 y_1^{\delta}}{2} - \rho_1 v_1\, y_1^{\delta} (x_1 - x_5) \right] \tag{4.160}$$

Points 1-3:

$$\dot{m}_{1-3} = (2\pi)^{\delta} \left[\frac{(\rho_1 u_1 + \rho_3 u_3)\, y_1 y_1^{\delta}}{2} - \rho_1 v_1\, y_1^{\delta} (x_1 - x_3) \right] . \tag{4.161}$$

The particle density relationship at point 3 may now be determined by equating Eqs. (4.160) and (4.161) and solving for ρ_3,

Equation (4.159) becomes:

$$(\rho_1 u_1 + \rho_5 u_5)\, y_1 y_1^{\delta} - 2\rho_1 v_1 y_1^{\delta}\,(x_1 - x_5) = (\rho_1 u_1 + \rho_3 u_3)\, y_1 y_1^{\delta} - 2\rho_1 v_1 y_1^{\delta}\,(x_1 - x_3) \quad (4.162)$$

To solve for ρ_3:

combine terms of Eq. (4.162) to form coefficients of ρ_1, ρ_3 and ρ_5

$$\rho_1\left[2v_1 y_1^{\delta}\,(x_5 - x_3)\right] + \rho_5 u_5\, y_1 y_1^{\delta} = \rho_3 u_3\, y_1 y_1^{\delta}$$

and then divide through by $u_3 y_1 y_1^{\delta}$

$$\rho_3 = \frac{\rho_5 u_5 - 2\rho_1 v_1\,(x_3 - x_5)}{u_3} \quad . \quad (4.163)$$

4.4.3 Particle Limiting Streamline Point Solution

Consider the characteristic net for a point on a particle limiting streamline

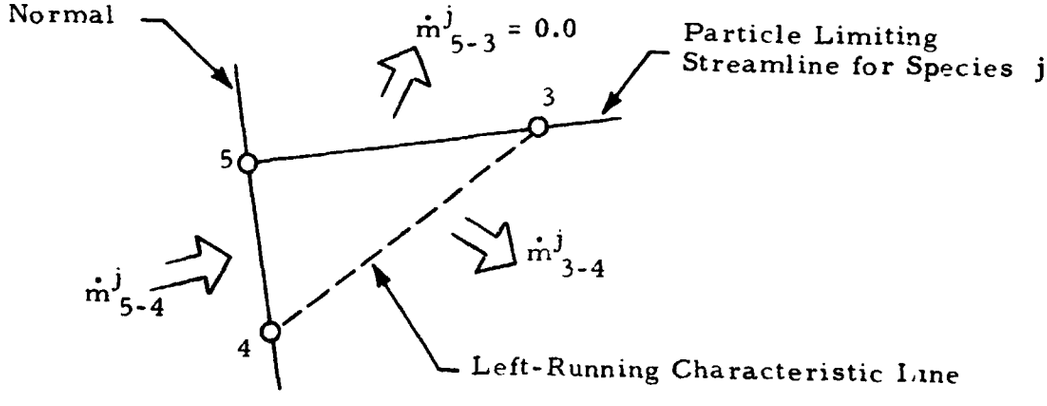

Applying the principle of conservation of mass to species j in the above system, we may write

$$\dot{m}^j_{5-4} = \dot{m}^j_{5-3} + \dot{m}^j_{3-4} \quad . \tag{4.164}$$

By definition of a particle limiting streamline, the entire mass of particle species j is contained in the streamtube formed by the particle limiting streamline for species j. Therefore $\dot{m}^j_{5-3}$ may be set equal to zero. Note that this condition applys only to particle species j; other particle species may pass through the particle limiting streamline for species j. Equation (3.164) then becomes

$$\dot{m}_{3-4} = \dot{m}_{5-4} \quad . \tag{4.165}$$

Each term in the above equation may be solved for by applying Eq. (4.137) between the proper points.

Points 3-4:

$$\dot{m}_{3-4} = (2\pi)^\delta \left[\frac{(\rho_3 u_3 + \rho_4 u_4)}{2} \frac{(y_3 y_3^\delta - y_4 y_4^\delta)}{2^\delta} - \frac{(\rho_3 v_3 + \rho_4 v_4)}{2} \frac{(y_3^\delta + y_4^\delta)}{2^\delta} (x_3 - x_4) \right] \tag{4.166}$$

Points 5-4:

$$\dot{m}_{5-4} = (2\pi)^\delta \left[\frac{(\rho_5 u_5 + \rho_4 u_4)}{2} \frac{(y_5 y_5^\delta - y_4 y_4^\delta)}{2^\delta} - \frac{(\rho_5 v_5 + \rho_4 v_4)}{2} \frac{(y_5^\delta + y_4^\delta)}{2^\delta} (x_5 - x_4) \right] \tag{4.167}$$

The particle density relationship at point 3 may now be determined by equating Eqs. (4.166) and (4.167) and solving for ρ_3. Equation (4.165) becomes:

$$\begin{aligned} &(\rho_3 u_3 + \rho_4 u_4)(y_3 y_3^\delta - y_4 y_4^\delta) - (\rho_3 v_3 + \rho_4 v_4)(y_3^\delta + y_4^\delta)(x_3 - x_4) = \\ &(\rho_5 u_5 + \rho_4 u_4)(y_5 y_5^\delta - y_4 y_4^\delta) - (\rho_5 v_5 + \rho_4 v_4)(y_5^\delta + y_4^\delta)(x_5 - x_4) \quad . \end{aligned} \tag{4.168}$$

To solve for ρ_3:

expand Eq. (3.168)

$$\rho_3 u_3 (y_3 y_3^\delta - y_4 y_4^\delta) - \rho_3 v_3 (y_3^\delta + y_4^\delta)(x_3 - x_4) + \rho_4 u_4 (y_3 y_3^\delta - y_4 y_4^\delta)$$

$$- \rho_4 v_4 (y_3^\delta + y_4^\delta)(x_3 - x_4) = \rho_5 u_5 (y_5 y_5^\delta - y_4 y_4^\delta) - \rho_5 v_5 (y_5^\delta + y_4^\delta)(x_5 - x_4)$$

$$+ \rho_4 u_4 (y_5 y_5^\delta - y_4 y_4^\delta) - \rho_4 v_4 (y_5^\delta + y_4^\delta)(x_5 - x_4) ;$$

combine terms to form coefficients of ρ_3, ρ_4 and ρ_5

$$\rho_3 \left[u_3 (y_3 y_3^\delta - y_4 y_4^\delta) - v_3 (y_3^\delta + y_4^\delta)(x_3 - x_4) \right] = \rho_5 \left[u_5 (y_5 y_5^\delta - y_4 y_4^\delta) \right.$$

$$\left. - v_5 (y_5^\delta + y_4^\delta)(x_5 - x_4) \right] + \rho_4 \left\{ u_4 (y_5 y_5^\delta - y_3 y_3^\delta) - v_4 \left[(y_5^\delta + y_4^\delta)(x_5 - x_4) \right. \right.$$

$$\left. \left. - (y_3^\delta + y_4^\delta)(x_3 - x_4) \right] \right\} ;$$

and finally solving for ρ_3

$$\rho_3 = \frac{1}{u_3 (y_3 y_3^\delta - y_4 y_4^\delta) - v_3 (y_3^\delta + y_4^\delta)(x_3 - x_4)} \left\{ \rho_5 \left[u_5 (y_5 y_5^\delta - y_4 y_4^\delta) \right. \right.$$

$$\left. - v_5 (y_5^\delta + y_4^\delta)(x_5 - x_4) \right] + \rho_4 \left\{ u_4 (y_5 y_5^\delta - y_3 y_3^\delta) - v_4 \left[(y_5^\delta + y_4^\delta)(x_5 - x_4) \right. \right.$$

$$\left. \left. \left. - (y_3^\delta + y_4^\delta)(x_3 - x_4) \right] \right\} \right\} . \qquad (4.169)$$

4.4.4 Upper Boundary Point Solution

The upper wall point and free boundary point are the two types of upper boundary points encountered in a typical gas-particle flow problem. Consider

the characteristic net for a point on an upper boundary

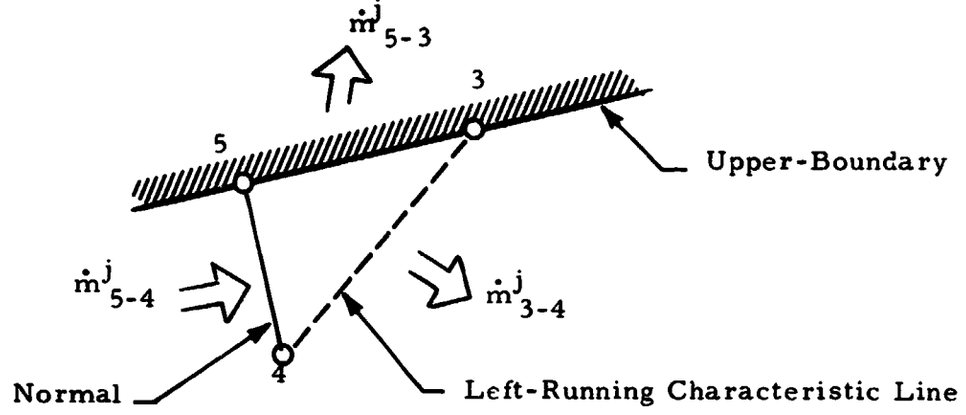

Applying the principle of conservation of mass to species j in the above system, we may write

$$\dot{m}^j_{5-4} = \dot{m}^j_{5-3} + \dot{m}^j_{3-4} \quad . \tag{4.170}$$

Unlike the assumption made in the lower boundary solution, the particle streamlines are not restricted to run parallel to the upper boundary in the vicinity of the boundary. Therefore, the particle mass flow rate $\dot{m}^j_{5-3}$ is not necessarily equal to zero. Physically speaking, $\dot{m}^j_{5-3}$ may be considered to be equivalent to particles "sticking" to the upper wall or passing through the free boundary.

The particle density relationship at the upper boundary is derived by following the same mathematical procedure used in the solution for the particle density relationship at an interior point. The final result is

$$\rho_3 = \frac{1}{u_3(y_5 y_5^\delta - y_4 y_4^\delta) - v_3\left[(y_5^\delta + y_3^\delta)(x_5 - x_3) + (y_4^\delta + y_3^\delta)(x_3 - x_4)\right]}\left[\rho_5\left\{u_5(y_3 y_3^\delta - y_4 y_4^\delta) - v_5\left[(y_5^\delta + y_4^\delta)(x_5 - x_4) - (y_5^\delta + y_3^\delta)(x_5 - x_3)\right]\right\} + \rho_4\left\{u_4(y_5 y_5^\delta - y_3 y_3^\delta) - v_4\left[(y_5^\delta + y_4^\delta)(x_5 - x_4) - (y_4^\delta + y_3^\delta)(x_3 - x_4)\right]\right\}\right] . \tag{4.171}$$

5. SHOCK CAPTURING OPTION

A shock capturing option has been included in the RAMP code to permit the computation of two-phase (gas-particle) nozzle flows with embedded shocks. The gas phase may be treated as either an ideal or real gas with equilibrium/frozen chemistry. The particle phase is treated as a discrete distribution of particle sizes. The two phases interact only in the transfer of momentum and energy. There is no mass transfer between phases, i.e., the particles do not evaporate, and the gas does not solidify or condense.

The inviscid steady state conservation equations for a gas-particle mixture are given as follows in vector notation:

Gas

Mass $$\nabla \cdot \rho \vec{q} = 0$$

Momentum $$\nabla \cdot [(\vec{q}) \rho q] + \nabla p + \sum_{j=1}^{NP} \rho^j A^j \Delta \vec{q}^j = 0$$

Energy $$\nabla \cdot (\rho \vec{q} H) - \sum_{j=1}^{NP} \rho^j A^j (B^j - \vec{q} \cdot \Delta \vec{q}^j) = 0$$

Particles

Mass $$\nabla \cdot \rho^j \vec{q} = 0$$

Momentum $$\nabla \cdot [(\vec{q})^j \rho^j \vec{q}^j] - \rho^j A^j \Delta \vec{q}^j = 0$$

Energy $$\nabla \cdot (\rho^j \vec{q}^j h^j) + \rho^j A^j (B^j - \Delta \vec{q}^j \cdot \Delta \vec{q}^j) = 0 \qquad (5.1)$$

These equations, expressed in compact form in nozzle coordinates, become:

$$\frac{\partial E}{\partial x} - \frac{R'}{R}\eta\frac{\partial E}{\partial \eta} + \frac{1}{R\eta^{\delta}}\frac{\partial}{\partial \eta}\left[\eta^{\delta}(F - \delta\kappa P)\right] + \delta\kappa\frac{1}{R}\frac{\partial P}{\partial \eta} + H = 0 \qquad (5.2a)$$

and, for axis solution:

$$\frac{\partial E}{\partial x} + \frac{2}{R}\frac{\partial}{\partial \eta}(F - \kappa P) + H \qquad (5.2b)$$

where E, F and H are the following arrays of variables:

Gas

$$E = \begin{pmatrix} \rho u \\ \rho u^2 + P \\ \rho uv \\ \rho uH \end{pmatrix} \quad F = \begin{pmatrix} \rho v \\ \rho uv \\ \rho v^2 + P \\ \rho vH \end{pmatrix} \quad H = \begin{pmatrix} 0 \\ \Sigma \rho^j A^j \Delta u^j \\ \Sigma \rho^j A^j \Delta v^j \\ \Sigma \rho^j A^j (B^j - u\,\Delta u^j - v\,\Delta v^j) \end{pmatrix}$$

Particles

$$E = \begin{pmatrix} \rho^j u^j \\ \rho^j u^{j2} \\ \rho^j u^j v^j \\ \rho^j u^j h^j \end{pmatrix} \quad F = \begin{pmatrix} \rho^j v^j \\ \rho^j u^j v^j \\ \rho^j v^{j2} \\ \rho^j v^j h^j \end{pmatrix} \quad H = \begin{pmatrix} 0 \\ -\rho^j A^j \Delta u^j \\ -\rho^j A^j \Delta v^j \\ \rho^j A^j (B^j - \Delta u^{j2} - \Delta v^{j2}) \end{pmatrix} \qquad (5.4)$$

and where

$$\delta = \begin{matrix} 0 & \text{2D planer} \\ 1 & \text{axisymmetric} \end{matrix}$$

$$\kappa = \begin{matrix} 1 & \text{r or y momentum eq.} \\ 0 & \text{all others} \end{matrix}$$

The nozzle coordinates x and $\eta = r/R$ or y/R are based on an expanding scale in the r or y direction proportional to the nozzle radius (or half-width) R. This permits a uniform distribution of grid points in the r or y direction.

Equation (5.2) is numerically integrated by the McCormack predictor/ corrector algorithm which is second-order accurate. This algorithm is given as follows:

Predictor Step

$$\bar{E}_m = E_m^n + \frac{R'}{R^n}\frac{\Delta x}{\Delta\eta}\eta_m (E_{m+1}^n - E_m^n) - \frac{1}{R^n \eta_m^\delta}\frac{\Delta x}{\Delta\eta}\left[\eta_m^\delta (F_{m+1}^n - \delta\kappa P_{m+1}^n) - (\eta_m^\delta - \delta\Delta\eta)(F_m^n - \delta\kappa P_m^n)\right] - \delta\varsigma\frac{\Delta x}{R^n \Delta\eta}(P_{m+1}^n - P_m^n) - H_m^n \Delta x \qquad (5.6a)$$

and, on axis (m = 1)

$$\bar{E}_1 = E_1^n - \frac{2}{R^n}\frac{\Delta x}{\Delta\eta}\left[(F_2^n - \kappa P_2^n) - (F_1^n - \kappa P_1^n)\right] - H_1^n \Delta x \qquad (5.6b)$$

Corrector Step

$$E_m^{n+1} = \frac{1}{2}\left\{(E_m^n + \bar{E}_m) + \frac{R'}{R^{n+1}}\frac{\Delta x}{\Delta\eta}\eta_m (\bar{E}_m - \bar{E}_{m-1}) - \frac{1}{R^{n+1}\eta_m^\delta}\frac{\Delta x}{\delta\Delta\eta}\left[(\eta_m^\delta + \Delta\delta\eta)(\bar{F}_m - \delta\kappa\bar{P}_m) - \eta_m^\delta (\bar{F}_{m-1} - \delta\kappa\bar{P}_{m-1})\right] - \delta\kappa\frac{\Delta x}{\Delta\eta}(\bar{P}_m - \bar{P}_{m-1}) - \bar{H}_m \Delta x\right\} \qquad (5.7a)$$

and, on axis (m = 1)

$$E^{n+1} = \frac{1}{2}\left\{E_m^n + \bar{E}_m - \frac{2}{R^{n+1}}\frac{\Delta x}{\Delta\eta}[(\bar{F}_2 - \kappa\bar{P}_2) - (\bar{F}_1 - \kappa\bar{P}_1)] - \bar{H}_1 \Delta x\right\} \qquad (5.7b)$$

The nozzle wall boundary is treated using the MOC option in RAMP for the gas phase. The particle phase upper boundary does not necessarily follow the nozzle wall boundary, and, hence, must be tracked for each particle specie by integrating the following equations of motion:

$$\ddot{x} = A\,\Delta u$$
$$\ddot{r} \text{ (or } \ddot{y}) = A\,\Delta v \qquad (5.8)$$

These equations are integrated with two steps along with Eqs. (5.6) and (5.7) to find the limiting streamline for each particle specie:

Predictor Step

$$\bar{R}_p = R_p^n + A_m^n\ \Delta v_m^n\ \frac{\Delta x^2}{2(u_m^n)^2} + \frac{v_m^n}{u_m^n}\ \Delta x \qquad (5.9a)$$

Corrector Step

$$R_p^{n+1} = \frac{1}{2}\left\{ \bar{R}_p^n + \bar{R}_p + \bar{A}_m\ \Delta \bar{v}_m\ \frac{\Delta x^2}{2(u_m)^2} + \frac{v_m}{u_m}\ \Delta x \right\} \qquad (5.9b)$$

The flowfield properties are obtained by decoding the computed flux variables E obtained by integrating Eqs. (5.6) and (5.7). The decode procedure for the gas phase depends on the type of chemistry involved. For both ideal and real gas decodes the radial (vertical) velocity v and total enthalpy H are obtained by

$$v^{n+1} = E_3/E_1$$

$$H^{n+1} = E_4/E_1$$

In the ideal gas decode, the axial velocity u is obtained from:

$$u^{n+1} = \frac{\gamma}{\gamma+1} \left\{ \frac{E_2}{E_1} + \sqrt{\left(\frac{E_2}{E_1}\right)^2 - \frac{2-1}{2} \left[2\frac{E_4}{E_1} - \left(\frac{E_3}{E_1}\right)^2 - 2A \right]} \right\} \qquad (5.10)$$

where

$$A = h^n - \frac{\gamma}{\gamma-1} P^n/\rho^n$$

The real gas decode procedure makes use of real gas chemistry tables in RAMP. These tables, by a look-up procedure, recover temperature, pressure, density, Mach number, gas constant and ratio of specific heats from an input of total enthalpy, entropy and velocity. The shock capture option real gas decode uses Newton iteration to solve the following equation:

$$v^2 - v^2 - \frac{1}{4}\left[\left(\frac{E_2}{E_1}\right) + \sqrt{\left(\frac{E_2}{E_1}\right)^{\kappa^2} - 4RT} \right]^2 = 0 \qquad (5.11)$$

where the gas constant, R, and temperature, T, are obtained from the real gas tables from known values of entropy, S, total velocity, V, and total enthalpy, H. Following convergence of the iteration on velocity, V, the axial velocity, u, is obtained from:

$$u^{n+1} = \sqrt{v^2 - (v^{n+1})^2} \qquad (5.12)$$

For both ideal and real gas decodes, the density, ρ, and pressure, p, are then obtained from:

$$\rho^{n+1} = E_1/u^{n+1} \qquad (5.13)$$

$$p^{n+1} = E_2 - E_1 u^{n+1} \qquad (5.14)$$

The particle phase decode is:

$$(u^j)^{n+1} = E_2^j/E_1^j \tag{5.15}$$

$$(\rho^j)^{n+1} = (E_1^j)^2/E_2^j \tag{5.16}$$

$$(v^j)^{n+1} = E_3^j/E_1^j \tag{5.17}$$

$$(h^j)^{n+1} = E_4^j/E_1^j \tag{5.18}$$

The Shock Capture option was checked out by comparison with the existing streamline/normal method-of-characteristics option. Three test cases were considered: (1) SSME nozzle flow, single phase, ideal gas, (2) SSME nozzle flow, single phase, equilibrium chemistry, and (3) two-phase ideal gas with solid particles. Computed Mach number and pressure distributions are shown in Figs. 5-1 through 5-3 for case 1 (SSME nozzle, ideal gas). Axial distributions are shown in Figs. 5-1 and 5-2, and exit radial distributions are shown in Fig. 5-3. Generally good agreement is shown between the Shock Capture and Streamline/Normal options. Similar results are shown in Figs. 5-4 through 5-6 for case 2 (SSME nozzle, equilibrium chemistry). Computed Mach number and pressure distributions along the exit radius are shown in Fig. 5-7 for case 3 (Space Shuttle SRM, two-phase, ideal gas). Solid particle densities, velocities and temperature exit radial distributions are shown in Figs. 5-8 through 5-10. In all cases, good agreement is shown between the Shock Capture and Streamline/Normal options.

On the basis of the demonstrated good agreement with the Streamline/Normal option, we conclude that the Shock Capture option is operational and error free.

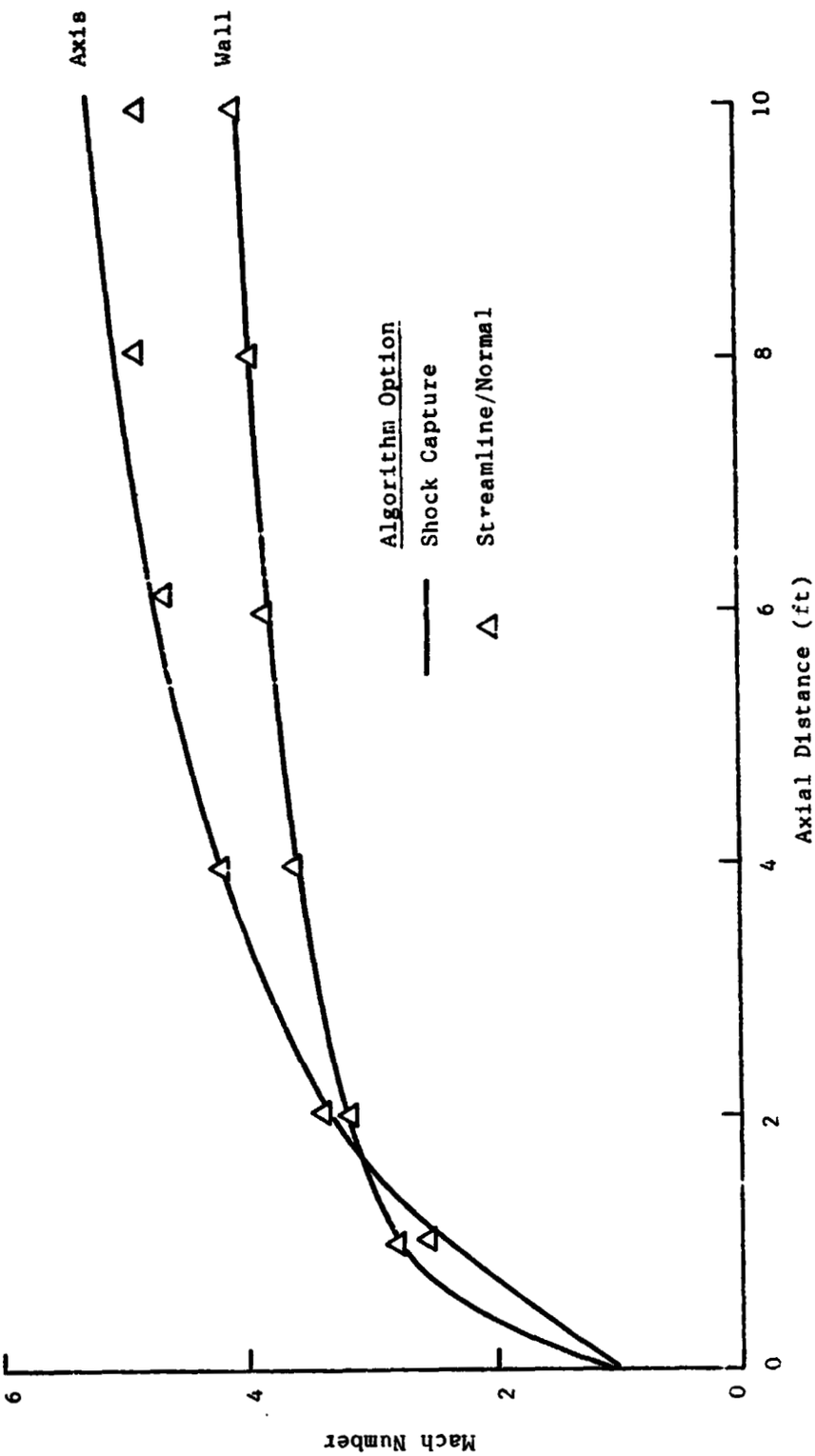

Fig. 5-1 Mach Number Distribution Along SSME Nozzle Axis, Ideal Gas Solution

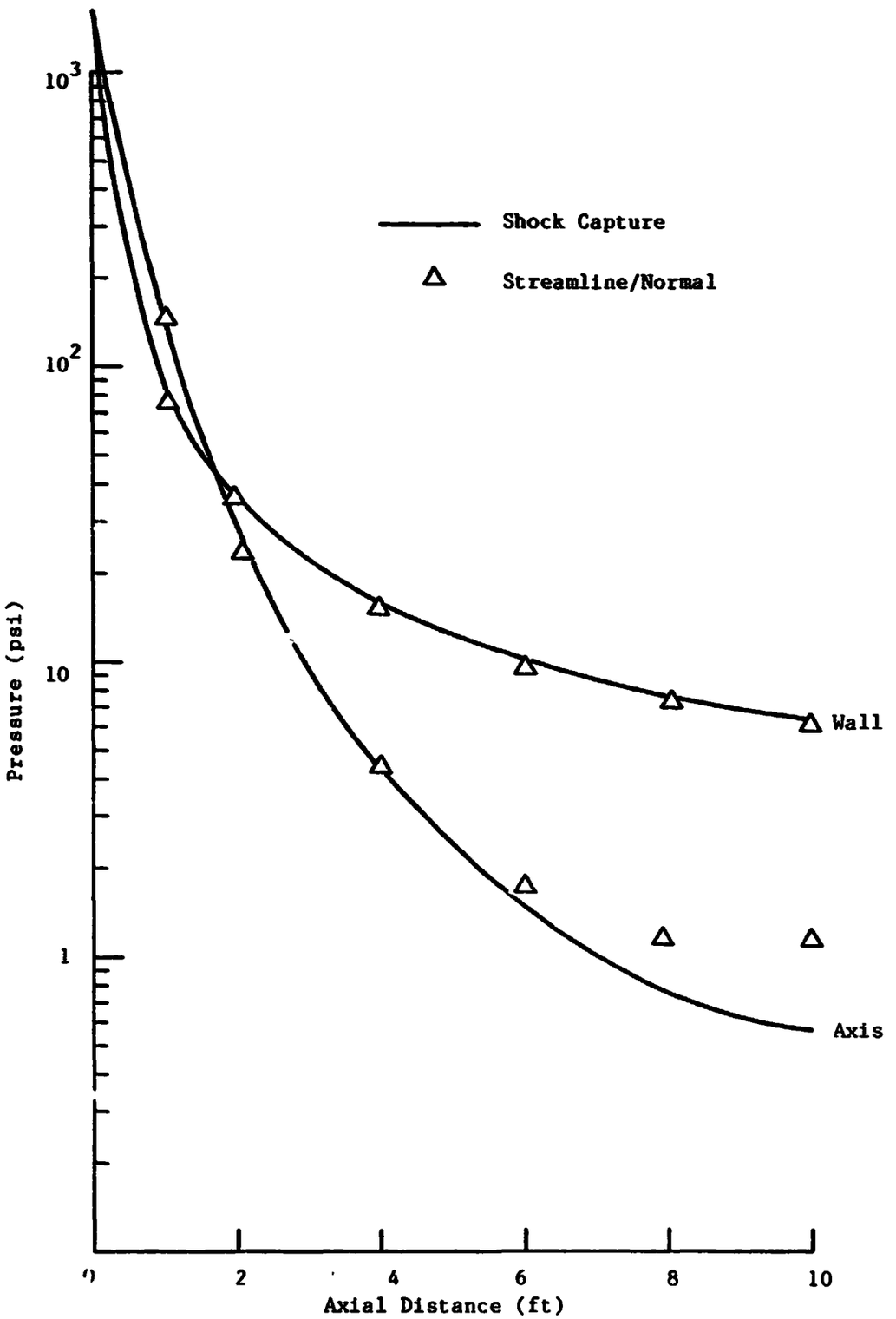

Fig. 5-2 Pressure Distribution Along SSME Nozzle Axis
Ideal Gas Solution

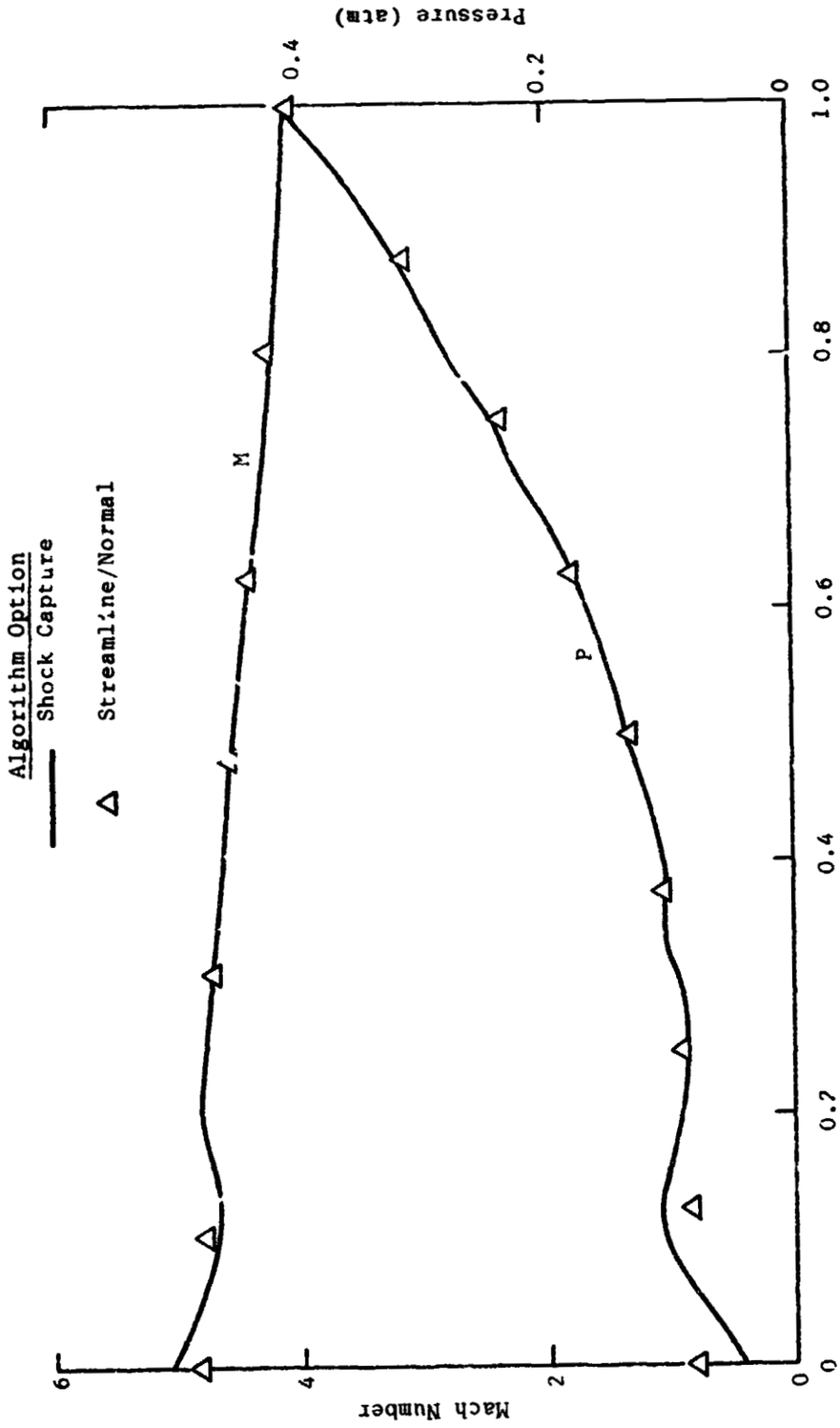

Fig. 5-3 Mach Number and Pressure Distributions Along SSME Nozzle Exit Radius, Ideal Gas Solution

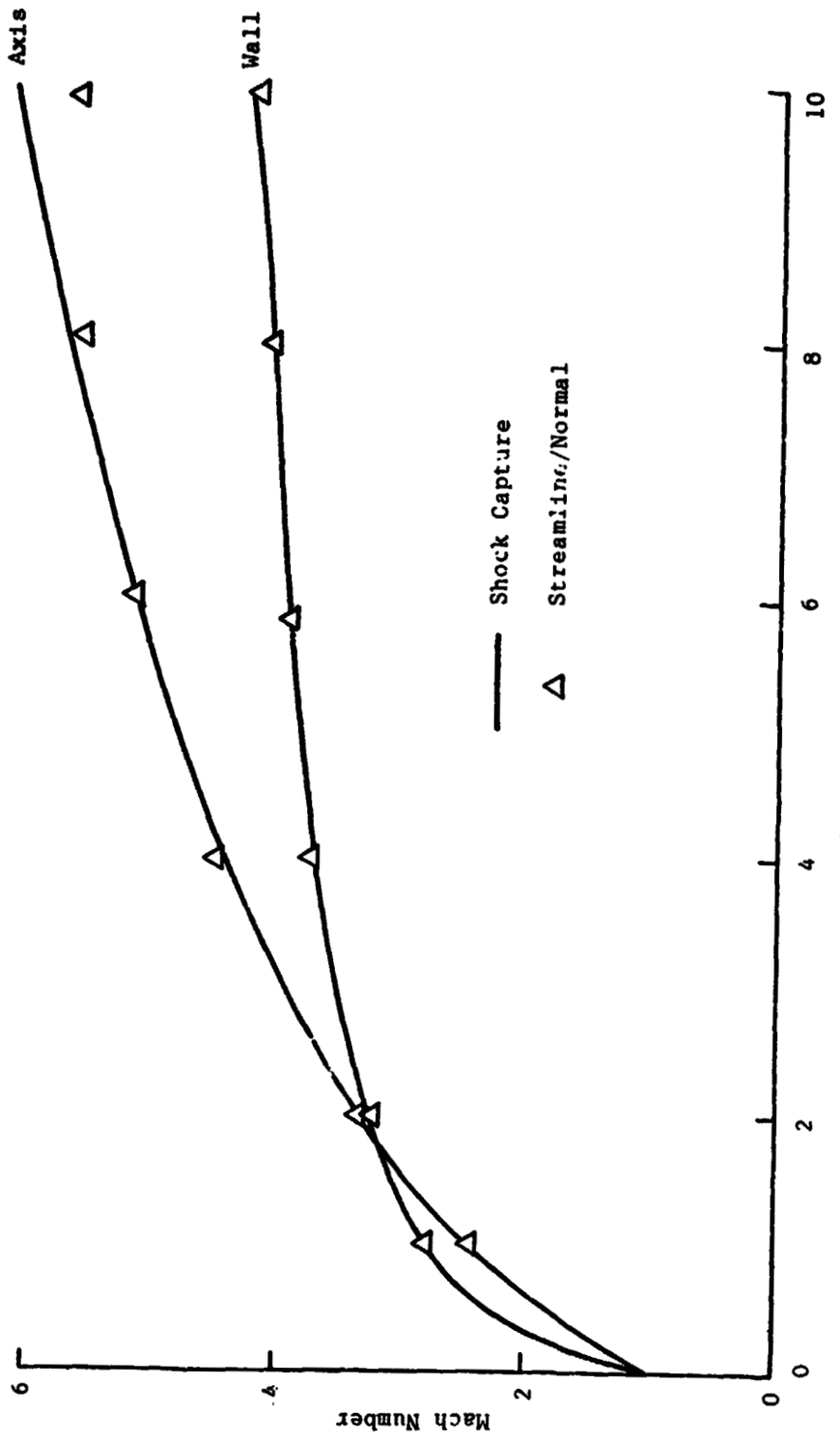

Fig. 5-4 Mach Number Distribution Along SSME Nozzle Axis, Equilibrium Chemistry Solution

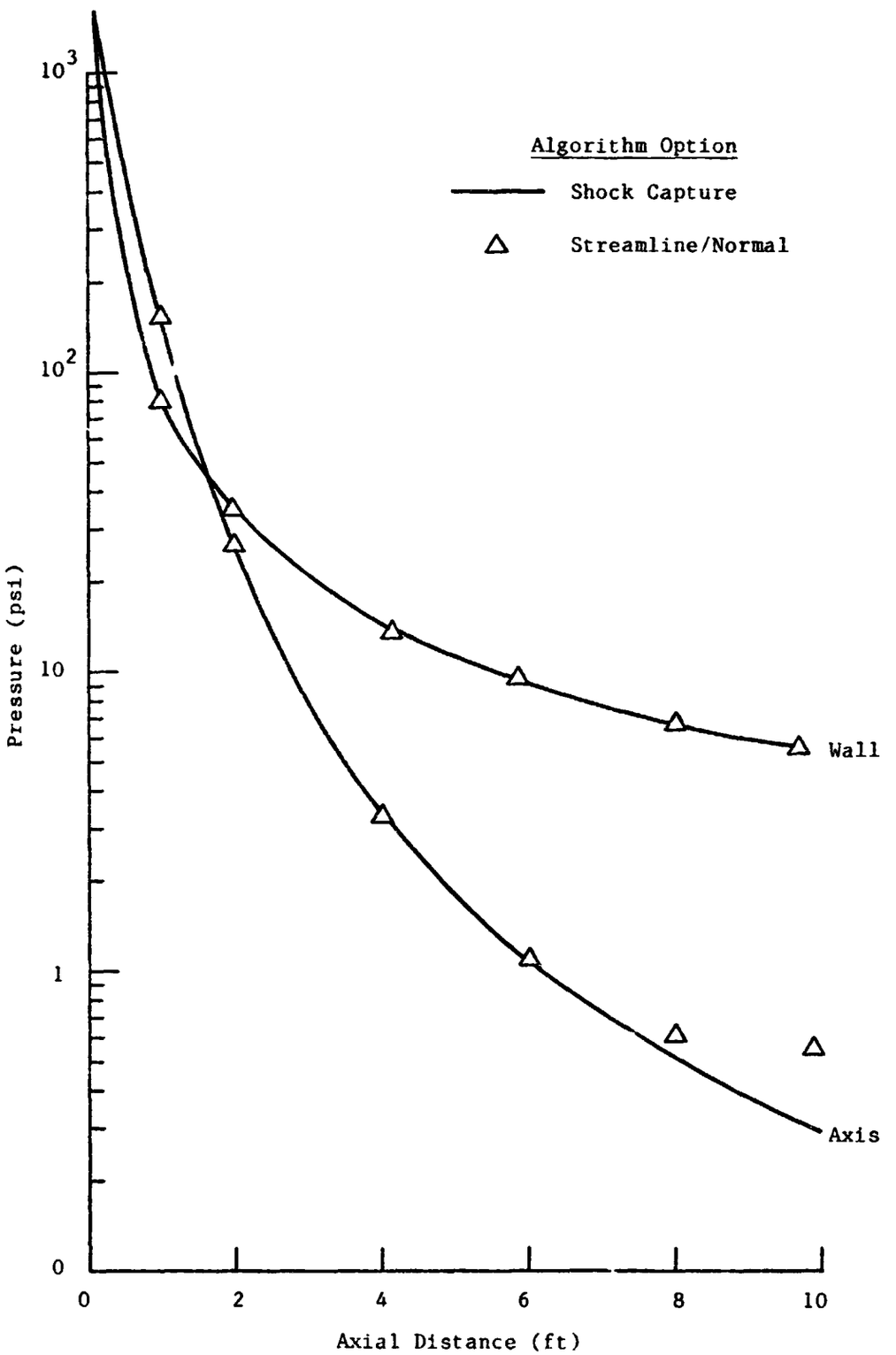

Fig. 5-5 Pressure Distribution Along SSME Nozzle Axis, Equilibrium Chemistry Solution

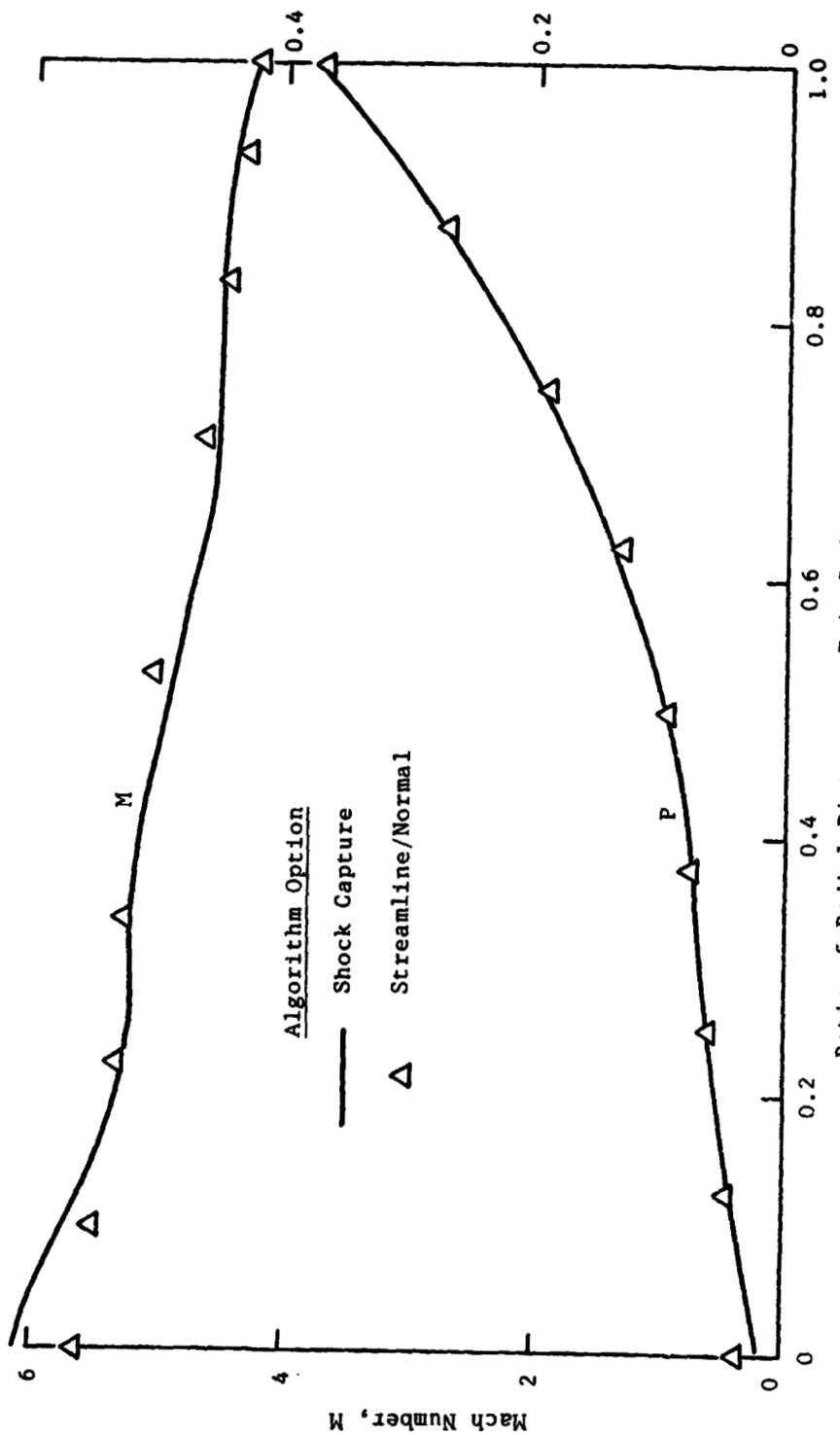

Fig. 5-6 Mach Number and Pressure Distributions at SSME Nozzle Exit, Equilibrium Chemistry Solution

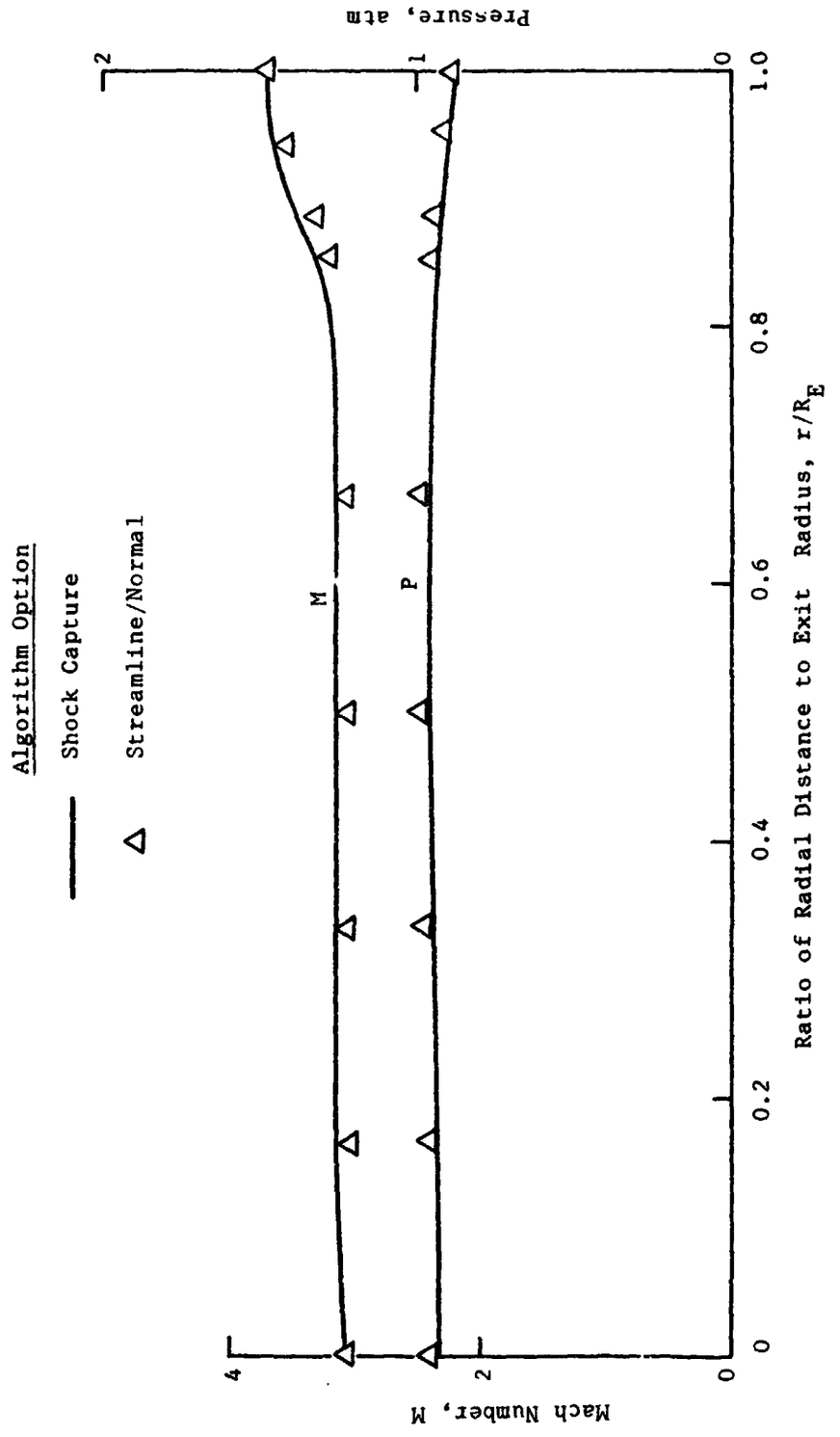

Fig. 5-7 Mach Number and Pressure Distributions Along Nozzle Exit Radius, Two Phase/Ideal Gas Case

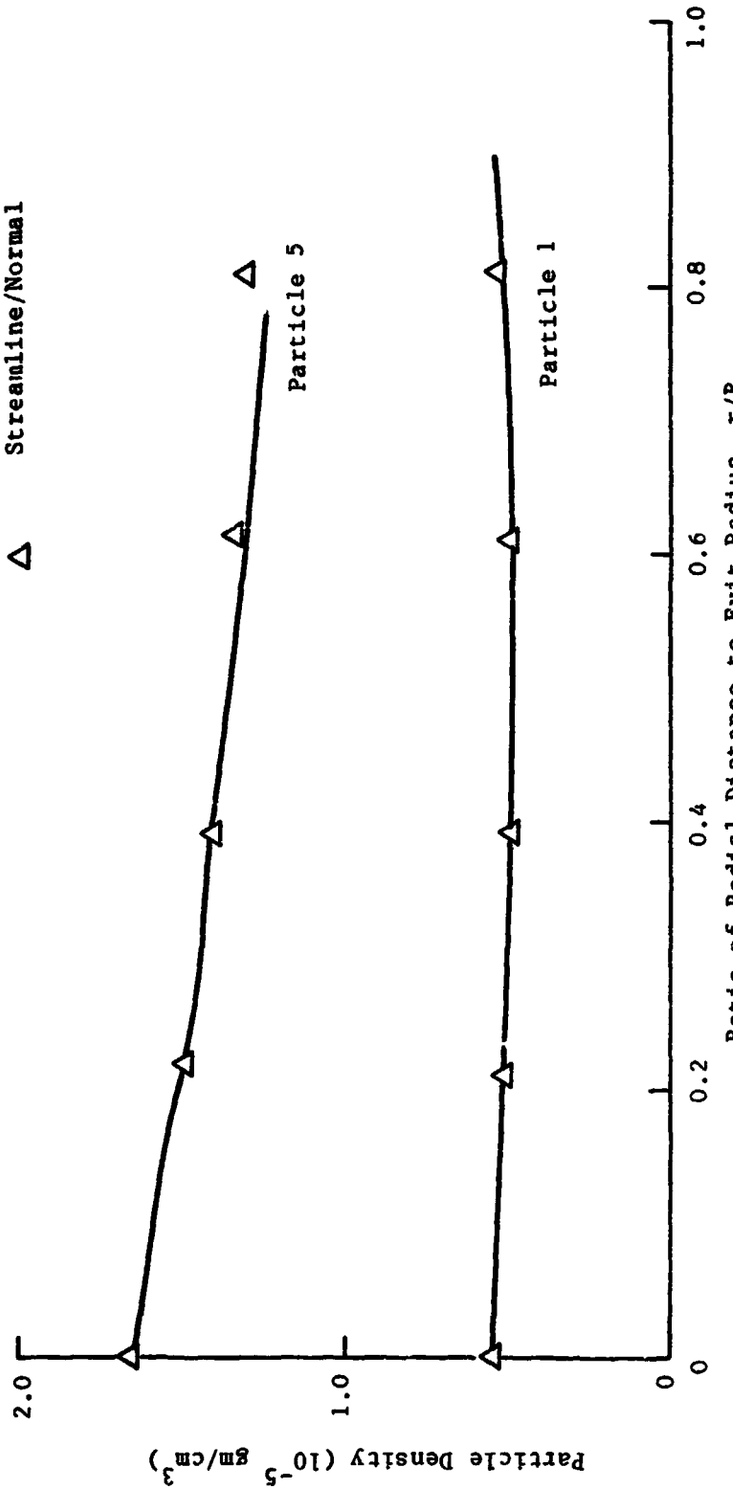

Fig. 5-8 Solid Particle Density Distributions Along Nozzle Exit Radius, Two Phase/Ideal Gas Case

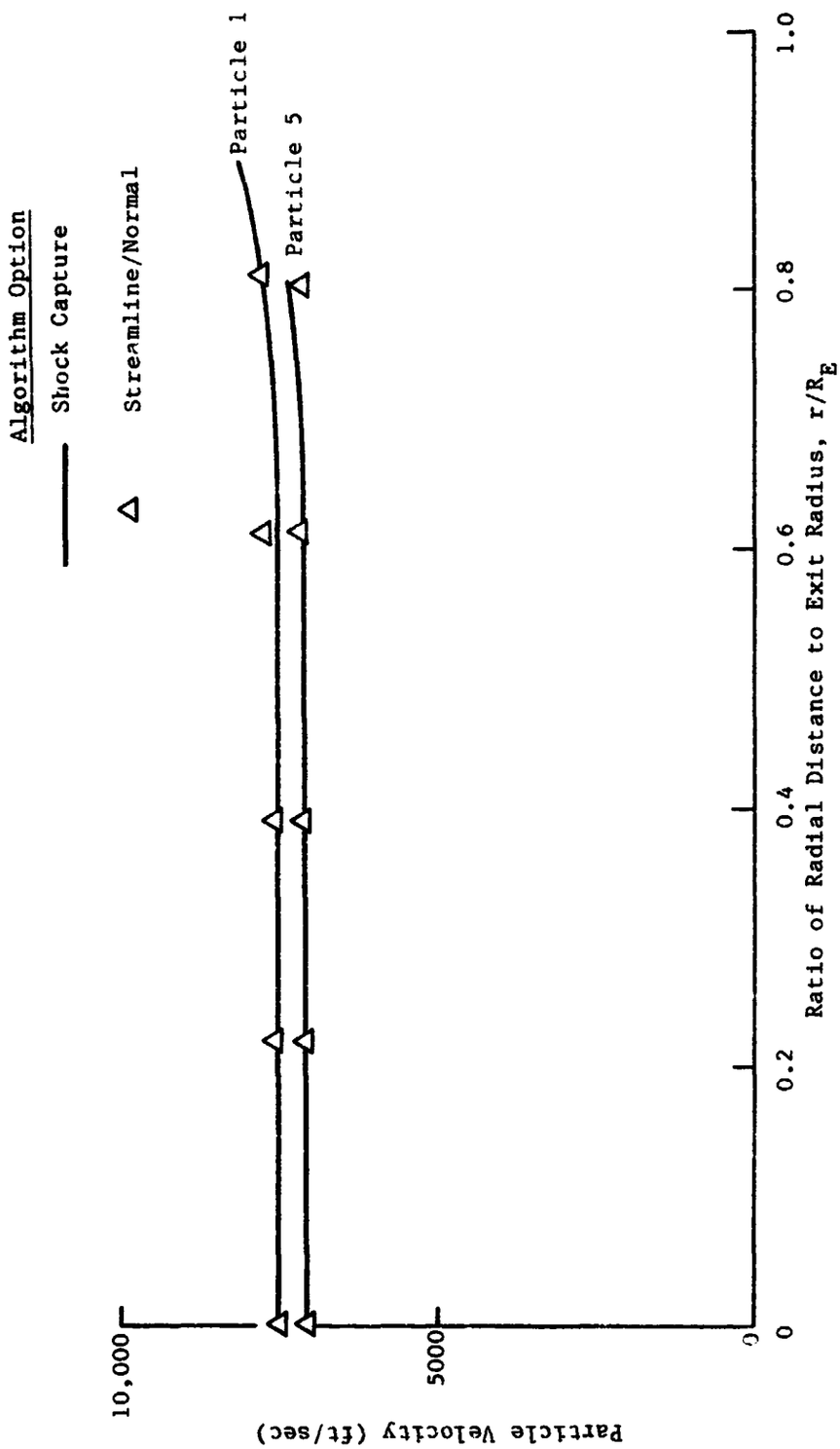

Fig. 5-9 Solid Particle Velocity Distributions Along Nozzle Exit Radius, Two Phase/Ideal Gas Case

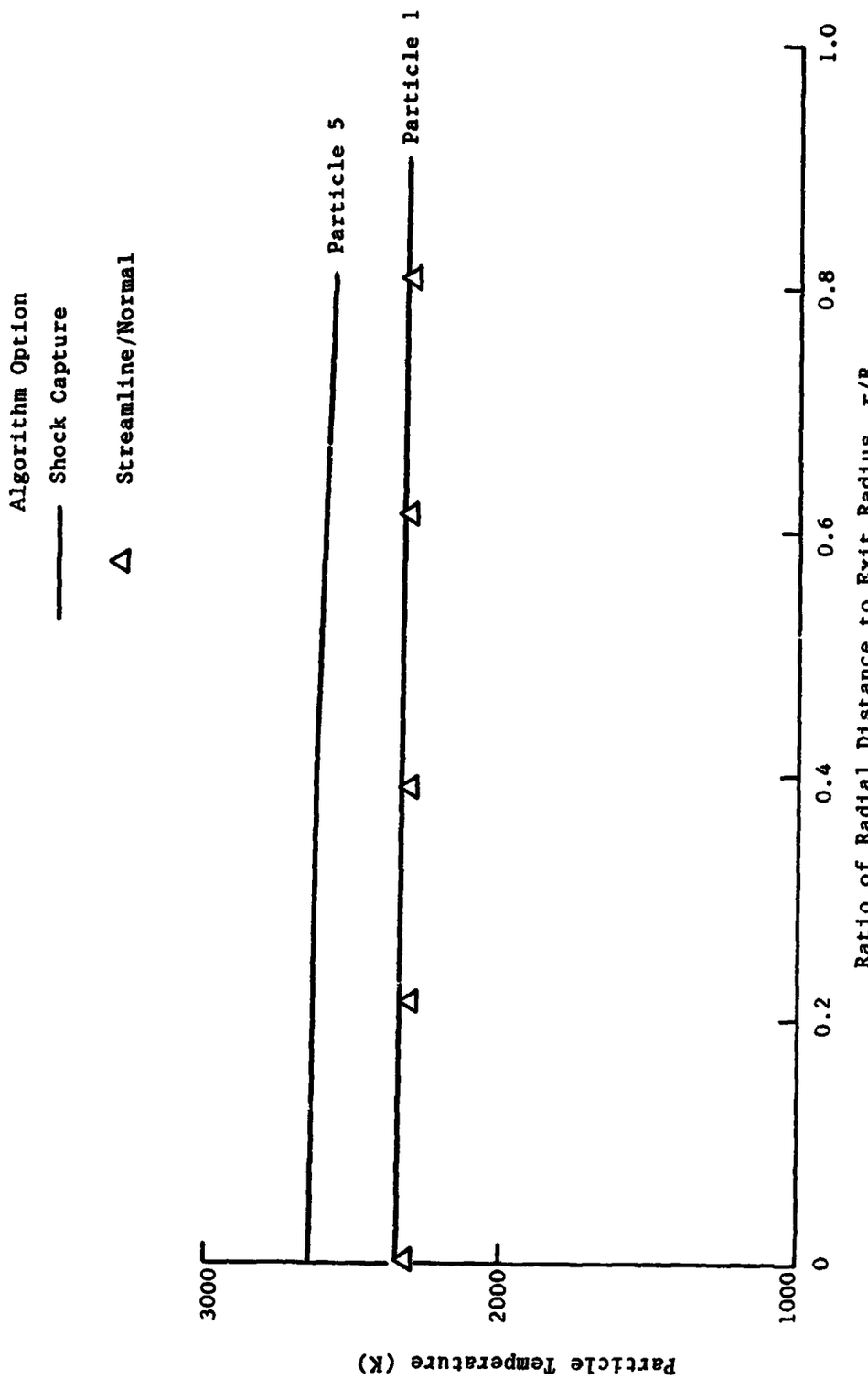

Fig. 5-10 Solid Particle Temperature Distributions Along Nozzle Exit Radius, Two Phase/Ideal Gas Case

6. EXPANSION CORNER – PRANDTL-MEYER FAN

In some cases the flow may be required to negotiate a sharp expansion turn. The problem becomes two dimensional at a sharp corner (it is impossible to conceive of an expansion corner on an axis of symmetry) and may be treated with a Prandtl-Meyer expansion.

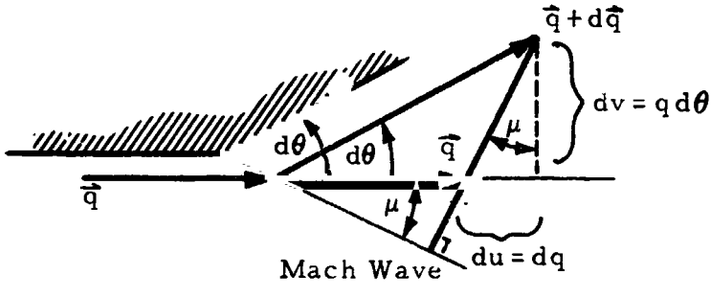

Fig. 6-1 - Nomenclature for Mach Wave Analysis

Since a Mach wave will support pressure changes only in a direction normal to itself (Ref. 41):

$$dv = qd\theta$$

$$du = dq$$

$$\frac{du}{dy} = \tan\mu = \frac{1}{\sqrt{M^2 - 1}}$$

or

$$d\theta = \sqrt{M^2 - 1}\ \frac{dq}{q} \tag{6.1}$$

The solution to Eq. (6.1) is a straightforward numerical integration for the case of a known final velocity (free-boundary case). If the turning angle is known, however, and the final velocity is not known, an iterative solution is necessary to determine the upper limit.

$$\int_{q_1}^{q_2} \sqrt{M^2 - 1}\ \frac{dq}{q} - \Delta\theta = f(q_2) = 0 \tag{6.2}$$

In the mesh construction to be discussed later a fan of rays must be generated to allow a numerical description through a large turning angle. The turning angle is subdivided into a number of small turns, each of which is integrated numerically. Corresponding to each of these small turns is a Mach wave or characteristic line emanating from the corner.

7. NUMERICAL SOLUTION (MESH POINT CONSTRUCTION)

The calculations described previously are point or small region solutions. This section presents the mesh construction and calculation procedure required to describe the entire flow field in a typical gas-particle flow problem. The general principles adopted in the numerical solution are similar to those used in the method-of-characteristics solutions. The major difference is in the technique of mesh construction; here, the calculation proceeds along normals to the streamlines instead of along characteristic lines.

To begin the problem of describing the entire flow field all necessary boundary conditions must, of course, be supplied. In addition, a start line whose properties are completely defined must be designated.

Figure 7-1 illustrates a flow field in which there are no discontinuities and in which the mesh construction is terminated when the region of interest has been computed.

Figure 7-2a presents the mesh construction required to solve for the properties of any interior point in Fig. 7-1. The J line is considered to be the known normal line. The J-line may be the input startline or the line just calculated. The K-line is the new normal line to be calculated. Calculation always starts from the lowest point and moves upward along the K-line. The first point on the new normal is located by extending the right-running characteristic from a properly selected point (based on desired mesh size) on the preceding known normal to intersect the lower boundary based on the flow properties of that point. The rest of the points including the last point (boundary point) of the normal are located by extending the normal to the local streamline to intersect the next streamline (A boundary is also a

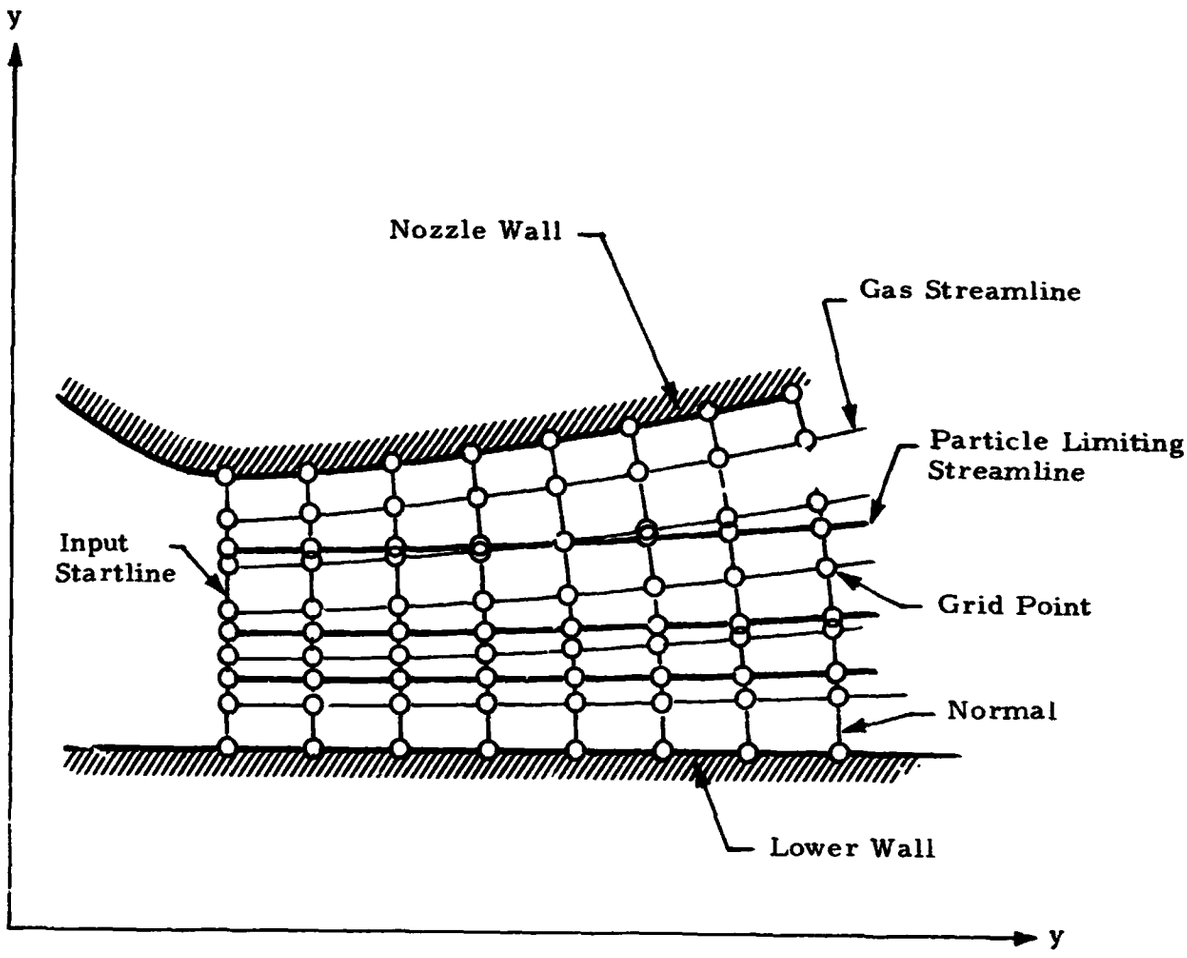

Fig. 7-1 - Basic Mesh Construction for the Streamline-Normal Two-Phase Numerical Solution

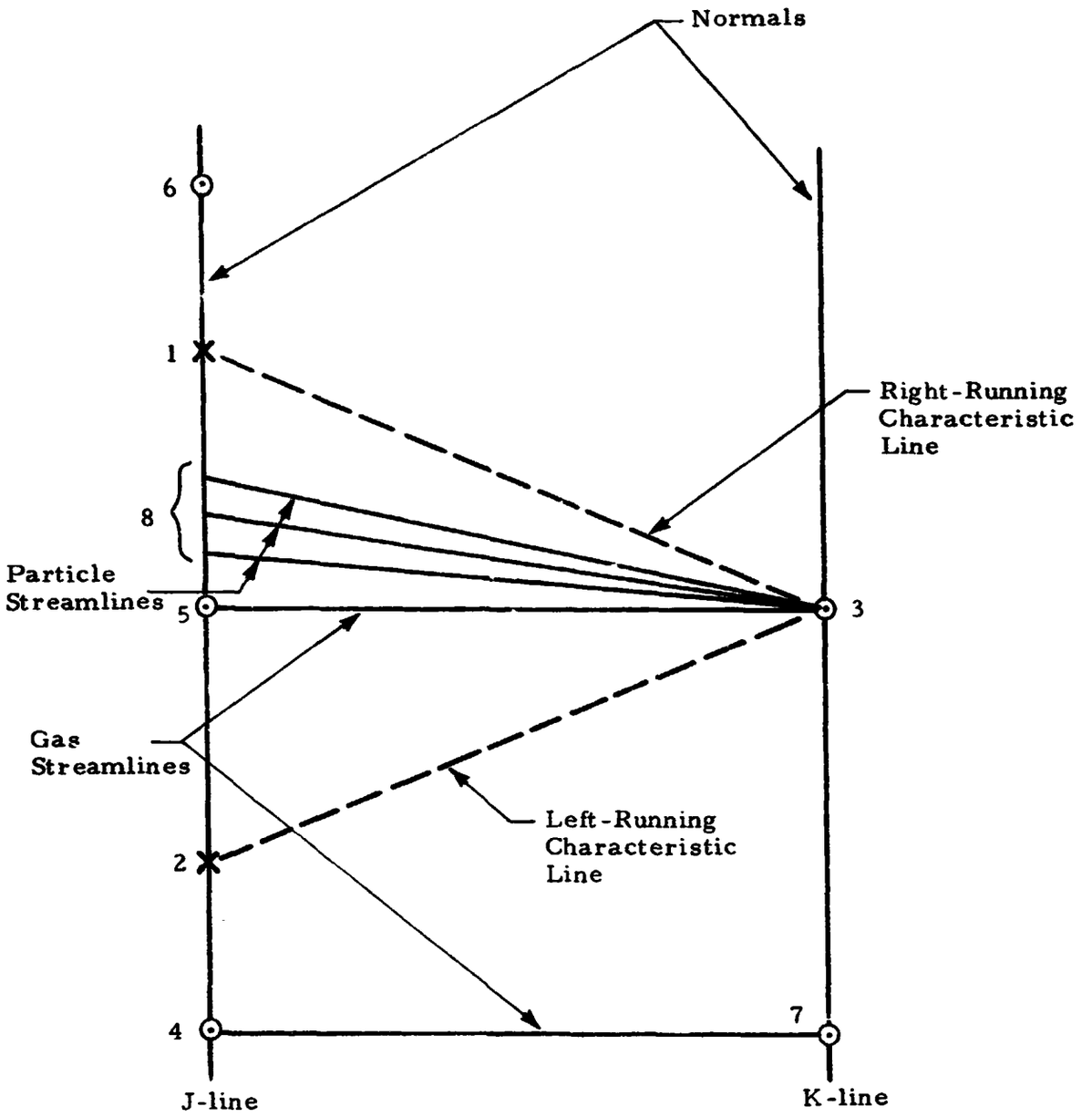

Fig. 7-2a - Mesh Construction for an Interior Point

streamline.) Once the location of the new point is known (point 3 in Fig. 7-2a), the characteristic line(s) and particle streamline(s) can be made to intersect the preceding known normal (points 1, 2 and 8 in Fig. 7-2a). The properties of points 1, 2 and 8 on the known normal can be interpolated from the known points. The properties at point 3 can then be calculated by solving the applicable compatibility equations. For an interior point, both the right-running and left-running characteristics are used to compute the velocity and the flow angle at the new point (point 3 in Fig. 7-2a). For a boundary point, either the flow angle or the velocity can be found with the boundary condition; therefore, only one physical characteristic is needed depending on the relative location of the boundary with the main flow. For shock points and Prandtl-Meyer expansion calculations, the mesh construction is appropriately modified to accommodate each individual case. The general method of computation, however, remains the same as described above.

The mesh construction and calculation procedure for an interior point solution forms the basis for the solution of the flow properties at all other types of points in the flow field. For that reason, the mesh construction and calculation procedure for an interior point will be first described in detail, then, to further aid in the understanding of the numerical solution, presented in flow chart form. Using the knowledge gained in the discussion of the interior point solution, the calculation procedure for each of the remaining cases will be described. Any important problems that may arise, or other points of interest involved in the calculational procedure will be discussed.

7.1 INTERIOR POINT

This section presents the details of the numerical solution for the gas and particle flow properties at an interior point of the flow field being analyzed. The solution is outlined in a step-by-step procedure and is for the case when particles are present at all points which enter into the calculation of the flow properties at the new point.

Consider again Fig. 7-2a and assume that the flow properties are known along the J-line. The J-line can be the input start line or the line just calculated. The point 7K will also be a known data point since it is the last point calculated on the K-line.

Before the calculation procedure can be started a decision must be made to use either the enthalpy-entropy-velocity form or the pressure-density-velocity form of the compatibility equations to solve for the properties at the new point. This decision is based on the type of chemistry being considered in the flow field. If finite rate chemistry is being considered, the pressure-density-velocity form of the compatibility equations is the more convenient form to be used. If equilibrium or frozen chemistry is being considered, the enthalpy-entropy-velocity form of the compatibility equations is the more convenient form to be used. In either case, the method of calculation is the same. For purposes of discussion, it will be assumed that the chemistry of the flow field being analyzed may be considered to be in chemical equilibrium.

Step 1: For the first pass of the solution, the properties at 3K are set equal to those of the base point 5J.

Step 2: The physical location (x_3, y_3) of the point 3K is found by intersecting the normal from the point 7K with the projection of the streamline from the point 5J.

Step 3: The intersection of the characteristic lines with the J-line is now found. These lines will in general fall between two known data points and an interpolation scheme is employed to find the flow properties at these points. The interpolation is of the following form:

$$P_{1,2} = P_{5,4} + F(P_{6,5} - P_{5,4})$$

where

F = interpolation factor.

For the gas flow properties P assumes the following

$$P = q, \theta, S, H$$

with

$$\left.\begin{aligned} T &= f(q, S, H) \\ \rho &= f(q, S, H) \\ \nu &= f(T, H) \\ C_P &= f(T, H) \\ Pr &= f(T, H) \end{aligned}\right\} \text{ tabulated}$$

while for the particle properties P assumes

$$P = u^j, v^j, h^j, \rho^j$$

with

$$T^j_{1,2} = f(h^j)_{1,2} \quad \text{tabulated}$$

$$Re^j_{1,2} = \frac{2 r^j_{1,2} \rho_{1,2} \left|\Delta q^j\right|_{1,2}}{\nu_{1,2}}$$

$$f_{1,2} = f(Re^j)_{1,2} \quad \text{tabulated}$$

$$G^j_{1,2} = f(Re^j_{1,2}, Pr_{1,2}) \quad \text{Ref. 12}$$

$$A^j_{1,2} = \frac{9}{2}\left(\frac{f^j \nu}{m^j (r^j)^2}\right)_{1,2} \tag{3.46}$$

$$C^j_{1,2} = \frac{G^j_{1,2}\, C_{p_{1,2}}}{f^j_{1,2}\, Pr_{1,2}} \tag{3.83}$$

and,

$$B^j_{1_{1,2}} = \frac{1}{\frac{C_{p_{1,2}}}{R_{1,2}} - 1}\left\{\bar{q}_{1,2}\cdot\Delta\bar{q}^j_{1,2} - \bar{q}^j_{1,2}\cdot\Delta\bar{q}^j_{1,2} + \frac{2}{3}C^j_{1,2}\,(T^j_{1,2} - T_{1,2})\right.$$

$$\left. + \frac{3\sigma_{1,2}}{A^j_{1,2}\, m^j_{1,2}\, r^j_{1,2}}\left[\epsilon^j_{1,2}\,(T^j_{1,2})^4 - \alpha^j_{1,2}\, T^4_{1,2}\right]\right\} \tag{3.86c}$$

Note that the points 1, 2 and 8 are not necessarily as shown in Fig. 7-2a. Their locations can vary along the J-line depending on the mesh size and the Mach number in the vicinity of point 3. Figure 7-2b presents one example when the point m + 2 is an upper boundary point and the point 1' is outside the flow field under consideration. Instead of the point 1' the point 1 is used in the calculation. However, the properties at point 1 are not available nor can they be interpolated because point n + 2 is not yet known. For this particular case, the flow properties at point 1 are assumed to be identical to those of point m + 2 so that the properties at point 3 can be approximated. The same method is used to calculate point n + 1. The boundary point n + 2 of the K-line can then be calculated without problem. Once the boundary point is determined the calculation goes back to point 1 and the right running characteristic

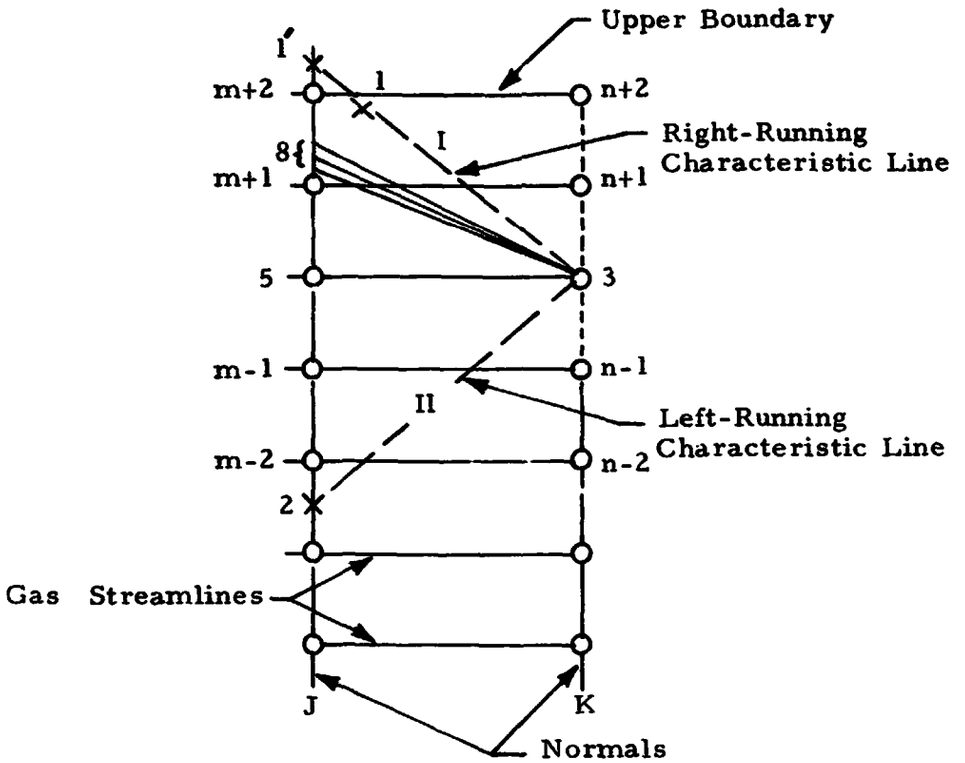

Fig. 7-2b - Mesh Construction for an Interior Point

intersection is made using the two boundary points. Point 1 is then solved for and the solution proceeds to the plume boundary.

Step 4: The particle density at point 3K is calculated using the relationship:

$$\rho_3^j = \frac{1}{u_3^j (y_1^j y_1^{j\delta} - y_2^j y_2^{j\delta}) - v_3^j \left[(y_1^{j\delta} + y_3^{j\delta})(x_1^j - x_3^j) + (y_2^{j\delta} + y_3^{j\delta})(x_3^j - x_2^j)\right]}$$

$$\left[\rho_1^j \left\{u_1^j (y_3^j y_3^{j\delta} - y_2^j y_2^{j\delta}) - v_1^j \left[(y_1^{j\delta} + y_2^{j\delta})(x_1^j - x_2^j) - (y_1^{j\delta} + y_3^{j\delta})(x_1^j - x_3^j)\right]\right\}\right.$$

$$\left. + \rho_2^j \left\{u_2^j (y_1^j y_1^{j\delta} - y_3^j y_3^{j\delta}) - v_2^j \left[(y_1^{j\delta} + y_2^{j\delta})(x_1^j - x_2^j) - (y_2^{j\delta} + y_3^{j\delta})(x_3^j - x_2^j)\right]\right\}\right] \quad (4.157)$$

Step 5: The particle streamline intersections with the J data line are now located (point 8 of Fig. 7-2a) using the particle streamline relationship:

$$\frac{y_3^j - y_8^j}{x_3^j - x_8^j} = \frac{v_3^j}{u_3^j} \tag{4.42}$$

Step 6: The gas and particle properties at point 8J are now found by employing an interpolation scheme as described in Step 3.

Step 7: The coefficients for the particle compatibility relations are now calculated from Eq. (4-150a).

$$C2_{8,3}^j = \frac{\left(u_{8,3} - u_{8,3}^j\right)}{u_{8,3}^j} A_{8,3}^j$$

$$C3_{8,3}^j = \frac{\left(v_{8,3} - v_{8,3}^j\right)}{u_{8,3}^j} A_{8,3}^j$$

$$C4_{8,3}^j = \frac{-\left\{\frac{2}{3} A_{8,3}^j C_{8,3}^j (T_{8,3}^j - T_{8,3}) + \frac{3\sigma_{8,3}}{m_{8,3}^j r_{8,3}^j}\left[\epsilon_{8,3}^j (T_{8,3}^j)^4 - \alpha_{8,3}^j T_{8,3}^4\right]\right\}}{u_{8,3}^j}$$

Step 8: The new particle properties at point 3K are then found by expanding the difference Eqs. (4.148), (4.149) and (4.150) to obtain

$$u_3^j = u_8^j + \overline{C2_{8,3}^j}\, \Delta x_{8-3}^j$$

$$v_3^j = v_8^j + \overline{C3}_{8,3}^j \Delta x_{8-3}^j$$

$$h_3^j = h_8^j + \overline{C4}_{8,3}^j \Delta x_{8-3}^j$$

with the remaining properties defined as

$$T_3^j = f(h)_3^j \quad \text{tabulated}$$

$$Re_3^j = \frac{2 r_3^j \rho_3 \left|\Delta q_3^j\right|}{\nu_3}$$

$$f_3^j = f(Re_3^j) \text{ tabulated}$$

$$G_3^j = f(Re_3^j, Pr_3) \quad \text{Ref. 12}$$

$$A_3^j = \frac{9}{2} \frac{f_3^j \nu_3}{m_3^j (r_3^j)^2} \tag{3.46}$$

$$C_3^j = \frac{G_3^j C_{p_3}}{f_3^j Pr_3} \tag{3.83}$$

and,

$$B_{1_3}^j = \frac{1}{C_{p_3}/R_3 - 1} \left\{ \bar{q}_3 \cdot \Delta \bar{q}_3{}^j - \bar{q}_3{}^j \cdot \Delta \bar{q}_3{}^j + \frac{2}{3} C_3^j (T_3^j - T_3) \right.$$

$$\left. + \frac{3\sigma_3}{A_3^j m_3^j r_3^j} \left[\epsilon_3^j (T_3^j)^4 - \alpha_3^j T_3^4 \right] \right\} \tag{3.86c}$$

Step 9: The coefficients for the gas streamline compatibility relations are now calculated

$$C_2 = \left(\frac{\overline{C}_{p_{5,3}}}{\overline{R}_{5,3}} - 1 \right) \left[\sum_{j=1}^{NP} \overline{\rho}^{j}_{5,3} \, \overline{A}^{j}_{5,3} \, \overline{B}^{j}_{1_{5,3}} \right] \frac{\Delta L_{5-3}}{\overline{\rho}_{5,3} \, \overline{T}_{5,3} \, \overline{q}_{5,3}}$$

and

$$C_{3_p} = \frac{1}{\overline{\rho}_{5,3}} \sum_{j=1}^{NP} \overline{\rho}^{j}_{5,3} \, \overline{A}^{j}_{5,3} \left[(\overline{u}_{5,3} - \overline{u}^{j}_{5,3}) \cos\overline{\theta}_{5,3} + (\overline{v}_{5,3} - \overline{v}^{j}_{5,3}) \sin\overline{\theta}_{5,3} \right] \Delta L_{5-3} \, .$$

Step 10: The rate of change of entropy in the direction of the gas streamline and the entropy at the point 3K are calculated in the following manner:

$$\Delta S_{5-3} = C_2 \tag{4.143}$$

and the entropy at point 3K is

$$S_3 = S_5 + C_2 \, .$$

Step 11: The rate of change of enthalpy in the direction of the gas streamline and the enthalpy at the point 3K are calculated in the following manner:

$$\Delta H_{5-3} = \overline{T}_{5,3} \, \Delta S_{5-3} - C_{3_p} \tag{4.142}$$

and the enthalpy at point 3K is

$$H_3 = H_5 + \bar{T}_{5,3}\,\Delta S_{5-3} - C_{3_p}\,.$$

Step 12: The remaining gas properties to be calculated at point 3K are the velocity and flow angle. Expanding equation (4.146) in terms of both the right and left-running characteristics and solving for the velocity gives

$$q_3 = \frac{\theta_1-\theta_2+Q_1q_1+Q_2q_2-B_1-B_2+CI_1(H_3-H_1)+CI_2(H_3-H_2)+G_1+G_2-Cl_1-Cl_2}{Q_1+Q_2}$$

The new flow angle is then

$$\theta_3 = \theta_2 + Q_2 q_3 - Q_2 q_2 + B_2 - CI_2(H_3 - H_2) - G_2 + Cl_2$$

Step 13: The properties T_3, ρ_3, ν_3, C_{p_3}, Pr_3, A_3^j, C_3^j and B_3^j are recalculated to reflect the new gas properties. The solution is then checked to determine if the desired accuracy has been obtained. If the solution has not converged, return to step 2 and repeat the process. The flow of the numerical solution is summarized in Chart 7-1.

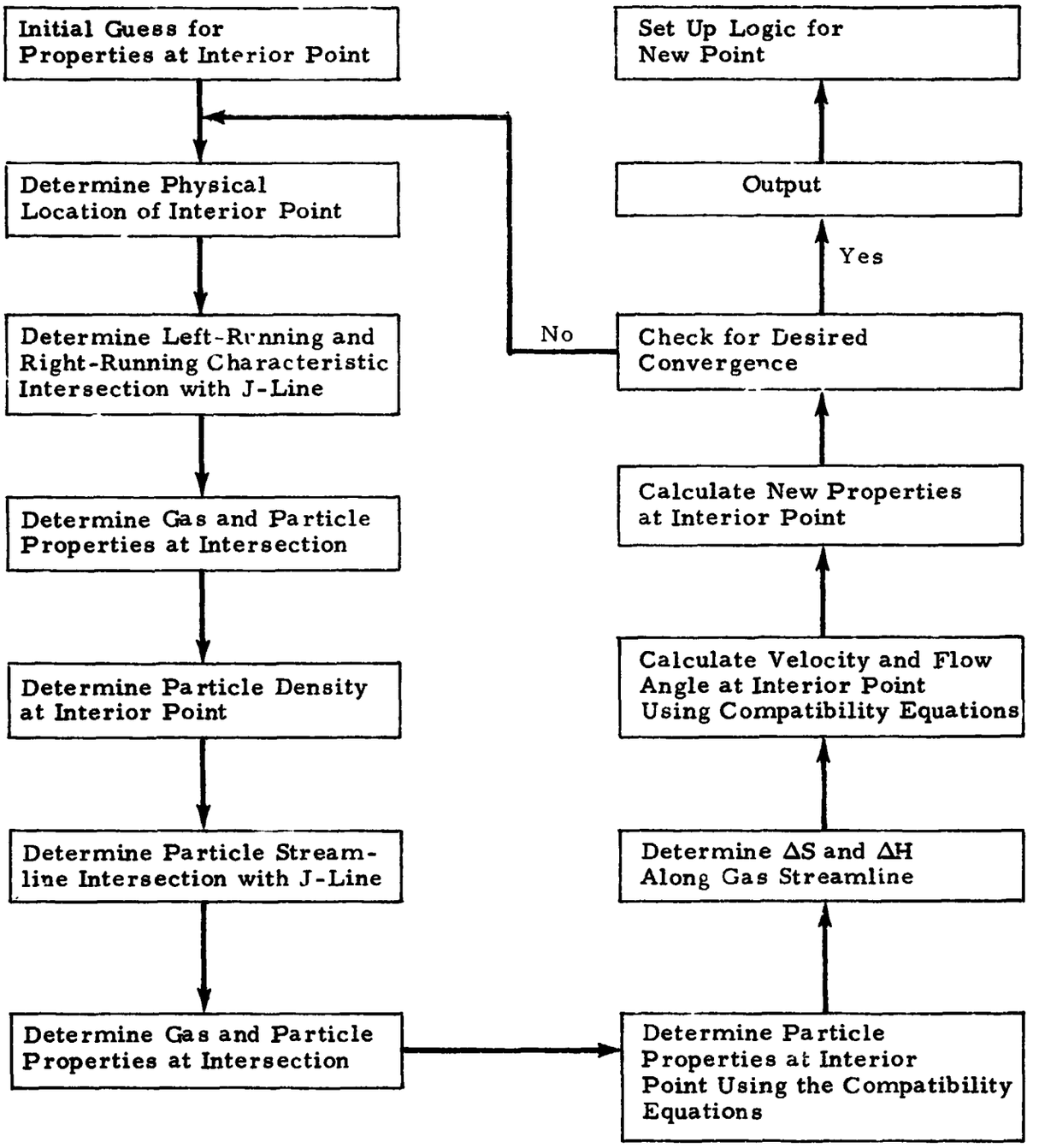

Chart 7-1 - Flow Chart of the Calculation Procedure for an Interior Point Solution

7.2 LOWER WALL POINT

Figure 7-3 presents the mesh construction required to solve for gas and particle properties at any lower wall point in Figure ·-1.

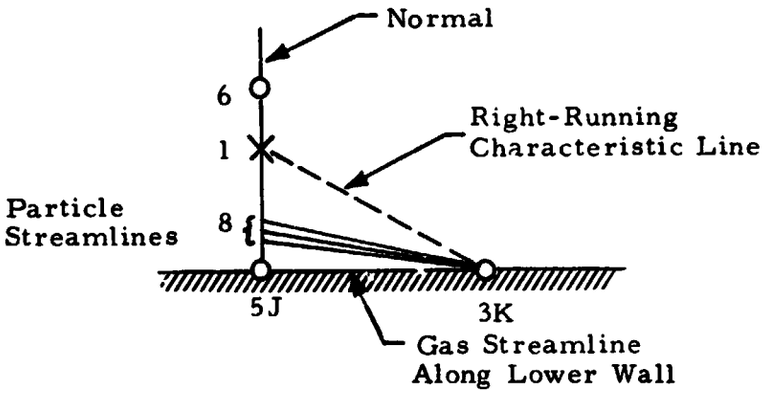

Fig. 7-3 - Mesh Construction for a Lower Wall Point

The calculational procedure followed to determine the flow properties at a lower all point is very similar to that of an interior point solution. The lower wall point is always the first point calculated on a K-line. Before the point 3K can be located, point 1J must first be selected as a function of the desired mesh size. Once point 1J is located and its properties determined using the interpolation scheme employed for an interior point; the physical location (x_3, y_3) of point 3K is found by intersecting the right-running characteristic from point 1J and the projection of the streamline from the point 5J. The particle density at point 3K is then calculated using the relationship

$$\rho_3^j = \frac{\rho_5^j u_5^j - 2\rho_1^j v_1^j (x_3 - x_5)}{u_3^j} \qquad (4.163)$$

and is based on the assumptions that: (1) the lower boundary runs parallel to the X-axis; and (2) the particle streamlines run parallel to the lower boundary when in the vicinity of the lower boundary.

Finally, since the flow angle along the lower wall is known, only the right running characteristic line is needed to calculate the velocity at the lower wall point. Solving for velocity in Eq. (4.146) gives

$$q_3 = \frac{[\theta_1 - \theta_3 + Q_1 q_1 - B_1 + CI_1(H_3 - H_1) + G_1 - CI_1]}{Q_1}$$

Once the velocity is found, the calculational procedure is continued as in the case of an interior point.

7.3 UPPER WALL POINT

Figure 7-4 presents the mesh construction required to solve for the gas and particle properties at any upper wall point in Fig. 7-1.

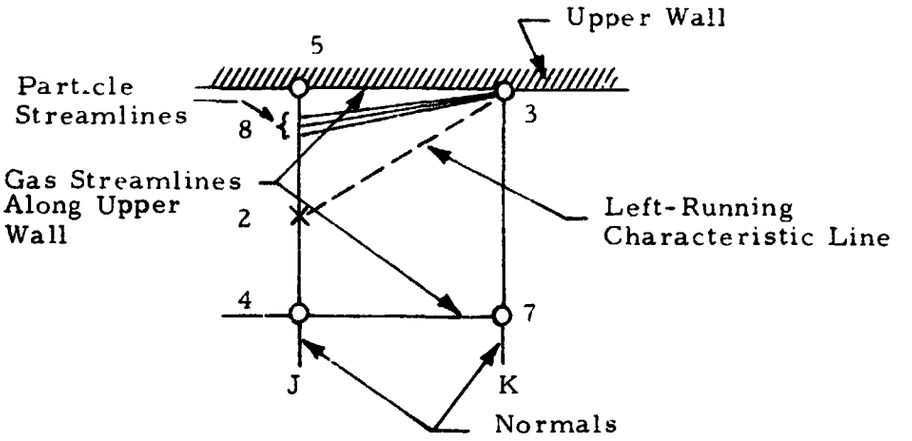

Fig. 7-4 - Mesh Construction for an Upper Wall Point

The calculational procedure followed to determine the flow properties at an upper wall point is almost identical to that of an interior point solution. The exception is that the flow angle on the upper wall is known and, therefore, only the left-running characteristic line is needed to calculate the velocity at the upper boundary point. Solving for velocity in Eq. (4.146) gives:

$$q_3 = \frac{\theta_3 - \theta_2 + Q_2 q_2 - B_2 + Cl_2(H_3 - H_2) + G_2 - Cl_2}{Q_2} .$$

7.4 FREE BOUNDARY POINT

Figure 6-5 presents the mesh construction required to solve for the gas and particle properties at a free boundary point. Note that the mesh construction is the same as that for an upper wall point.

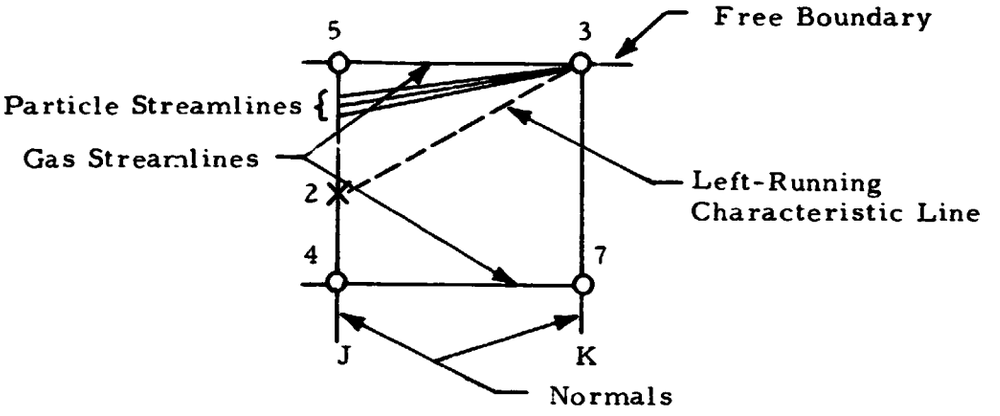

Fig. 7-5 - Mesh Construction for a Free Boundary Point

The calculational procedure followed to determine the flow properties at a free boundary point is like that of an upper wall point solution. The one difference is that the velocity and not the flow angle at the free boundary point is known. Applying Eq. (4.146) to the left-running characteristic and solving for the flow angle at the free boundary point gives

$$\theta_3 = \theta_2 + Q_2(q_3 - q_2) + B_2 - Cl_2(H_3 - H_2) - G_2 + Cl_2 .$$

The velocity at the free boundary, though assumed to be known, is not easily obtained. The velocity at the free boundary must be solved for iteratively using the relation

$$q_3 = \left\{ \frac{2\gamma RT}{\gamma - 1} \left[\left(\frac{P}{P_0} \right)^{-\frac{\gamma - 1}{\gamma}} - 1 \right] \right\}^{1/2} .$$

An interative solution is required because the gas properties R, T and P are functions of a variable γ. If an ideal gas was being considered, γ would be constant and v_3 may be solved for directly.

7.5 PARTICLE LIMITING STREAMLINE POINT

Figure 7-6 presents the mesh construction required to solve for the gas and particle properties at any particle limiting streamline point in Figure 7-1.

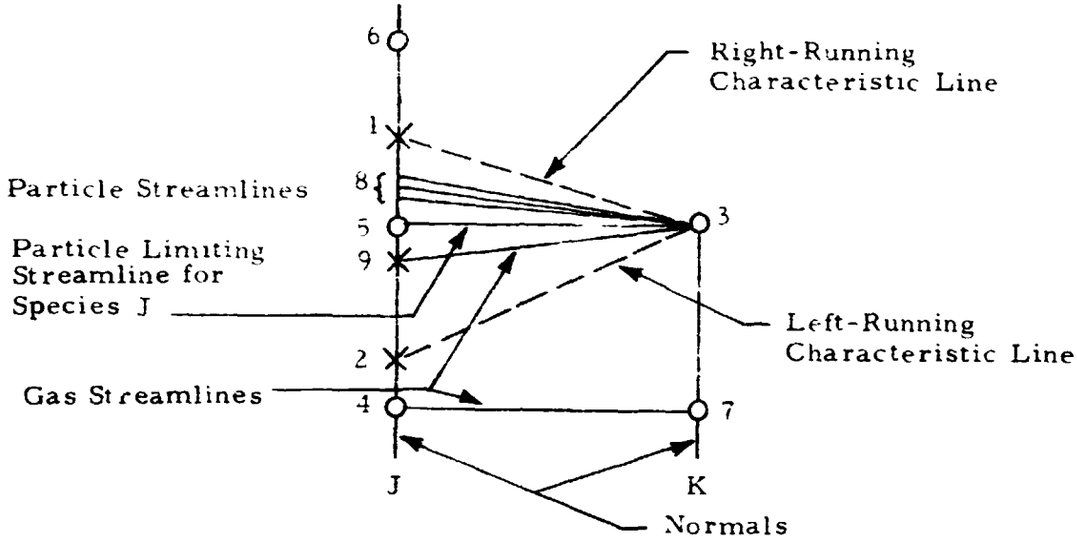

Fig. 7-6 - Mesh Construction for a Particle Limiting Streamline Point

The calculational procedure followed to determine the flow properties at a particle limiting streamline point is somewhat different from that of an interior point solution. The differences in the calculational procedure are brought about by the fact that the J and K normals are constructed between a gas streamline and a particle limiting streamline rather than between two gas streamlines.

The physical location (x_3, y_3) of point 3K is found by intersecting the normal from the point 7K with the projection of the particle limiting streamline of species J from the point 5J. Once point 3K is located, the gas streamline

intersection with the J data line must be located (point 9 of Figure 7-6) using the gas streamline relationship

$$\frac{y_3 - y_9}{x_3 - x_9} = \frac{v_3}{u_3} \quad . \tag{4.41}$$

The properties at this point are found by interpolation between the known points 4J and 5J.

The particle density at point 3K for all particle species except particle species J is determined in the same manner as for an interior point. The particle density of species J is calculated using the relationship

$$\rho_3 = \frac{1}{u_3 (y_3 y_3^{\delta} - y_2 y_2^{\delta}) - v_3 (y_3^{\delta} + y_2^{\delta})(x_3 - x_2)} \left\{ \rho_5 \left[u_5 (y_5 y_5^{\delta} - y_2 y_2^{\delta}) - v_5 (y_5^{\delta} + y_2^{\delta}) \right.\right.$$

$$\left.\left. (x_5 - x_2) \right] + \rho_2 \left\{ u_2 (y_5 y_5^{\delta} - y_3 y_3^{\delta}) - v_2 \left[(y_5^{\delta} + y_2^{\delta}) (x_5 - x_2) - (y_3^{\delta} + y_2^{\delta}) (x_3 - x_2) \right] \right\} \right\} \tag{4.169}$$

and is based on the fact that the entire mass of particle species J is contained in the streamtube formed by the particle limiting streamline for species J.

Once the particle densities have been found, the calculation procedure is continued as in the case of an interior point.

7.6 PARTICLE LIMITING STREAMLINE-BOUNDARY INTERSECTION

Figure 7-7 presents the mesh construction required to solve for the gas and particle properties at the particle limiting streamline-boundary intersection.

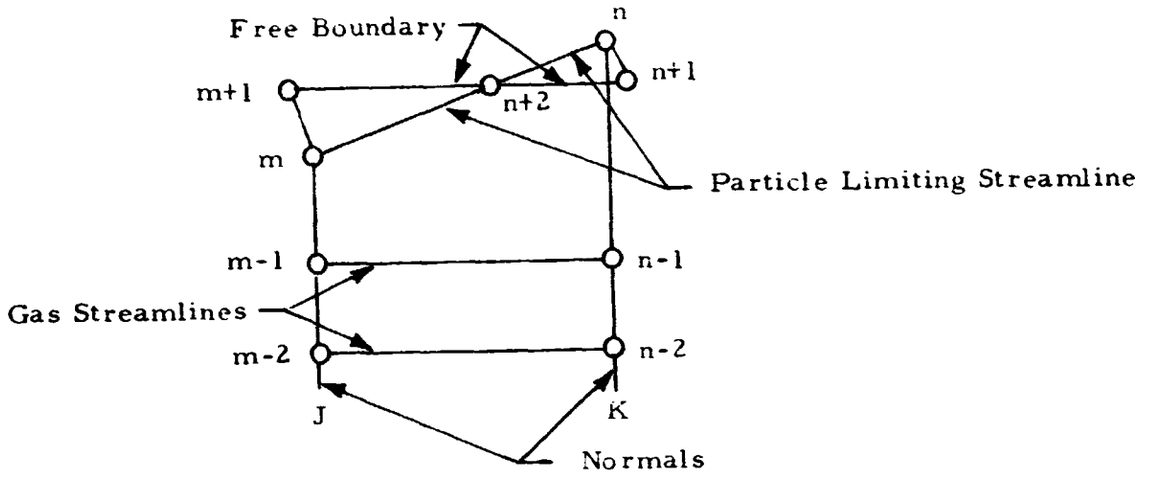

Fig. 7-7 - Mesh Construction for a Particle Limiting Streamline-Boundary Intersection

Assume that the particle limiting streamline point (n, K) has just been completed and the next point to be calculated is that of a free boundary point (n+1, K). Under these circumstances, the free boundary point is calculated in the normal manner, and then upon completion of the free boundary point a comparison is made of the physical location of the two points. If $y_{n+1} < y_n$, an intersection of the particle limiting streamline and free boundary is indicated. The physical location of (n+2, K) is found intersecting the projection of the streamline from the point (m+1, J) and the particle limiting streamline between the points (m, J) and (n, K). The gas and particle properties at the point (n+2, K) are then found by interpolation between the points (m, J) and (n, K).

Once the properties at the point (n+2, K) are found, the point (n+1, K) is assumed to no longer exist. The point (n+2, K) is used as the base point the next time an upper boundary point is calculated.

The description of the entire flow field now proceeds onto the calculation of the lower boundary point of the new K-line.

7.7 EXPANSION CORNER – PRANDTL-MEYER FAN

Expansion corners are found when the slope of the solid boundary has a discontinuity in such a way that the flow must negotiate a sharp turn away from the oncoming flow or when the flow issuing into an open space is under-expanded in a nozzle or a flow channel. The expansion takes place either in a channel or at the channel exit. The amount of turn the flow must make and the final flow velocity can be found with the aid of the Prandtl-Meyer expansion relation, Eq.(6.1),and the boundary conditions.

After the total turning angle is found, it is subdivided into a number of small turning angles. The flow properties at the expansion corner corresponding to each of the small turns are calculated and the angle's corresponding characteristic lines emanating from the corner are constructed. The final line of the expansion is a streamline rather than a characteristic line and, normally, the Mach angle corresponding to this streamline is substantially greater than the small turning angle. An extra point is inserted to fill the gap after the expansion corner computation has been completed. Note that this final expansion line, a streamline, can be a solid boundary or a free boundary.

In the example shown in Figure 7- 8, the turning angle is subdivided into four small turns. The corresponding characteristic lines emanating from the corner are designated as A, B, C and D in Figure 7- 8. The final expansion line E is a streamline corresponding to the last corner point (d, J). The properties at the corner corresponding to every small turn are stored in (a, J), (b, J), (c, J) and (d, J) arrays. The properties at the corner before the expansion takes place can be found as usual and are stored in (m, J) array; its characteristic line is designated as M in Figure 7- 8.

A weak shock is initialized at point (n+4, K) for the upper corner expansion point or (n-4,K) for the lower corner expansion, which is done simply by defining a double point at those points with identical flow properties. The initial shock angle is assumed equal to the Mach angle.

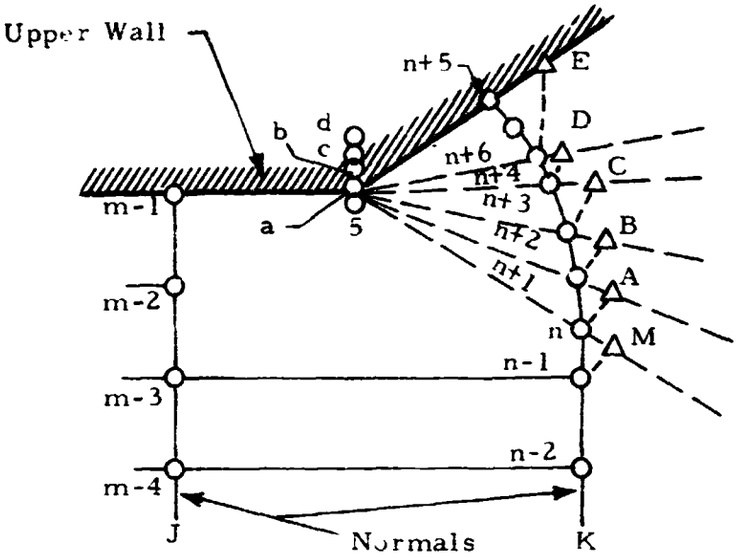

Fig. 7- 8a - Mesh Construction for an Upper Expansion Corner Point

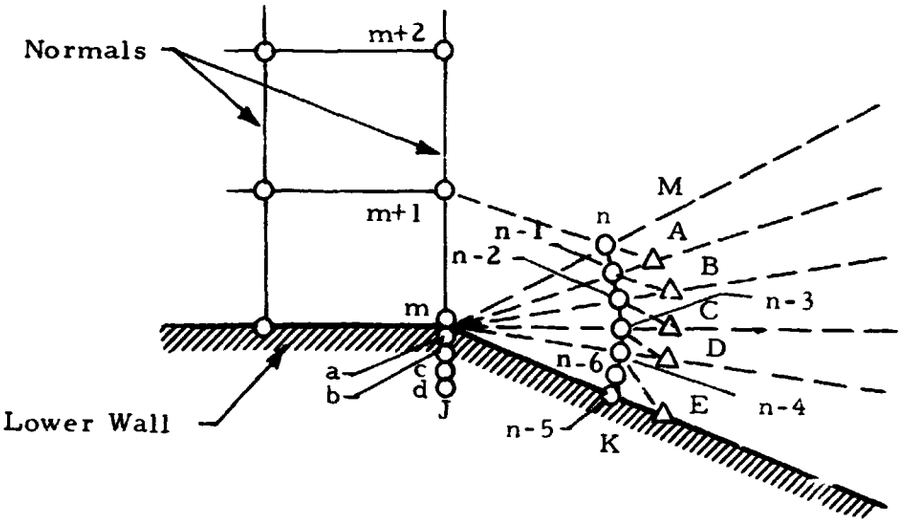

Fig. 7- 8b - Mesh Construction for a Lower Expansion Corner Point

7.7.1 Upper Corner Expansion

As shown in Figure 7- 8(a), the point (n-1, K) is considered to be complete. A left-running characteristic is drawn from the point (n-1, K) to intersect the right-running characteristic from point (m, J) at M, which is an interior point. The properties can be calculated in the usual manner. A normal is drawn from point (n-1, K) to intersect the right-running characteristic from point (m, J) at n. The properties at this point are then interpolated between points (m, J) and M. Similarly, the properties at points (n+1, K) through (n+4, K) can be calculated. Point (n+5, K) is calculated by the same technique provided that the point E is treated as an upper boundary point. If the distance between points (n+4, K) and (n+5, K) is greater than other meshes in the expansion fan, one extra point (n+6, K) is inserted and its properties are found by interpolation between points (n+4, K) and (n+5, K).

7.7.2 Lower Corner Expansion

This case is shown in Figure 7- 8 (b). When an expansion at the lower boundary is detected, the normal line starting from the corner point (m, J) is completed first. The flow properties at the corner and the corresponding characteristic line for each small turn can be found by the same method described in the preceding paragraph. Point (n, K) is the intersection of the right-running characteristic from point (m+1, J) and the left-running characteristic from point (m, J); its properties can be calculated without problem. The flow properties at point A can also be calculated. A normal from point (n, K) and the left-running characteristic from point (a, J) intersects at (n-1, K); flow properties at this point are then interpolated between points (a, J) and A. Points (n-2, K) through (n-4, K) can be calculated by the same method. Point (n-5, K) is a lower boundary point which can be calculated with the technique used to find the point (n+5, K) in Figure 7- 8(a). An extra point may also be inserted between points (n-4, K) and (n-5, K) if needed.

8. NUMERICAL INTEGRATION OF THE CONSERVATION EQUATIONS

Examination of the mass flow rate, momentum flux and energy flux through a nozzle and exhaust plume will yield considerable information about the nozzle performance and the status of the flowfield numerical solution. The momentum flux is used to determine the thrust produced by the nozzle while the thrust ratioed to the mass flow rate is a measure of the nozzle performance. Deviations of the fluxes in the conservative parameters from surface to surface (Fig. 8-1) are indicators of the validity of a numerical solution such as the one used in the gas-particle code.

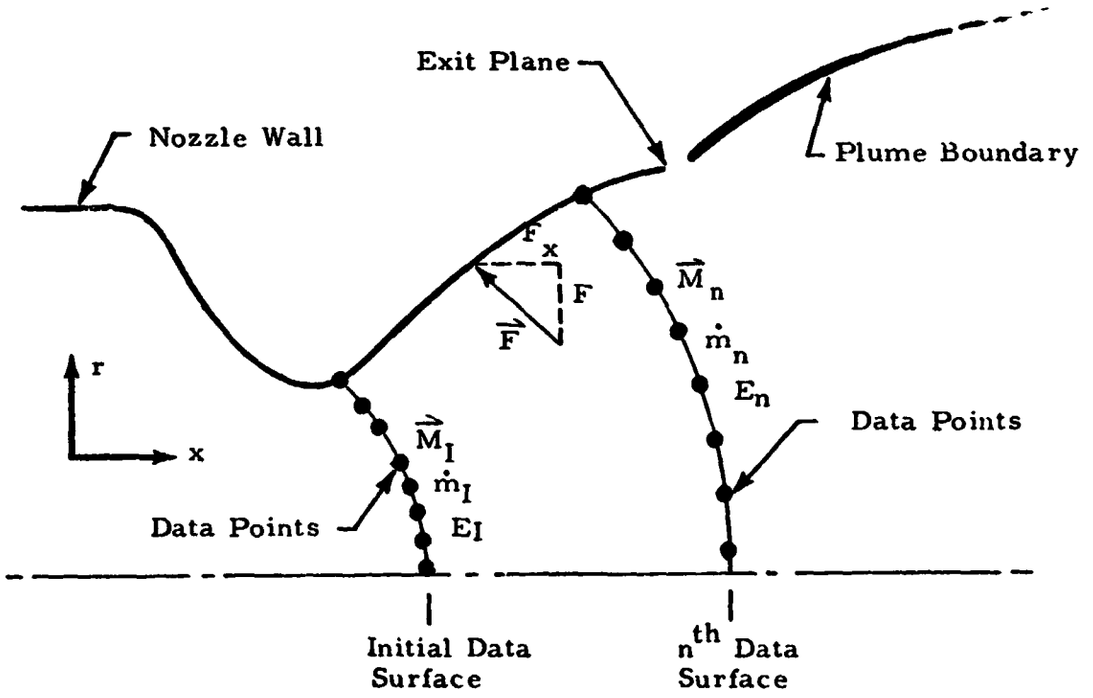

Fig. 8-1 - Schematic of Conservation Parameters in a Nozzle Plume

8.1 CONTINUITY

The mass flow rate through a surface is calculated by numerically integrating the incremental mass flow through adjacent streamtubes. A streamtube is defined as the flow area bounded by adjacent data points (Fig. 8-2a) and the incremental flow rate is calculated as follows.

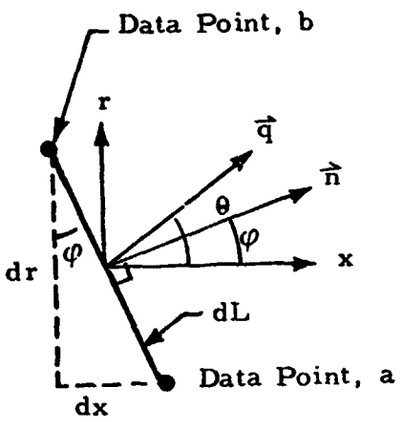

Fig. 8-2a - Schematic of Surface Geometry

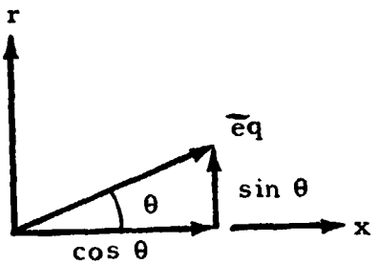

Fig. 8-2b - Schematic of Velocity Unit Vector

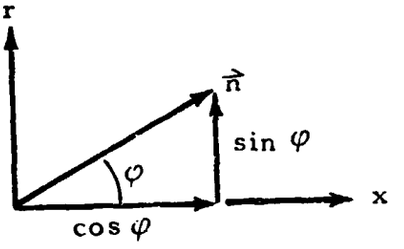

Fig. 8-2c - Schematic of Surface Normal Unit Vector

Fig. 8-2 - Schematic of Elemental Geometry on a Data Surface

Let points a and b be any two points on a data surface within the flow field. The incremental flow area for axisymmetric or two-dimensional flow is given by

$$dA = (2\pi r)^{\delta} dL . \qquad (8.1)$$

In terms of the coordinate directions, the incremental area is

$$dA = (2\pi r)^{\delta} \left\{(dr)^2 + (dx)^2\right\}^{1/2} \tag{8.2}$$

The flow area in the direction normal to the surface, dL, is now

$$\vec{dA} = (2\pi r)^{\delta} \left\{(dr)^2 + (dx)^2\right\}^{1/2} \hat{e}_n \tag{8.3}$$

where the unit normal vector, $\hat{e}_n$, is defined by the geometry of Fig. 8-2c as

$$\hat{e}_n = \cos\varphi\, \hat{i} + \sin\varphi\, \hat{j}\,; \tag{8.4}$$

and the angular location of the unit normal vector relative to the x-axis is

$$\varphi = -\tan^{-1}\left(\frac{dx}{dr}\right) \tag{8.5}$$

The quantity of mass flowing through the incremental area is found from the relation

$$d\dot{m} = \rho \left|\vec{q}\right| dA\, \hat{e}_q \cdot \hat{e}_n\,; \tag{8.6}$$

where the unit velocity vector, $\hat{e}_q$ is defined by the geometry of Fig. 8-2b. The relation for $\dot{m}$ is now

$$\dot{m} = \rho \left|\vec{q}\right| dA \left\{\cos\theta\, \hat{i} + \sin\theta\, \hat{j}\right\} \cdot \left(\cos\varphi\, \hat{i} + \sin\varphi\, \hat{j}\right\}.$$

Performing the indicated dot product the relation reduces to

$$\dot{m} = \rho \left|\vec{q}\right| dA \left\{\cos\theta\, \cos\varphi + \sin\theta\, \sin\varphi\right\}.$$

The trigometric identity for sine-cosine function is

$$\cos\theta\, \cos\varphi + \sin\theta\, \sin\varphi = \cos(\theta - \varphi)\,.$$

Substituting, the incremental mass flow is

$$d\dot{m} = \rho \left| \vec{q} \right| dA \cos(\theta - \varphi) \ . \tag{8.7}$$

The total mass flow through the surface is simply

$$\dot{m} = \sum d\dot{m} \tag{8.8}$$

for all the incremental flow areas.

So far the discussion has been directed toward a general expression for the mass flow rate. For gas-particle flows the surface geometry is the same. The only change is in the definition of the flow variables. The expression for the respective phases are as follows:

Gas Phase

$$\dot{m} = \rho \left| \vec{q} \right| dA \cos(\theta - \varphi) \ ; \tag{8.9a}$$

Particle (j^{th} particle)

$$\dot{m}^j = \rho^j \left| \vec{q}^j \right| dA \cos(\theta^j - \varphi) \ ; \tag{8.9b}$$

Mixture

$$\dot{m}_m = \dot{m} + \sum_{j=1}^{NP} \dot{m}^j \tag{8.9c}$$

8.2 MOMENTUM

As with the mass flow relations, a general expression for the momentum flux will be developed. This expression will then be extended to include the treatment of gas-particle flows.

The general expression for the momentum flux is

$$\vec{M}_M = \left\{ P\bar{\bar{\delta}} + \rho \vec{q}\,\vec{q} \right\} \cdot d\vec{A} \tag{8.10}$$

where $\bar{\bar{\delta}}$ is the Kronecker delta and $d\vec{A}$ is given by Eq. (8.3). Substituting for $d\vec{A}$ and performing the indicated algebraic operations, Eq. (7.10) becomes

$$\vec{M}_M = \left\{ P\vec{n} + \rho \vec{q}\,\vec{q} \cdot \vec{n} \right\} dA \tag{8.11}$$

where dA is now defined by Eq. (8.2). Equation (8.11) yields an expression for each coordinate direction in the equation in terms of the scalar components given by the expressions

$$\vec{M}_M = \left\{ P(\cos\varphi \hat{i} + \sin\varphi \hat{j}) + \rho(u\hat{i} + v\hat{i})\,(u\hat{i} + v\hat{j}) \cdot (\cos\varphi \hat{i} + \sin\varphi \hat{j}) \right\} dA ;$$

$$\vec{M}_M = \left\{ P(\cos\varphi \hat{i} + \sin\varphi \hat{j}) + \rho(u^2 \hat{i}\hat{i} + uv\hat{i}\hat{j} + uv\hat{j}\hat{i} + v^2 \hat{j}\hat{i}) \cdot (\cos\varphi \hat{i} + \sin\varphi \hat{j}) \right\} dA ;$$

$$\vec{M}_M = \left\{ P(\cos\varphi \hat{i} + \sin\varphi \hat{j}) + \rho(u^2 \cos\varphi \hat{i} + uv \cos\varphi \hat{j} + uv\sin\varphi \hat{i} + v^2 \sin\varphi \hat{j}) \right\} dA .$$

The scalar equations in the coordinate directions are then

$$M_{M_x} = \left\{ P\cos\varphi + \rho\,(u^2 \cos\varphi + uv \sin\varphi) \right\} dA ,$$

and

$$M_{M_n} = \left\{ P\sin\varphi + \rho(uv\cos\varphi + v^2 \sin\varphi) \right\} dA;$$

Substituting for the velocity components

$$M_{M_x} = \left\{ P\cos\varphi + \rho q^2 (\cos\theta \cos\theta \cos\varphi + \cos\theta \sin\theta \sin\varphi) \right\} dA$$

and

$$M_{M_r} = \left\{ P\sin\varphi + \rho q^2 (\cos\theta \sin\theta \cos\varphi + \sin\theta \sin\theta \sin\varphi) \right\} dA .$$

Factoring common terms and substituting the trigometric identity as before the final result for the incremental momentum flux is

$$M_{M_x} = \left\{P \cos\varphi + \rho q^2 \cos(\theta - \varphi) \cos\theta\right\} dA , \tag{8.12a}$$

and

$$M_{M_r} = \left\{P \sin\varphi + \rho q^2 \cos(\theta - \varphi) \sin\theta\right\} dA \tag{8.12b}$$

The only difference between the expression for the gas and particle contributions to the momentum flux is that the particles do not contribute to the pressure of the mixture. The respective expressions for the momentum flux through the surface are:

Gas

$$M_{M_x} = \left\{P \cos\varphi + \rho q^2 \cos(\theta - \varphi) \cos\theta\right\} A \tag{8.13a}$$

$$M_{M_r} = \left\{P \sin\varphi + \rho q^2 \cos(\theta - \varphi) \sin\theta\right\} A \tag{8.13b}$$

Particles (j^{th} Particle)

$$M^j_{M_x} = \rho^j (q^2)^j \cos(\theta - \varphi) \cos(\theta^j) A \tag{8.13c}$$

$$M^j_{M_r} = \rho^j (q^2) \cos(\theta - \varphi) \sin(\theta^j) A \tag{8.13d}$$

Mixture

$$M_{M_{m_x}} = M_{M_x} + \sum_{j=1}^{NP} M^j_{M_x} \tag{8.14a}$$

$$M_{M_{m_r}} = M_{M_r} + \sum_{j=1}^{NP} M^j_{M_r} \tag{8.14b}$$

8.3 ENERGY

The general relation is

$$E = (h + \tfrac{1}{2} q^2)\, \dot{m} \tag{8.15}$$

Applied to gas and particulate phases the respective relations for a given surface are:

Gas

$$E = (h + \tfrac{1}{2} q^2)\, \dot{m} \tag{8.16a}$$

Particles (j^{th} Particle)

$$E^j = (h^j + \tfrac{1}{2} (q^2)^j)\, \dot{m}^j \tag{8.16b}$$

Mixture

$$E_m = E + \sum_{j=1}^{NP} E^j \tag{8.16c}$$

8.4 NOZZLE PERFORMANCE

Performance parameters considered are the thrust produced and the associated specific impulse, I_{sp}. The force vector is calculated as the mixture momentum on the initial data surface (Fig. 8-1) plus the pressure force on the nozzle wall. Mathematically this is expressed as

$$\vec{F}_T = \vec{M}_{m_I} + \int P_w \, \vec{dA}_w \tag{8.17}$$

The integral term in Eq. (8.17) is obtained by numerically integrating the pressure force along the nozzle wall. Consider the elemental surface, dL, bounded by the nozzle wall points a and b on any two successive data

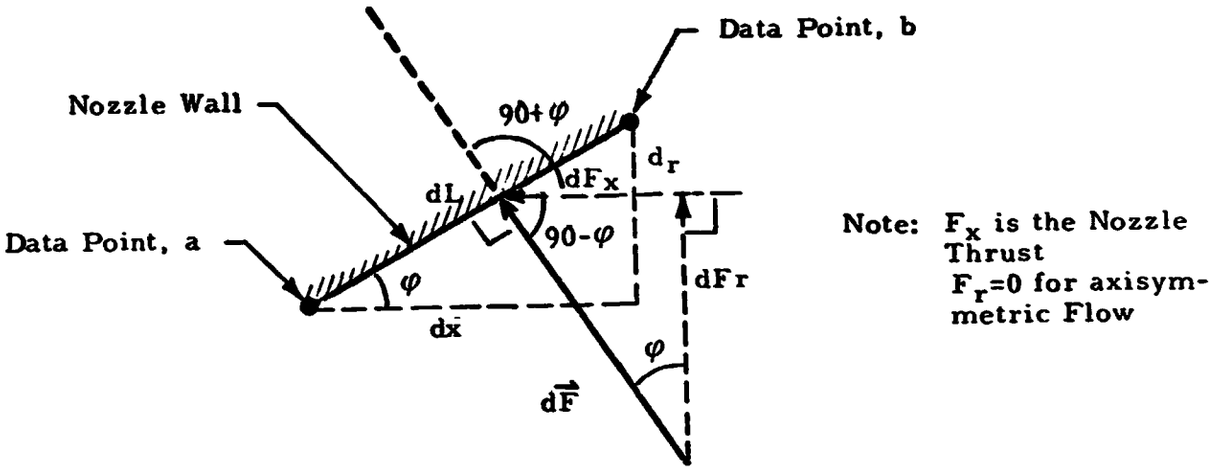

Fig. 8-3 - Schematic of Pressure Force Acting on the Nozzle Wall

surfaces. The slop e surface, dL, is given by

$$\varphi_L = \tan^{-1}\left(\frac{dr}{dx}\right) \quad . \tag{8.18}$$

However, the force due to the pressure loading acts normal to the sur e which is given by the angular relation 90 + φ. The local surface area over which the pressure is acting is

$$dA = (2\pi r)^{\delta} \left\{(dr)^2 + (dx)^2\right\}^{1/2} ; \tag{8.19}$$

and the unit normal to the surface is

$$\vec{n}_L = -\sin\varphi\hat{i} + \cos\varphi\hat{j} , \tag{8.20}$$

so that

$$\vec{dA} = dA\,\vec{n}$$

$$\vec{dA} = (2\pi r)\delta \left\{(dr)^2 + (dx)^2\right\}^{1/2} \left\{-\sin\varphi\hat{i} + \cos(\varphi)\hat{j}\right\} \qquad (8.21)$$

Equation (8.21) can be generalized to reflect the loading increment to either an upper or lower wall in the following manner. Define a parameter λ which has a value of $\pm$ 1 for an upper or lower wall, respectively. The orientation of the surface unit normal with respect to the x-axis is

$$\varphi_1 = \varphi_L + \lambda\, 90 \qquad (8.22)$$

From the sine and cosine trigometric identities, Eq. (8.22) reduces to

$$\cos\varphi_1 = -\sin\varphi$$

and

$$\sin\varphi_1 = \cos\varphi$$

so that the unit normal vector is now given by

$$\vec{n} = \cos\varphi_1\hat{i} + \sin\varphi_1\hat{j}\,;$$

and the surface area term is now

$$\vec{dA}_w = (2\pi r)\delta \left\{(dr)^2 + (dx)^2\right\}^{1/2} \left\{\cos(\varphi_1)\hat{i} + \sin(\varphi_1)\hat{j}\right\}.$$

The resultant force relation for the nozzle is then

$$\vec{F}_T = \vec{M}_{m_I} + \sum_{i=1}^{NS}\left[P\,(2\pi r)\delta \left\{(dr)^2 + (dx)^2\right\}^{1/2} \left\{\cos(\varphi_1)\hat{i} + \sin\varphi_1\hat{j}\right\}\right] \qquad (8.23)$$

and the nozzle thrust is just F_x. The specific impulse, I_{sp}, is then

$$I_{sp} = F_x/\dot{m}_{m_I} \quad . \tag{8.24}$$

8.5 PERCENT CHANGES IN THE CONSERVATION QUANTITIES

One check on the validity of the numerical solution is to monitor the change in the conservation quantities mass flow, momentum and energy. If these quantities do not change relative to the initial surface values, then the mass, momentum and energy have been conserved; this is a good indication that the numerical solution is proceeding satisfactorily. However, since a numerical solution is employed some changes in the conservation quantities is to be expected. The objective then is to keep the error as small as possible. When large errors occur, the input data, wall equations, mesh construction, etc., should be checked.

The changes in the conservation quantities are found by comparing the integrated value at a given data surface relative to the initial data surface. These are as follows:

Mass Flow Rate (Mixture):

$$\%\Delta\dot{m} = \frac{(\dot{m}_N - \dot{m}_I) \cdot 100}{\dot{m}_I} \tag{8.25}$$

Momentum (Mixture)

$$\%\Delta|M| = \frac{(|\vec{M}_N| - |\vec{M}_I|) \cdot 100}{|\vec{M}_I|} \tag{8.26}$$

Energy (Mixture)

$$\%\Delta E = \frac{(E_N - E_I) \cdot 100}{E_I} \tag{8.27}$$

The individual changes for the respective phases are computed in a similar fashion as specified by Eqs. (8.25) through (8.27). One important item to remember is that when gas particle flows are being considered the

solution is coupled in the sense that momentum and energy is exchanged between the phases. This means that relatively large changes in the momentum and energy quantities for each phase can occur. What should be of concern for gas-particle flows is the change in the mixture conservation quantities (momentum and energy). The respective mass flows should be conserved since the assumption has been made that the phases do not exchange mass via chemical reactions, condensation, etc.

Finally, the specific impulse for a nozzle can be calculated in one of several ways. One way has already been outlined where the thrust is computed as the sum of the initial surface momentum and the pressure force acting on the nozzle wall. The specific impulse is then calculated by dividing the thrust by the mass flow rate through the initial surface. Using the initial surface mass flow rate is a matter of choice and can be argued from either a pro or con view. However, use of the initial surface mass flow rate eliminates the use of one variable which would be numerically calculated. Computation of the specific impulse by the second procedure is as follows.

The thrust generated by the nozzle is first obtained by calculating the momentum in the nozzle axial direction ($M_{M_{m_x}}$, Eq. (8.14a)). The specific impulse is then calculated by dividing by the mixture mass flow rate. This gives a means to compare the I_{sp} calculation previously discussed. The change in I_{sp} is

$$\%\Delta I_{sp} = \frac{(M_{M_{m_x}}/\dot{m}_m - I_{sp}) * 100}{I_{sp}} \qquad (8.28)$$

where the term I_{sp} is obtained from Eq. (8.24).

9. CONCLUSIONS AND RECOMMENDATIONS

A computer code has been developed which can be used to model the dominant phenomena which affect the prediction of liquid and solid rocket nozzle and orbital (as well as low altitude) plume flow fields. With a single computer run it is possible for the designer to predict a high altitude plume starting from the combustion chamber. This code is intended to be a user-oriented design tool that will allow rocket nozzle/plume calculations that can range from the simplest preliminary design calculations to final design predictions.

The emphasis in developing this tool was to require very little user interface and data manipulation which has previously been required to adequately treat such influences as nozzle boundary layer, two-phase and variable O/F transonic startlines, boundary layer effects on particulates entering the boundary layer, and the transition from continuum to free molecular flow. Development of the program to this stage also allows the RAM2F code to generate an exit plane startline for both single and two phase motors which will interface with the JANNAF Standardized Plume Flowfield (SPF) Code.

The program is being used to generate nozzle and plume data for numerous applications such as:

- o Gas/Gas-Particle Impingement (Heat-Transfer-Loads)
- o Rocket Nozzle Performance (Thrust, I_{sp})
- o IR Signatures (Radiating Species)
- o RF Attenuation (Electron Densities)
- o Plume Radiation (Radiative Heat Transfer Gas/Particles)
- o Vehicle Base Pressure
- o Base Heating (Convection-Recirculation), and
- o Flowfield Properties for Contamination Predictions.

This three-volume report describes the program and is intended to provide the user the necessary information to use the code. It is anticipated that there may be some areas of the operation of the code that are not discussed in sufficient depth. Through feedback from the user the documentation will be periodically updated to reflect the experience of the various users. Additionally, coding errors which are uncovered will also be periodically provided to users.

The code has been checked out and compared with a wide range of data. Validation of the program in the low density area of the plume has been verified with limited amounts of data. High altitude (vacuum) plume data are still required to further verify the applicability and range of use of the RAMP2F code. As these data become available the code will be further verified or modified to improve its applicability.

10. REFERENCES

1. Penny, M.M. et al., "Supersonic Flow of Chemically Reacting Gas-Particle Mixtures - Volume I - A Theoretical Analysis and Development of the Numerical Solution," LMSC-HREC TR 476555-I, Lockheed Missiles & Space Company, Huntsville, Ala., January 1976.

2. Penny, M.M. et al., "Supersonic Flow of Chemically Reacting Gas-Particle Mixtures - Volume II - RAMP, A Computer for Analysis of Chemically Reacting Gas-Particle Flows," LMSC-HREC TR 496555, Lockheed Missiles & Space Company, Huntsville, Ala., January 1976.

3. Dash, S.M., H.S. Pergament and R.D. Thorpe, "A Modular Approach for the Coupling of Viscous and Inviscid Processes in Exhaust Plume Flows," 17th Aerospace Sciences Meeting, New Orleans, 15-17 January 1979.

4. Smith, S.D., "High Altitude Supersonic Flow of Chemically Reacting Gas-Particle Mixtures - Volume II - Program Manual for RAMP2," LMSC-HREC TR D867400-I, Lockheed Missiles & Space Company, Huntsville, Ala., October 1984.

5. Smith, S.D., "High Altitude Supersonic Flow of Chemically Reacting Gas-Particle Mixtures - Volume III - RAMP2 - Computer Code User's and Applications Manual," Lockheed Missiles & Space Company, Huntsville, Ala., LMSC-HREC TR D867400-III, October 1984.

6. Svehla, R.A, and B.J. McBride, "FORTRAN IV Computer Program for Calculation of Thermodynamics and Transport Properties of Complex Chemical Systems," NASA TN D-7056, January 1976.

7. Evans, R.M., "Boundary Layer Integral Matrix Procedure BLIMP-J User's Manual," Aerotherm UM-75-64, July 1975.

8. Hoffman, J.D., "An Analysis of the Effects of Gas-Particle Mixtures on the Performance of Rocket Nozzles," TM 63-1, Jet Propulsion Center, Purdue University, Lafayette, Ind., January 1963.

9. Kliegel J.R., "Gas Particle Nozzle Flows," Ninth International Combustion Symposium, Cornell University, Ithaca, N.Y., August 1962.

10. Kliegel, J.R., and G.R. Nickerson, "The Calculation of Supersonic Gas-Particle Flows in Axisymmetric Nozzles by the Method of Characteristics," STL 6120-8345-TU000, Space Technology Laboratories, Inc., Redondo Beach, Calif., May 1962.

11. Laderman, A.J. et al., "Study of Thermal Radiation, Particle Impingement Heating and Flowfield Analysis of Solid Propellant Rocket Exhaust," No. 2386 Philco-Ford Aeronutronics Division, Newport, Calif., April 1967.

12. Hoffman, R.J. et al., "Plume Contamination Effects Predication," Report AFRPL-TR-71-109, McDonnell Douglas Astronautics Company, Huntington Beach, Calif., December 1971.

13. Penny, M.M. et al., "A Study of the Plume Impingement Environment Experienced by the Booster During the Space Shuttle Nominal Staging Maneuver," AIAA Paper 72-1171, AIAA/SAE 9th Joint Propulsion Specialist Conference, November 1972.

14. F ker, L.R., M.M. Penny, and R.W. McCanna, "Design and Calibration of Model Nozzles for Use in Gasdynamic Simulation of the Space Shuttle Propulsion System Exhaust Plumes," LMSC-HREC TR D306555, Lockheed Missiles & Space Company, Huntsville, Ala., April 1973.

15. Greenwood, T.R. et al., "Analysis of Liquid Rocket Propellant Engine Exhaust Plumes," Paper 70-844, presented at AIAA 5th Thermophysics Conference, Los Angeles, June 1970.

16. Prozan, R.J., "Solution of Non-Isoenergetic Supersonic Flows by Method of Characteristics," LMSC-HREC D162220-III-A Lockheed Missiles & Space Company, Huntsville, Ala., July 1971.

17. Ruo, S.R., "Development of a Multiple Shock Computer Program Using a Streamline-Normal Technique," LMSC-HREC A791047, Lockheed Missiles & Space Company, Huntsville, Ala., January 1968.

18. Penny, M.M., "Analytical Data for the APS R-1E Engine Plume Impingement Forces and Moments on the S-IVB Protuberances and the OWS Panels (Small Version), LMSC-HREC A148628, TN 54/20-51, Lockheed Missiles & Space Company, Huntsville, Ala., January 1969.

19. Boynto, F.P., "Exhaust Plumes from Nozzles with Wall Boundary Layers," J. Spacecraft Roc., Vol. 5, October 1968, pr. 1143-1147.

20. Simons, G.A., "Effect of Nozzle Boundary Layers on Rocket Exhaust Plumes," AIAA J., Vol. 10, November 1972, pp. 1534-1535.

21. Curtis, J.T. e ..., "Plume Interference Prediction (PIP) Code: User's Manual and Tes. and Evaluation Report - Vols. I and II," KC-5900-A-6, Calspan Corp., Buffalo, N.Y., April 1977.

22. Spradley, L.W., and M.L. Pearson, "GIM Code User's Manual for the STAR-100 Computer," NASA CR-3157, November 1979.

23. Smith,S.D., "Definition of Solid Particle Plume Flow Fields of the Space Shuttle Interim Upper Stage (IUS, SSUS-A, SSUS-D) Solid Booster Motors," LMSC-HREC TN D568087, Lockheed Missiles & Space Company, Huntsville, Ala., November 1977.

24. Smith, S.D., and A.W. Ratliff, "User's Manual - Variable O/F Ratio Method of Characteristics Program for Nozzle and Plume Analysis," LMSC-HREC D162220-IV, Lockheed Missiles & Space Company, Huntsville, Al_ , June 1971.

25. Seubold, J.G., and R.H. Edwards, "A Simple Method for Calculating Expansion of a Rocket Engine Nozzle Boundary Layer into a Vacuum," Seventh JANNAF Plume Technology Conference, April 1973, pp. 35-44.

26. Bird, G.A., "The Nozzle Lip Problem," Rarefied Gas Dynamics: Proceedings of the 9th International Symposium, Vol. 1, 1974, pp. A.22-1 -A.22-8.

27. Wiernbaum, S., "Rapid Expansion of a Supersonic Boundary Layer and Its Application to the Near Wake," AIAA J., Vol. 4, No. 2, 1966, pp. 217-226.

28. Baum, E., "An Interaction Model of a Supersonic Laminar Boundary Layer on Sharp and Backward Facing Steps," AIAA J., Vol. 6, No. 3, March 1966, pp. 440-447.

29. Cooper, B.P., "Nozzle Boundary Layer Model Including the Subsonic Sublayer Usable for Determining Boundary Layer Effects on Plume Flow Fields," JANNAF 11th Plume Technology Meeting, Huntsville, Ala, May 1979.

30. Prozan, R.J., "Striated Combustion Solution," LMSC-HREC A791356, Lockheed Missiles & Space Company, Huntsville, Ala., May 1968.

31. Combs, L.P., "Liquid Rocket Performance Computer Model with Distributed Energy Release," NASA CR-11462, 10 June 1972.

32. Ring, L.R., "Evaluation of Combustion/Nozzle Gasdynamic Models for Liquid Rocket Engine Applications," AFRPL-TR-77-46, Air Force Rocket Propulsion Laboratory, Edwards, Calif., July 1977.

33. Stephens, J.T., and A.W. Ratliff, "Studies of Rocket Engine Combustion Chamber Geometry Using an Equilibrium Reacting Gas Transonic Flow Program," LMSC-HREC A784898, Lockheed Missiles & Space Company, Huntsville, Ala., November 1967.

34. Ratliff, A.W. et al., "Analysis of Exhaust Plumes from Skylab-Configuration R-4D Attitude Control Motors," LMSC-HREC D162171, Lockheed Missiles & Space Company, Huntsville, Ala., March 1970.

35. Ring, L.R. et al., "Analysis and Correlation of High Altitude Rocket Exhaust Plume Experimental Data," JANNAF 7th Plume Technology Meeting, Huntsville, Ala., April 1973.

36. Nickerson, G.R. et al., "Solid Rocket Motor Performance Predictions Using the Improved SPP Computer Model," 16th JANNAF Combustion Meeting, Monterey, Calif., September 1979.

37. Bird, G.A., "Breakdown of Translational and Rotational Equilibrium in Gaseous Expansions," AIAA J., Vol. 8, November 1970, pp. 1998-2003.

38. Penny, M.M. and C.J. Wojciechowski, "User's Manual and Description of a Computer Program for Calculating Heating Rates, Forces and Moments Acting on Bodies Immersed in Rocket Exhaust Plumes," LMSC-HREC D162867-II, Lockheed Missiles & Space Company, Huntsville, Ala, March 1971.

39. Thoenes, J. et al., "Analysis of Chemical Lasers - Volume I - Laser and Mixing Program (LAMP) Theory and User's Guide," TR RK-CR-74-13, Lockheed Missiles & Space Company, Huntsville, Ala., June 1974.

40. Denbigh, K., The Principles of Chemical Equilibrium, Cambridge University Press, Great Britain, 1968.

41. Shapiro, A.H., The Dynamics and Thermodynamics of Compressible Fluid Flow, Vol. 1, Ronald Press, New York, 1953.

Appendix A

DISCUSSION OF PARTICLE DRAG AND HEAT TRANSFER COEFFICIENTS

Appendix A
SYMBOLS AND NOTATION

Symbol	Description
C_D	drag coefficient, dimensionless
f	incompressible drag coefficient defined by Eq. (A-2)
Kn	Knudsen number, dimensionless
M	Mach number, dimensionless
Nu	Nusselt number, dimensionless
Pr	Prandtl number, dimensionless
q	velocity, ft/sec
r	particle radius, ft
R	gas constant, $ft^2/sec^2/^oR$
Re	Reynolds number, dimensionless
T	temperature, ^oR

Greek

γ	specific heat ratio, dimensionless
μ	viscosity, lbf-sec/ft^2
ρ	density, slug/ft^3

Subscripts

C	indicates the quantity	pertains to the continuum flow regime
FM	indicates the quantity	pertains to the free molecular flow regime
I	indicates the quantity	pertains to incompressible flow

Superscript

j	indicates the quantity	pertains to a particle species

APPENDIX A

Particle drag and heat transfer quantities are calculated in terms of non-dimensional coefficients. These coefficients are functions of the local Reynolds number or the Knudsen number depending on the parameter being calculated. The following discussion summarizes the calculations employed in the gas-particle flow analyses. Details of the theory are given in the cited references.

A.1 PARTICLE DRAG COEFFICIENTS

Particles in solid rocket motor nozzle and exhaust plume flow-fields encounter a wide range of flow regimes. Consequently any expression chosen for the drag coefficient must have the ability to take this into account. In a rocket nozzle and exhaust plume flow field the particles are continually being accelerated by the turbulent flow which has a temperature different than the particles. This situation is further complicated by rarefaction effects because the mean free path in the gas is comparable to dimensions of the particle boundary layer. Obviously the "standard drag curve" of a sphere as a function of Reynolds number (Ref. A-1) does not fit this description. This drag coefficient can only be applied to

- Single solid sphere
- Constant velocity
- Still, isothermal, incompressible flow of infinite extent

In early two-phase studies the sphere drag coefficient was taken as the Stokes drag coefficient;

$$C_D = \frac{24}{Re} \qquad (A.1)$$

This expression, however, is valid only for Re $\angle$ 1 if rarefaction effects are not taken into account.

The Stokes drag coefficient is now used as a reference drag coefficient. An incompressible drag parameter defined by the relation

$$f^j = C_D{}^j / C_{D_{Stokes}}^j ; \; j=1, \; NP \qquad (A.2)$$

was tabulated as a function of Reynolds number by Kliegel (Ref. A-2). This was corrected for rarefaction effects (Ref. A-3) by the relation

$$C_D = C_{D_I} \left\{ \frac{(1+ 7.5\,Kn)\,(1+2\,Kn) + 1.91\,Kn^2}{(1+7.5\,Kn)\,(1+3\,Kn) + (2.29+ 5.16\,Kn)\,Kn^2} \right\} \qquad (A.3)$$

The Knudsen number, Kn, (a measure of flow rarefaction) is related to the Mach and Reynolds numbers by

$$Kn^j = 1.26\sqrt{\gamma}\; M^j/Re^j , \qquad (A.4)$$

$$M^j = |\Delta q^j|/\sqrt{\gamma RT} \; . \qquad (A.5)$$

A more recent formulation for the drag coefficient is taken from the work of Crowe (Ref. A-4). The drag coefficient is defined as

$$C_D = (C_{D_{FM}} - C_{D_I})\,\bar{C}_D + C_{D_I} \;;$$

where

$$\bar{C}_D = \left\{\frac{1.1}{1+1.1\,(Kn)^{-.3}}\;\exp\left(-Kn^{1/2}\right)\right\}\left\{1 - \exp\left[-Kn^{.7}e^{\frac{Kn(C_{D_{inc}} - .48)}{6.6}}\,Re\right]\right\}$$

A.2 PARTICLE HEAT TRANSFER COEFFICIENTS

At present there appear to be no specific experimental heat transfer data for spheres of the particle sizes in the flow regimes encountered in a rocket nozzle-exhaust plume flow field. A review of semi-empirical expressions is given by Miller and Barrington (Ref. A-5). Until further work is done that is directly applicable to particle flows the continuum expression of Drake (Ref. A-6)

$$Nu^j_{cont} = 2 + 0.459\,(Re^j)^{0.55}\,Pr^{0.333} \;;$$

where

$$Re^j = 2\rho\,|\,\Delta\bar{q}\,|\,r^j/\,\mu$$

modified for rarefaction effects by Kawanau (Ref. A-6)

$$Nu = \frac{Nu_{cont}}{1.0 + 3.42\,M/Re^j\,Pr\,Nu_{cont}}$$

appears to be the most applicable to two-phase flows.

Section A-1
REFERENCES

A.1 Schlichting, H., Boundary Layer Theory, McGraw-Hill, New York, N. Y., March 1958.

A.2 Kliegel, J. R., and G. R. Nickerson, "Axisymmetric Two-Phase Perfect Gas Performance Program – Vol. I," NASA - CR 92069, April 1967.

A.3 Kliegel, J. R., "Gas Particle Nozzle Flows," Ninth Symposium on Combustion, Academic Press, New York, N.Y., 1963.

A.4 Crowe, C.J., "Drag Coefficient of Particles in Rocket Nozzles," AIAA J., Vol. 5, No. 5, May 1967.

A.5 Miller, W.H., and D. K. Barrington, "A Review of Contemporary Solid Rocket Motor Performance Prediction Techniques," J. Spacecraft Roc., Vol. 7, No. 3, March 1970.

A.6 Drake, R. M., "Discussion on G. C. Bliet and G. Leppert; Forced Convection Heat Transfer from an Isothermal Sphere to Water," J. Heat Trans., Am. Soc. Mech. Engrs., Vol. 83, 1961.

A.7 Kavanau, L.L., "Heat Transfer from Spheres to a Rarefied Gas in Subsonic Flow," Trans. Am. Soc. Mech. Engrs., Vol. 77, 1955.

Appendix B

NON-ISOENERGETIC GAS PHASE FLOW TREATMENT

Appendix B
SYMBOLS AND NOTATION

Symbol	Description
h	local enthalpy, ft^2/sec^2
H	total enthalpy, ft^2/sec^2
P	pressure, lbf/ft^2
q	velocity, ft/sec
s	entropy, $ft^2/sec^2/^oR$
T	temperature, ^oR
Greek	
η	weight flow ratio of oxidizer to fuel, dimensionless
ρ	density, $slug/ft^3$
Δ	denotes a change in a variable over a step length
Subscripts	
o	indicates the quantity pertains to the oxidizer
f	indicates the quantity pertains to the fuel
Superscript	
$\vec{}$	denotes a vector quantity
$\bar{}$	denotes an average value over a step length

PRECEDING PAGE BLANK NOT FILMED

Appendix B

The bulk of this document is concerned with the discussion of the analysis of gas-particle flows which have been shown to be non-isentropic as well as non-isoenergetic in the gas phase. However, one of the original objectives of the RAMP code development was to provide for a single phase (gas) calculation as an option. Computationally this entails simply considering the coefficients reflecting particle contributions to the compatibility equation as numerically equal to zero. As expected, there is no change in entropy and gas total enthalpy along gas streamlines, that is, the flow is seen to be isentropic and isoenergetic. However, for many liquid propellant motor applications a fuel rich mixture of the chamber combustion products is used to film cool the nozzle walls. This results in fuel striations across the nozzle where each streamline has a different energy level associated with it (i.e. non-isoenergetic flow).

This case can be treated with a non-equilibrium chemical analysis by simply specifying the appropriate initial gas total conditions on each streamline. Recall that the pressure-density-velocity form of the compatibility equation is then used. Gas chemical concentrations are required for each streamline so that the gas thermodynamics are computed locally as the solution proceeds downstream in the nozzle-exhaust plume flowfield. However, if the flow is to be considered in chemical equilibrium or equilibrium/frozen, the applicable compatibility relations must reflect the non-isoenergetic nature of the striated flow condition. These relations are developed in the following paragraphs.

To begin, the development of the species continuity equation (starting with equation 2.6) could be replaced by atomic conservation

equations. Moreover if the conservation of those atoms associated with the fuel and the oxidizer were considered then, for steady state,

$$\nabla \cdot (\rho_f \vec{q}) = 0 \qquad \text{(B•1)}$$

and

$$\nabla \cdot (\rho_o \vec{q}) = 0 \qquad \text{(B•2)}$$

would result.

If the weight flow ratio of oxidizer to fuel (O/F ratio) is denoted by η then Eq. (B•1) and B•2) are satisfied if,

$$\vec{q} \cdot \nabla \eta = 0 \qquad \text{(B•3)}$$

and

$$\nabla \cdot (\rho \vec{q}) = 0 \qquad \text{(B•4)}$$

The assumptions inherent in arriving at Eq. (2•50) did not involve isoenergetic flow so that the momentum equation remains valid. The energy Eq. (2•105), however, remains valid only along each streamline and must be replaced by

$$h + \frac{\vec{q}^2}{2} = H(\eta) \qquad \text{(B•5)}$$

The compatibility equations which apply along each Mach line are unaltered by the non-isoenergetic analysis since it is constructed based on the momentum equation and the global continuity equation (neither of which are altered by the non-isoenergetic flow phenomena).

The numerical solution to the governing equations is not greatly affected by the modification to the compatibility equation. In Eq. (3•146)

$$\Delta s_{1,2} \Leftarrow -\frac{1}{\bar{T}_{1,2}} \left(\frac{\Delta P_{1,2}}{\bar{\rho}_{1,2}} + \bar{q}_{1,2} \Delta q_{1,2} \right) \qquad \text{(B•6)}$$

while for a lower pressure boundary

$$(s_3 - s_{1,2}) \Leftarrow \frac{1}{\bar{T}_{1,2}} \left(\frac{\Delta P_{1,2}}{\bar{\rho}_{1,2}} + \bar{q}_{1,2} \Delta q_{1,2} \right) \qquad \text{(B•7)}$$

The finite difference analog to the streamline equation may be written:

a. interior point

$$\eta_3 = \eta_5$$

b. an upper wall or upper free boundary point

$$\eta_3 = \eta_1$$

c. a lower wall or lower pressure boundary point

$$\eta_3 = \eta_2$$

The oblique shock relations of Section 4 are unaffected since the discussion concerns a single streamline. All references to flow variables are understood to be a function of the O/F ratio. Since that ratio does not change across the shock the only alteration necessary is that of Eq. (4•11) which is altered to read

$$P_2 = P(s_2, q_2, \eta_1), \; \rho_2 = \rho(s_2, q_2, \eta_1) \qquad \text{(B•8)}$$

Since the Prandtl-Meyer calculation of Section 5 is also concerned with a single streamline, hence a constant value of η, it to is unaffected.

It can readily be seen from the above discussion that the alterations necessary to incorporate the non-isoenergetic analysis are straightforward from an analytic point of view.

Appendix C

CHEMICAL EQUILIBRIUM CALCULATIONS IN GAS-PARTICLE FLOWS

Appendix C
SYMBOLS AND NOTATION

Symbols	Description
A	parameter defined by Eq. (2-46), 1/sec
B_1	parameter defined by Eq. (2-103)
c_p	specific heat at constant pressure, $ft^2/sec^2/^oR$
H	total enthalpy, ft^2/sec^2
M_w	molecular weight, lbm/lb mole
N	number of moles
N_p	number of discrete particles
P	pressure, lbf/ft^2
q	velocity, ft/sec
R	gas constant, $ft^2/sec^2/^oR$
S	entropy, $ft^2/sec^2/^oR$
T	temperature, ^oR
u, v	velocity components, ft/sec
V	velocity, ft/sec
$\dot{w}$	flow rate, lbm/sec
x	position coordinate, ft
Greek	
ρ	density, $slugs/ft^3$
θ	inclination of the flow vector with respect to the x-axis, deg

SYMBOLS AND NOTATION (Cont'd)

Subscripts

c	denotes chamber conditions
g,G	indicates the quantity pertains to the gaseous species
m	indicates the quantity pertains to the gas-particle mixture
p	indicates the quantity pertains to the particle species

Superscript

j	indicates the quantity pertains to the particle species

Appendix C

One of the basic assumptions made in the development of equations describing the gas-particle flow is that there is no mass transfer between the phases. Consequently, calculations treating chemical reactions in gas-particle flows must reflect this assumption. Prozan (Ref. C-1) has shown for chemical equilibrium that the gas thermochemistry calculations can be uncoupled from gas-dynamic considerations. Gas thermodynamic properties (Ref. C-2) for chemical equilibrium or frozen flow are precalculated for nozzle chamber conditions. Tabulated thermodynamic data are then constructed in terms of the independent variables by expanding the flow from the chamber conditions.

Thermochemistry calculations are, however, complicated by condensed species produced in the combustion process. Since the particles are inert, they perform no expansion work. Particle acceleration is accomplished by viscous drag forces exerted by the gas. This, coupled with the gas cooling resulting from expansion, produces dynamic and thermal lags. The work required to accelerate the particles combined with the heat exchanged between the particle and gas phases is a non-isentropic process as shown by the following relations:

$$Tds - \frac{(C_p - R)}{R\rho q \cos\theta} \sum_{j=1}^{NP} \rho^j A^j B_1^j \, dx = 0; \qquad (C\text{-}1)$$

$$dH - Tds + \frac{1}{\rho} \sum_{j=1}^{NP} \rho^j A^j \left[(u - u^j) + \frac{v}{u}(v - v^j)\right] dx = 0. \qquad (C\text{-}2)$$

The term B_1^j is a function of the velocity and thermal lags and in essence reflects the loss in work potential. Equation (C•1) indicates that if the algebraic sign on B_1^j is positive then the change in the entropy level along a streamline will be positive. This is the case when the entropy increase resulting from the work required to accelerate the particle is greater than the heat transferred from the particles to the gas. Consequently there will be a corresponding decrease in gas total enthalpy. It should be noted that just the reverse is true if the increase in work potential due to heat transfer is greater than the work required to accelerate the particles.

The original chemical equilibrium formulation (Ref. C-2) assumed that the gas and particles comprising the flow mixture were in dynamic and thermal equilibrium. Condensed species resulting from the combustion process were treated in the same fashion as the gas chemical species in that chemical reactions were permitted. The expansion process was then isentropic since gas-particle equilibrium was assumed. However, the correct thermochemical properties can be obtained if certain modifications to the analysis are made. A step-by-step description of the modifications is contained in the following paragraphs.

First the adiabatic flame calculation is made for the gas-particle mixture (Step 1, Fig. C-1). The mixture concentrations comprise the gas chemical species as well as the particulate species. Examination of the concentrations permits identification of the particulates. Since the assumption has been made that the gas and particulate phases do not exchange mass, the chemical reactions between the phases are suppressed by removing these from the list of possible reactions. Particle energy and mass are removed from the mixture (Step 2). The particle loading is then calculated from the relation

$$\frac{\dot{w}_p}{\dot{w}_g} = \frac{M_{wp} N_p}{M_{wg} N_g} \qquad (C•3)$$

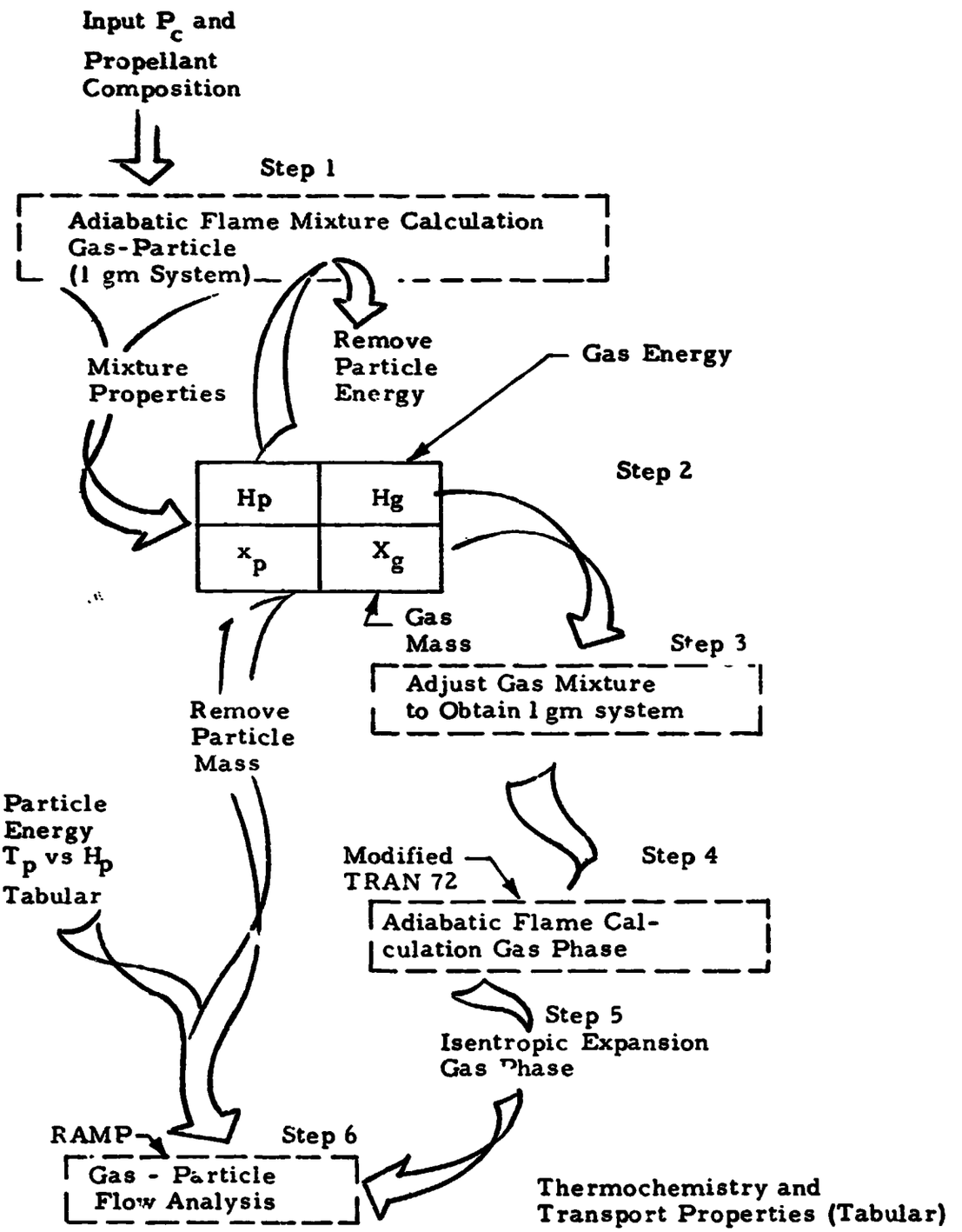

Fig. C-1 - Schematic of Two-Phase Thermochemical Calculations

Equation (C•3) gives the total particle mass loading relative to the gas. Individual particle loadings are obtained from empirical data for a given motor class and size. These data along with the particle enthalpy - temperature data (Ref. C-3) which defines the energy removed from the mixture become input data to the RAMP code. Next, the remaining gas energy and molar concentrations are then readjusted to obtain a one gram system (Step 3). The adiabatic flame calculation is made for the gas phase at the chamber pressure and temperature computed for the gas-particle mixture (Step 1).

Equations (C•1) and (C•2) indicated the gas phase expansion process to be non-isentropic. Hence the thermochemistry calculation must reflect this condition. This is accomplished in the following manner.

Equation (C-2) defines the change in gas total enthalpy as a function of entropy change and particle velocity lags. A schedule of gas total enthalpy changes can now be defined by the relation

$$H_{G_i} = H_c + \Delta H_i \; ; \; i = 1, n \qquad \text{(C•4)}$$

The values of ΔH_i are defined to cover the expected change in gas total enthalpy for a given analysis.

Figure C-2 shows a typical schematic of an H-S diagram for gas-particle flows. Each point H_{G_i}, Pc defines a particular point on the diagram from which the flow can be isentropically expanding for the corresponding value of S_1. However, the flow is non-isentropic so that for each H_{G_i}, Pc an expansion from one or more states defined by a change in entropy must be made. This is depicted schematically in Fig. C-2. Computationally this is accomplished by inputing to the code a schedule of ΔH_i and a corresponding change in entropy for each ΔH_i. The chamber calculation is made for the gas phase (Step 3,

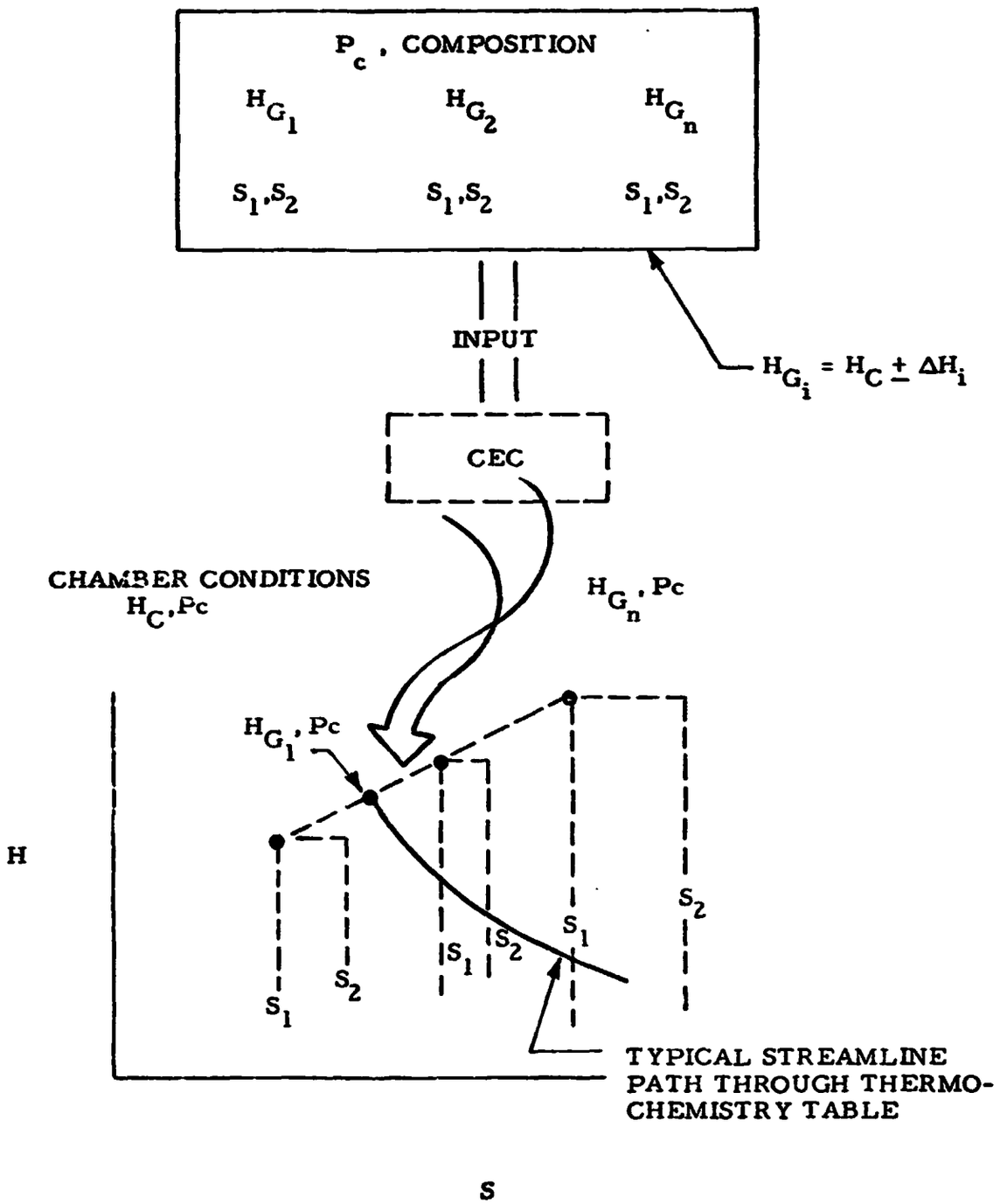

Fig. C-2 - Schematic of Thermochemistry Table Construction

Fig. C-1) and an isentropic expansion from the reference conditions calculated for the number of entropy levels desired. These data are generated in tabular form as a function of ΔH_i, ΔS_j and V_k respectively as indicated by the following schematic. This process is subsequently

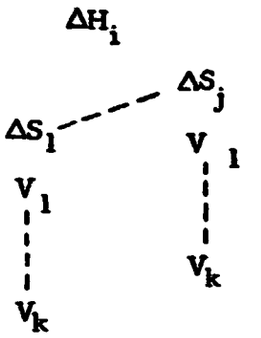

Fig. C-3 - Schematic of Tabulated Thermochemistry Data

repeated for each ΔH_i. Since for a chemical equilibrium analysis the independent variables chosen are ΔH, ΔS and V the local thermodynamic and transport properties at a given point in the flow are obtained by interpolating within the tables.

Appendix C
REFERENCES

C.1 Prozan, R.J., "Solution of Non-Isoenergetic, Supersonic Flows by the Method-of-Characteristics," LMSC-HREC D162220-III-A, Lockheed Missiles & Space Company, Huntsville, Alabama, July 1971.

C.2 Gordon, S. and B. J. McBride, "Computer Program for Calculations of Complex Chemical Equilibrium Compositions, Rocket Performance, Incident and Reflected Shocks and Chapman-Jouguet Detonations," NASA SP-273, Lewis Research Center, Cleveland, Ohio, 1968.

C.3 JANNAF Thermochemical Tables, Second Edition, H.S. Dept. of Commerce, National Bureau of Standards, NSRDS-NBS 37, Washington, D.C., June 1971.

Appendix D

NON-CONTINUUM FLOW EXPANSIONS

Appendix D
SYMBOLS AND NOTATION

Symbol	Description
Kn	Knudsen number, dimensionless
M	Mach number, dimensionless
N	number of collisions per molecule required for the gas to achieve relaxation
R	gas constant, $ft^2/sec^2/^oR$
Re	Reynolds number, dimensionless
Ro	characteristic dimension of the flow field, ft
S	distance along a streamline, ft
T	temperature, ^oR
V	gas velocity, ft/sec
$\overline{V}$	mean molecular velocity, ft/sec
Greek	
γ	specific heat ratio, dimensionless
μ	viscosity, $lbf\text{-}sec/ft^2$
ρ	density, $slug/ft^3$
λ	mean free path, ft

Appendix D

D.1 DETERMINATION OF THE LOCAL KNUDSEN NUMBER, Kn

The expansion of exhaust gases to very low back pressures results in a decrease in the gas pressure and density. This inturn produces a decrease in the number of intermolecular collisions. At some point, the effect of intermolecular collisions will cease to be a governing factor in determining the flowfield characteristics. The local Knudsen number (Kn) is used to indicate the local flow regime, i.e., continuum, vibrationally frozen, rotationally frozen or translationally frozen. The local Knudsen number is defined as the ratio of the mean free path (which is a measure of the average distance between intermolecular collisions) to a characteristic dimension of the flowfield. Kn is given by this relation (Ref. D-1):

$$Kn = \left(\frac{V}{\bar{V}}\lambda\right)\left(\frac{1}{T}\frac{dT}{dS}\right) = \frac{1}{N}$$

In the relation for Kn, the mean free path is represented by $\frac{V}{\bar{V}}\lambda$ and the characteristic dimension is represented by $T/\frac{dT}{dS}$. The method employed here is to utilize the "sudden freeze" approximation (Ref. D-1) to determine when an energy mode freezes such that the gas temperature cannot relax fast enough to maintain the equilibrium rate of change. The RAMP program computes a local Kn at each mesh point and compares it to $1/N_i$ (the inverse of the collision number) to determine if the i^{th} energy mode has frozen.

Assuming that the mean molecular speed $\bar{V}$ is determined by the Maxwell distribution function

$$\bar{V} = \left(\frac{8}{\pi} RT\right)^{1/2} \qquad \text{(Ref. D-2)}$$

were R is the particular gas constant. Introducing the local Mach number M, Kn can be written:

$$Kn = \left(\frac{\pi}{8}\gamma\right)^{1/2} = M\lambda\left[\frac{d(\ell n\ T)}{dS}\right], \quad d(\ell n\ T) = \frac{dT}{T} .$$

For rarefied gases the mean free path can be related to the viscosity μ

$$\lambda = \frac{\mu}{0.499\rho\bar{V}} \qquad \text{(Ref. D-3)}$$

where ρ is the local gas density. Let $\bar{S} = \frac{S}{R_o}$, where R_o is the characteristic dimension of the flowfield. Then $dS = R_o\, d\bar{S}$. With the above relation $\lambda = f(\mu)$, and introducing the characteristic dimension R_o, Kn can be written:

$$Kn = \frac{\pi\ \gamma M^2}{8(.499)} \left(\frac{\mu}{\rho V R_o}\right) \frac{d(\ell n\ T)}{d\bar{S}} .$$

But the local Reynolds number Re is:

$$Re = \frac{\rho V R_o}{\mu}$$

Therefore,

$$Kn = 0.25050\ \pi\ \frac{\gamma M^2}{Re} \quad \frac{d(\ell n\ T)}{d\bar{S}} .$$

As a first approximation to the derivative $\frac{d(\ell n\ T)}{d\bar{S}}$, let

$$\frac{d(\ln T)}{d\bar{S}} \simeq \frac{\ln (T_1/T_2)}{dS/R_o}$$

so that the local Knudsen number, Kn as coded is given by:

$$Kn = 0.25050 \ \pi \frac{\gamma M^2}{Re} \left[\frac{\ln T_1 - \ln T_2}{dS/R_o} \right]$$

The characteristic mesh is shown below to illustrate the flowfield variables used to determine the local Knudsen number

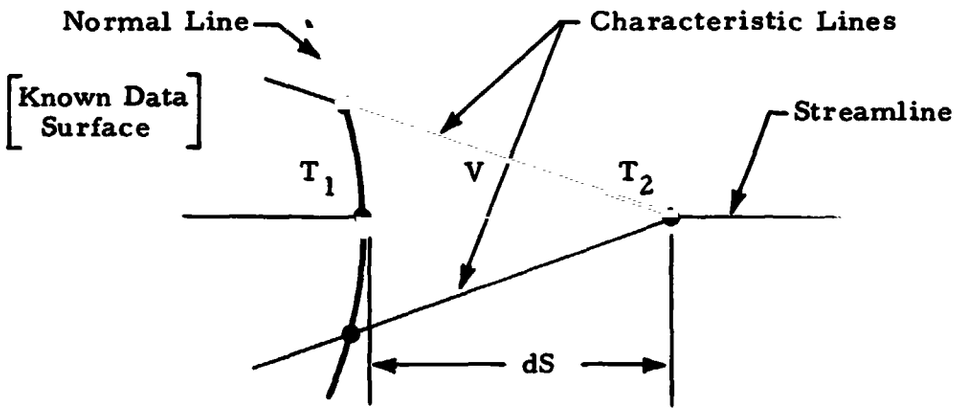

D.2 NON-CONTINUUM FLOW REGIME CRITERIA

The criteria used by the RAMP program to determine the "freezing" of particular energy modes is to compare the local Knudsen number (Kn) with the reciprocal of the collision number. When Kn is equal to or greater than the reciprocal of the collision number for the vibrational, rotational, or translational modes that particular mode is considered to be frozen. The freezing of the first two energy modes (vibrational and rotational) represents a transitional computational region from the continuum to free molecular regimes. During this transitional period the

gaseous flowfield calculation is performed using the characteristic equations with the thermodynamic properties modified to reflect the respective flow regime. That is, the gaseous ratio of specific heats is altered to reflect the transition to a non-continuum regime. Once the translational energy mode has frozen the flowfield becomes "free molecular." In this case the solution becomes a source flow solution with a constant gaseous ratio of specific heats.

D.2.1 Non-Continuum Flowfield Gas Properties

The energy modes of the gaseous flowfield freeze one at a time in order of increasing energy requirements. The vibrational mode freezes first, the ratio of specific heats (gamma) is set to 7/5 and the flowfield solution proceeds in the conventional streamline normal fashion. See Ref. D-4 for the characteristics equations. The rotational mode freezes next in which case gamma is computed as a function of Kn (third order polynomial) and varies from 7/5 to 5/3. This flowfield solution is not altered except for the determination of gamma. The last energy mode to freeze is the translational mode. Once the translational mode has frozen, the flowfield is considered to be in the free molecular regime. Gamma is set to 5/3 and is held constant. The effect of the freezing of the three gaseous internal energy modes on the gas ratio of specific heats is depicted pictorially in Fig. D-1.

Once the flowfield calculation has switched to the free molecular regime the gas streamlines remain straight and the gas velocity which is directed along streamlines remains constant. The gas constant, temperature, and flow angle also remain constant. The gas density varies inversely as the streamtube area and the gas pressure is obtained from the equation of state.

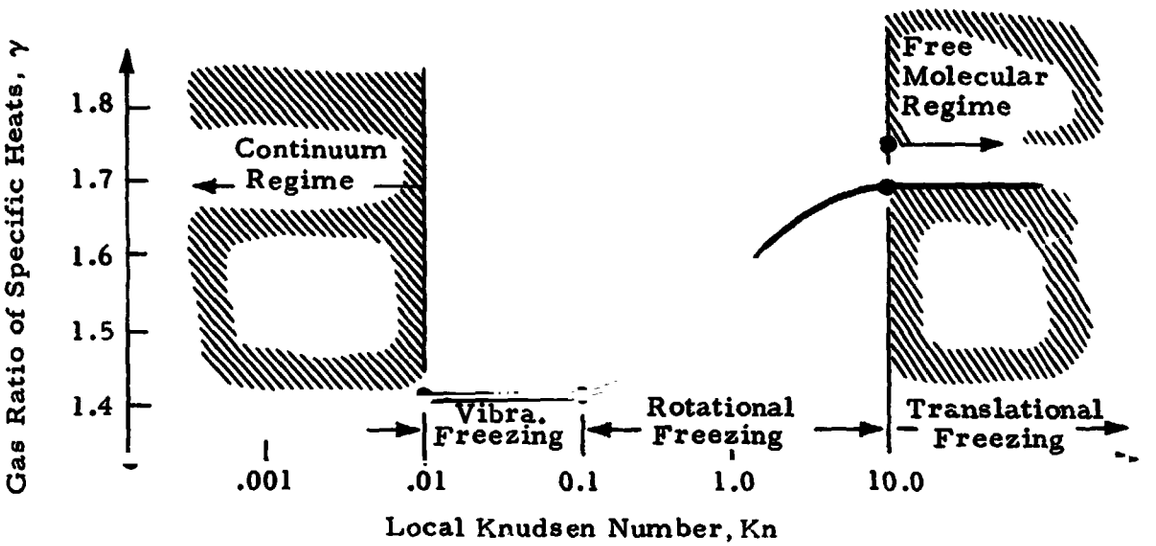

Fig. D-1 - Variation of Gamma with the Local Knudsen Number

D.2.2 Non-Continuum Flowfield Particle Properties

If particles are present in the free molecular flowfield their status is computationally very similar to the gas. Particle velocity, temperature, and enthalpy remain constant. The particle flow angle remains constant, and the particles are directed along straight streamlines. The particle and gas streamlines are not necessarily parallel. The particle density varies inversely as particle stream tube cross-sectional area.

Appendix D
REFERENCES

D.1 Robertson, S.J., "A Method for Calculating Flow Field Properties in Low Density Plumes," Lockheed Missiles & Space Company, Huntsville Research & Engineering Center, LMSC/HREC A784697, October 1967.

D.2 Present, R.D., Kinetic Theory of Gases, McGraw-Hill Book Company, New York, N.Y., 1958.

D.3 Kennazo, E. H., Kinetic Theory of Gases, McGraw-Hill Book Company, New York, N.Y., 1938.

D.4 Penny, M. M., et al, "Two-Phase Flow Development Final Report," Lockheed Missiles & Space Company, Huntsville Research & Engineering Center, LMSC/HREC TRD390040, January 1974.

Appendix E

INTEGRATION OF THE FINITE RATE CHEMICAL KINETIC EQUATIONS

Appendix E

In flow problems where the gas may be considered in equilibrium (chemical and thermodynamic) at every point, two parameters are sufficient to define any of the other thermodynamic variables, either by assuming a perfect gas or by utilizing the results of chemical equilibrium calculations of the gases involved. If the gases cannot be considered to be in equilibrium, a point-by-point evaluation of its composition via integrating the individual species continuity equations is required. This appendix addresses the procedure utilized in the RAMP program to perform such calculations.

A detailed description of the rate processes that occur in rocket exhaust flows requires that a myriad of mechanisms be considered to include all the possible chemical reactions of dissociation, formation, recombination, etc.

All of these, however, can be treated with a very general formalism. In the form usually quoted in chemical kinetics (Ref. E-1) the phenomenological law of mass action states that the rate of a reaction is proportional to the product of the concentrations of the reactants. Thus, for a general reaction of the form

$$\sum_{i=1}^{N} \nu_i' A_i \rightleftharpoons \sum_{i=1}^{N} \nu_i'' A_i \tag{E.1}$$

the net rate of production $\dot{w}_i$ for any participating species for which the stoichiometric coefficients ν_i' and ν_i'' are not equal can then be written as

$$\dot{w} = k_f \prod_{i=1}^{N} (C_i)^{\nu_i'} - k_b \prod_{i=i}^{N} (C_i)^{\nu_i''} \tag{E.2}$$

where C_i is the species concentration defined as $C_i = \rho F_i$ with ρ being the density and F_i being the species mol/mass ratio, respectively. Assuming small deviations from equilibrium, the forward and backward reaction rate constants, k_f and k_b, respectively, can be related to the concentration equilibrium constant and to the pressure equilibrium constant as follows:

$$\frac{k_f}{k_b} = K_c = K_p (\Re T)^{\sum_{i=1}^{N} (\nu_i' - \nu_i'')} \tag{E.3}$$

The significance of the pressure equilibrium constant K_p is that it can be easily evaluated for any reaction using tabulated values of K_f the equilibrium constant for formation from the elements. Values of K_f are commonly tabulated in conjunction with specific heats, entropies and enthalpies as a function of temperature, and are available in general for most species. An equally convenient method exists for determining K_p from the change of free energy accompanying the reaction, i.e.,

$$K_p = \exp(-\Delta G / \Re T) \tag{E.4}$$

where ΔG is the change in free energy during the reaction process. Free energy values are also available for most species in tabular form. This method is used to compute K_p in the RAMP program.

Using Eq. (E.3) to eliminate the backward rate constant from Eq. (E.2) the general production rate equation can be written as

$$\dot{w} = k_f \left\{ \prod_{i=1}^{N} (C_i)^{\nu_i'} - \frac{(\Re T)^{\sum_{i=1}^{N} (\nu_i'' - \nu_i')}}{K_p} \prod_{i=i}^{N} (C_i)^{\nu_i''} \right\} \tag{E.5}$$

Finally, the net rate of production for any species participating in the reaction, either as a reaciant or as a reaction product, is then given by

$$\dot{w}_i = (\nu_i'' - \nu_i') \dot{w} \tag{E.6}$$

Since most reaction systems involve numerous simultaneous reactions, the net rate of production of species i usually equals a sum of terms. Thus, for an aribitrary number of M simultaneous reactions, all involving species i,

$$\dot{w}_i = \sum_{k=1}^{M} \dot{w}_{i,k} \qquad k = 1, \ldots, M \tag{E.7}$$

where $\dot{w}_{i,k}$ denotes the net rate of production of species i due to reaction k only.

For reasons of computational speed and efficiency, the program contains explicit expressions, as obtained from Eq. (E.5), for the most commonly encountered reaction mechanisms. Twelve types of reaction mechanisms are considered as possible contributors to the calculation of the net rate of production, $\dot{w}_i$:

Reaction type

(1, 7)	A + B	$\rightleftharpoons$	C + D	
(2, 8)	A + B + M	$\rightleftharpoons$	C + M	
(3, 9)	A + B	$\rightleftharpoons$	C + D + E	
(4, 10)	A + B	$\rightleftharpoons$	C	(E.8)
(5, 11)	A + M	$\rightleftharpoons$	C + D + M	
(6, 12)	A + M	$\rightleftharpoons$	C + M	

Reaction types (7) through (12) correspond to reaction types (1) through (6), but proceed in the forward direction only.

To reduce roundoff and truncation errors, the forward and backward rates for each reaction are computed separately. All contributions to the

molar rate of production of a given species are then computed and added algebraically to form matrix coefficients (discussed later). Since reaction types (7) through (14) proceed in the forward direction only, the second term on the right-hand side of Eq. (E.5) is disregarded in calculating the contributions to the coefficient matrix.

In reactions (2), (5) and (6) as well as in (8), (11) and (12), M denotes a third body species which can be specified. For these reactions the situation often occurs where for various third bodies the respective rate constants differ only by a constant multiplier. These multipliers can be considered as third body efficiencies or weighting factors. If such a case is encountered, the third body species mole mass ratio F_M becomes effectively a fictitious mole mass ratio, consisting of the weighted sum over all those species having a nonzero weighting factor, i.e.,

$$F_M = \sum_i f_i F_{M_i} \tag{E.9}$$

where f_i are the weighting factors.

The forward rate constant, k_f, is generally a function of temperature. It is most often expressed in Arrhenius form. Again, for speed and efficiency in computation, the rate constants are divided into five types:

Rate Constant Type

(1)	$k_f = A$	
(2)	$k_f = AT^{-N}$	
(3)	$k_f = A \exp(B/\Re T)$	(E.10)
(4)	$k_f = AT^{-N} \exp(B/\Re T)$	
(5)	$k_f = AT^{-N} \exp(B/\Re T^M)$	

The equations presented in this appendix provide a very general formalism for the evaluation of various rate processes. The specification of particular systems and associated rate constants is up to the program user.

Considering now the general species continuity equation

$$\rho \vec{q} \cdot \nabla C_i = \dot{w} \tag{E.11}$$

and making use of the foregoing discussion of the rate process we now proceed to describe a calculational technique for determining the individual species composition on a point-by-point basis. The description of this process is substantially simplified if Eq. (E.5) is specialized to a particular reaction type, say number (7) from Eq. (E.8) which is a one-way, two-body reaction.

$$A + B \rightarrow C + D \tag{E.12}$$

the net production rate for this process is

$$\dot{w} = k_f \rho^2 F_A F_B \tag{E.13}$$

and the species continuity equation for species B then becomes

$$\rho \vec{q} \cdot \nabla F_B = k_f \rho^2 F_A F_B \tag{E.14}$$

which along streamlines becomes

$$\rho q \frac{\partial F_B}{\partial S} = k_f \rho^2 F_A F_B \tag{E.15}$$

This equation can readily be solved using finite difference techniques employing explicit relationships, such as Euler or more sophisticated schemes, such as Runge-Kutta. The step size for integrating this equation however is severely limited by stability criteria. It can be seen from Eq. (E.15) that the rate of change of a species along the streamline becomes increasingly larger as the flow speed is slowed, the density increased, or for fast reaction rates. In rocket engine problems, combinations of slow speeds, high densities and fast reaction rates (i.e., quasi-equilibrium) are quite common and integration step sizes so small (i.e., $< 10^{-8}$ meters) are encountered that the solution becomes impractical in terms of computation time.

For this reason, the technique described in Ref. E-2 based on a linearization of the production rates was utilized. Writing Eq. (E.15) in finite difference form over a streamline step from station n to n+1.

$$F_{B_{n+1}} = F_{B_n} - \frac{\Delta S \rho}{q} F_{A_{n+1}} F_{B_{n+1}} \tag{E.16}$$

And evaluating all the species concentrations at the downstream point results in a set of simultaneous nonlinear algebraic equations. In order to solve these equations we must then linearize the term $F_{A_{n+1}} F_{B_{n+1}}$ which is accomplished following the lead of Ref. E-2. If this term is expanded in terms of its values at station n along with the increments over n to n+1 we can obtain the following expression.

$$F_{A_{n+1}} F_{B_{n+1}} = F_{A_n} F_{B_{n+1}} + F_B F_{A_{n+1}} \tag{E.17}$$

neglecting products of differentials which are assumed to be of second order importance. Equation (E.16) can now be written in its linearized form.
Let $C = \Delta S \rho / q$

$$\begin{aligned} F_{B_{n+1}} &= F_{B_n} - C\left[F_{A_n} F_{B_{n+1}} + F_B F_{A_{n+1}}\right] \\ \text{and} \quad F_{A_{n+1}} &= F_{A_n} - C\left[F_{A_{n+1}} F_B + F_{B_{n+1}} F_A\right] \end{aligned} \tag{E.18}$$

Equation (E.18) can then be expressed in terms of a set of unknowns and calculable coefficients, C. Rewriting these we obtain

$$\begin{aligned} F_{A_{n+1}} &= F_{A_n} - C F_{A_n} (F_{B_{n+1}}) - C F_{B_n} (F_{A_{n+1}}) \\ F_{B_{n+1}} &= F_{B_n} - C F_{B_n} (F_{A_{n+1}}) - C F_{A_n} (F_{B_{n+1}}) \end{aligned} \tag{E.19}$$

$$F_{A_{n+1}}(1 + C F_{B_n}) + (C F_{A_n}) F_{B_{n+1}} = F_{A_n}$$

$$F_{A_{n+1}}(C F_{B_n}) + (1 - C F_{A_n}) F_{B_{n+1}} = F_{B_n} \qquad \text{(E.19) Cont'd}$$

A matrix can now be formed using totally known information.

$$\begin{bmatrix} 1 + C F_{B_n} & C F_{A_n} \\ C F_{E_n} & 1 - C F_{An} \end{bmatrix} \begin{bmatrix} F_{A_{n+1}} \\ F_{B_{n+1}} \end{bmatrix} = \begin{bmatrix} F_{A_n} \\ F_{B_n} \end{bmatrix} \qquad \text{(E.20)}$$

The matrix $[A][X] = [B]$ is then solved for the unknown compositions $F_{A_{n+1}}$, $F_{B_{n+1}}$ via a triangulation technique. Although consuming more time per integration step than an explicit formulation, the implicit technique employed here is unconditionally stable permitting much larger step sizes, thus allowing solutions to be obtained for problems where the small steps required by the explicit technique prevented even the consideration of the case. Finally it should be recalled that an extremely simple case was chosen only for purposes of illustration and the general technique coded in RAMP handles many species (see input guide) with multiple reactions.

REFERENCES

E-1. Williams, F.A., Combustion Theory, Addison-Wesley Publishing Co., Inc., Reading, Mass., 1965.

E-2. Moretti, G., "A New Technique for the Numerical Analysis of Non-Equilibrium Flows," AIAA J., Vol. 3, No. 2, February 1965.